



Universiteit  
Leiden

The Netherlands

## Unraveling multifaceted roles of Grainyhead-like transcription factor-2 in breast cancer

Coban, B.

### Citation

Coban, B. (2024, November 5). *Unraveling multifaceted roles of Grainyhead-like transcription factor-2 in breast cancer*. Retrieved from <https://hdl.handle.net/1887/4107667>

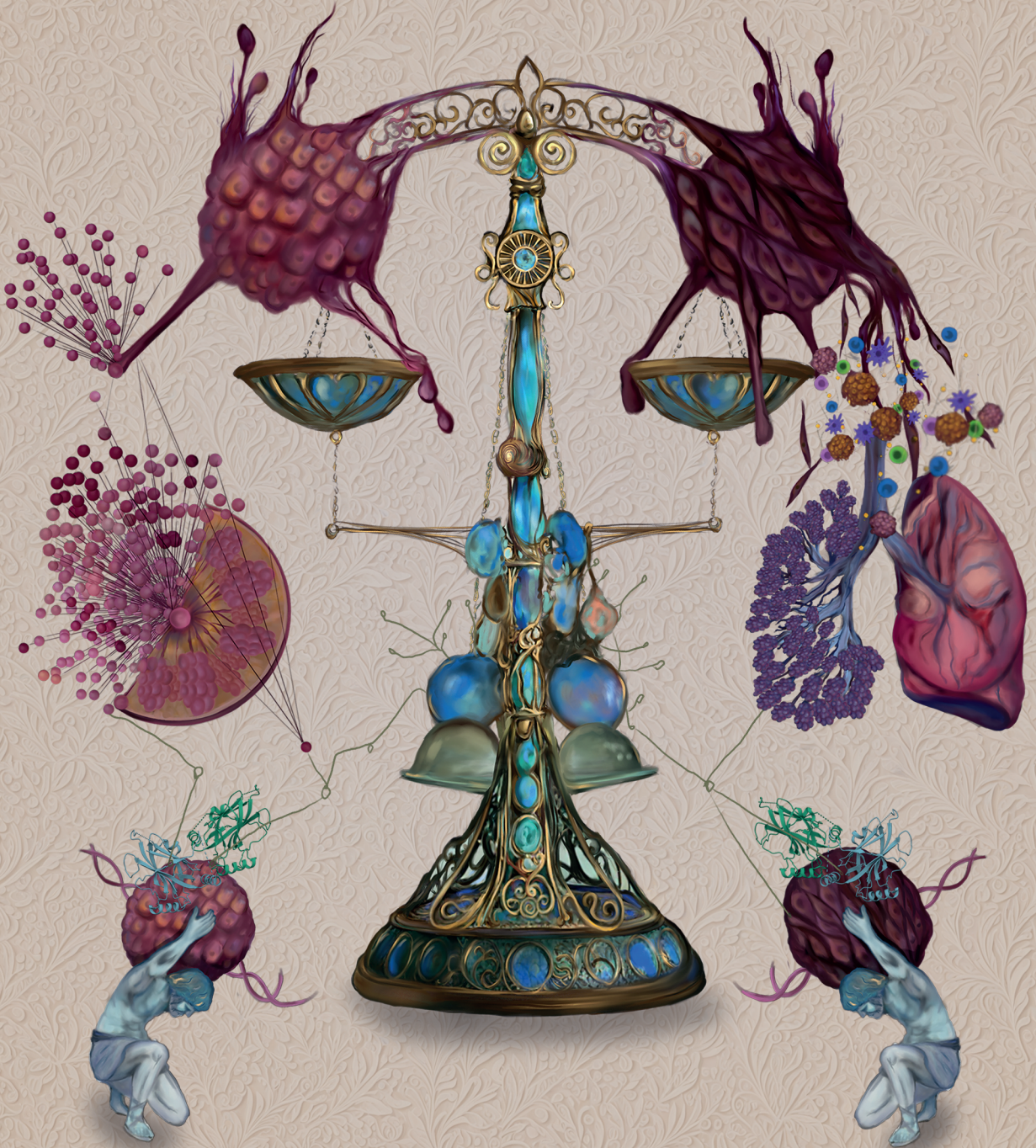
Version: Publisher's Version

License: [Licence agreement concerning inclusion of doctoral thesis in the Institutional Repository of the University of Leiden](#)

Downloaded from: <https://hdl.handle.net/1887/4107667>

**Note:** To cite this publication please use the final published version (if applicable).

# Unraveling Multifaceted Roles of Grainyhead-Like Transcription Factor-2 in Breast Cancer



**Bircan Çoban**



**Unraveling Multifaceted Roles of  
Grainyhead-like Transcription Factor-2  
in Breast Cancer**

**Bircan Çoban**

*Cover design:* Roshni R. Nair  
*Thesis lay-out:* Bircan Çoban  
*Printing:* Ipskamp Printing

© Copyright, Bircan Çoban, 2024  
ISBN: 978-94-6473-611-3

All rights reserved. No part of this book may be reproduced in any form or by any means without permission of the author.



# **Unraveling Multifaceted Roles of Grainyhead-like Transcription Factor-2 in Breast Cancer**

**Proefschrift**

ter verkrijging van  
de graad van doctor aan de Universiteit Leiden,  
op gezag van rector magnificus prof.dr.ir. H. Bijl,  
volgens besluit van het college voor promoties  
te verdedigen op dinsdag 5 november 2024  
klokke 10:00 uur

door  
Bircan Çoban  
geboren te Izmir, Turkije  
in 1990

**Promotor:** Prof.dr. E.H.J. Danen

**Co-promotor:** Dr. E. Neubert

**Promotiecommissie:**

Prof. dr. H. Irth

Prof. dr. E.C.M. de Lange

Prof. dr. B. van de Water

Prof. dr. P. ten Dijke (Leiden University Medical Centre)

Dr. G. van der Pluijm (Leiden University Medical Centre)

The research described in this thesis was performed at the Leiden Academic Centre for Drug Research (LACDR), Leiden University (Leiden, The Netherlands). The research was financially supported by the Dutch Cancer Society (KWF).



# Table of Contents

<b>Chapter 1</b>	Introduction, aim and scope of the thesis	<b>9</b>
<b>Chapter 2</b>	Metastasis: crosstalk between tissue mechanics and tumour cell plasticity	<b>27</b>
<b>Chapter 3</b>	GRHL2-controlled gene expression networks in luminal breast cancer	<b>57</b>
<b>Chapter 4</b>	GRHL2 regulation of growth/motility balance in luminal versus basal breast cancer	<b>117</b>
<b>Chapter 5</b>	Limited control of EMT/MET balance and targetable vulnerabilities by GRHL2 alone in breast cancer cells	<b>147</b>
<b>Chapter 6</b>	GRHL2 suppression of NT5E/CD73 in breast cancer modulates CD73-mediated adenosine production and T cell recruitment	<b>171</b>
<b>Chapter 7</b>	Summary, discussion and future perspectives	<b>207</b>
<b>Appendix</b>		<b>221</b>
	Nederlandse samenvatting	
	List of commonly used abbreviations	
	Curriculum vitae	
	List of publications	





This thesis is dedicated to my father, the most valuable person in my life, whose hard work, dedication and endeavor have been a constant source of inspiration.





# Chapter 1

---

Introduction, aim and scope of  
the thesis

### Breast Cancer

Breast cancer is the leading cause of death among women worldwide.<sup>1</sup> The highly heterogeneous and complex nature of the disease, characterized by diverse biological and histological features influence the breast cancer prognosis and response to the treatments. To overcome this heterogeneity and tailor the treatment options, breast cancer has been subcategorized into four groups based on the expression of estrogen receptor (ER), progesterone receptor (PR) and human epidermal growth factor receptor 2 (HER2); Luminal A, Luminal B, Human epidermal growth factor receptor 2 enriched (HER2<sup>+</sup>) and Triple-negative Basal-like.<sup>2</sup>

Luminal A tumors accounts for the most prevalent subtype with ER, PR and low Ki67 expression (a proliferation marker) but not HER2. It shows good prognosis and hormone therapy response. Compared to Luminal A, Luminal B has a higher level of Ki67 expression, causing a worse prognosis. It represents 20% of luminal tumors and expresses ER, PR and Her2. The Her2 enriched subtype is characterized by overexpression of Her2 and absence of ER and PR. HER2<sup>+</sup> breast tumors are associated with poor prognosis and require therapies targeting Her2 such as trastuzumab.<sup>3,4</sup> The last subtype Basal-like lacks ER, PR and Her2 expression. The high metastatic potential and the aggressiveness of TNBC tumors result in poor prognosis and survival outcomes.<sup>5,6</sup>

While this categorization based on the molecular markers guides the disease prognosis and treatment strategies, metastasis remains a major challenge for achieving therapeutic success. Metastasis accounts for more than 90% of cancer related deaths. It has been previously reported that the interactions between the components of tumor microenvironment (TME) (extracellular matrix, tumor cells, fibroblasts, blood and lymph vessels, immune cells and cytokines) promotes tumor progression and metastasis.<sup>7-10</sup> Therefore, it is crucial to identify key molecules and processes modulating the TME to channel novel targeted therapies to combat metastasis.

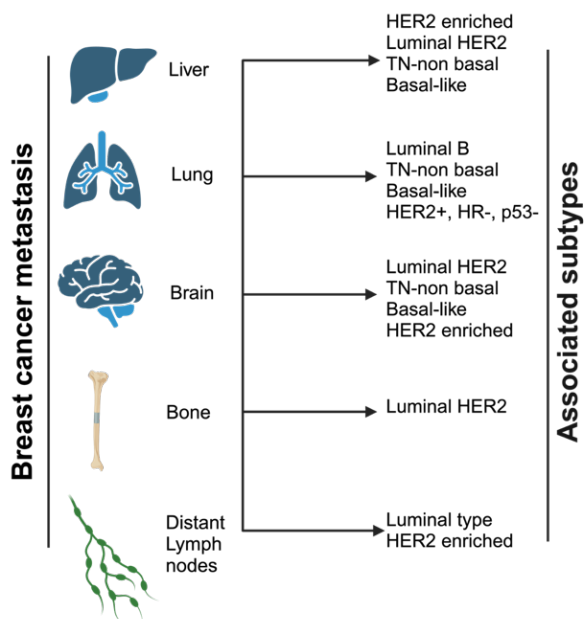


**Figure 1: Association of breast cancer molecular subtypes with metastasis.**

Organ-specific metastasis of breast cancer is governed by the molecular subtypes of breast cancer. The most prevalent metastatic site in breast cancer patients is the bone, followed by the brain as the second most common site, with the liver and lungs being subsequent sites. (Created by Biorender.com)

## Grainyhead-like transcription factors

Transcriptional regulatory networks play pivotal roles in embryogenesis, wound healing and disease-onset (e.g., cancer) in humans. The Grainyhead-like (Grhl) family of transcription factors belong to such group of genes. It was initially identified in *Drosophila melanogaster* which harbor an embryonic mutation, resulting in a unique head defect phenotype characterized by holes in specific large cuticular regions and abnormal cuticular structures.<sup>11</sup> Three orthologues of Grhl; GRHL1-3 are expressed in mammals.<sup>12,13</sup> GRHL transcription factors consist of an N-terminal transactivation domain, a DNA binding domain homologous to tumor suppressor gene p53, a DNA binding domain, and a C-terminal dimerization domain, enabling GRHL proteins to form homo and heterodimers.<sup>14</sup>

GRHL family members exert tissue-specific functions during mammalian development by being involved in the regulation of neural tube closure,<sup>15,16</sup> formation of the lungs,<sup>17,18</sup> skin barrier function,<sup>19,20</sup> and epithelial morphogenesis.<sup>21</sup> They are also involved in the repair of epidermal barrier after tissue damage modulated by receptor tyrosine kinases.<sup>22</sup> These important roles are facilitated in part by the negative regulation of epithelial-mesenchymal transition (EMT); a cellular process where epithelial cells lose apical-basal polarity and cell-cell adhesion through downregulation of epithelial genes<sup>23,24</sup> (i.e. E-cadherin, OVOL2) enabling to gain mesenchymal features such as motility, invasion and plasticity through upregulation of mesenchymal genes (i.e.; ZEB1, Vimentin SNAIL1).<sup>25</sup> EMT in embryonic development also lead to the differentiation of germ layers (ectoderm, endoderm and mesoderm), giving rise to the formation of different organs.<sup>26</sup> The members of GRHL family act as master regulators of epithelial characteristics and drive the establishment and maintenance of tissue integrity and epithelial differentiation in the embryonic development and tissue homeostasis.

In addition to their roles in the developmental processes, GRHL family transcription factors have been linked to various types of cancer including breast cancer,<sup>23,27</sup> lung cancer,<sup>28,29</sup> ovarian cancer,<sup>30</sup> colorectal cancer (CRC),<sup>31,32</sup> skin cancer,<sup>33,34</sup> and neuroblastoma.<sup>35</sup> This association is characterized by the disruption of the epithelial integrity and the dysregulation of growth and survival pathways, exhibiting both tumor suppressive and supportive functions, in part through modulation of EMT.<sup>36–38</sup>

### **Deregulation of GRHL1 and GRHL3 in cancer**

GRHL1 has been associated with squamous cell carcinoma of the skin. Grhl1 deletion in mice resulted in skin barrier defects, accompanied by more chemically-induced skin tumor formations.<sup>33</sup> This implied that GRHL1 functions as a tumor suppressor gene. Another significant role of GRHL1 as tumor suppressor has been reported in neuroblastoma. GRHL1 was identified as an early response gene to the treatment with histone deacetylase inhibitors. Its overexpression in neuroblastoma cell lines inhibited proliferation and hampered anchorage independent growth. Neuroblastoma patients with high

GRHL1 expression had favorable prognosis.<sup>35</sup> In contrast, a tumor promoter function of GRHL1 in cell-cycle regulation via EGFR-ERK axis has been shown in lung cancer.<sup>28</sup>

Similar to GRHL1, GRHL3 also exhibits context-specific activities in multiple tumors types. GRHL3 was found to be expressed mainly in early stage and hormone receptor positive breast cancers and decreased GRHL3 expression was observed during tumor progression. This indicated a possible function of GRHL3 in suppressing the tumor growth.<sup>39</sup> However, an overexpression study of GRHL3 in skin and breast cancer cell lines showed the direct transcriptional repression of E-cadherin by GRHL3, resulting in induction of cell migration and invasion.<sup>40</sup> Furthermore, decreased GRHL3 expression levels promoted EMT and deregulated MAPK/ERK pathway in CRC cells, demonstrating the tumor promoter role of GRHL3.<sup>41</sup> In addition to CRC, reduced levels of GRHL3 in squamous cell carcinoma of the skin also contributed to the tumor progression and upregulated of the oncomir miR-21, an indicator of malignant transformation.<sup>42</sup>

### **GRHL2 transcription factor in tumorigenesis**

GRHL2 is located on the chromosome 8q22 within human genome, a region that is commonly amplified in different tumor types.<sup>43</sup> Dysregulation of GRHL2 expression has been linked to numerous cellular processes, affecting the tumor progression and metastasis. In this regard, GRHL2 confers both tumor suppressive<sup>44,45</sup> and oncogenic roles in cancers.<sup>46,47</sup>

#### *GRHL2 as a tumor suppressor*

It has been demonstrated that the overexpression of GRHL2 expression prevented the invasive and migratory capabilities of gastric cancer cell lines and transforming growth factor- $\beta$  (TGF $\beta$ )-induced EMT in both gastric cancer<sup>48</sup> and oral carcinogenesis.<sup>49</sup> Downregulation of GRHL2 expression in lung cancer cell lines induced partial EMT -a hybrid state where the expression of both epithelial and mesenchymal genes coexists- by influencing the cell proliferation and colony formation.<sup>29</sup> Moreover, functional studies on GRHL2 expression revealed that GRHL2 inhibits EMT through its direct interactions with E-

cadherin and ZEB1. Silencing GRHL2 expression in a human mammary epithelial cell line resulted in downregulation of E-cadherin (CDH-1) expression and EMT.<sup>50</sup> ZEB1 was found to interact with the GRHL2 promoter upon activation of an important EMT-supporting pathway, Transforming growth factor- $\beta$  (TGF- $\beta$ ), thereby suppressing GRHL2 in different cancer types including breast cancer and colorectal cancer.<sup>46,51</sup> In contrast, it has been shown that GRHL2 also inhibits ZEB1 expression by upregulating the miR200b/c, a known EMT suppressor.<sup>52</sup> These results suggested a double negative feedback loop between GRHL2 and ZEB1 in the regulation of EMT and tumor progression. A direct and indirect regulation of epithelial phenotype via GRHL2 is further represented in Figure 2.

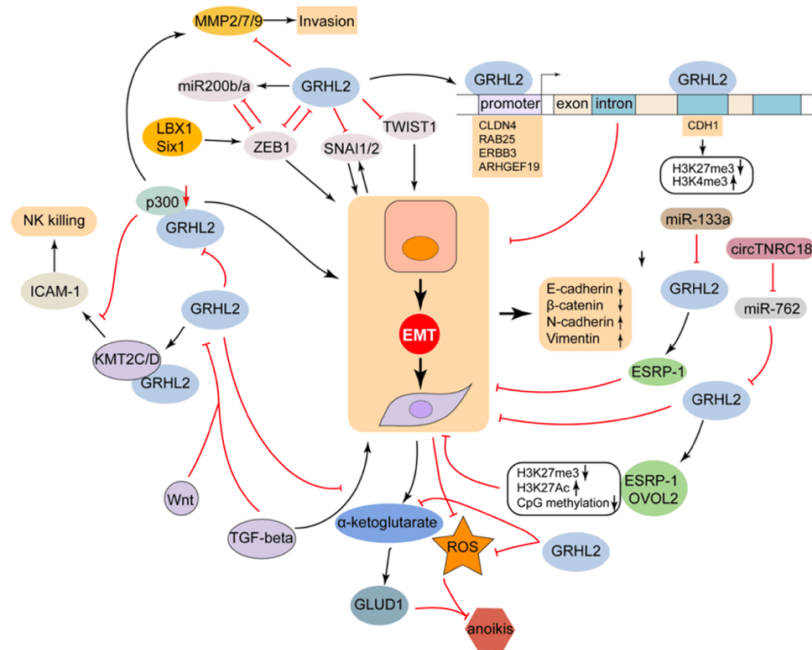


**Figure 2: Complex regulatory loops illustrating GRHL2-mediated EMT suppression.**

Here, a double-negative feedback loop between GRHL2 and ZEB1 is indicated upon GRHL2 suppression by ZEB1. Additionally, miR-200 is a direct target of GRHL2, thereby allowing the regulation of ZEB1 and EMT by GRHL2. GRHL2 bound



to the promoters of RAB25, CLDN4, ARHGEF19, and ERBB as well as intron of E-cadherin/CDH1, resulting in alterations in histone methylation. GRHL2 also inhibits SNAIL2, TWIST1 and TGF-beta/Wnt-induced EMT. Furthermore, it increases ICAM-1 expression and the sensitivity of NK killing via KMT2C/D interactions and inhibition of p300. GRHL2 is downregulated by miR-133a, resulting in decreased ESRP1 expression and EMT inhibition. MiR-762 reduction by circTNRC18 increases GRHL2 expression. EMT enhances mitochondrial oxidative phosphorylation accompanied by the overall declined level of ROS and increased GLUD1 expression which is restored by GRHL2. EMT elevates mitochondrial oxidative phosphorylation, leading to a decrease in ROS levels and an increase in GLUD1 expression. This effect is reversed by GRHL2. (Adopted from He J. et.al.; 2020)

### *GRHL2 as an oncoprotein*

Several studies have also attributed a tumor supportive role for GRHL2. A study with colorectal cancer cell lines identified GRHL2 as an oncoprotein due to its ability for enhancing cell viability and decreasing apoptosis through PI3K/Akt pathway.<sup>31</sup> Increased GRHL2 expression has been associated with poor prognosis and resistance to cisplatin, regulated by via ERK/MAPK signaling in ovarian cancer.<sup>53</sup> GRHL2 also employed oncogenic roles in lung cancer by stabilizing partial EMT; a hybrid epithelial/mesenchymal phenotype that holds a higher metastatic potential than the mesenchymal state.<sup>24</sup> Lastly, it has been found that GRHL2 functions as a key player for telomerase activity by controlling hTERT expression, thereby enhancing the viability of tumor cells.<sup>54</sup>

### *Role of GRHL2 in stemness and epigenetic regulation*

A mechanism based mathematical modeling analyzed the tumor initiating potential (stemness) of GRHL2 in stemness through EMT. GRHL2-centered positive and negative feedback loops including ZEB1 and SNAIL constituted a regulatory network between GRHL2 and stemness associated genes such as Oct4 and LIN28.<sup>24</sup> Direct regulation of Oct4 by GRHL2 modulated the stemness and plasticity in oral cancer cells.<sup>47</sup> Notably, decreased GRHL2 expression enabled pancreatic cancer cells to retain their stem-like characteristics, including self-renewal capacity and resistance to anoikis.<sup>45</sup>

Multiple studies have examined the interaction between GRHL2 and epigenetic modifiers, particularly Histone deacetylases (HDACs). HDACs are enzymes that induce loss of gene expression through chromatin condensation, impacting cellular processes such as cancer stemness, cell proliferation, and EMT.<sup>55</sup> The induction of GRHL2 suppresses the expression of mesenchymal proteins like ZEB1 and SNAI2 and augments apoptosis mediated by HDAC inhibitors in glioblastoma.<sup>56</sup> In a study on Basal-like breast cancer, the mechanisms behind cell survival upon treatment with conventional therapy were linked to the loss of histone acetylation by H3K27ac, a known transcription enhancer, at regulatory regions of epithelial master regulators like GRHL2.<sup>57</sup>

### **GRHL2 in breast cancer**

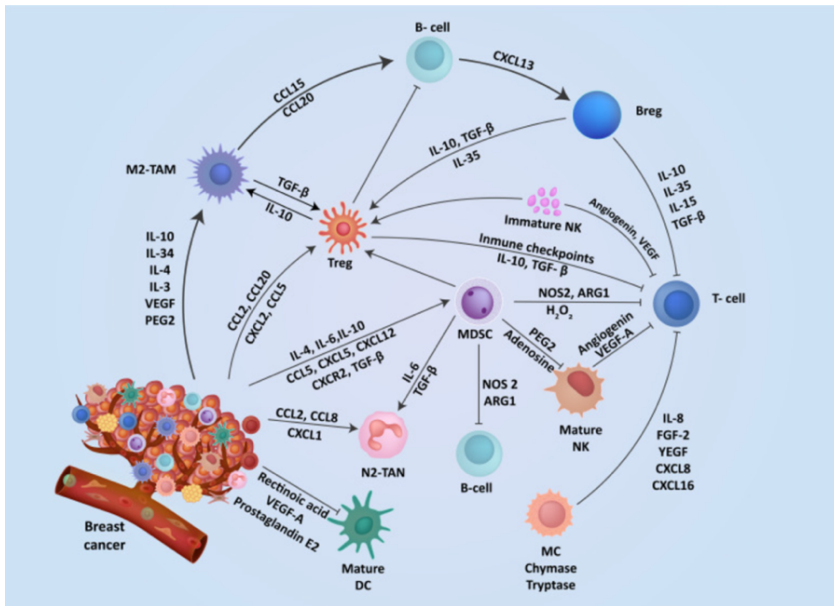
GRHL2 exhibits context-specific and subtype-specific functions in breast cancer, similar to its behavior in other cancer types. The role of GRHL2 in maintaining epithelial phenotype of breast cancer cells was highlighted above. This was further supported by Werner et al., who demonstrated that GRHL2 knockdown led to the downregulation of its target gene *ErbB3*, resulting in phenotypic and genotypic changes related to EMT in Basal subtype of breast cancer cells.<sup>58</sup> In contrast, elevated expression of GRHL2 has been associated with increased metastatic potential and poor relapse-free survival in breast cancer patients.<sup>59</sup>

Downregulated GRHL2 expression was observed in the Basal-B subtype.<sup>46</sup> Accumulating evidence suggested a specific role for GRHL2 in modulating transcriptional activity of ER in hormone receptor positive breast cancer. A virtual ChIP-seq based network analysis revealed that GRHL2 restricts estrogen transcriptional activity by downregulating the estrogen responsive enhancer RNAs.<sup>60</sup> In Tamoxifen-resistant breast tumors, FOXA1, a pioneer factor for ER transcriptional activity, has been discovered to interact with GRHL2. This interaction further regulated the LYPD3/AGR2 complex, promoting therapy resistance.<sup>61</sup> It was further shown that GRHL2 not only controls the ER activity but also prevents estrogen-induced migration of ER-positive breast cancer cells.<sup>62</sup> Altogether, these studies manifest a multifaceted role for GRHL2 function across multiple breast cancer subtypes.

### **Role of GRHL2 in immune modulation**

The immune landscape of the TME is heterogenous and determines tumor progression. Therefore, it is important to understand the dynamic interplay between tumor and immune cells.<sup>63</sup> The immune cells exert functional adaptations to the local TME and perform dual roles. These can be tumor growth promoting: Regulatory T cells (Treg), M2-like Tumor-associated Macrophages, Mast cells, Innate Lymphoid Cells type 2 and 3 (ILC2/3). Or they can be tumor growth inhibiting: Natural killer cells (NK) and Tumor infiltrating CD4+ and CD8+ Lymphocytes (TILs), Dendritic cells (DC).<sup>64</sup> During tumor progression, tumor cells adopt several immune evasive mechanisms to limit infiltration of anti-tumor immune cells and impair their cytotoxic or effector functions.<sup>65</sup> An overview of immune evasive mechanisms in breast cancer is shown in Figure 3.

Besides enabling the tumor cells to gain the cellular plasticity, EMT also confer immune evasion in different cancer types including breast cancer.<sup>66</sup> It has been previously reported that diverse epithelial and mesenchymal phenotypes modulate the sensitivity to the immune cells, thereby determining the therapy response in metastatic melanoma patients.<sup>67</sup> A comprehensive study on immune infiltration in breast cancer patient tumors revealed a correlation between EMT signature and the immune response by using the expression of epithelial markers associated with EMT. It has found out that in the triple-negative tumors and poorly differentiated tumors where E-cadherin and GRHL2 expression was downregulated, the inflammatory infiltrate was more prominent.<sup>68</sup> This was further supported by Song S. et.al, demonstrating the inverse correlation between GRHL2 expression and CD8+T cell infiltration in breast tumors.<sup>69</sup> Moreover, type I interferon (IRF1) has been identified as a direct target of GRHL2 and GRHL2 upregulated the expressions of both IRF1 and IRF3; stimulants of immune responses. Therefore, high GRHL2 protein expression was found to be associated with suppression of tumor recurrence.<sup>27</sup> Regulation of interferon response genes by GRHL2 has been also demonstrated in another study. Upon GRHL2 overexpression, an interaction of GRHL2 with two the histone methyltransferase genes was formed and this further induced mesenchymal-epithelial transition and sensitized the cells



The tumor microenvironment (TME) harbors various resident cells, pivotal for tumor progression and metastasis. These cells, along with their secretory elements and receptors such as cytokines, chemokines, and growth factors, form a complex network. This diverse network actively promotes an immunosuppressive TME. (Adopted from Akinsipe T. et.al., *Frontiers in Immunology*, 2024)

This thesis aimed to decipher GRHL2-mediated signaling networks, cellular processes and targetable vulnerabilities in multiple breast cancer subtypes to identify novel therapeutic avenues for breast cancer. We discuss how the interplay between cellular plasticity and mechanical cues in the TME enable tumor cells to navigate during dissemination, providing an overview of therapeutic opportunities to prevent metastasis in chapter 2. We explore DNA

binding sites as well as direct and indirect targets of GRHL2 in luminal breast cancer in chapter 3. ChIP-seq analysis revealed few overlapping binding sites of GRHL2 with ER $\alpha$  in luminal breast cancer cell lines. We found the direct and indirect targets of GRHL2 in response to GRHL2 loss in luminal breast cancer using Bru-seq. An integrative analysis of ChIP-seq and Bru-seq data identified distinct gene regulatory networks controlled by GRHL2 in luminal breast cancer, differ from those in other tissues. Chapter 4 demonstrates the shared and distinct roles for GRHL2 in growth and motility of luminal and basal breast cancers. A common outcome of GRHL2 deletion was characterized by cell cycle arrest. We observed a reduction in epithelial markers particularly in the luminal line while mesenchymal markers were induced only in basal cells alongside enhanced migration in response to GRHL2 loss. This is further confirmed by an in vivo model with silenced GRHL2 which demonstrated reduced primary tumor growth and fewer lung colonies, indicating that growth suppression predominated upon GRHL2 deletion. We focus on delineating GRHL2-mediated drug resistance/sensitivities in the Basal B subtype of breast cancer in Chapter 5. GRHL2 overexpression did not result in any MET-like changes in Basal B cell line in contrast to the literature previously reported. We also didn't find an effect of elevated GRHL2 expression on the cellular proliferation. A kinase inhibitor approach was implemented on GRHL2 overexpressing Basal B cells that four kinase candidates have been associated with the presence GRHL2. However, this needs further validations to confirm GRHL2 mediated responses. Chapter 6 focuses on the impact of GRHL2 deletion in immune modulation via NT5E/CD73 in luminal breast cancer. Loss of GRHL2 increased the expression of NT5E/CD73, resulting in elevated levels of adenosine production in the TME. This further enhanced the CD8 $^{+}$  T cell migration. In chapter 7, we provide an overview of the research presented in this thesis, accompanied by the discussions and future perspectives. Overall, this thesis unveils the novel regulatory roles of GRHL2 across breast cancer subtypes and highlighting novel GRHL2-mediated pathways for potential therapeutic interventions in breast cancer.

### References:

1. Sung H, Ferlay J, Siegel RL, et al. Global cancer statistics 2020: GLOBOCAN estimates of incidence and mortality worldwide for 36 cancers in 185 countries. *CA Cancer J Clin*. 2021;71(3):209-249. doi:10.3322/caac.21660
2. Al-Thoubaity FK. Molecular classification of breast cancer: A retrospective cohort study. *Ann Med Surg Lond*. 2020;49:44-48. doi:10.1016/j.amsu.2019.11.021
3. Ellis MJ, Perou CM. The genomic landscape of breast cancer as a therapeutic roadmap. *Cancer Discov*. 2013;3(1):27-34. doi:10.1158/2159-8290.CD-12-0462
4. Orrantia-Borunda E, Anchondo-Nuñez P, Acuña-Aguilar LE, Gómez-Valles FO, Ramírez-Valdespino CA. Subtypes of Breast Cancer. In: Mayrovitz HN, ed. *Breast Cancer*. Exon Publications; 2022. Accessed May 20, 2024. <http://www.ncbi.nlm.nih.gov/books/NBK583808/>
5. Milioli HH, Tishchenko I, Riveros C, Berretta R, Moscato P. Basal-like breast cancer: molecular profiles, clinical features and survival outcomes. *BMC Med Genomics*. 2017;10(1):19. doi:10.1186/s12920-017-0250-9
6. Yin L, Duan JJ, Bian XW, Yu SC. Triple-negative breast cancer molecular subtyping and treatment progress. *Breast Cancer Res*. 2020;22(1):61. doi:10.1186/s13058-020-01296-5
7. Ferreira Almeida C, Correia-da-Silva G, Teixeira N, Amaral C. Influence of tumor microenvironment on the different breast cancer subtypes and applied therapies. *Biochem Pharmacol*. 2024;223:116178. doi:10.1016/j.bcp.2024.116178
8. Zarrilli G, Businello G, Dieci MV, et al. The tumor microenvironment of primitive and metastatic breast cancer: Implications for novel therapeutic strategies. *Int J Mol Sci*. 2020;21(21):8102. doi:10.3390/ijms21218102
9. Wei R, Liu S, Zhang S, Min L, Zhu S. Cellular and extracellular components in tumor microenvironment and their application in early diagnosis of cancers. *Anal Cell Pathol*. 2020;2020:6283796. doi:10.1155/2020/6283796
10. Terry S, Savagner P, Ortiz-Cuaran S, et al. New insights into the role of EMT in tumor immune escape. *Mol Oncol*. 2017;11(7):824-846. doi:10.1002/1878-0261.12093
11. Bray SJ, Kafatos FC. Developmental function of Elf-1: an essential transcription factor during embryogenesis in *Drosophila*. *Genes Dev*. 1991;5(9):1672-1683. doi:10.1101/gad.5.9.1672
12. Ting SB, Wilanowski T, Cerruti L, Zhao LL, Cunningham JM, Jane SM. The identification and characterization of human Sister-of-Mammalian Grainyhead (SOM) expands the grainyhead-like family of developmental transcription factors. *Biochem J*. 2003;370(Pt 3):953-962. doi:10.1042/BJ20021476
13. Wilanowski T, Tuckfield A, Cerruti L, et al. A highly conserved novel family of mammalian developmental transcription factors related to *Drosophila* grainyhead. *Mech Dev*. 2002;114(1-2):37-50. doi:10.1016/s0925-4773(02)00046-1
14. Kokoszynska K, Ostrowski J, Rychlewski L, Wyrwicz LS. The fold recognition of CP2 transcription factors gives new insights into the function and evolution of tumor



- suppressor protein p53. *Cell Cycle*. 2008;7(18):2907-2915. doi:10.4161/cc.7.18.6680
15. Rifat Y, Parekh V, Wilanowski T, et al. Regional neural tube closure defined by the Grainy head-like transcription factors. *Dev Biol*. 2010;345(2):237-245. doi:10.1016/j.ydbio.2010.07.017
  16. Ting SB, Wilanowski T, Auden A, et al. Inositol- and folate-resistant neural tube defects in mice lacking the epithelial-specific factor Grhl-3. *Nat Med*. 2003;9(12):1513-1519. doi:10.1038/nm961
  17. Kersbergen A, Best SA, Dworkin S, et al. Lung morphogenesis is orchestrated through Grainyhead-like 2 (Grhl2) transcriptional programs. *Dev Biol*. 2018;443(1):1-9. doi:10.1016/j.ydbio.2018.09.002
  18. Varma S, Cao Y, Tagne JB, et al. The transcription factors Grainyhead-like 2 and NK2-homeobox 1 form a regulatory loop that coordinates lung epithelial cell morphogenesis and differentiation. *J Biol Chem*. 2012;287(44):37282-37295. doi:10.1074/jbc.M112.408401
  19. Cangkrama M, Darido C, Georgy SR, et al. Two ancient gene families are critical for maintenance of the mammalian skin barrier in postnatal life. *J Invest Dermatol*. 2016;136(7):1438-1448. doi:10.1016/j.jid.2016.02.806
  20. Ting SB, Caddy J, Wilanowski T, et al. The epidermis of grhl3-null mice displays altered lipid processing and cellular hyperproliferation. *Organogenesis*. 2005;2(2):33-35. doi:10.4161/org.2.2.2167
  21. Senga K, Mostov KE, Mitaka T, Miyajima A, Tanimizu N. Grainyhead-like 2 regulates epithelial morphogenesis by establishing functional tight junctions through the organization of a molecular network among claudin3, claudin4, and Rab25. *Mol Biol Cell*. 2012;23(15):2845-2855. doi:10.1091/mbc.E12-02-0097
  22. Caddy J, Wilanowski T, Darido C, et al. Epidermal wound repair is regulated by the planar cell polarity signaling pathway. *Dev Cell*. 2010;19(1):138-147. doi:10.1016/j.devcel.2010.06.008
  23. Wang Z, Coban B, Liao CY, Chen YJ, Liu Q, Danen EHJ. GRHL2 regulation of growth/motility balance in luminal versus basal breast cancer. *Int J Mol Sci*. 2023;24(3):2512. doi:10.3390/ijms24032512
  24. Jolly MK, Tripathi SC, Jia D, et al. Stability of the hybrid epithelial/mesenchymal phenotype. *Oncotarget*. 2016;7(19):27067-27084. doi:10.18632/oncotarget.8166
  25. Kalluri R, Weinberg RA. The basics of epithelial-mesenchymal transition. *J Clin Invest*. 2009;119(6):1420-1428. doi:10.1172/JCI39104
  26. Kim DH, Xing T, Yang Z, Dudek R, Lu Q, Chen YH. Epithelial mesenchymal transition in embryonic development, tissue repair and cancer: A comprehensive overview. *J Clin Med*. 2017;7(1). doi:10.3390/jcm7010001
  27. MacFawn I, Farris J, Pifer P, et al. Grainyhead-like-2, an epithelial master programmer, promotes interferon induction and suppresses breast cancer recurrence. *Mol Immunol*. 2024;170:156-169. doi:10.1016/j.molimm.2024.04.012

28. He Y, Gan M, Wang Y, et al. EGFR-ERK induced activation of GRHL1 promotes cell cycle progression by up-regulating cell cycle related genes in lung cancer. *Cell Death Dis.* 2021;12(5):430. doi:10.1038/s41419-021-03721-9
29. Kawabe N, Matsuoka K, Komeda K, et al. Silencing of GRHL2 induces epithelial-to-mesenchymal transition in lung cancer cell lines with different effects on proliferation and clonogenic growth. *Oncol Lett.* 2023;26(3):391. doi:10.3892/ol.2023.13977
30. Chung VY, Tan TZ, Ye J, et al. The role of GRHL2 and epigenetic remodeling in epithelial-mesenchymal plasticity in ovarian cancer cells. *Commun Biol.* 2019;2(1):272. doi:10.1038/s42003-019-0506-3
31. Hu F, He Z, Sun C, Rong D. Knockdown of GRHL2 inhibited proliferation and induced apoptosis of colorectal cancer by suppressing the PI3K/Akt pathway. *Gene.* 2019;700:96-104. doi:10.1016/j.gene.2019.03.051
32. Wang XK, Zhou FF, Tao HR, et al. Knockdown of GRHL3 inhibits activities and induces cell cycle arrest and apoptosis of human colorectal cancer cells. *J Huazhong Univ Sci Technol Med Sci.* 2017;37(6):880-885. doi:10.1007/s11596-017-1821-x
33. Mlacki M, Darido C, Jane SM, Wilanowski T. Loss of Grainy head-like 1 is associated with disruption of the epidermal barrier and squamous cell carcinoma of the skin. *PLoS One.* 2014;9(2):e89247. doi:10.1371/journal.pone.0089247
34. Kikulska A, Rausch T, Krzywinska E, et al. Coordinated expression and genetic polymorphisms in Grainyhead-like genes in human non-melanoma skin cancers. *BMC Cancer.* 2018;18(1):23. doi:10.1186/s12885-017-3943-8
35. Fabian J, Lodrini M, Oehme I, et al. GRHL1 acts as tumor suppressor in neuroblastoma and is negatively regulated by MYCN and HDAC3. *Cancer Res.* 2014;74(9):2604-2616. doi:10.1158/0008-5472.CAN-13-1904
36. Frisch SM, Farris JC, Pifer PM. Roles of Grainyhead-like transcription factors in cancer. *Oncogene.* 2017;36(44):6067-6073. doi:10.1038/onc.2017.178
37. Gasperoni JG, Fuller JN, Darido C, Wilanowski T, Dworkin S. Grainyhead-like (grhl) target genes in development and cancer. *Int J Mol Sci.* 2022;23(5):2735. doi:10.3390/ijms23052735
38. Kotarba G, Taracha-Wisniewska A, Wilanowski T. Grainyhead-like transcription factors in cancer - Focus on recent developments. *Exp Biol Med Maywood.* 2020;245(5):402-410. doi:10.1177/1535370220903009
39. Xu H, Liu C, Zhao Z, et al. Clinical implications of GRHL3 protein expression in breast cancer. *Tumour Biol.* 2014;35(3):1827-1831. doi:10.1007/s13277-013-1244-7
40. Zhao P, Guo S, Tu Z, et al. Grhl3 induces human epithelial tumor cell migration and invasion via downregulation of E-cadherin. *Acta Biochim Biophys Sin Shanghai.* 2016;48(3):266-274. doi:10.1093/abbs/gmw001
41. Tan L, Qu W, Wu D, et al. GRHL3 promotes tumor growth and metastasis via the MEK pathway in colorectal cancer. *Anal Cell Pathol.* 2021;2021:6004821. doi:10.1155/2021/6004821
42. Bhandari A, Gordon W, Dizon D, et al. The Grainyhead transcription factor Grhl3/Get1 suppresses miR-21 expression and tumorigenesis in skin: modulation

- of the miR-21 target MSH2 by RNA-binding protein DND1. *Oncogene*. 2013;32(12):1497-1507. doi:10.1038/onc.2012.168
43. Dompe N, Rivers CS, Li L, et al. A whole-genome RNAi screen identifies an 8q22 gene cluster that inhibits death receptor-mediated apoptosis. *Proc Natl Acad Sci U A*. 2011;108(43):E943-51. doi:10.1073/pnas.1100132108
44. Pan X, Zhang R, Xie C, et al. GRHL2 suppresses tumor metastasis via regulation of transcriptional activity of RhoG in non-small cell lung cancer. *Am J Transl Res*. 2017;9(9):4217-4226.
45. Nishino H, Takano S, Yoshitomi H, et al. Grainyhead-like 2 (GRHL2) regulates epithelial plasticity in pancreatic cancer progression. *Cancer Med*. 2017;6(11):2686-2696. doi:10.1002/cam4.1212
46. Cieply B, Riley P 4th, Pifer PM, et al. Suppression of the epithelial-mesenchymal transition by Grainyhead-like-2. *Cancer Res*. 2012;72(9):2440-2453. doi:10.1158/0008-5472.CAN-11-4038
47. Chen W, Yi JK, Shimane T, et al. Grainyhead-like 2 regulates epithelial plasticity and stemness in oral cancer cells. *Carcinogenesis*. 2016;37(5):500-510. doi:10.1093/carcin/bgw027
48. Xiang J, Fu X, Ran W, Wang Z. Grhl2 reduces invasion and migration through inhibition of TGF $\beta$ -induced EMT in gastric cancer. *Oncogenesis*. 2017;6(1):e284. doi:10.1038/oncsis.2016.83
49. Chen W, Kang KL, Alshaikh A, et al. Grainyhead-like 2 (GRHL2) knockout abolishes oral cancer development through reciprocal regulation of the MAP kinase and TGF- $\beta$  signaling pathways. *Oncogenesis*. 2018;7(5):38. doi:10.1038/s41389-018-0047-5
50. Xiang X, Deng Z, Zhuang X, et al. Grhl2 determines the epithelial phenotype of breast cancers and promotes tumor progression. *PLoS One*. 2012;7(12):e50781. doi:10.1371/journal.pone.0050781
51. Quan Y, Jin R, Huang A, et al. Downregulation of GRHL2 inhibits the proliferation of colorectal cancer cells by targeting ZEB1. *Cancer Biol Ther*. 2014;15(7):878-887. doi:10.4161/cbt.28877
52. Gregory PA, Bracken CP, Smith E, et al. An autocrine TGF-beta/ZEB/miR-200 signaling network regulates establishment and maintenance of epithelial-mesenchymal transition. *Mol Biol Cell*. 2011;22(10):1686-1698. doi:10.1091/mbc.E11-02-0103
53. Nie Y, Ding Y, Yang M. GRHL2 upregulation predicts a poor prognosis and promotes the resistance of serous ovarian cancer to cisplatin. *Onco Targets Ther*. 2020;13:6303-6314. doi:10.2147/OTT.S250412
54. Kang X, Chen W, Kim RH, Kang MK, Park NH. Regulation of the hTERT promoter activity by MSH2, the hnRNPs K and D, and GRHL2 in human oral squamous cell carcinoma cells. *Oncogene*. 2009;28(4):565-574. doi:10.1038/onc.2008.404
55. Tam WL, Weinberg RA. The epigenetics of epithelial-mesenchymal plasticity in cancer. *Nat Med*. 2013;19(11):1438-1449. doi:10.1038/nm.3336
56. Kotian S, Carnes RM, Stern JL. Enhancing transcriptional reprogramming of mesenchymal glioblastoma with Grainyhead-like 2 and HDAC inhibitors leads to

- apoptosis and cell-cycle dysregulation. *Genes Basel*. 2023;14(9). doi:10.3390/genes14091787
57. Pantelaiou-Prokaki G, Mieczkowska I, Schmidt GE, et al. HDAC8 suppresses the epithelial phenotype and promotes EMT in chemotherapy-treated basal-like breast cancer. *Clin Epigenetics*. 2022;14(1):7. doi:10.1186/s13148-022-01228-4
58. Werner S, Frey S, Riethdorf S, et al. Dual roles of the transcription factor grainyhead-like 2 (GRHL2) in breast cancer. *J Biol Chem*. 2013;288(32):22993-23008. doi:10.1074/jbc.M113.456293
59. Yang X, Vasudevan P, Parekh V, Penev A, Cunningham JM. Bridging cancer biology with the clinic: relative expression of a GRHL2-mediated gene-set pair predicts breast cancer metastasis. *PLoS One*. 2013;8(2):e56195. doi:10.1371/journal.pone.0056195
60. Holding AN, Giorgi FM, Donnelly A, et al. Correction to: VULCAN integrates ChIP-seq with patient-derived co-expression networks to identify GRHL2 as a key co-regulator of ERα at enhancers in breast cancer. *Genome Biol*. 2019;20(1):122. doi:10.1186/s13059-019-1733-0
61. Cocce KJ, Jasper JS, Desautels TK, et al. The lineage determining factor GRHL2 collaborates with FOXA1 to establish a targetable pathway in endocrine therapy-resistant breast cancer. *Cell Rep*. 2019;29(4):889-903.e10. doi:10.1016/j.celrep.2019.09.032
62. Reese RM, Helzer KT, Allen KO, Zheng C, Solodin N, Alarid ET. GRHL2 enhances phosphorylated estrogen receptor (ER) chromatin binding and regulates ER-mediated transcriptional activation and repression. *Mol Cell Biol*. 2022;42(10):e0019122. doi:10.1128/mcb.00191-22
63. Wellenstein MD, de Visser KE. Cancer-cell-intrinsic mechanisms shaping the tumor immune landscape. *Immunity*. 2018;48(3):399-416. doi:10.1016/j.immuni.2018.03.004
64. Salemme V, Centonze G, Cavallo F, Defilippi P, Conti L. The crosstalk between tumor cells and the immune microenvironment in breast cancer: Implications for immunotherapy. *Front Oncol*. 2021;11:610303. doi:10.3389/fonc.2021.610303
65. Binnewies M, Roberts EW, Kersten K, et al. Understanding the tumor immune microenvironment (TIME) for effective therapy. *Nat Med*. 2018;24(5):541-550. doi:10.1038/s41591-018-0014-x
66. Dongre A, Rashidian M, Reinhardt F, et al. Epithelial-to-mesenchymal transition contributes to immunosuppression in breast carcinomas. *Cancer Res*. 2017;77(15):3982-3989. doi:10.1158/0008-5472.CAN-16-3292
67. Hugo W, Zaretsky JM, Sun L, et al. Genomic and transcriptomic features of response to anti-PD-1 therapy in metastatic melanoma. *Cell*. 2016;165(1):35-44. doi:10.1016/j.cell.2016.02.065
68. Khadri FZ, Issac MSM, Gaboury LA. Impact of epithelial-mesenchymal transition on the immune landscape in breast cancer. *Cancers Basel*. 2021;13(20):5099. doi:10.3390/cancers13205099

69. Song S, Zhang D, Chen J, et al. CHMP4A stimulates CD8<sup>+</sup> T-lymphocyte infiltration and inhibits breast tumor growth via the LSD1/IFN $\beta$  axis. *Cancer Sci.* 2023;114(8):3162-3175. doi:10.1111/cas.15844
70. MacFawn I, Wilson H, Selth LA, et al. Grainyhead-like-2 confers NK-sensitivity through interactions with epigenetic modifiers. *Mol Immunol.* 2019;105:137-149. doi:10.1016/j.molimm.2018.11.006
71. Liang Y, Liu Y, Zhang Q, Zhang H, Du J. Corrigendum to Tumor-derived extracellular vesicles containing microRNA-1290 promote immune escape of cancer cells through the Grhl2/ZEB1/PD-L1 axis in gastric cancer [Translational Research 231C (2021)102-112]. *Transl Res.* 2022;247:168. doi:10.1016/j.trsl.2021.12.010



# Chapter 2

---

## Metastasis: crosstalk between tissue mechanics and tumour cell plasticity

Published in: Bircan Coban<sup>\*1</sup>, Cecilia Bergonzini<sup>\*1</sup>, Annelien JM Zweemer<sup>1</sup>, Erik HJ Danen<sup>1,2</sup>. Metastasis: crosstalk between tissue mechanics and tumour cell plasticity. Br J Cancer. 2021 Jan;124(1):49-57.

<sup>1</sup>Leiden Academic Center for Drug Research, Leiden University,  
The Netherlands

<sup>2</sup>Correspondance to E.H.J. Danen, e.danen@lacdr.leidenuniv.nl

\* These authors contributed equally to this work

### Abstract

Despite the fact that different genetic programs drive metastasis of solid tumours, the ultimate outcome is the same: tumour cells are empowered to pass a series of physical hurdles to escape the primary tumour and disseminate to other organs. Epithelial-to-mesenchymal transition (EMT) has been proposed to drive the detachment of individual cells from primary tumour masses and facilitate the subsequent establishment of metastases in distant organs. However, this concept has been challenged by observations from pathologists and from studies in animal models, in which partial and transient acquisition of mesenchymal traits is seen but tumour cells travel collectively rather than as individuals. In this review, we discuss how crosstalk between a hybrid E/M state and variations in the mechanical aspects of the tumour microenvironment can provide tumour cells with the plasticity required for strategies to navigate surrounding tissues *en route* to dissemination. Targeting such plasticity provides therapeutic opportunities to combat metastasis.

### Introduction

Metastasis is the major cause of mortality associated with solid tumours. Tumour cells escape from the primary tumour mass, move through surrounding tissues, enter the circulation, and colonize distant organs to form secondary tumours. During this process, tumour cells have to navigate mechanical hurdles consisting of various extracellular matrix (ECM) structures and layers of cells. Cross talk between intrinsic properties of the tumour cells and mechanical aspects of their surroundings drives cellular plasticity that enables tumour cells to make this journey.

The cells of solid tumours are typically surrounded by a dense fibrotic tissue composed of cellular and acellular elements — the tumour microenvironment (TME) — which plays an active role in the aggressive metastatic behaviour of cancer.<sup>1,2</sup> The TME comprises cancer-associated fibroblasts (CAFs), blood vessels and lymphatic vessels, immune-inflammatory cells, and neuroendocrine and adipose cells, all of which are embedded in an ECM, a structural network that sustains and shapes the three-dimensional architecture of



tissues and organs. Within the TME, tumour cells are subjected to chemical (cytokines, growth factors) and physical cues that originate from the cellular elements as well as from the ECM. Together, these cues impinge on cellular signalling cascades in tumour cells thereby promoting tumour development and metastasis.

What triggers a cluster of tumour cells to transit to a motile state, crawl through surrounding tissues, and start the metastatic process? One concept is that this involves an epithelial-to-mesenchymal transition (EMT; Fig. 1), whereby epithelial cells lose their cell–cell contacts and apico–basal polarity, and acquire features of mesenchymal cells, allowing them to migrate and invade.<sup>3</sup> This process is orchestrated by signalling molecules such as transforming growth factor (TGF)- $\beta$  and Wnt, which induce downstream pathways that regulate a network of transcription factors to control the balance between key epithelial proteins (including mediators of cell–cell adhesion such as E-cadherin and claudins) and mesenchymal proteins (such as vimentin).<sup>3–5</sup> Transcription factors such as TWIST, SNAIL and ZEB induce EMT whereas GRHL2 and OVOL2 suppress EMT.<sup>6,7</sup> EMT is important in embryonic development for cell migration and regulation of tissue differentiation and homeostasis,<sup>8,9</sup> but has also been associated with cancer initiation, development, and progression.<sup>7,10,11</sup> However, the idea that a full transition from an epithelial to a mesenchymal state is required for metastasis has been challenged by observations from pathologists and studies using genetically-modified mouse models.<sup>12–14</sup>

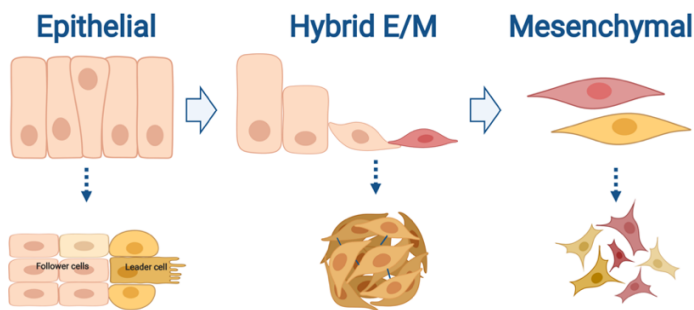


**Figure 1: EMT regulates cell migration strategies.** Upper row: During epithelial–mesenchymal transition (EMT), epithelial cells lose their tight intercellular

junctions, form a transient hybrid E/M phenotype, and eventually lose their epithelial features while gaining mesenchymal features. This process is driven by a series of changes in gene transcription programs. Lower row: migration strategies shift from collective migration, to migration with a high degree of plasticity, to individual migration as EMT progresses.

An alternate concept explaining how groups of (cancer) cells may initiate movement is derived from active matter physics. It describes how changes in mechanical and geometric parameters such as extracellular pressure, cell density, and cortical tension, can trigger a shift from solid to fluid-like behaviour in cell clusters, without the need for transcriptional alterations such as those underlying EMT<sup>15</sup> (Fig. 2). This shift is referred to as “unjamming” and transient shifts between jammed and unjammed states likely occur as tumour cell clusters navigate mechanical hurdles during the metastatic process. Notably, tumour cells are known to adopt a state referred to as partial EMT or a hybrid E/M state where epithelial and mesenchymal markers are combined. Crosstalk between mechanical aspects of the TME and the hybrid E/M state may drive plasticity and prime tumour cell clusters to unjamming, thereby allowing tumour cells to adapt to, and navigate physical hurdles and increase their metastatic potential.

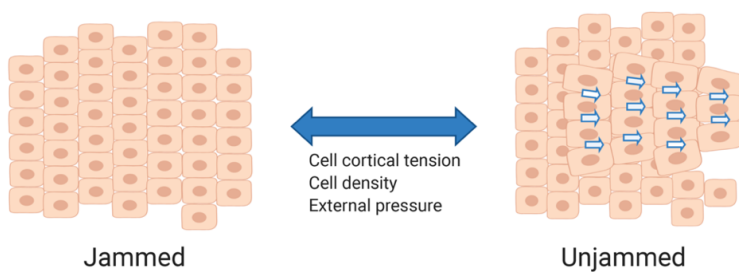


**Figure 2: Unjamming transitions as an alternative means to trigger migration.** Clusters of cells can switch between solid-like (jammed) and fluid-like (unjammed) states. In this case, changes in mechanical and geometric parameters in the tissue

can trigger fluidization (unjamming) in absence of the changes in gene transcription required for EMT.

Here, we focus on the early stage of the metastatic cascade where tumour cells leave the primary tumour, invade surrounding tissues, and enter the circulation. We present an overview of mechanical properties of the TME and discuss roles for (partial) EMT and unjamming in tumour cell migration strategies. We then explore bidirectional cross talk between the TME and partial EMT and discuss how this may contribute to plasticity and unjamming. While a detailed description of underlying molecular pathways is beyond the scope of this review, we discuss candidate therapeutic opportunities for targeting the TME and the hybrid E/M state to break crosstalk and plasticity in order to interfere with metastatic strategies.

### **Mechanical aspects of the TME**

Tumour cells are subjected to multifaceted physical cues within the TME.<sup>2</sup> Increased stiffness and pressure, both solid and fluid, are the main macroscopic mechanical alterations that can be observed in the tumour bulk.

#### *Mechanical alterations within the TME*

The components of the TME are not malignant *per se* — in fact, they are an important source of support for tissues in physiological conditions. However, as cancer progresses, many of these components are exploited by the tumour cells, causing a change in the mechanical properties of the TME. For example, CAFs can arise from resident fibroblasts and become activated in response to the release of growth factors such as TGF- $\beta$  to acquire a tumour-promoting function.<sup>2</sup> This process triggers a series of intercellular feedback loops: tumour cells recruit and activate stromal cells; these stromal cells contribute to the increased production and secretion of ECM, which, in turn, stimulates tumour progression. Ultimately, these events result in a stiffer TME, which confers increased resistance to physical deformation. This alteration in tissue tensional homeostasis has been reported to enhance cancerous transformation.<sup>16,17</sup> The dysregulation of ECM deposition, named

desmoplasia, involves not only changes in terms of ECM quantity, but also its architecture and organisation.<sup>18</sup> In particular, the main components of ECM that are dysregulated and associated with cancer progression are fibrillar collagens, fibronectin and hyaluronic acid (HA).<sup>19</sup> These alterations in ECM contribute to the increased stiffness of the TME, which has been associated with increased malignancy and invasiveness in pancreatic ductal adenocarcinoma, breast cancer, colorectal cancer and prostate cancer.<sup>20-24</sup>

Besides alterations in stiffness, the mechanical TME is affected by increased solid and interstitial pressure as the tumour increases in size. ECM components such as HA and proteoglycans absorb water, which leads to an increase in solid pressure due to the resistance conferred by the surrounding tissue. In addition, proliferation of tumour cells generates solid pressure, as an increased uptake of soluble factors results in enhanced conversion into insoluble biomass.<sup>25</sup> Expansion of the tumour bulk compresses tumour-associated blood and lymphatic vasculature, which, in turn, can affect the vascular integrity, ultimately leading to leaks and impaired drainage of lymphatic vessels. This impairment of the normal function of vessels leads to an increase in interstitial fluid pressure, which contributes to therapy resistance by inhibiting drug delivery to the tumour.<sup>26</sup> In addition, impaired vascular integrity creates hypoxic regions, which induce activation of the transcription factor hypoxia-inducible factor (HIF)-1 $\alpha$ , leading to tumour invasion and promotion of angiogenesis.<sup>16,27</sup>

### *Active cellular mechanical remodelling of the TME*

The physical alterations that occur within the tumour stroma are not just passive consequences of tumour growth. Tumour cells and CAFs actively change the mechanical properties of the TME through their interaction with the ECM. They adhere to ECM components through integrin receptors and use contractility mediated by the actin cytoskeleton and myosin motors to apply force onto these adhesions, causing cell-mediated deformation of the ECM proteins (termed strain stiffening), which contributes to the stiffening of tumour stroma.<sup>25</sup> In a positive-feedback loop, the stiffer environment triggers an increase in actomyosin contractility and force application by tumour cells,

causing further ECM stiffening.<sup>28</sup> The tensile forces on the ECM also lead to the unmasking of new binding sites for integrins, further promoting cell–ECM interactions.<sup>25,29</sup> In addition, tumour cells and CAFs remodel the ECM by enhancing collagen alignment through a process that requires contractility mediated by the GTPase Rho and its downstream effector Rho-associated kinase (ROCK), which has been associated with tumour invasion and attraction of vascular endothelial cells.<sup>30–32</sup> Moreover, tumour cells can enhance crosslinking of collagen fibres in the ECM, which further augments stiffness of the tumour stroma. The main enzymes responsible for this crosslinking are tissue transglutaminase 2 and lysyl oxidases (LOXs), the expression of which is up-regulated in several solid tumours. LOX enzymes, in particular LOX2, are up-regulated in response to hypoxia and high levels of TGF- $\beta$ , both of which are characteristic of the TME and associated with tumour progression and metastasis.<sup>25,33,34</sup>

The altered mechanical cues in the TME help to create a niche that supports tumour growth, invasion of surrounding tissues, and therapy evasion. Tumour cells sense the above-mentioned mechanical changes and transduce the mechanical input into intracellular biochemical signalling.<sup>35</sup> A force-transmitting cytoskeleton is essential for cells to sense the mechanical properties of the environment and several signal transducers have been implicated in this process, including ion channels, cell matrix adhesion complexes and membrane-associated phospholipases. Within cell matrix adhesion complexes, mechanoresponsive elements including integrin receptors and associated cytoplasmic proteins such as focal adhesion kinase (FAK)<sup>36</sup> couple the ECM to the cytoskeleton across the plasma membrane, providing mechanical homeostasis between cells and the ECM.<sup>37</sup> In conjunction with chemosensory signalling pathways (such as those activated by TGF- $\beta$  and hypoxia mentioned earlier), this bidirectional signalling controls cell shape and migratory and invasive behaviour, as well as cell survival and proliferation.<sup>38,39</sup>

### **Tumour cell migration: EMT and unjamming**

Changes in the TME induce adaptive mechanisms, such as metabolic reprogramming in tumour cells, that, in addition to the intrinsic lack of

homogeneity within tumours, contribute to the generation of tumour cell populations with diverse gene expression patterns and phenotypic features within a tumour mass.<sup>40,41</sup> This 'intra-tumour heterogeneity' provides plasticity and confers a survival advantage on tumour cells to migrate, invade and reach distant organs.<sup>42,43</sup> The conversion from a localized tumour to a full blown, disseminated cancer requires that tumour cells activate migration. EMT and unjamming represent two concepts explaining the acquisition of migratory capacity in tumours.

### *EMT*

EMT can contribute significantly to tumour heterogeneity and plasticity and has been proposed to drive the initiation of metastasis.<sup>1,44,45</sup> For example, ErbB2 is a metastasis-promoting oncogene that is frequently overexpressed in non-invasive ductal carcinoma in situ. However, only a subset of ErbB2-overexpressing cells progressed to invasive breast cancer in animal models and patient tumours and in this subpopulation ErbB2 was accompanied by overexpression of 14-3-3 $\zeta$ , which led to EMT.<sup>46</sup> The notion that EMT represents a critical step for the initiation of metastasis is challenged by the lack of evidence for EMT in the histopathology of metastatic tumour tissues as well as in several studies using animal models.<sup>12-14,47,48</sup> For example, depletion of the key EMT-promoting factors SNAIL or TWIST in a mouse model for pancreatic cancer or lineage-tracing using Fsp1 as an EMT marker in a mouse model for breast cancer failed to support a role for EMT in metastasis.<sup>13,14,47</sup> On the other hand, a study using loss of E-cadherin as an EMT marker in a mouse model for breast cancer, associated the occurrence of spontaneous EMT in a small subpopulation of tumour cells with increased migration capacity.<sup>48</sup> The interpretation of studies in favor of- and arguing against a critical role for EMT remains an ongoing debate.<sup>49-51</sup> Importantly, defining EMT based on the expression of a single marker underestimates the dynamic nature of EMT as this process is likely to be a transient event in cancer.<sup>52</sup> Moreover, EMT is a non-linear program that can be defined and controlled by distinct gene networks in a cancer-type specific manner.<sup>53,54</sup> It has been shown that a pro-metastatic effect of EMT depends not only on the final state but on the molecular route that leads tumour cells to that state.<sup>55</sup> The reverse process,

mesenchymal-to-epithelial transition (MET), occurs as tumour cells arrive at distant organs, and might be important for the formation of metastatic lesions, as disseminated tumour cells locked in a mesenchymal state fail to effectively colonise these organs.<sup>48,56-58</sup>

Notably, EMT also plays a role in other cell types in the TME including the generation of CAFs. CAFs can originate from normal resident tissue fibroblasts<sup>59</sup> or mesenchymal stem cells.<sup>60</sup> In addition, CAFs can arise from epithelial cells through EMT or from endothelial cells through endothelial-to-mesenchymal transition (EndMT) and both conversions are induced by TGF- $\beta$ .<sup>61,62</sup> It is largely unknown how these CAF populations differ in functionality, but they are all characterized by a myofibroblast phenotype that drives stiffening of the TME as described above.

### *Partial EMT or hybrid E/M*

Rather than a complete EMT, transient subtle changes in the balance between pro- and anti-EMT transcription factors that result in a partial EMT or 'hybrid E/M' state might be more relevant in the context of cancer (Fig. 1). Indeed, both epithelial and mesenchymal markers can be co-expressed in a single tumour cell in hybrid E/M and a range of intermediate states may exist.<sup>63-66</sup> One advantage of maintaining an epithelial phenotype, such as expression of E-cadherin in a hybrid E/M state is an increased survival fitness through cell-cell contacts in tumour clusters in the circulation.<sup>67</sup> Hybrid E/M is also associated with increased stemness, which, in turn, is linked to elevated plasticity and self-renewal capacities as compared to completely E or M states in breast cancer.<sup>64,68,69</sup> Additionally, a tumour that harbours subpopulations of cells residing at different stages of a fluid, cancer-associated hybrid E/M state might have an optimal capacity to cope with variations in the TME and progress towards metastasis. A hybrid E/M state confers phenotypic and molecular diversity, which provides cellular plasticity, empowering tumour cells to navigate various physical hurdles during their journey to metastatic sites while maintaining expression of epithelial markers and intercellular adhesion.<sup>3,7,64,65,70-73</sup> Indeed, in a mouse model for breast cancer, a hybrid E/M state induced the formation of tumour cell subpopulations with varying

degrees of invasiveness and metastatic potential.<sup>64</sup> The existence of hybrid E/M cell populations and their association with enhanced metastatic features including migration and intravasation, were corroborated by studies on ovarian and pancreatic cancers.<sup>74,75</sup> A biophysical model also showed that hybrid E/M states give rise to heterogeneous clusters migrating collectively and leading to the circulating tumour cell clusters as observed in animal models and patients.<sup>76</sup>

### *Unjamming transitions*

The collective movement of cell clusters has also been studied using principles from active matter to describe transitions between arrested (“jammed”) and moving states (“unjammed”) in cell aggregates.<sup>77</sup> In this case, changes in mechanical and geometric parameters in the tissue trigger fluidization in absence of EMT<sup>15</sup> (Fig. 2). In epithelial cells grown as a monolayer, introducing a wound or perturbing endocytosis induces unjamming and creates a transition from a static to a flowing state.<sup>78-80</sup> Likewise, compressive stress mimicking a bronchospasm triggers a transition in a monolayer of airway epithelial cells from a solid-like jammed phase to a fluid-like unjammed phase.<sup>81</sup> A solid-to-fluid transition is also observed during development in *Xenopus laevis*, in which a hybrid E/M is associated with a fluid, but still collective, state of migrating neural crest cells.<sup>82</sup> A study using MCF10-derived tumouroids showed that a similar fluidisation process occurs at the edges of densely packed breast cancer cells.<sup>83</sup>

If and how the early steps of metastasis follow similar principles, represents an urgent, unresolved issue. In breast cancer, clusters of invading tumour cells are more prone than individual cells to survive. These clusters promote metastasis formation in mouse models and give rise to oligoclonal clusters in the circulation that are associated with poor prognosis in patients.<sup>84,85</sup> Likewise, circulating tumour cell clusters can arise from collective cell migration and intravasation in renal cell carcinoma, lung cancer and invasive melanoma.<sup>86-88</sup> Whether cluster invasion in complete absence of a partial EMT fully explains these findings is unresolved. EMT-like changes have been detected in circulating tumor cells.<sup>89</sup> Yet, clusters of circulating tumour cells are



largely epithelial and evidence in favor of E/M hybrid clusters is still scarce, suggesting that unjamming of fully epithelial tumour tissues may occur.

Tumour cells in the centre of a tumour mass are likely to be jammed but increased pressure might drive a switch from a solid to a fluid-like state. Indeed, multiphoton microscopy in a spontaneous mouse model for intestinal cancer has shown coordinated migratory patterns in the tumour core that are indicative of a fluid-like behaviour.<sup>90</sup> Such movement has been suggested to be critical for cell mixing inside the tumour, which allows the most aggressive clones to effectively replace all other cells.<sup>91</sup> In the outer regions, tumour cells are prone to mechanical stress due to a high abundance of ECM, which results in further unjamming.<sup>77</sup>

### *Collectivity in tumour cell migration strategies*

Unjamming, as well as a hybrid E/M state, leads to a fluid-like migration of clusters of tumour cells that maintain cell–cell contacts. It has been reported that high expression of EMT-promoting transcription factors such as Snail and Twist leads to the collective migration of tumour cells that exhibit epithelial and incomplete mesenchymal features.<sup>92,93</sup> Likewise, unjamming of breast cancer cells triggered by a cascade of growth factor receptor internalization, activation of extracellular signal-regulated kinase/mitogen-activated protein kinase and cytoskeletal remodelling, induces collective migration.<sup>81</sup> Glioma cells infiltrate the brain as multicellular networks and breaking cell-cell interactions by downregulating p120-catenin was found to decrease infiltration capacity, again indicating that the ability to maintain cell-cell contacts is important.<sup>94</sup> It is likely that the interaction between molecular programs induced by hybrid E/M and local, physical cues in the TME creates routes for subpopulations of tumour cells to unjam and start disseminating.<sup>46,95</sup>

Mixed individual and collective migration modes are observed in tumours of distinct origin: even mesenchymal tumours such as sarcomas switch from an individual to a collective migration mode in areas of particularly dense ECM structures.<sup>96</sup> Single cells can move through ECM networks by adopting amoeboid or spindle-like mesenchymal shapes:<sup>97</sup> amoeboid cells generate few

## Chapter 2

ECM adhesions and stress fibres whereas mesenchymal migration is associated with strong ECM interaction and actomyosin contractility.<sup>95</sup> Collectively migrating cells adopt different morphologies such as sheets, strands, multicellular tubes and masses with irregular forms (Fig. 3).<sup>98</sup> Inside groups of collectively migrating cells, intercellular junctions can sense and integrate chemical and mechanical cues from the environment. Migrating clusters are usually organized into two cellular populations: leader and follower cells. The leader cells are responsible for sensing the microenvironment and generating traction forces to move the remainder of the group, which they do by proteolytically remodelling the matrix in order to create a path through which the collective group can navigate.<sup>99</sup> It has been suggested that a collective migration strategy might be thermodynamically favorable by alternating leader cells that are exposed to a long-range strain field at the invasive front.<sup>100</sup> In vitro models also showed how switching leader and follower positions, enables groups of breast cancer cells to invade through areas of high ECM density.<sup>101</sup>

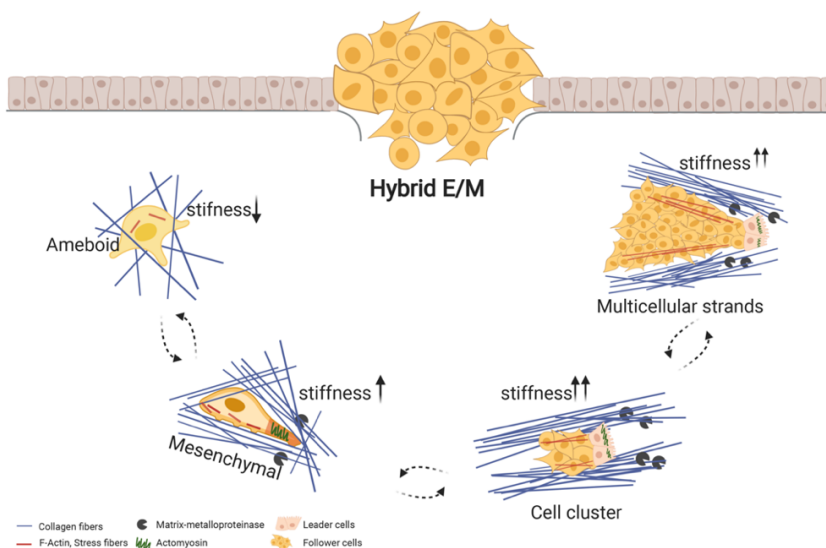


**Figure 3: The hybrid E/M state provides plasticity and the local TME dictates collective and individual migration strategies.** In a low stiffness environment, hybrid E/M cells migrate individually through ECM networks in an amoeboid or mesenchymal fashion. Amoeboid cells move through existing openings in a soft ECM of high porosity using few ECM adhesions and stress fibres, independent of protease activity. Mesenchymal migration in regions of somewhat higher stiffness and lower porosity is accompanied by increased formation of ECM adhesions, stress fibres and actomyosin contractility, and requires protease activity (mediated for instance by matrix metalloproteases (MMPs)) to generate openings through which to migrate. A further increase in TME stiffness promotes collective migration of hybrid E/M cells. Collective migration can take the shape of cell clusters or multicellular strands, and involves contractile and proteolytically active leader cells creating the path for follower cells. Collectively migrating cells can make use of pre-existing large-scale mechanical structures in the TME such as channels or interphases between cell layers. Interconversion between the different migration strategies is dictated by local variations in the mechanical aspects of the TME, and the hybrid E/M state provides tumour cells with enhanced plasticity to respond to such cues.

### Crosstalk between partial EMT and TME mechanics

Plasticity of tumour cells allows them to switch between distinct modes of migration, which provides them with the means to navigate the mechanical complexity of their environment.<sup>102</sup> A transition between escaping individual cells and regrouping collectives can be observed in collective strands of invasive cells.<sup>103</sup> The hybrid E/M state probably supports such plasticity and the local physical properties of the TME can determine the level of individualization. Indeed, using theoretical, *in vitro* and *in vivo* models shows how a weakening of cell–cell adhesion (as occurs in hybrid E/M) cooperates with ECM confinement to drive unjamming, fluidization and, ultimately, cell individualisation.<sup>104</sup> Thus, the interaction between molecular features of tumour cells and local properties of the TME can drive metastasis by mediating interconversions between collective and individual behaviour (Fig. 3).

### *TME stiffening promotes EMT*

Tumour cells sense and respond to mechanical stimuli from the TME.<sup>35,39</sup> Integrins and associated intracellular proteins bidirectionally transmit force between the ECM and the cytoskeletal network and associated molecular motors (e.g. myosins), which facilitates ECM remodelling and regulates canonical signal transduction pathways that control cell fate.<sup>105</sup> Mechanical cues from the TME, such as increased ECM density and stiffness, can stimulate EMT<sup>20,106-109</sup> and act in concert with soluble EMT-stimulating factors, such as TGF- $\beta$ .<sup>106,110,111</sup> Important mediators of mechanically-induced EMT are the transcription factors TWIST1 and YAP/TAZ,<sup>112,113</sup> which, upon matrix stiffening and subsequent intracellular transduction of mechanical signals, are induced to translocate to the nucleus to influence the expression of several genes that promote EMT (Fig. 4).<sup>106,113-115</sup> A positive feedback loop is also generated by the interaction with HA in the TME. The interaction between CD44 on the cell surface and HA in the ECM induces the activation of Zeb1, which, in addition to promoting EMT also inhibits epithelial splicing regulatory protein 1 (ESRP1) leading to the up-regulation of hyaluronic acid synthase 2 (HAS2) and increased HA production.<sup>116</sup> Thus, the chemical composition and stiffening of the TME can promote (partial) EMT in tumour cells. Notably, cells appear to possess a “mechanical memory”. I.e., prolonged exposure to a stiff ECM causes EMT-like behaviour with nuclear localization of YAP, high actomyosin contractility, and large cell matrix adhesions and this phenotype is maintained when the cells move to a soft environment for as long as the factors mediating the mechanical memory suppress a transcriptional switch.<sup>116-118</sup>

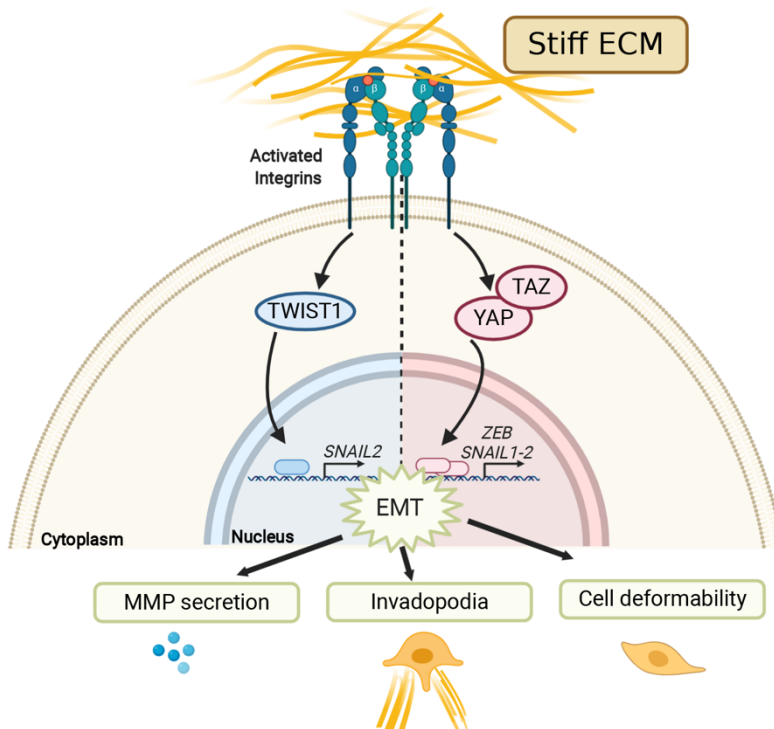


**Figure 4. Mechanotransduction drives EMT in response to mechanical cues from the TME.** An increased stiffness in the TME is sensed by integrins, which activate downstream intracellular signalling, ultimately resulting in the nuclear translocation of EMT-associated transcription factors and transcriptional co-activators, such as TWIST and YAP/TAZ. In the nucleus, these factors will bind to and regulate the transcription of target genes such as SNAIL and ZEB, causing a shift between epithelial (E) and mesenchymal (M) features. As tumour cells undergo EMT, cell deformability, proteolytic activity and the formation of invadopodia increase, driving enhanced migratory and invasive capacity.

### *EMT and tumour cell mechanics*

Whereas stiffening of the TME drives EMT and the aggressive behaviour of tumours,<sup>119</sup> tumour cells themselves have been observed to be ‘more deformable’ or ‘softer’.<sup>120</sup> EMT might play a role in such softening of tumour cells. Cells undergoing EMT change their morphology, lose adhesive

properties and undergo actin cytoskeletal rearrangement, which all influence cell stiffness and tension with neighbouring cells and the ECM.<sup>121</sup> Mesenchymal-like cells tend to reduce their stiffness and become softer in response to force application, while epithelial cells are more likely to stiffen in response to the same force application.<sup>122</sup> Accordingly, EMT-promoting transcription factors such as SNAIL and TWIST1 promote increased cellular deformability,<sup>123</sup> which facilitates migration through ECM networks and intravasation.<sup>122</sup> Actin fibres connect integrin-containing adhesions with the nuclear envelope through the linker of nucleoskeleton and cytoskeleton (LINC) complex, thereby creating a physical connection between the ECM and the nucleus.<sup>124</sup> This interaction is important for tuning the mechanical properties of the nucleus during migration in confined spaces. Indeed, nuclear deformability is a rate-limiting step for cell migration and some level of nuclear rupture has been observed during the migration of tumour cells in a confined space.<sup>125-127</sup> The nucleoskeletal lamins regulate stiffness of the nuclear envelope and thereby determine a cell's migratory capacity in confinement.<sup>128</sup> How (partial) EMT affects nuclear mechanics remains to be elucidated but a hybrid E/M will increase cellular and, perhaps, nuclear deformability to increase plasticity, allowing tumour cells to adapt to confinement and enhance migratory potential.

### *EMT and tumour cell mediated modulation of the TME*

As tumour cells undergo EMT, they also increase the production of soluble proteases or membrane-anchored MMPs, which allows invading tumour cells or tumour cell clusters to remove barriers or create tracks.<sup>29,129,130</sup> The number of invadopodia — specialised actin-based membrane protrusions in which localised proteolytic activity degrades ECM — is also increased in tumour cells that are subjected to a stiffer environment or dense fibrillar collagen structures.<sup>131,132</sup> Likewise, EMT induced by transcription factors including TWIST1 and ZEB1, promotes the formation of invadopodia in tumour cells.<sup>133,134</sup> Thus, the interconnection between stiffening of the TME and EMT discussed above might enhance the ability of tumour cells and tumour-cell clusters to proteolytically degrade the ECM and break through tissue barriers. The importance of proteolytic ECM degradation, however, depends on the

migratory strategy. While enzymatic breakdown of ECM is necessary for collective migration, individually migrating cells can either proteolytically remodel their surrounding ECM or adapt their shape to the already existing gaps.<sup>95</sup> EMT driven by ZEB1 also leads to increased expression of LOXL2,<sup>135</sup> which not only causes enhanced collagen crosslinking and TME stiffening but has been found to stimulate an EMT-associated transcription network,<sup>136</sup> providing yet another positive feedback loop between EMT and the TME.

### Targeting the TME and hybrid E/M state

Interfering with the metastatic process remains a major challenge. Crosstalk between tumour cells and the TME is complex and dynamic, and provides plasticity that allows tumour cells to adapt to different environments and escape therapy. We have discussed the mechanical interplay between the TME and tumour cells and a role for partial EMT in this process. Several candidate targets exist, which, when inhibited, might block this mechanical interaction and prevent tumour cell plasticity, including integrins,<sup>137,138</sup> vimentin,<sup>139</sup> Rho/ROCK and actomyosin contractility,<sup>140</sup> and FAK.<sup>36,137,138,141</sup> Notably, however, interfering with tumour–TME interactions can also have unexpected and undesirable effects. For example, whereas inhibition of FAK in a mouse model for pancreatic cancer attenuated the cancer-promoting activity of the fibrotic stroma, limited tumour progression and enhanced survival,<sup>141</sup> depletion of CAFs, which might be expected to have a similar effect, actually led to more aggressive tumours and reduced survival.<sup>142</sup> One explanation is the heterogeneity of CAFs in pancreatic and other cancers that may have diverse impacts on tumour growth and progression within the TME, including immune-modulation.<sup>143,144</sup>

Strategies that simultaneously target different mechanisms of tumour cell plasticity, including the hybrid E/M state, might prevent tumour cells from adapting to changes in the TME.<sup>141,145</sup> A network topology-based modelling approach has been applied to identify approaches for interfering with feedback loops in EMT networks, which may point to new strategies to interfere with plasticity and, hence with metastasis.<sup>146</sup> Signal transduction cascades and transcription factors promoting a stable hybrid E/M state might serve as

promising therapeutic targets, including GRHL2, OVOL2, NUMB and NRF2.<sup>76,147,148</sup> Such a strategy has been successfully explored in breast cancer cells, in which the expression of SNAIL is associated with the hybrid E/M state. Deletion of SNAIL or either deletion or overexpression of ZEB1 pushed cells either in a complete E or in an M state, in each case resulting in attenuated capacity to form tumours.<sup>149</sup> Despite these promising results, strategies that drive hybrid E/M cells into MET pose the risk of driving metastatic outgrowth of already disseminated tumour cells.<sup>48,56-58</sup> On the other hand, strategies that lock cells in the M state might attenuate the outgrowth of primary and secondary tumours but drive the dissemination of individual tumour cells.<sup>57</sup> An alternative promising strategy that exploits the highly plastic hybrid E/M state has made use of a combination of peroxisome proliferator-activated receptor  $\gamma$  (PPAR $\gamma$ ) activation and MEK inhibition to enforce trans-differentiation of the tumour cells into post-mitotic adipocytes.<sup>150</sup> This points to an exciting possibility that while plasticity allows tumour cells to adapt to different environments during metastasis it also represents a state that is vulnerable to differentiation therapy.

### Conclusions

In this review, we have discussed the dynamic interactions of tumour cells with the TME. In particular, we highlighted the importance of tissue mechanics and the role of (partial) EMT in the early steps of the metastatic cascade. The TME provides a pathological mechanical environment that tumour cells sense and respond to. The initiation of the metastatic cascade requires acquisition of a migratory phenotype that is influenced by this environment. The role of EMT in this process is likely different in different tumour types and in most cases involves a partial EMT or hybrid E/M state. EMT and unjamming provide distinct mechanisms to initiate movement and to what extent hybrid E/M sets the stage for unjamming of epithelial tumour cell clusters is poorly understood. The hybrid E/M state provides tumour cells with plasticity affecting stemness, tumour growth, and migration, allowing them to navigate variations in the mechanical TME as they use collective strategies to invade local surrounding tissues and enter the circulation. It is the bidirectional cross talk between partial EMT-driving molecular programs in the



tumour cells and the heterogeneous local mechanical properties of the environment that drive the early stages of the metastatic cascade. Further insight into the dynamic nature of this process at different stages of the metastatic cascade is required. This will depend on integration of multiscale theoretical models, in vitro models incorporating tumour heterogeneity and relevant mechanical variations in the TME, and in vivo models that capture the full complexity of the metastatic process. Disrupting mechanical tumour–TME interactions and/or tumour plasticity at the level of the hybrid E/M state offers promising avenues for therapeutic strategies. In this area we have only just begun to scratch the surface of what might be possible.

### Additional Information

**Acknowledgements:** This work was supported by grants from the Dutch Cancer Society to Bircan Coban (KWF Research Project 10967) and Cecilia Bergonzini (KWF Research Project 11957).

The figures were created using the BioRender.com Illustrating tool.

**Authors' contributions:** B.C., C.B., A.J.M.Z., and E.H.J.D. jointly prepared the manuscript.

**Funding:** This work was supported by grants from the Dutch Cancer Society to Bircan Coban (KWF Research Project 10967) and Cecilia Bergonzini (KWF Research Project 11957).

### References

1. Hanahan, D., Weinberg, R.A. Hallmarks of cancer: the next generation. *Cell* **144**, 646-74 (2011)
2. Jang, I., Beningo, K.A. Integrins, CAFs and Mechanical Forces in the Progression of Cancer. *Cancers (Basel)* **11**, 721 (2019)
3. Thiery, J.P., Acloque, H., Huang, R.Y., Nieto, M.A. Epithelial-mesenchymal transitions in development and disease. *Cell* **139**, 871-90 (2009)
4. Ansieau, S., Bastid, J., Doreau, A., Morel, A.P., Bouchet, B.P., Thomas, C., et al. Induction of EMT by twist proteins as a collateral effect of tumor-promoting inactivation of premature senescence. *Cancer Cell* **14**, 79-89 (2008)

5. Lamouille, S., Xu, J., Derynck, R. Molecular mechanisms of epithelial-mesenchymal transition. *Nat Rev Mol Cell Biol* **15**, 178-96 (2014)
6. Peinado, H., Olmeda, D., Cano, A. Snail, Zeb and bHLH factors in tumour progression: an alliance against the epithelial phenotype? *Nat Rev Cancer* **7**, 415-28 (2007)
7. De Craene, B., Berx, G. Regulatory networks defining EMT during cancer initiation and progression. *Nat Rev Cancer* **13**, 97-110 (2013)
8. Yang, J., Weinberg, R.A. Epithelial-mesenchymal transition: at the crossroads of development and tumor metastasis. *Dev Cell* **14**, 818-29 (2008)
9. Nieto, M.A. Epithelial plasticity: a common theme in embryonic and cancer cells. *Science* **342**, 1234850 (2013)
10. Polyak, K., Weinberg, R.A. Transitions between epithelial and mesenchymal states: acquisition of malignant and stem cell traits. *Nat Rev Cancer* **9**, 265-73 (2009)
11. Krebs, A.M., Mitschke, J., Lasierra Losada, M., Schmalhofer, O., Boerries, M., Busch, H., et al. The EMT-activator Zeb1 is a key factor for cell plasticity and promotes metastasis in pancreatic cancer. *Nat Cell Biol* **19**, 518-29 (2017)
12. Tarin, D., Thompson, E.W., Newgreen, D.F. The fallacy of epithelial mesenchymal transition in neoplasia. *Cancer Res* **65**, 5996-6000; discussion -1 (2005)
13. Fischer, K.R., Durrans, A., Lee, S., Sheng, J., Li, F., Wong, S.T., et al. Epithelial-to-mesenchymal transition is not required for lung metastasis but contributes to chemoresistance. *Nature* **527**, 472-6 (2015)
14. Zheng, X., Carstens, J.L., Kim, J., Scheible, M., Kaye, J., Sugimoto, H., et al. Epithelial-to-mesenchymal transition is dispensable for metastasis but induces chemoresistance in pancreatic cancer. *Nature* **527**, 525-30 (2015)
15. Oswald, L., Grosser, S., Smith, D.M., Kas, J.A. Jamming transitions in cancer. *J Phys D Appl Phys* **50**, 483001 (2017)
16. Northey, J.J., Przybyla, L., Weaver, V.M. Tissue Force Programs Cell Fate and Tumor Aggression. *Cancer Discov* **7**, 1224-61 (2017)
17. Panciera, T., Citron, A., Di Biagio, D., Battilana, G., Gandin, A., Giullitti, S., et al. Publisher Correction: Reprogramming normal cells into tumour precursors requires ECM stiffness and oncogene-mediated changes of cell mechanical properties. *Nat Mater* **19**, 475 (2020)
18. Di Maggio, F., El-Shakankery, K.H. Desmoplasia and Biophysics in Pancreatic Ductal Adenocarcinoma. *Pancreas* **49**, 313-25 (2020)
19. Walker, C., Mojares, E., Del Río Hernández, A. Role of Extracellular Matrix in Development and Cancer Progression. *Int J Mol Sci* **19**, 3028 (2018)
20. Rice, A.J., Cortes, E., Lachowski, D., Cheung, B.C.H., Karim, S.A., Morton, J.P., et al. Matrix stiffness induces epithelial-mesenchymal transition and promotes chemoresistance in pancreatic cancer cells. *Oncogenesis* **6**, e352 (2017)
21. Boyd, N.F., Lockwood, G.A., Byng, J.W., Trichler, D.L., Yaffe, M.J. Mammographic densities and breast cancer risk. *Cancer Epidemiol Biomarkers Prev* **7**, 1133-44 (1998)

22. Acerbi, I., Cassereau, L., Dean, I., Shi, Q., Au, A., Park, C., et al. Human breast cancer invasion and aggression correlates with ECM stiffening and immune cell infiltration. *Integr Biol (Camb)* **7**, 1120-34 (2015)
23. Baker, A.M., Bird, D., Lang, G., Cox, T.R., Erler, J.T. Lysyl oxidase enzymatic function increases stiffness to drive colorectal cancer progression through FAK. *Oncogene* **32**, 1863-8 (2013)
24. Hoyt, K., Castaneda, B., Zhang, M., Nigwekar, P., di Sant'agnese, P.A., Joseph, J.V., et al. Tissue elasticity properties as biomarkers for prostate cancer. *Cancer Biomark* **4**, 213-25 (2008)
25. Mohammadi, H., Sahai, E. Mechanisms and impact of altered tumour mechanics. *Nat Cell Biol* **20**, 766-74 (2018)
26. Dewhirst, M.W., Secomb, T.W. Transport of drugs from blood vessels to tumour tissue. *Nat Rev Cancer* **17**, 738-50 (2017)
27. Stylianopoulos, T., Martin, J.D., Chauhan, V.P., Jain, S.R., Diop-Frimpong, B., Bardeesy, N., et al. Causes, consequences, and remedies for growth-induced solid stress in murine and human tumors. *Proc Natl Acad Sci U S A* **109**, 15101-8 (2012)
28. Malandrino, A., Mak, M., Kamm, R.D., Moeendarbary, E. Complex mechanics of the heterogeneous extracellular matrix in cancer. *Extreme Mech Lett* **21**, 25-34 (2018)
29. Te Boekhorst, V., Preziosi, L., Friedl, P. Plasticity of Cell Migration In Vivo and In Silico. *Annu Rev Cell Dev Biol* **32**, 491-526 (2016)
30. Conklin, M.W., Keely, P.J. Why the stroma matters in breast cancer: insights into breast cancer patient outcomes through the examination of stromal biomarkers. *Cell Adh Migr* **6**, 249-60 (2012)
31. Balcioglu, H.E., van de Water, B., Danen, E.H.J. Tumor-induced remote ECM network orientation steers angiogenesis. *Sci Rep* **6**, 22580 (2016)
32. Provenzano, P.P., Inman, D.R., Eliceiri, K.W., Trier, S.M., Keely, P.J. Contact Guidance Mediated Three-Dimensional Cell Migration is Regulated by Rho/ROCK-Dependent Matrix Reorganization. *Biophys J* **95**, 5374-84 (2008)
33. Finger, E.C., Giaccia, A.J. Hypoxia, inflammation, and the tumor microenvironment in metastatic disease. *Cancer Metastasis Rev* **29**, 285-93 (2010)
34. Pickup, M.W., Laklai, H., Acerbi, I., Owens, P., Gorska, A.E., Chytil, A., et al. Stromally derived lysyl oxidase promotes metastasis of transforming growth factor-beta-deficient mouse mammary carcinomas. *Cancer Res* **73**, 5336-46 (2013)
35. Chin, L., Xia, Y., Discher, D.E., Janmey, P.A. Mechanotransduction in cancer. *Curr Opin Chem Eng* **11**, 77-84 (2016)
36. Sulzmaier, F.J., Jean, C., Schlaepfer, D.D. FAK in cancer: mechanistic findings and clinical applications. *Nature Reviews: Cancer* **14**, 598-610 (2014)
37. Huveneers, S., Danen, E.H.J. Adhesion signaling – crosstalk between integrins, Src and Rho. *J Cell Sci* **122**, 1059-69 (2009)
38. Kalli, M., Stylianopoulos, T. Defining the Role of Solid Stress and Matrix Stiffness in Cancer Cell Proliferation and Metastasis. *Front Oncol* **8**, 55 (2018)
39. Sheetz, M. A Tale of Two States: Normal and Transformed, With and Without Rigidity Sensing. *Annu Rev Cell Dev Biol* **35**, 169-90 (2019)

40. Hermann, P.C., Huber, S.L., Herrler, T., Aicher, A., Ellwart, J.W., Guba, M., et al. Distinct populations of cancer stem cells determine tumor growth and metastatic activity in human pancreatic cancer. *Cell Stem Cell* **1**, 313-23 (2007)
41. Sormendi, S., Wielockx, B. Hypoxia Pathway Proteins As Central Mediators of Metabolism in the Tumor Cells and Their Microenvironment. *Front Immunol* **9**, 40 (2018)
42. Dieter, S.M., Ball, C.R., Hoffmann, C.M., Nowrouzi, A., Herbst, F., Zavidij, O., et al. Distinct types of tumor-initiating cells form human colon cancer tumors and metastases. *Cell Stem Cell* **9**, 357-65 (2011)
43. Netea-Maier, R.T., Smit, J.W.A., Netea, M.G. Metabolic changes in tumor cells and tumor-associated macrophages: A mutual relationship. *Cancer Lett* **413**, 102-9 (2018)
44. Kalluri, R., Weinberg, R.A. The basics of epithelial-mesenchymal transition. *J Clin Invest* **119**, 1420-8 (2009)
45. Micalizzi, D.S., Farabaugh, S.M., Ford, H.L. Epithelial-mesenchymal transition in cancer: parallels between normal development and tumor progression. *J Mammary Gland Biol Neoplasia* **15**, 117-34 (2010)
46. Lu, J., Guo, H., Treekitkarnmongkol, W., Li, P., Zhang, J., Shi, B., et al. 14-3-3zeta Cooperates with ErbB2 to promote ductal carcinoma in situ progression to invasive breast cancer by inducing epithelial-mesenchymal transition. *Cancer Cell* **16**, 195-207 (2009)
47. Lourenco, A.R., Ban, Y., Crowley, M.J., Lee, S.B., Ramchandani, D., Du, W., et al. Differential Contributions of Pre- and Post-EMT Tumor Cells in Breast Cancer Metastasis. *Cancer Research* **80**, 163-9 (2020)
48. Beerling, E., Seinstra, D., de Wit, E., Kester, L., van der Velden, D., Maynard, C., et al. Plasticity between Epithelial and Mesenchymal States Unlinks EMT from Metastasis-Enhancing Stem Cell Capacity. *Cell Rep* **14**, 2281-8 (2016)
49. Aiello, N.M., Brabletz, T., Kang, Y., Nieto, M.A., Weinberg, R.A., Stanger, B.Z. Upholding a role for EMT in pancreatic cancer metastasis. *Nature* **547**, E7-E8 (2017)
50. Krebs, A.M., Mitschke, J., Lasierra Losada, M., Schmalhofer, O., Boerries, M., Busch, H., et al. The EMT-activator Zeb1 is a key factor for cell plasticity and promotes metastasis in pancreatic cancer. *Nat Cell Biol* **19**, 518-29 (2017)
51. Ye, X., Brabletz, T., Kang, Y., Longmore, G.D., Nieto, M.A., Stanger, B.Z., et al. Upholding a role for EMT in breast cancer metastasis. *Nature* **547**, E1-E3 (2017)
52. Yang, J., Antin, P., Berx, G., Blanpain, C., Brabletz, T., Bronner, M., et al. Guidelines and definitions for research on epithelial–mesenchymal transition. *Nat Rev Mol Cell Biol* **21**, 341-52 (2020)
53. Cook, D.P., Vanderhyden, B.C. Context specificity of the EMT transcriptional response. *Nat Commun* **11**, 2142 (2020)
54. Jolly, M.K., Ware, K.E., Gilja, S., Somarelli, J.A., Levine, H. EMT and MET: necessary or permissive for metastasis? *Mol Oncol* **11**, 755-69 (2017)
55. Celia-Terrassa, T., Bastian, C., Liu, D.D., Ell, B., Aiello, N.M., Wei, Y., et al. Author Correction: Hysteresis control of epithelial-mesenchymal transition dynamics

conveys a distinct program with enhanced metastatic ability. *Nat Commun* **10**, 527 (2019)

56. Tsai, J.H., Donaher, J.L., Murphy, D.A., Chau, S., Yang, J. Spatiotemporal regulation of epithelial-mesenchymal transition is essential for squamous cell carcinoma metastasis. *Cancer Cell* **22**, 725-36 (2012)

57. Truong, H.H., Xiong, J., Ghotra, V.P., Nirmala, E., Haazen, L., Le Devedec, S.E., et al. beta1 integrin inhibition elicits a prometastatic switch through the TGFbeta-miR-200-ZEB network in E-cadherin-positive triple-negative breast cancer. *Sci Signal* **7**, ra15 (2014)

58. Del Pozo Martin, Y., Park, D., Ramachandran, A., Ombrato, L., Calvo, F., Chakravarty, P., et al. Mesenchymal Cancer Cell-Stroma Crosstalk Promotes Niche Activation, Epithelial Reversion, and Metastatic Colonization. *Cell Rep* **13**, 2456-69 (2015)

59. Kojima, Y., Acar, A., Eaton, E.N., Mellody, K.T., Scheel, C., Ben-Porath, I., et al. Autocrine TGF-beta and stromal cell-derived factor-1 (SDF-1) signaling drives the evolution of tumor-promoting mammary stromal myofibroblasts. *Proc Natl Acad Sci U S A* **107**, 20009-14 (2010)

60. Jung, Y., Kim, J.K., Shiozawa, Y., Wang, J., Mishra, A., Joseph, J., et al. Recruitment of mesenchymal stem cells into prostate tumours promotes metastasis. *Nat Commun* **4**, 1795 (2013)

61. Iwano, M., Plieth, D., Danoff, T.M., Xue, C., Okada, H., Neilson, E.G. Evidence that fibroblasts derive from epithelium during tissue fibrosis. *J Clin Invest* **110**, 341-50 (2002)

62. Zeisberg, E.M., Potenta, S., Xie, L., Zeisberg, M., Kalluri, R. Discovery of endothelial to mesenchymal transition as a source for carcinoma-associated fibroblasts. *Cancer Res* **67**, 10123-8 (2007)

63. Klymkowsky, M.W., Savagner, P. Epithelial-mesenchymal transition: a cancer researcher's conceptual friend and foe. *Am J Pathol* **174**, 1588-93 (2009)

64. Pastushenko, I., Brisebarre, A., Sifrim, A., Fioramonti, M., Revenco, T., Boumahdi, S., et al. Identification of the tumour transition states occurring during EMT. *Nature* **556**, 463-8 (2018)

65. Jordan, N.V., Johnson, G.L., Abell, A.N. Tracking the intermediate stages of epithelial-mesenchymal transition in epithelial stem cells and cancer. *Cell Cycle* **10**, 2865-73 (2011)

66. Pastushenko, I., Blanpain, C. EMT Transition States during Tumor Progression and Metastasis. *Trends Cell Biol* **29**, 212-26 (2019)

67. Padmanaban, V., Krol, I., Suhail, Y., Szczerba, B.M., Aceto, N., Bader, J.S., et al. E-cadherin is required for metastasis in multiple models of breast cancer. *Nature* **573**, 439-44 (2019)

68. Grosse-Wilde, A., Fouquier d'Herouel, A., McIntosh, E., Ertaylan, G., Skupin, A., Kuestner, R.E., et al. Stemness of the hybrid Epithelial/Mesenchymal State in Breast Cancer and Its Association with Poor Survival. *PLoS One* **10**, e0126522 (2015)

69. Bierie, B., Pierce, S.E., Kroeger, C., Stover, D.G., Pattabiraman, D.R., Thiru, P., et al. Integrin-beta4 identifies cancer stem cell-enriched populations of partially mesenchymal carcinoma cells. *Proc Natl Acad Sci U S A* **114**, E2337-E46 (2017)
70. Savagner, P. Epithelial-mesenchymal transitions: from cell plasticity to concept elasticity. *Curr Top Dev Biol* **112**, 273-300 (2015)
71. Olmeda, D., Moreno-Bueno, G., Flores, J.M., Fabra, A., Portillo, F., Cano, A. SNAI1 is required for tumor growth and lymph node metastasis of human breast carcinoma MDA-MB-231 cells. *Cancer Res* **67**, 11721-31 (2007)
72. Gibbons, D.L., Lin, W., Creighton, C.J., Rizvi, Z.H., Gregory, P.A., Goodall, G.J., et al. Contextual extracellular cues promote tumor cell EMT and metastasis by regulating miR-200 family expression. *Genes Dev* **23**, 2140-51 (2009)
73. De Craene, B., Denecker, G., Vermassen, P., Taminiau, J., Mauch, C., Derore, A., et al. Epidermal Snail expression drives skin cancer initiation and progression through enhanced cytoprotection, epidermal stem/progenitor cell expansion and enhanced metastatic potential. *Cell Death Differ* **21**, 310-20 (2014)
74. Strauss, R., Li, Z.Y., Liu, Y., Beyer, I., Persson, J., Sova, P., et al. Analysis of epithelial and mesenchymal markers in ovarian cancer reveals phenotypic heterogeneity and plasticity. *PLoS One* **6**, e16186 (2011)
75. Aiello, N.M., Maddipati, R., Norgard, R.J., Balli, D., Li, J., Yuan, S., et al. EMT Subtype Influences Epithelial Plasticity and Mode of Cell Migration. *Dev Cell* **45**, 681-95 e4 (2018)
76. Bocci, F., Tripathi, S.C., Vilchez Mercedes, S.A., George, J.T., Casabar, J.P., Wong, P.K., et al. NRF2 activates a partial epithelial-mesenchymal transition and is maximally present in a hybrid epithelial/mesenchymal phenotype. *Integrative Biology: Quantitative Biosciences From Nano To Macro* **11**, 251-63 (2019)
77. Oswald, L., Grosser, S., Smith, D.M., Kas, J.A. Jamming transitions in cancer. *J Phys D Appl Phys* **50**, 483001 (2017)
78. Malinverno, C., Corallino, S., Giavazzi, F., Bergert, M., Li, Q., Leoni, M., et al. Endocytic reawakening of motility in jammed epithelia. *Nat Mater* **16**, 587-96 (2017)
79. Sigismund, S., Scita, G. The 'endocytic matrix reloaded' and its impact on the plasticity of migratory strategies. *Curr Opin Cell Biol* **54**, 9-17 (2018)
80. Chepizhko, O., Lionetti, M.C., Malinverno, C., Giampietro, C., Scita, G., Zapperi, S., et al. From jamming to collective cell migration through a boundary induced transition. *Soft Matter* **14**, 3774-82 (2018)
81. Park, J.A., Kim, J.H., Bi, D., Mitchel, J.A., Qazvini, N.T., Tantisira, K., et al. Unjamming and cell shape in the asthmatic airway epithelium. *Nature Materials* **14**, 1040-8 (2015)
82. Kuriyama, S., Theveneau, E., Benedetto, A., Parsons, M., Tanaka, M., Charras, G., et al. In vivo collective cell migration requires an LPAR2-dependent increase in tissue fluidity. *J Cell Biol* **206**, 113-27 (2014)
83. Palamidessi, A., Malinverno, C., Frittoli, E., Corallino, S., Barbieri, E., Sigismund, S., et al. Unjamming overcomes kinetic and proliferation arrest in terminally differentiated cells and promotes collective motility of carcinoma. *Nat Mater* **18**, 1252-63 (2019)

84. Cheung, K.J., Padmanaban, V., Silvestri, V., Schipper, K., Cohen, J.D., Fairchild, A.N., et al. Polyclonal breast cancer metastases arise from collective dissemination of keratin 14-expressing tumor cell clusters. *Proc Natl Acad Sci U S A* **113**, E854-63 (2016)
85. Aceto, N., Bardia, A., Miyamoto, D.T., Donaldson, M.C., Wittner, B.S., Spencer, J.A., et al. Circulating tumor cell clusters are oligoclonal precursors of breast cancer metastasis. *Cell* **158**, 1110-22 (2014)
86. Kats-Ugurlu, G., Roodink, I., de Weijert, M., Tiemessen, D., Maass, C., Verrijp, K., et al. Circulating tumour tissue fragments in patients with pulmonary metastasis of clear cell renal cell carcinoma. *J Pathol* **219**, 287-93 (2009)
87. Hou, J.M., Krebs, M.G., Lancashire, L., Sloane, R., Backen, A., Swain, R.K., et al. Clinical significance and molecular characteristics of circulating tumor cells and circulating tumor microemboli in patients with small-cell lung cancer. *J Clin Oncol* **30**, 525-32 (2012)
88. Khoja, L., Shenjere, P., Hodgson, C., Hodgetts, J., Clack, G., Hughes, A., et al. Prevalence and heterogeneity of circulating tumour cells in metastatic cutaneous melanoma. *Melanoma Res* **24**, 40-6 (2014)
89. Yu, M., Bardia, A., Wittner, B.S., Stott, S.L., Smas, M.E., Ting, D.T., et al. Circulating breast tumor cells exhibit dynamic changes in epithelial and mesenchymal composition. *Science* **339**, 580-4 (2013)
90. Staneva, R., El Marjou, F., Barbazan, J., Krndija, D., Richon, S., Clark, A.G., et al. Cancer cells in the tumor core exhibit spatially coordinated migration patterns. *J Cell Sci* **132**, jcs220277 (2019)
91. Waclaw, B., Bozic, I., Pittman, M.E., Hruban, R.H., Vogelstein, B., Nowak, M.A. A spatial model predicts that dispersal and cell turnover limit intratumour heterogeneity. *Nature* **525**, 261-4 (2015)
92. Westcott, J.M., Prechtel, A.M., Maine, E.A., Dang, T.T., Esparza, M.A., Sun, H., et al. An epigenetically distinct breast cancer cell subpopulation promotes collective invasion. *J Clin Invest* **125**, 1927-43 (2015)
93. Cheung, K.J., Gabrielson, E., Werb, Z., Ewald, A.J. Collective invasion in breast cancer requires a conserved basal epithelial program. *Cell* **155**, 1639-51 (2013)
94. Gritsenko, P.G., Atlasy, N., Dieteren, C.E.J., Navis, A.C., Venhuizen, J.H., Veelken, C., et al. p120-catenin-dependent collective brain infiltration by glioma cell networks. *Nat Cell Biol* **22**, 97-107 (2020)
95. Friedl, P., Wolf, K. Plasticity of cell migration: a multiscale tuning model. *J Cell Biol* **188**, 11-9 (2010)
96. Haeger, A., Krause, M., Wolf, K., Friedl, P. Cell jamming: collective invasion of mesenchymal tumor cells imposed by tissue confinement. *Biochim Biophys Acta* **1840**, 2386-95 (2014)
97. Friedl, P., Alexander, S. Cancer invasion and the microenvironment: plasticity and reciprocity. *Cell* **147**, 992-1009 (2011)
98. Friedl, P., Gilmour, D. Collective cell migration in morphogenesis, regeneration and cancer. *Nat Rev Mol Cell Biol* **10**, 445-57 (2009)

99. Khalil, A.A., Friedl, P. Determinants of leader cells in collective cell migration. *Integr Biol (Camb)* **2**, 568-74 (2010)
100. Liu, L., Duclos, G., Sun, B., Lee, J., Wu, A., Kam, Y., et al. Minimization of thermodynamic costs in cancer cell invasion. *Proc Natl Acad Sci U S A* **110**, 1686-91 (2013)
101. Zhang, J., Goliwas, K.F., Wang, W., Taufalele, P.V., Bordeleau, F., Reinhart-King, C.A. Energetic regulation of coordinated leader-follower dynamics during collective invasion of breast cancer cells. *Proc Natl Acad Sci U S A* **116**, 7867-72 (2019)
102. Westcott, J.M., Prechtel, A.M., Maine, E.A., Dang, T.T., Esparza, M.A., Sun, H., et al. An epigenetically distinct breast cancer cell subpopulation promotes collective invasion. *J Clin Invest* **125**, 1927-43 (2015)
103. Ilina, O., Campanello, L., Gritsenko, P.G., Vullings, M., Wang, C., Bult, P., et al. Intravital microscopy of collective invasion plasticity in breast cancer. *Dis Model Mech* **11**, dmm034330 (2018)
104. Ilina, O., Gritsenko, G.P., Syga, S., Lippoldt, J., La Porta, A.M.C., Chepizhko, O., et al. Cell-cell adhesion and 3D matrix confinement determine jamming transitions in breast cancer invasion. *Nat Cell Biol*, (2020 (in press))
105. Kumar, S., Weaver, V.M. Mechanics, malignancy, and metastasis: the force journey of a tumor cell. *Cancer Metastasis Rev* **28**, 113-27 (2009)
106. Wei, S.C., Fattet, L., Tsai, J.H., Guo, Y., Pai, V.H., Majeski, H.E., et al. Matrix stiffness drives epithelial-mesenchymal transition and tumour metastasis through a TWIST1-G3BP2 mechanotransduction pathway. *Nat Cell Biol* **17**, 678-88 (2015)
107. Dong, Y., Zheng, Q., Wang, Z., Lin, X., You, Y., Wu, S., et al. Higher matrix stiffness as an independent initiator triggers epithelial-mesenchymal transition and facilitates HCC metastasis. *J Hematol Oncol* **12**, 112 (2019)
108. Matte, B.F., Kumar, A., Placone, J.K., Zanella, V.G., Martins, M.D., Engler, A.J., et al. Matrix stiffness mechanically conditions EMT and migratory behavior of oral squamous cell carcinoma. *J Cell Sci* **132**, jcs224360 (2019)
109. Kumar, S., Das, A., Sen, S. Extracellular matrix density promotes EMT by weakening cell-cell adhesions. *Mol Biosyst* **10**, 838-50 (2014)
110. Ondeck, M.G., Kumar, A., Placone, J.K., Plunkett, C.M., Matte, B.F., Wong, K.C., et al. Dynamically stiffened matrix promotes malignant transformation of mammary epithelial cells via collective mechanical signaling. *Proc Natl Acad Sci U S A* **116**, 3502-7 (2019)
111. Leight, J.L., Wozniak, M.A., Chen, S., Lynch, M.L., Chen, C.S. Matrix rigidity regulates a switch between TGF- $\beta$ 1-induced apoptosis and epithelial-mesenchymal transition. *Mol Biol Cell* **23**, 781-91 (2012)
112. Warren, J.S.A., Xiao, Y., Lamar, J.M. YAP/TAZ Activation as a Target for Treating Metastatic Cancer. *Cancers (Basel)* **10**, 115 (2018)
113. Dupont, S., Morsut, L., Aragona, M., Enzo, E., Giulitti, S., Cordenonsi, M., et al. Role of YAP/TAZ in mechanotransduction. *Nature* **474**, 179-83 (2011)
114. Casas, E., Kim, J., Bendesky, A., Ohno-Machado, L., Wolfe, C.J., Yang, J. Snail2 is an essential mediator of Twist1-induced epithelial mesenchymal transition and metastasis. *Cancer Research* **71**, 245-54 (2011)



115. Noguchi, S., Saito, A., Nagase, T. YAP/TAZ Signaling as a Molecular Link between Fibrosis and Cancer. *International Journal of Molecular Sciences* **19**, 3674 (2018)
116. Jolly, M.K., Preca, B.-T., Tripathi, S.C., Jia, D., George, J.T., Hanash, S.M., et al. Interconnected feedback loops among ESRP1, HAS2, and CD44 regulate epithelial-mesenchymal plasticity in cancer. *APL Bioeng* **2**, 031908- (2018)
117. Nasrollahi, S., Walter, C., Loza, A.J., Schimizzi, G.V., Longmore, G.D., Pathak, A. Past matrix stiffness primes epithelial cells and regulates their future collective migration through a mechanical memory. *Biomaterials* **146**, 146-55 (2017)
118. Mathur, J., Shenoy, V.B., Pathak, A. Mechanical memory in cells emerges from mechanotransduction with transcriptional feedback and epigenetic plasticity. *bioRxiv*, 2020.03.20.000802 (2020)
119. Levental, K.R., Yu, H., Kass, L., Lakins, J.N., Egeblad, M., Erler, J.T., et al. Matrix crosslinking forces tumor progression by enhancing integrin signaling. *Cell* **139**, 891-906 (2009)
120. Alibert, C., Goud, B., Manneville, J.B. Are cancer cells really softer than normal cells? *Biol Cell* **109**, 167-89 (2017)
121. Yu, H., Mouw, J.K., Weaver, V.M. Forcing form and function: biomechanical regulation of tumor evolution. *Trends Cell Biol* **21**, 47-56 (2011)
122. Osborne, L.D., Li, G.Z., How, T., O'Brien, E.T., Blobe, G.C., Superfine, R., et al. TGF- $\beta$  regulates LARG and GEF-H1 during EMT to affect stiffening response to force and cell invasion. *Mol Biol Cell* **25**, 3528-40 (2014)
123. Chen, Y.-Q., Lan, H.-Y., Wu, Y.-C., Yang, W.-H., Chiou, A., Yang, M.-H. Epithelial-mesenchymal transition softens head and neck cancer cells to facilitate migration in 3D environments. *J Cell Mol Med* **22**, 3837-46 (2018)
124. Kechagia, J.Z., Ivaska, J., Roca-Cusachs, P. Integrins as biomechanical sensors of the microenvironment. *Nat Rev Mol Cell Biol* **20**, 457-73 (2019)
125. Davidson, P.M., Denais, C., Bakshi, M.C., Lammerding, J. Nuclear deformability constitutes a rate-limiting step during cell migration in 3-D environments. *Cell Mol Bioeng* **7**, 293-306 (2014)
126. Wolf, K., Te Lindert, M., Krause, M., Alexander, S., Te Riet, J., Willis, A.L., et al. Physical limits of cell migration: control by ECM space and nuclear deformation and tuning by proteolysis and traction force. *J Cell Biol* **201**, 1069-84 (2013)
127. Denais, C.M., Gilbert, R.M., Isermann, P., McGregor, A.L., te Lindert, M., Weigel, B., et al. Nuclear envelope rupture and repair during cancer cell migration. *Science* **352**, 353-8 (2016)
128. Harada, T., Swift, J., Irianto, J., Shin, J.W., Spinler, K.R., Athirasala, A., et al. Nuclear lamin stiffness is a barrier to 3D migration, but softness can limit survival. *J Cell Biol* **204**, 669-82 (2014)
129. van Helvert, S., Storm, C., Friedl, P. Mechanoreciprocity in cell migration. *Nat Cell Biol* **20**, 8-20 (2018)
130. Mitschke, J., Burk, U.C., Reinheckel, T. The role of proteases in epithelial-to-mesenchymal cell transitions in cancer. *Cancer Metastasis Rev* **38**, 431-44 (2019)

131. Artym, V.V., Swatkoski, S., Matsumoto, K., Campbell, C.B., Petrie, R.J., Dimitriadis, E.K., et al. Dense fibrillar collagen is a potent inducer of invadopodia via a specific signaling network. *J Cell Biol* **208**, 331-50 (2015)
132. Juin, A., Billottet, C., Moreau, V., Destaing, O., Albiges-Rizo, C., Rosenbaum, J., et al. Physiological type I collagen organization induces the formation of a novel class of linear invadosomes. *Mol Biol Cell* **23**, 297-309 (2012)
133. Eckert, M.A., Lwin, T.M., Chang, A.T., Kim, J., Danis, E., Ohno-Machado, L., et al. Twist1-induced invadopodia formation promotes tumor metastasis. *Cancer Cell* **19**, 372-86 (2011)
134. Sundararajan, V., Gengenbacher, N., Stemmler, M.P., Kleemann, J.A., Brabletz, T., Brabletz, S. The ZEB1/miR-200c feedback loop regulates invasion via actin interacting proteins MYLK and TKS5. *Oncotarget* **6**, 27083-96 (2015)
135. Peng, D.H., Ungewiss, C., Tong, P., Byers, L.A., Wang, J., Canales, J.R., et al. ZEB1 induces LOXL2-mediated collagen stabilization and deposition in the extracellular matrix to drive lung cancer invasion and metastasis. *Oncogene* **36**, 1925-38 (2017)
136. Cao, C., Lin, S., Zhi, W., Lazare, C., Meng, Y., Wu, P., et al. LOXL2 Expression Status Is Correlated With Molecular Characterizations of Cervical Carcinoma and Associated With Poor Cancer Survival via Epithelial-Mesenchymal Transition (EMT) Phenotype. *Front Oncol* **10**, 284 (2020)
137. Hamidi, H., Ivaska, J. Every step of the way: integrins in cancer progression and metastasis. *Nat Rev Cancer* **18**, 533-48 (2018)
138. Xiong, J., Balcioglu, H.E., Danen, E.H. Integrin signaling in control of tumor growth and progression. *Int J Biochem Cell Biol* **45**, 1012-5 (2013)
139. Strouhalova, K., Prechova, M., Gandalovicova, A., Brabek, J., Gregor, M., Rosel, D. Vimentin Intermediate Filaments as Potential Target for Cancer Treatment. *Cancers (Basel)* **12**, 184 (2020)
140. Rodriguez-Hernandez, I., Cantelli, G., Bruce, F., Sanz-Moreno, V. Rho, ROCK and actomyosin contractility in metastasis as drug targets. *F1000Res* **5**, F1000 Faculty Rev-783 (2016)
141. Jiang, H., Hegde, S., Knolhoff, B.L., Zhu, Y., Herndon, J.M., Meyer, M.A., et al. Targeting focal adhesion kinase renders pancreatic cancers responsive to checkpoint immunotherapy. *Nat Med* **22**, 851-60 (2016)
142. Özdemir, B.C., Pentcheva-Hoang, T., Carstens, J.L., Zheng, X., Wu, C.-C., Simpson, T.R., et al. Depletion of carcinoma-associated fibroblasts and fibrosis induces immunosuppression and accelerates pancreas cancer with reduced survival. *Cancer Cell* **25**, 719-34 (2014)
143. Neuzillet, C., Tijeras-Raballand, A., Ragulan, C., Cros, J., Patil, Y., Martinet, M., et al. Inter- and intra-tumoural heterogeneity in cancer-associated fibroblasts of human pancreatic ductal adenocarcinoma. *J Pathol* **248**, 51-65 (2019)
144. Ohlund, D., Handly-Santana, A., Biffi, G., Elyada, E., Almeida, A.S., Ponz-Sarvisé, M., et al. Distinct populations of inflammatory fibroblasts and myofibroblasts in pancreatic cancer. *J Exp Med* **214**, 579-96 (2017)

145. Jolly, M.K., Somarelli, J.A., Sheth, M., Biddle, A., Tripathi, S.C., Armstrong, A.J., et al. Hybrid epithelial/mesenchymal phenotypes promote metastasis and therapy resistance across carcinomas. *Pharmacol Ther* **194**, 161-84 (2019)
146. Hari, K., Sabuwala, B., Subramani, B.V., La Porta, C.A.M., Zapperi, S., Font-Clos, F., et al. Identifying inhibitors of epithelial-mesenchymal plasticity using a network topology-based approach. *NPJ Syst Biol Appl* **6**, 15 (2020)
147. Bocci, F., Jolly, M.K., Tripathi, S.C., Aguilar, M., Hanash, S.M., Levine, H., et al. Numb prevents a complete epithelial-mesenchymal transition by modulating Notch signalling. *J R Soc Interface* **14**, 20170512 (2017)
148. Jolly, M.K., Tripathi, S.C., Jia, D., Mooney, S.M., Celiktaş, M., Hanash, S.M., et al. Stability of the hybrid epithelial/mesenchymal phenotype. *Oncotarget* **7**, 27067-84 (2016)
149. Kröger, C., Afeyan, A., Mraz, J., Eaton, E.N., Reinhardt, F., Khodor, Y.L., et al. Acquisition of a hybrid E/M state is essential for tumorigenicity of basal breast cancer cells. *Proc Natl Acad Sci U S A* **116**, 7353-62 (2019)
150. Ishay-Ronen, D., Diepenbruck, M., Kalathur, R.K.R., Sugiyama, N., Tiede, S., Ivanek, R., et al. Gain Fat - Lose Metastasis: Converting Invasive Breast Cancer Cells into Adipocytes Inhibits Cancer Metastasis. *Cancer Cell* **35**, 17-32.e6 (2019)



# Chapter 3

---

## GRHL2-controlled gene expression networks in luminal breast cancer

Published in: Zi Wang<sup>1</sup>, Bircan Coban<sup>1</sup>, Haoyu Wu<sup>2</sup>, Jihed Chouaref<sup>2</sup>, Lucia Daxinger<sup>2</sup>, Michelle T Paulsen<sup>3</sup>, Mats Ljungman<sup>3</sup>, Marcel Smid<sup>4</sup>, John W.M. Martens<sup>4</sup>, Erik HJ Danen<sup>1,5</sup>. GRHL2-controlled gene expression networks in luminal breast cancer. *Cell Commun Signal*. 2023 Jan 23;21(1):15.

<sup>1</sup>Leiden Academic Center for Drug Research, Leiden University, Leiden, The Netherlands; <sup>2</sup>Department of Human Genetics, Leiden University Medical Centre, Leiden, The Netherlands; <sup>3</sup>Departments of Radiation Oncology and Environmental Health Sciences, University of Michigan Medical School, Ann Arbor, MI, USA; <sup>4</sup>Department of Medical Oncology, Erasmus MC Cancer Institute, Erasmus University Medical Center, Rotterdam, The Netherlands; <sup>5</sup>correspondence to Erik HJ Danen, [e.danen@lacdr.leidenuniv.nl](mailto:e.danen@lacdr.leidenuniv.nl)

### Abstract

Grainyhead like 2 (GRHL2) is an essential transcription factor for development and function of epithelial tissues. It has dual roles in cancer by supporting tumor growth while suppressing epithelial to mesenchymal transitions (EMT). GRHL2 cooperates with androgen (AR) and estrogen receptors (ER) to regulate gene expression. We explore genome wide GRHL2 binding sites conserved in three ER $\alpha$ /GRHL2 positive luminal breast cancer cell lines by ChIP-Seq. Interaction with the ER $\alpha$ /FOXA1/GATA3 complex is observed, however, only for a minor fraction of conserved GRHL2 peaks. We determine genome wide transcriptional dynamics in response to loss of GRHL2 by nascent RNA Bru-seq using an MCF7 conditional knockout model. Integration of ChIP- and Bru-seq pinpoints candidate direct GRHL2 target genes in luminal breast cancer. Multiple connections between GRHL2 and proliferation are uncovered, including transcriptional activation of ETS and E2F transcription factors. Among EMT-related genes, direct regulation of CLDN4 is corroborated but several targets identified in other cells (including *CDH1* and *ZEB1*) are ruled out by both ChIP- and Bru-seq as being directly controlled by GRHL2 in luminal breast cancer cells. Gene clusters correlating positively (including known GRHL2 targets such as *ErbB3*, *CLDN4/7*) or negatively (including *TGFB1* and *TGFB2*) with GRHL2 in the MCF7 knockout model, display similar correlation with GRHL2 in ER positive as well as ER negative breast cancer patients. Altogether, this study uncovers gene sets regulated directly or indirectly by GRHL2 in luminal breast cancer, identifies novel GRHL2-regulated genes, and points to distinct GRHL2 regulation of EMT in luminal breast cancer cells.

### Keywords

Breast cancer, luminal, GRHL2, CHIP-seq, BRU-seq, transcription, gene regulation

### Background

The *Grh* gene was discovered in *Drosophila* and its mammalian homologs have three members (*GRHL1*, *GRHL2* and *GRHL3*) [1]. Mice lacking GRHL1, 2, or 3 display neural tube closure defects and a variety of defects in epithelia

of several organs with disruption of epithelial adhesion complexes as a major common event [2-7]. GRHLs support expression of genes encoding key epithelial cell-cell junction proteins in desmosomes, adherens junctions, and tight junctions as well as targets involved in cytoskeletal regulation, membrane trafficking, and guidance cues. Several of these genes have been identified as direct GRHL transcriptional targets [3, 4, 8-15]. ChIP-seq in placenta, kidney, and lung epithelial cells has revealed >5000 GRHL2 binding peaks [11, 14, 15]. GRHL2 depletion in these same tissues identified a few hundred to a thousand genes whose expression was altered. Notably, i) overlap between these different tissues with respect to GRHL2 binding peaks and candidate target genes is limited pointing to common and tissue specific functions of GRHL2 and ii) for many of the GRHL2 target genes regulation appears indirect, which may involve GRHL2-regulated expression of other transcription factors or epigenetic modifiers [16, 17].

*GRHL2* is located on chromosome 8q22 that is frequently amplified in many cancers, including breast cancer, colorectal cancer and oral squamous cell carcinoma [18-20]. GRHL2 acts as an activator or suppressor of target gene transcription by interacting with promotor and enhancer regions in competition or in cooperation with other transcription factors and epigenetic regulators [2]. GRHL2 may enhance proliferation, replicative potential, and evasion of cell death through activation of the *ErbB3* gene, epigenetically promoting expression of *hTERT*, and suppressing death receptor expression [9, 18, 19]. Indeed, GRHL2 expression was negatively correlated with metastasis-free survival in breast cancer patients [21, 22]. By contrast, others have reported that high GRHL2 expression in breast cancer cell lines is associated with sensitivity to anoikis and chemotherapy and reduced tumor initiation capacity [23, 24].

Loss of GRHL2 was reported in gastric cancer and GRHL2 was found down-regulated at the invasive front of breast cancers and loss of GRHL2 expression in primary breast cancers correlated with lymph node metastasis [9, 25]. A key mechanism by which GRHL2 may suppress aspects of tumor progression is through inhibition of epithelial-to-mesenchymal transition

(EMT). GRHL2 acts in a double negative feedback loop with ZEB1 and it activates the expression of miR-200s that, in turn, are in a double negative feedback loop with ZEBs, thereby enforcing the epithelial phenotype [9, 17, 23, 24, 26, 27]. The roles of GRHL2 may be tumor type- and stage-specific through regulating different target genes in different cancers [28].

Breast cancer represents a heterogeneous disease with multiple clinically relevant subtypes appearing to originate from luminal or basal epithelial cells in the duct [29-31]. The luminal subtype accounts for the majority of breast cancer cases and can be treated by therapies targeting estrogen receptor alpha (ER $\alpha$ ) signaling [32]. Recent studies have shown that GRHL2 cooperates with androgen receptor in prostate cancer [33] and with ER $\alpha$  in breast cancer. Like FOXA1, GRHL2 may act as a pioneer factor, promoting chromatin accessibility and GRHL2 has been found to co-occupy enhancer elements with FOXA1, GATA3, and ER $\alpha$  to regulate ER $\alpha$  signaling output in hormone receptor positive breast cancer [34-37].

In this study, we identify genomic binding sites of GRHL2 shared among 3 luminal breast cancer cell lines and find that only a small subset of these GRHL2 peaks is associated with ER binding sites. We integrate this ChIP-seq data with Bru-seq analysis of genes showing transcriptional responses at different time points after conditional GRHL2 knockout in MCF7 cells. For genes showing sustained up- or downregulation in response to GRHL2 deletion, we explore correlations with GRHL2 expression in breast cancer patients. Our findings reveal gene sets regulated directly or indirectly by GRHL2 in luminal breast cancer that partly overlap but also appear markedly distinct from targets identified in other tissues.

## Methods

### Cell lines and plasmids

Human breast cancer cell lines representing the luminal subtype (MCF7, T47D and BT474) were obtained from the American Type Culture Collection. The Hs578T human basal-B breast cancer cell line served as a GRHL2-negative control. Cells were cultured in RPMI1640 medium with 10% fetal bovine



serum, 25 U/mL penicillin and 25 µg/mL streptomycin in the incubator (37°C, 5% CO<sub>2</sub>). For production of lentiviral particles, VSV, GAG, REV and Cas9 or single guide (sg) RNA plasmids were transfected into HEK293 cells using Polyethylenimine (PEI). After 2 days, lentiviral particles were harvested and filtered. Conditional Cas9 cells were generated by infecting parental cells with lentiviral particles expressing the Edit-R Tre3G promotor-driven Cas9 (Dharmacon) and selected by blasticidin. Limited dilution was used to generate Cas9 monoclonal cells. Subsequently, Cas9-monoclonal cells were transduced with U6-gRNA:hPGK-puro-2A-tBFP control non-targeting sgRNAs or GRHL2-specific sgRNAs (Sigma) and selected by puromycin. The EHF plasmid was kindly provided by Dr. Giuseppina Carbone, Institute of Oncology Research, Bellinzona, Switzerland and described previously [38, 39]. The EHF plasmid was transfected into cells using Lipofectamin 2000 according to a protocol provided by the manufacturer.

### Western blot

Cells were lysed by radioimmunoprecipitation (RIPA) buffer (150 mM NaCl, 1% Triton X-100, 0.5% sodium deoxycholate and 0.1% Tris and 1% protease cocktail inhibitor (Sigma-Aldrich. P8340)). Lysates were sonicated and protein concentration was determined by bicinchoninic acid (BCA) assay. Cell lysates were mixed with protein loading buffer, separated by SDS-PAGE, and transferred to a methanol-activated polyvinylidene difluoride (PVDF) membrane (Milipore, The Netherlands). The membrane was blocked with 5% bovine serum albumin (BSA; Sigma-Aldrich) for 1 hour at room temperature (RT). Next, membranes were stained with primary antibody overnight at 4°C and HRP-conjugated secondary antibodies for half hour at room temperature (RT). After staining with Prime ECL Detection Reagent (GE Healthcare Life science), chemoluminescence was detected with an Amersham Imager 600 (GE Healthcare Life science, The Netherlands). The following antibodies were used: GRHL2 (Atlas-Antibodies, hpa004820) Cas9 (Cell Signaling, 14697), and GAPDH (SantaCruz, sc-32233).

### ChIP-seq

Cells were grown in RPMI-1640 complete, serum-containing medium. Cross-linking was performed by 1% formaldehyde for 10 minutes at room temperature (RT). Then 1M glycine (141  $\mu$ l of 1M glycine for 1 ml of medium) was used to quench for 5 minutes at RT. Cells were washed twice with ice-cold PBS containing 5  $\mu$ l/ml phenylmethylsulfonyl fluoride (PMSF). Cells were harvested by centrifugation (2095 g for 5 minutes at 4°C) and lysed with NP40 buffer (150 mM NaCl, 50mM Tris-HCl, 5mM EDTA, 0.5% NP40, 1% Triton X-100) containing 0.1% SDS, 0.5% sodium deoxycholate and protease inhibitor cocktail (EDTA-free Protease Inhibitor Cocktail, Sigma). Chromatin was sonicated to an average size of 300 bp (**Fig. S1**). GRHL2-bound chromatin fragments were immunoprecipitated with anti-GRHL2 antibody (Sigma; HPA004820). Precipitates were washed by NP buffer, low salt (0.1% SDS, 1% Triton X-100, 2mM EDTA, 20mM Tris-HCl (pH 8.1), 150mM NaCl), high salt (0.1% SDS, 1% Triton X-100, 2mM EDTA, 20mM Tris-HCl (pH 8.1), 500mM NaCl) and LiCl buffer (0.25M LiCl, 1%NP40, 1% deoxycholate, 1mM EDTA, 10mM Tris-HCl (pH 8.1)). Chromatin was de-crosslinked by 1% SDS at 65°C. DNA was purified by Phenol:Chloroform:Isoamyl Alcohol (PCI) and then diluted in TE buffer.

In order to examine the quality of our samples before sequencing, ChIP-qPCR (quantitative polymerase chain reaction) was performed to validate interaction of GRHL2 with the promoter region of Claudin-4 (*CLDN4*), a known direct target gene of GRHL2 [4]. The results confirmed the GRHL2 binding site around the *CLDN4* promoter (**Fig. S2**). The following primers were used for ChIP-qPCR: *CLDN4* forward: gtgacctcagcatgggctttga, *CLDN4* reverse: ctctctctgaccagtttctctg, Control (an intergenic region upstream of the *GAPDH* locus) forward: atgggtgccactggggatct, Control reverse: tgccaaagcctagggaaga, *ZEB1* promoter<sup>#</sup> forward: cggtccttagcaacaagggtt, *ZEB1* promoter<sup>#</sup> reverse: tcgcttggtctaaatgctcg. *ZEB1*<sup>##</sup> forward: gccgccgagcctccaacttt, *ZEB1*<sup>##</sup> reverse: tgctagggacggggcggttt, *OVOL2* exon forward: ccttaaactcgcgagtgaagacc, *OVOL2* exon reverse: gtagcgagcttggtgacacc, *CDH1* intron forward: gtatgaacggcaagcctctg, *CDH1* intron reverse: caaggagaccaggaagagaa. ChIP-qPCR data were collected and analyzed using the  $2^{-\Delta\Delta Ct}$  method [40].

For ChIP-seq, library preparation and paired-end (151bp) sequencing were performed by GenomeScan (Leiden, The Netherlands). MCF7, T47D and BT474 had 87393758, 84633440, and 82080866 pair-end reads, respectively.

### ChIP-seq analysis

Less than 5% of adapter sequences were present, and the mean per base sequence quality was >30, indicating high quality reads and no requirement for adapter-trimming (**Fig. S3, S4**). Paired-end reads were mapped to the human reference genome (hg38) using BWA-MEM [41] with default parameters. Over 93% of total reads were mapped to the human genome in T47D and MCF7 and 57.3% in BT474. Phred quality score (Q score) was used to measure base calling accuracy [42]. Q>30 scores (corresponding to a 0.1% error rate [43]) were >86% in T47D and MCF7 and 48.6% in BT474. Reads with low mapping quality ( $\leq Q30$ ) were filtered out. MACS version 2.1.0 [44] was used for peak calling by default settings. The q value was adjusted to 0.1 for BT474 cell line to avoid loss of peaks. The `annotatePeaks` and `MergePeaks` functions from HOMER [45] were used to annotate and overlap peaks, respectively. ChIPseeker was used for the analysis of ChIP-seq peaks coverage plot and the density profile of GRHL2 binding sites [46]. Motif analysis was performed using ChIP-seq peaks with high scores by the MEME-ChIP program with default settings. ChIP-seq data was visualized by the UCSC genome browser. To analyze coverage of GRHL2 peaks at consensus motifs for GRHL2, ER $\alpha$ , FOXA1, and GATA3 binding, the JASPAR 2022 database was used to identify motifs [47]. To analyze colocalization of our GRHL2 binding events with published ER $\alpha$  peaks in luminal breast cancer cells, ChIP-seq data files from a study mapping ER $\alpha$  binding sites in MCF7, BT474, and T47D [48] were intersected using bedtools (v2.3.0) [PMID: 20110278] and ChIP-seq data files from two different studies mapping ER-alpha binding sites in MCF7 were intersected [49, 50].

### Bru-seq

MCF7 cells expressing inducible Cas9 and control non-targeting sgRNAs or GRHL2-specific sgRNAs were exposed to 1  $\mu$ g/ml doxycycline. At different timepoints after doxycycline-induced deletion of GRHL2, cells were

## Chapter 3

---

incubated with a final concentration of 2 mM Bru at 37°C for 30 minutes. Cells were lysed in TRIzol reagent (Sigma) and Bru-labelled nascent RNA was isolated using an anti-BrdU antibody conjugated to magnetic beads [51]. Subsequently, cDNA libraries were generated using the Illumina TruSeq library kit and sequenced using the Illumina NovaSeq 6000 Sequencing System. Sequence reads were strand-specific, paired-ended with read lengths of ~150 nucleotides. Reads were pre-mapped to the ribosomal RNA (rRNA) repeating unit (GenBank U13369.1) and the mitochondrial and EBV genomes (from the hg38 analysis set) using Bowtie2 (2.3.3). Unaligned reads were subsequently mapped to human genome build hg38/GRCh38 using STAR (v 2.5.3a) and a STAR index created from GENCODE annotation version 27 [51, 52].

### Bru-seq analysis

To identify GRHL2-regulated genes, an inter-sample comparison analysis was performed comparing RPKM (reads per kilobase per million mapped reads) for each gene in the doxycycline-treated samples compared to the untreated sample, to obtain fold-change (FC) and *p* values. Genes with  $p < 0.05$  and  $FC > 2$  or  $FC < 0.5$  in any of the doxycycline-treated samples relative to untreated cells were filtered. Subsequently, genes responding to Cas9 induction in the context of both GRHL2 sgRNAs were selected and genes responding also in the context of control sgRNA were eliminated from this list. A heatmap was generated by R. The function “fviz\_nbclust()” from the R package “factorextra” was used to determine and visualize the optimal numbers of clusters using the method “within cluster sums of square”. The graph is attached. The STRING database (version 11.5) was used to assign protein interaction networks to Bru-seq data [53].

### Breast cancer patient mRNA expression data analysis

A compendium microarray dataset, all Affymetrix U133a, was used, containing RNA expression data of primary tumors of 867 untreated, lymph node negative patients (MA-867 dataset [59]; publicly available at [GSE2034](#), [GSE5327](#), [GSE2990](#), [GSE7390](#) and [GSE11121](#)). Raw .cel files were downloaded, processed with fRMA and batch effects were corrected using ComBat.

RNAseq data retrieved from the Molecular Taxonomy of Breast Cancer International Consortium (METABRIC) data set [54, 55] was used consisting of targeted sequencing data of 1904 primary breast tumors with matched normal tissues. Data visualization and calculation of co-expression z-scores were performed using cBioPortal (<https://www.cbioportal.org/>).

### SRB assay

For Sulforhodamine B (SRB) assays, cells were seeded into 96-well plates. At indicated time points, cells were fixed with 50% Trichloroacetic acid (TCA, Sigma-Aldrich) for 1 hour at 4 °C and then plates were washed with demineralized water four times and air-dried at RT. Subsequently, 0.4% SRB (60 µl/well) was added and kept for at least 2 hours at RT. The plates were washed five times with 1% acetic acid and air-dried. 10 mM (150 µl/well) Tris was added and kept for half hour at RT with gentle shaking. The absorbance value was measured by a plate-reader Fluostar OPTIMA.

## Results

### Genome-wide identification of GRHL2 binding sites in luminal breast cancer cells

To identify GRHL2 binding sites, ChIP-seq was performed in the human luminal breast cancer cell lines, MCF7, T47D and BT474. As a quality control of the ChIP samples, ChIP-qPCR confirmed the interaction of GRHL2 with the promoter region of *CLDN4*, a known direct target gene of GRHL2 [4] in all three luminal, GRHL2-positive cell lines but not in the GRHL2-negative Hs578T human basal-B breast cancer cell line (**Fig. S2**). Subsequently, ChIP-seq was performed and the coverage of peak regions across chromosomes was analyzed [46]. In each sample, GRHL2 was associated with all chromosomes (**Fig. S5**).

GRHL2 binding sites were mainly located in intergenic regions and introns, with ~3-5% of the peaks located in -1000 bp to +100 bp promoter regions (**Fig. 1a**). Analysis of read count frequency and density profiling of GRHL2 binding sites within -6000 bp to +6000 bp of the transcription start site (TSS)

# Chapter 3

showed no enrichment around the TSS (**Fig. 1b**). Intersection of the data in the 3 cell lines identified 6527 conserved GRHL2 binding sites in luminal breast cancer cells. Of these, 238 binding sites located in the -1000 bp to +100 bp regions, representing candidate interactions for direct GRHL2-mediated regulation of gene promoter activity (**Fig. 1c; Table S1**).

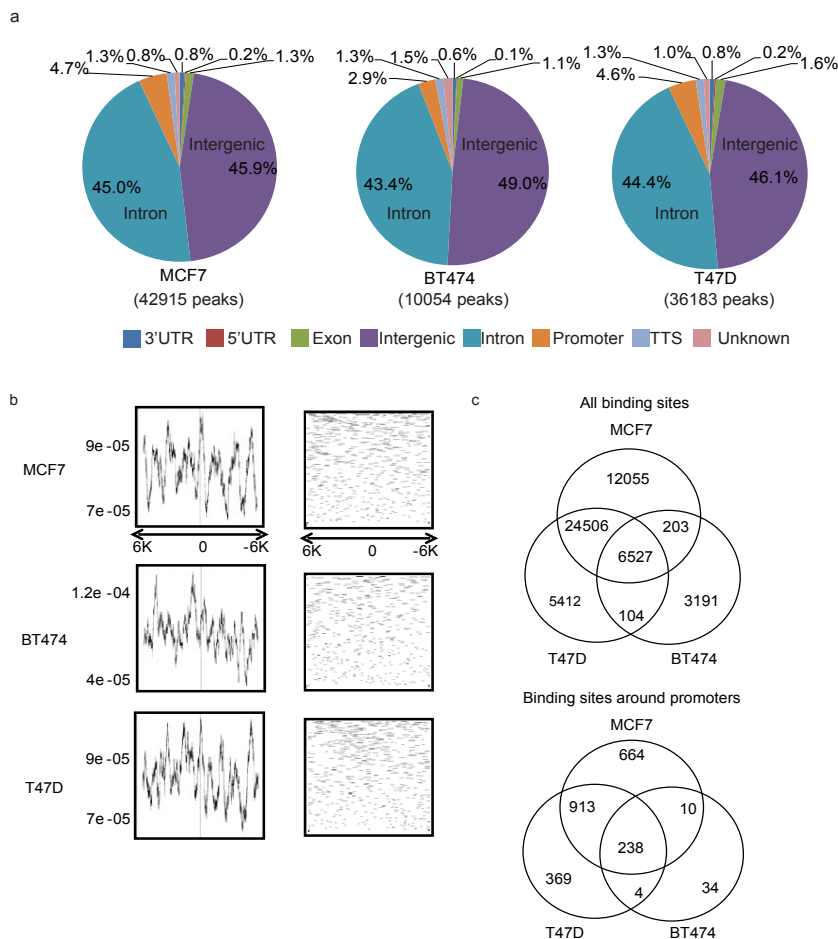


**Fig. 1. GRHL2 ChIP-seq in luminal breast cancer cells. (a)** Percentage of GRHL2 binding sites found at promoter regions, 5' untranslated regions (UTRs), 3' UTRs, exons, introns, intergenic regions, transcription termination sites (TTSs) and

unknown regions in the indicated luminal breast cancer cell lines. Promoter regions are defined as -1000 bp to +100 bp from the transcription start sites (TSS). **(b)** Read count frequency and density profile of GRHL2 binding sites within -6000 bp to +6000 bp of the TSS. Left panels show GRHL2 ChIP-seq read count frequencies in indicated cell lines (Y axis, read count frequency; X axis, genomic region). Right panels show density of ChIP-seq reads for GRHL2 binding sites in the indicated cell lines. **(c)** Venn diagrams showing overlap of GRHL2 binding sites among the three indicated cell lines. Top panel shows overlap for all peaks. Bottom panel shows overlap for peaks within the -1000 to +100 promoter region.

### **A small proportion of GRHL2 peaks is associated with ER $\alpha$ binding**

MEME-ChIP identified 3 GRHL2 binding motifs low *E* values in each cell line (**Fig. 2a**), whose core binding site matched previously published motifs [14, 15, 17, 56]. Based on the published interaction of GRHL2 with ER $\alpha$ , FOXA1, and GATA3 at enhancer elements of target genes [34-36, 57], we addressed to what extent the identified conserved GRHL2 binding sites in luminal breast cancer cells were flanked by putative binding sites for the ER $\alpha$ -mediated transcriptional complex. Heatmap visualization showed concentration of the GRHL2 peaks at the consensus GRHL2 motif [AACCGGTT] as expected (**Fig. 2b**). GRHL2 peaks showed only a weak trace for ER $\alpha$  [AGGTCAnnnTGACCT] and a barely detectable trace for the FOXA1 motif [TGTTT(A/G)C], and no concentration of the GATA3-binding motif [A/T]GATA(A/G) was observed. Indeed, among the shared GRHL2 peaks in luminal breast cancer cells ~5% was flanked by an ER $\alpha$  binding motif within +/- 1000bp (**Fig. 2c**).

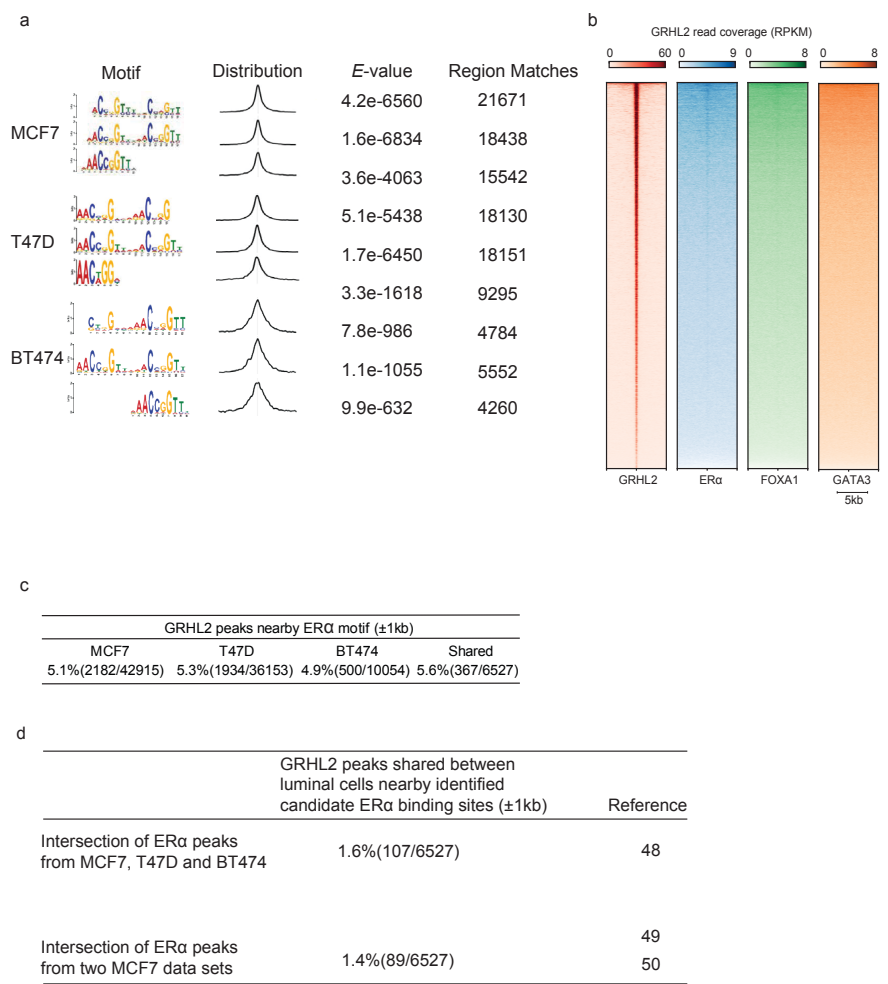


**Fig. 2. Association of GRHL2 motif with ER transcriptional complex in luminal breast cancer cells. (a)** DNA-binding motif of GRHL2 in luminal breast cancer. From left to right, the first panel shows the identified motifs in the indicated cell lines. The second panel shows distribution of the best matches to the motif in the sequences. The third panel shows the *E*-value, representing the significance of the motif according to the motif discovery. The last panel shows the number of regions that match the corresponding motif. **(b)** Heatmaps showing the coverage of identified GRHL2 peaks shared between MCF7, BT474 and T47D at GRHL2 motifs



(red) (n=20766), ER $\alpha$  motifs (blue) (n=76564), FOXA1 motifs (Green) (n=88923) and GATA3 motifs (Orange) (n=93403). Note that the read coverage scale differs for the different heatmaps. **(c)** Table indicating the occurrence of ER $\alpha$  consensus motif in a region spanning 1000bp up- and downstream of all GRHL2 peaks either identified in the indicated cell lines (left 3 columns) or shared between the indicated cell lines (right column). **(d)** Table indicating the occurrence of published ER $\alpha$  binding events in a region spanning 1000bp up- and downstream of all GRHL2 peaks shared between MCF7, BT474 and T47D (upper row) or shared between 2 MCF7 datasets (bottom row).

To further address colocalization of GRHL2 and ER $\alpha$  binding in luminal breast cancer, regions flanking +/- 1000bp of the conserved GRHL2 peaks in MCF7, BT474, and T47D were interrogated for the presence of previously reported ER $\alpha$  binding events. For this purpose, ChIP-seq data files from a study mapping ER $\alpha$  binding sites in MCF7, BT474, and T47D [48] and ChIP-seq data files from two studies mapping ER $\alpha$  binding sites in MCF7 were intersected [49, 50]. These studies had used similar culture conditions as ours, using phenol red medium and serum containing estrogen. Only a minor fraction of ~1.5% of conserved GRHL2 peaks identified in our study was flanked by established ER $\alpha$  binding sites in luminal breast cancer cells identified in those studies (**Fig. 2d**). Altogether, this data indicated that the majority of GRHL2 binding sites in luminal breast cancer cells were not associated with the ER $\alpha$ -mediated transcriptional complex.

### Changes in gene transcription in response to GRHL2 loss

Next, we employed nascent RNA Bru-seq to investigate genome-wide dynamic changes in DNA transcription triggered by GRHL2 loss. For this purpose, we made use of a conditional Cas9 MCF7 knockout model expressing a control or 2 different GRHL2 sgRNAs (sgCTR, sgGRHL2(1) and sgGRHL2(2), respectively). At 0, 2, 4, 8, or 16 days after GRHL2 knockout, cells were incubated with bromouridine (BrU) for 30 minutes to label nascent RNA (**Fig. 3a**) and analyzed in parallel by Western blot for the induction of Cas9 and deletion of GRHL2 (**Fig. 3b**). To identify GRHL2-regulated genes, for each time point, the average fold change (AFC) of transcription induced by doxycycline treatment in the two sgGRHL2 and sgCTR samples was determined. 262

# Chapter 3

genes were found to be upregulated and 226 genes were downregulated in at least one time point after GRHL2 loss in both sgGRHL2 samples ( $FC > 2$  or  $FC < 0.5$ ;  $p < 0.05$ ) but not in the sgCTR samples (**Fig. 3c**; **Table S2**).

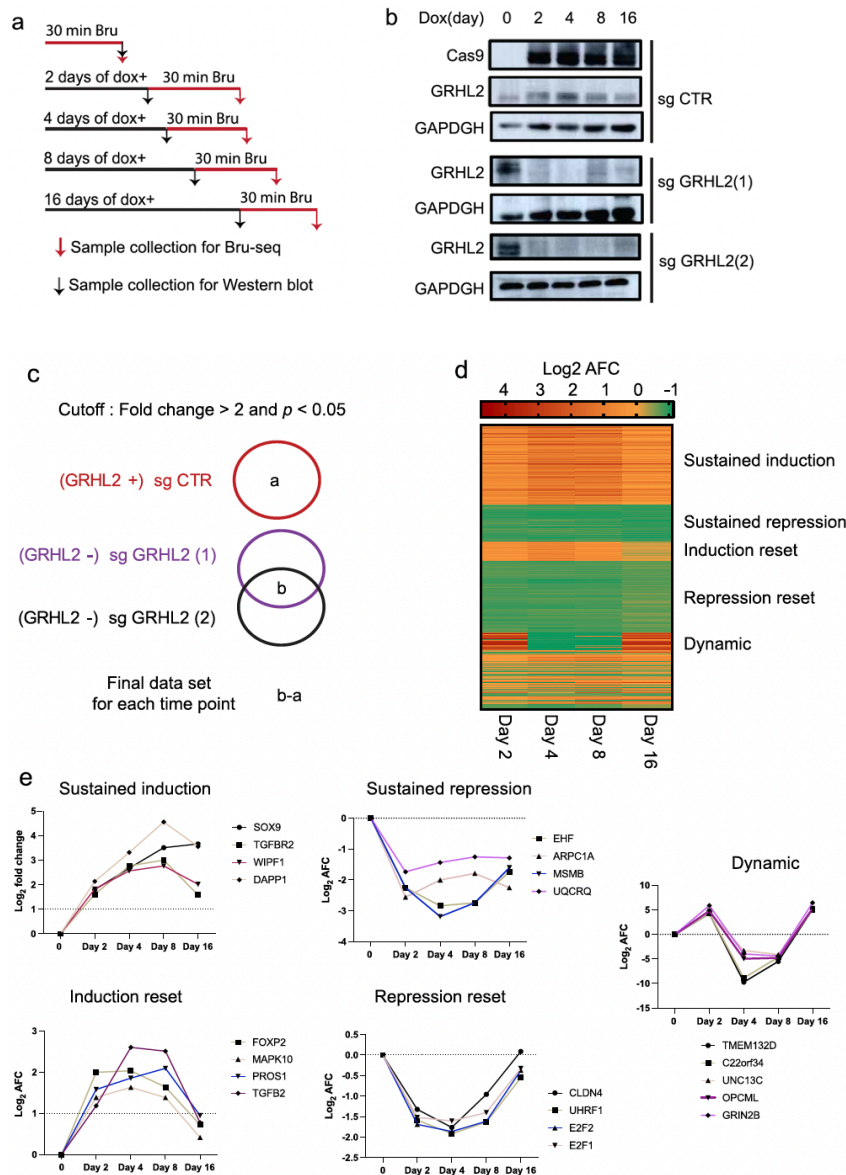


**Fig. 3.** Bru-seq analysis of transcriptional changes in response to GRHL2 loss in luminal breast cancer MCF7 cells. (a) Bru-seq sample preparation. Bromouridine

(Bru) labeling of nascent RNA was carried out for 30 minutes at the indicated time points after doxycycline (dox)-induced GRHL2 deletion. **(b)** Western blot analysis of GRHL2 expression levels at the indicated time points in sgCTR and sgGRHL2 transduced MCF7 cells. Cas9 induction is monitored and GAPDH serves as loading control. **(c)** Bru-seq data analysis approach. Each circle represents a gene set with differential transcription relative to the condition where no doxycycline was added. **(d)** Heatmap for genes whose transcription was altered in response to GRHL2 depletion. **(e)** Graphs depicting clusters of genes with distinct patterns of transcriptional changes in response to GRHL2 depletion. Graphs represent  $\log_2$  AFC of transcription in sgGRHL2(1) and sgGRHL2(2) cells. “Dynamic”: genes with  $\text{AFC} > 2$ ;  $p < 0.05$  at some and  $\text{AFC} < 0.5$ ;  $p < 0.05$  at other time points. “Sustained induction”: genes with  $\text{AFC} > 2$ ;  $p < 0.05$  at all time points. “Sustained repression”: genes with  $\text{AFC} < 0.5$ ;  $p < 0.05$  at all time points. “Induction reset”: genes with  $\text{AFC} > 2$ ;  $p < 0.05$  at early time points followed by a return to  $1 < \text{AFC} < 2$  at day 16. “Repression reset”: genes with  $\text{AFC} < 0.5$ ;  $p < 0.05$  at early time points followed by a return to  $0.5 < \text{AFC} < 1$  at day 16.

GRHL2-regulated genes were clustered in a heatmap using the AFC at each time point (**Fig. 3d**). Five clusters were identified based on transcriptional dynamics (**Fig. 3e; Table S2**). There was no preference for the subset of genes containing GRHL2 binding sites flanked by ER $\alpha$  binding in either of the clusters. Clusters displaying sustained upregulation of RNA synthesis or a transient induction that subsequently returned to baseline included *TGFB1*, *TGFB2*, and *TGFB2* pointing to enhanced TGF $\beta$  signaling. Other clusters showed sustained downregulation of RNA synthesis following GRHL2 deletion or a transient repression that subsequently returned to baseline. These included genes encoding the epithelial specific ETS transcription factor EHF, the *E2F1* and *E2F2* genes encoding E2F transcription factors involved in cell cycle progression, and the *CLDN4* gene encoding an epithelial tight junction protein. Another cluster showed responses that could be categorized as highly dynamic with alternating increased and decreased transcription.

### Identification of candidate genes regulated by GRHL2 promoter binding

GRHL2 can regulate gene transcription through interaction with gene promoter or enhancer elements [2]. We intersected the list of genes whose expression levels were significantly altered after GRHL2 loss in MCF7 at one or

more time points as identified by Bru-seq, with genes harboring GRHL2 binding sites in the -1000 bp to +100 bp promoter regions in MCF7 identified by ChIP-seq. 53 genes were identified where transcriptional regulation could be explained by direct GRHL2 interactions at the promoter region (**Table S2**; genes indicated in bold). Restricting this list to genes harboring GRHL2 binding sites in the promoter regions that were shared in all three luminal breast cancer cell lines, reduced this number to 9 (**Table S1**; genes indicated in bold). The presence or absence of GRHL2 binding sites in the promoter region did not correspond to the dynamic pattern of the transcriptional response of the gene (**Table S2**). Together, this indicated that the majority of the genes showing a transcriptional response to GRHL2 depletion was regulated either by direct interactions at enhancer elements or indirectly, e.g., through GRHL2 regulation of a transcription factor targeting the gene of interest.

### **EHF is a direct GRHL2-target inversely correlated with GRHL2 in breast cancer subtypes**

EHF was identified as a GRHL2 target harboring a GRHL2 binding site in its promoter region that was conserved in all three luminal breast cancer cell lines (**Fig. 3e**; **Table S1,2**). EHF had not been previously reported as a GRHL2 target gene while our Bru-seq tracks showed that EHF transcription was rapidly and continuously attenuated following GRHL2 loss (**Fig. 4a,b**). ChIP-qPCR confirmed the interaction between GRHL2 and the promoter region of the *EHF* gene (**Fig. 4c**). *EHF* is a member of the ETS transcription factor subfamily characterized by epithelial-specific expression [58]. Epithelial markers (e.g., GRHL2, CLDN4 and E-cadherin) are lost in basal B breast cancer cells as compared to the luminal and basal A subtype and we examined whether *EHF* expression followed this pattern. Indeed, RNA-seq data from a panel of 52 human breast cancer cell lines [59] showed a decrease of *EHF* RNA levels in the basal B subtype (**Fig. 4d**).

## GRHL2-controlled gene expression networks

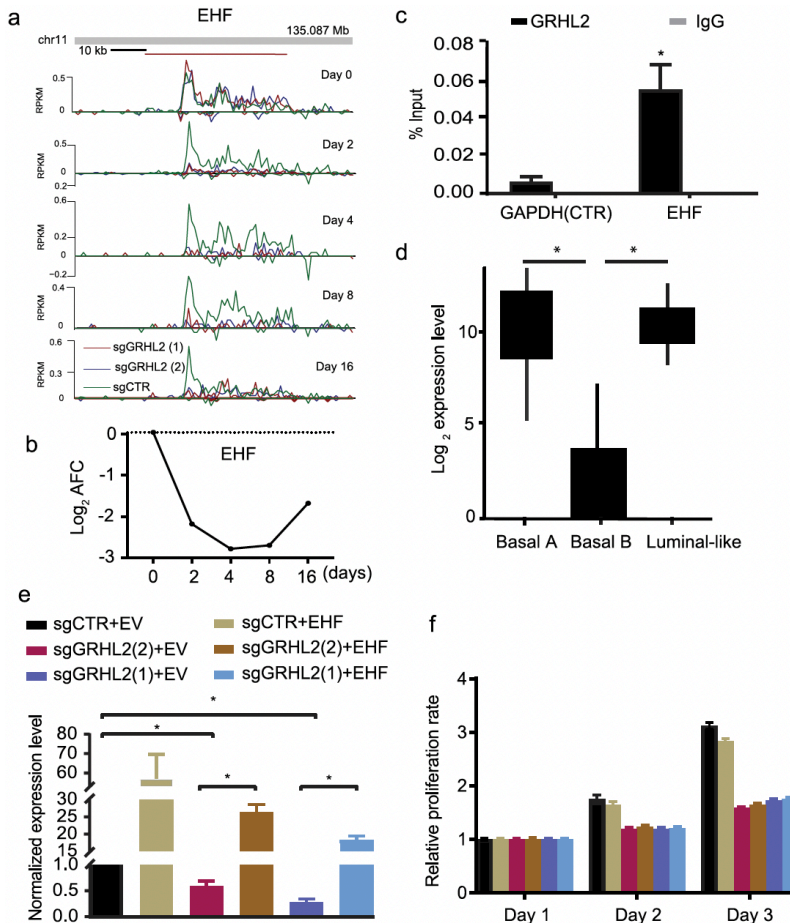


**Fig. 4. EHF represents a direct GRHL2 regulated gene.** **(a)** Bru-seq reads for *EHF* at indicated time points after to GRHL2 deletion. Track colors: green, sgCTR; red, sgGRHL2(1); blue, sgGRHL2(2). Positive y-axis indicates the plus-strand signal of RNA synthesis from left to right and the negative y-axis represents the minus-strand signal of RNA synthesis from right to left. **(b)** Line graph depicting the log<sub>2</sub> AFC of *EHF* transcription in sgGRHL2(1) and sgGRHL2(2) cells. **(c)** ChIP-qPCR showing enrichment of GRHL2 binding sites in *EHF* promoter region but not in the control *GAPDH* gene. Graph represents the efficiency of indicated genomic DNA co-precipitation with anti-GRHL2 Ab (black bars) or IgG control Ab (grey bars). Signals for IgG control and GRHL2 antibody pulldown samples are normalized to input DNA and are presented as % input with SEM from 3 technical replicates. Data are statistically analyzed by t-test and \* indicates  $p < 0.05$ . **(d)** *EHF* mRNA expression

in a panel of 52 human breast cancer cell lines covering luminal-, basal A-, and basal B subtypes extracted from RNA-seq data. Data is statistically analyzed by t-test and \* indicates  $p < 0.05$ . **(e)** qRT-PCR analysis of expression level of *EHF* mRNA after 4 days of doxycycline treatment of MCF7 cells transduced with dox-inducible Cas9 and sgCTR or sgGRHL2 constructs, in combination with ectopic expression of *EHF* or empty vector (EV) plasmids. Data are presented as mean  $\pm$  SEM from three technical replicates. Data are statistically analyzed by t-test. \* Indicates  $p < 0.05$ . **(f)** Graph showing results from SRB assay after 4 days doxycycline-treatment as in (e) and subsequent culture for the indicated time periods.

Studies in various cancer types have attributed tumor promoting as well as tumor suppressive roles to *EHF* but its role in breast cancer is largely unknown [60]. GRHL2 loss led to a rapid reduction in MCF7 cell growth and we tested whether ectopically overexpressed *EHF* could enhance proliferation in absence of GRHL2. However, overexpression of *EHF* did not rescue cell proliferation of GRHL2 KO MCF7 cells (**Fig. 4e,f**). The RNA synthesis rates of several other genes supporting cell cycle progression were rapidly suppressed in response to GRHL2 loss, including E2F transcription factors *E2F1* and *E2F2* and other genes such as *CDCA7L* and *MCM2* [61-63] (**Fig. 5a-d; Fig. 7a**). Our ChIP-seq data revealed GRHL2 binding sites in the promoter regions of *E2F2* and *CDCA7L* in MCF7 (**Table S2**) and this finding was corroborated by ChIP-qPCR analysis (**Fig. 5e**). Altogether, these results showed that several genes involved in cell cycle progression are rapidly downregulated following GRHL2 depletion with *EHF*, *E2F2*, and *CDCA7L* representing candidate targets for direct transcriptional regulation by GRHL2 at the gene promoter.

## GRHL2-controlled gene expression networks

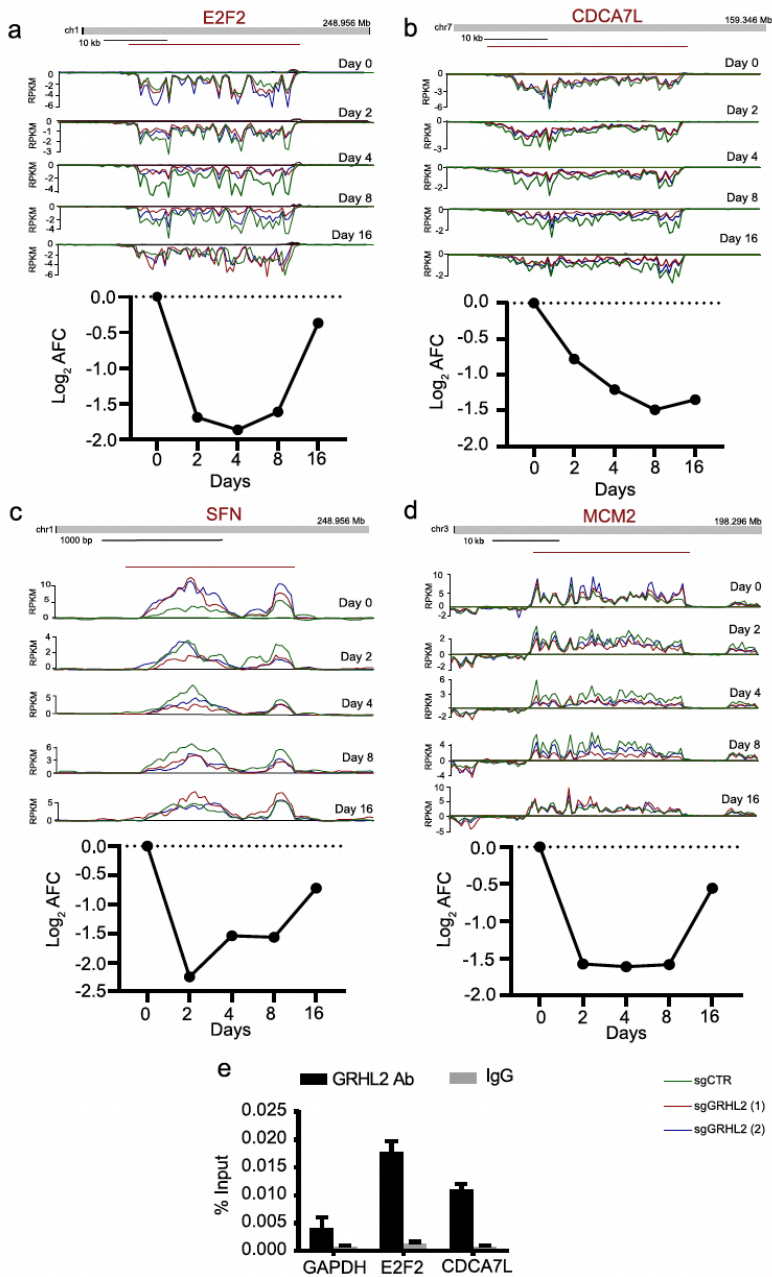


**Fig. 5. Downregulation of RNA synthesis for genes involved in cell cycle progression after GRHL2 loss. (a-d) Top: Bru-seq reads for indicated genes**

at indicated time point after to GRHL2 deletion. Track colors: green, sgCTR; red, sgGRHL2(1); blue, sgGRHL2(2). **Bottom:** Line graphs depicting the log<sub>2</sub> AFC of transcription in sgGRHL2(1) and sgGRHL2(2) cells for the indicated genes. The positive y-axis indicates the plus-strand signal of RNA synthesis from left to right and the negative y-axis represents the minus-strand signal of RNA synthesis from right to left. **(e)** Validation of interaction of GRHL2 binding sites with the promoter regions of indicated genes by ChIP-qPCR. Signals for IgG control and GRHL2 antibody pulldown samples are normalized to input DNA and are presented as % input with SEM from 3 technical replicates. Data are statistically analyzed by t-test and \* indicates  $p < 0.05$ .

### **Regulation of EMT-related genes: CLDN4 but not CDH1, ZEB1, and ZEB2 represent direct GRHL2 targets in luminal breast cancer**

GRHL2 and OVOL2 support an epithelial phenotype and counteract EMT transcription factors such as ZEB1, ZEB2, and SNAIL. Genes encoding epithelial adhesion components such as CLDN4 in tight junctions or E-cadherin (CDH1) in adherens junctions are regulated by this balance [64]. It has been reported that GRHL2 binding sites are present in the intronic region of *CDH1* and in the promoter regions of *CLDN4* and *OVOL2* for activation of transcription, and GRHL2 was reported to bind the *ZEB1* gene as a negative regulator [4, 12, 15, 23, 24, 65].

In our ChIP-seq data, a conserved intronic GRHL2 binding site was observed in *CDH1* that was validated by ChIP-qPCR (**Fig. 6a,b**). However, while GRHL2 was found to transcriptionally activate *CDH1* in earlier reports [4, 21, 33] we did not observe downregulation of *CDH1* nascent RNA synthesis in the first 16 days after GRHL2 loss (**Fig. 6c,d**). No GRHL2 peaks were associated with *CDH2* (encoding N-cadherin, a mesenchymal marker) while GRHL2 binding was conserved in the promoter regions of *CLDN4* and *OVOL2* (**Fig. 6a,b; Fig S2**). *CLDN4* also showed multiple GRHL2 binding sites across the coding and non-coding regions. *CLDN4* transcription was suppressed at 2, 4, and 8 days after GRHL2 depletion but recovered at 16 days (**Table S2; Fig. 6c,d**) whereas *OVOL2* was not affected (data not shown).



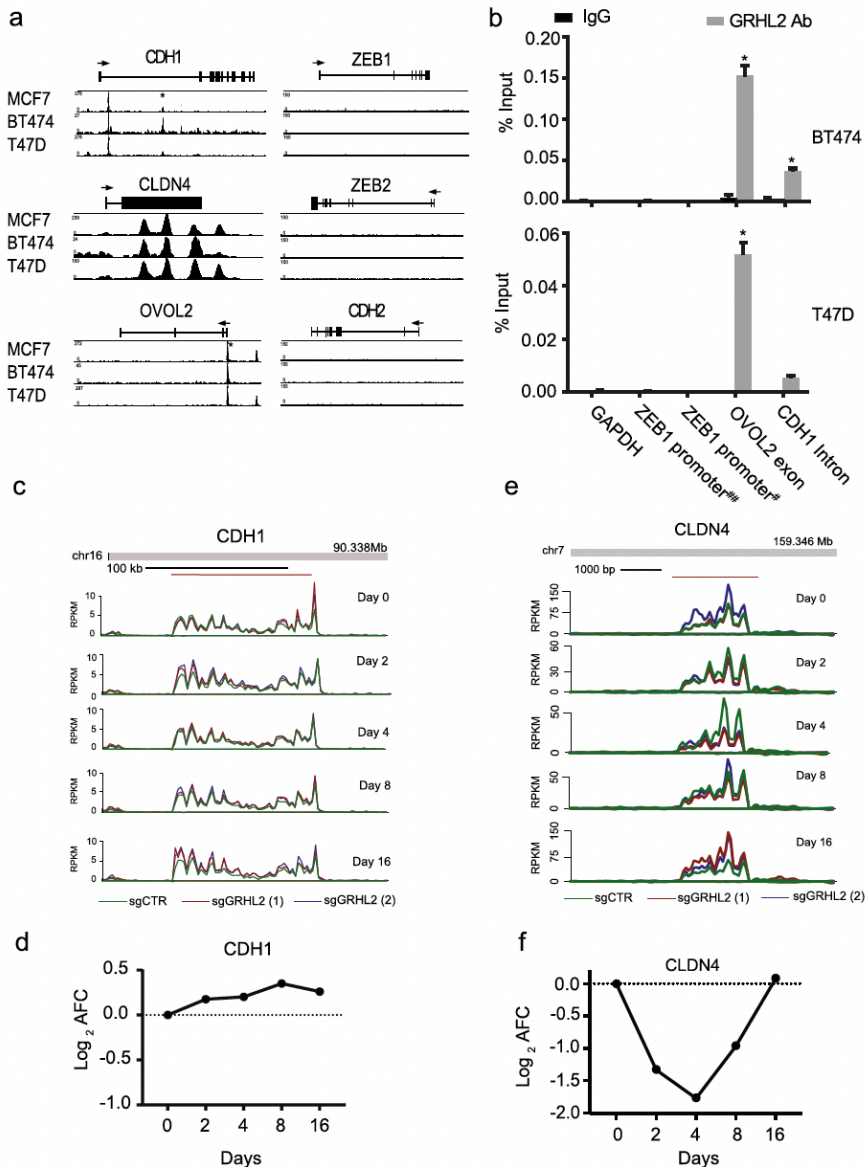


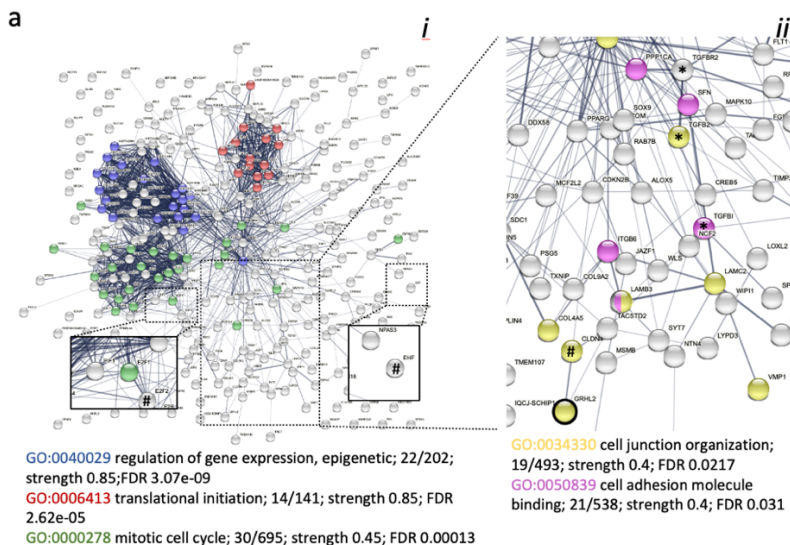
**Fig. 6. Regulation of EMT related genes by GRHL2. (a)** ChIP tracks for the indicated genes in three luminal breast cancer cell lines. The track height is scaled from 0 to the indicated number. The locus with its exon/intron structure is presented above the tracks. \*Indicates binding sites validated by ChIP-qPCR in (b). **(b)** ChIP-qPCR validation of presence and absence of GRHL2 binding sites identified by ChIP-seq. Graphs represent the efficiency

of indicated genomic DNA co-precipitation with anti-GRHL2 Ab (grey bars) or IgG control Ab (black bars). Note enrichment of GRHL2 binding at *OVOL2* exon and *CDH1* intron, but not at *ZEB1* promoter regions. For *ZEB1* detection, ChIP-qPCR was performed using primers that have been previously reported to amplify *ZEB1* promoter DNA sequences bound by GRHL2 in human mammary epithelial cells and in PEO1 but not OVCA429 human ovarian cancer cells (indicated by ##) [17, 23] and another primer set that did not confirm GRHL2 promoter interaction in ovarian cancer cells (indicated by #) [17]. Signals for IgG control and GRHL2 antibody pulldown samples were normalized to input DNA and presented as % input with SEM from 3 technical replicates. Data were statistically analyzed by t-test and \* indicates  $p < 0.05$ . **(c,e)** Bru-seq reads for indicated genes at indicated time point after to GRHL2 deletion. Track colors: green, sgCTR; red, sgGRHL2(1); blue, sgGRHL2(2). **(d,f)** Line graphs depicting the  $\log_2$  AFC of transcription in sgGRHL2(1) and sgGRHL2(2) cells for the indicated genes. The positive y-axis indicates the plus-strand signal of RNA synthesis from left to right and the negative y-axis represents the minus-strand signal of RNA synthesis from right to left.

No GRHL2 binding was observed at the promoter or other regions of *ZEB1* or *ZEB2* as opposed to findings in mammary epithelial cells [24] (**Fig. 6a**). ChIP-qPCR was performed using primers that have been previously reported to amplify *ZEB1* promoter DNA sequences bound by GRHL2 in human mammary epithelial cells and in PEO1 but not OVCA429 human ovarian cancer cells [17, 23] and another primer set that did not detect GRHL2 promoter interaction in ovarian cancer cells [17] (**Fig. 6b**). This confirmed the absence of GRHL2 binding in the promoter of *ZEB1* in luminal breast cancer cells. In agreement, no significant changes in transcription of *ZEB1* and *ZEB2* genes were observed after GRHL2 loss in MCF7(data not shown). Together, these results indicated that *CLDN4* is a direct GRHL2 target while *CDH1*, *ZEB1*, or *ZEB2* are unlikely to represent direct GRHL2 target genes in luminal breast cancer cells. The latter may be regulated at later timepoints indirectly through other transcriptional regulators [66] or by GRHL2-mediated post-transcriptional modification [17, 23, 67].

## Validation of GRHL2 associations in breast cancer patients

All genes identified by Bru-seq in the MCF7 conditional GRHL2 KO model falling in the categories “sustained induction/repression” or “induction/repression reset”, were imported in the STRING database to visualize clusters representing enriched functionalities regulated by GRHL2. Three clusters of proteins associated with i) epigenetic regulation of gene expression (including proteins also connected to GO:0098532, histone H3-K27 trimethylation; not shown), ii) translation initiation, and iii) mitosis were clearly visible (**Fig. 7a**). This was in agreement with the growth suppression observed in response to GRHL2 depletion (**Fig. 4**) and earlier reports involving GRHL2 in histone methylation [17]. E2F1 and E2F2 were connected to the mitosis cluster but EHF showed no connections. No connections of these clusters with GRHL2 were visible but the interaction of GRHL2 with CLDN4 was shown as well as co-expression of GRHL2 with TACSTD2, a transmembrane receptor regulating cell proliferation and migration in development and cancer [68]. The TGFB1, TGFB2, and TGFB2 axis was not closely connected to GRHL2 but both were surrounded by genes encoding extracellular matrix (ECM) components (e.g., laminin subunits and collagen chains), the ITGB6 integrin subunit, and LOXL2 encoding an ECM crosslinking enzyme [69] pointing to modification of ECM production and adhesion.



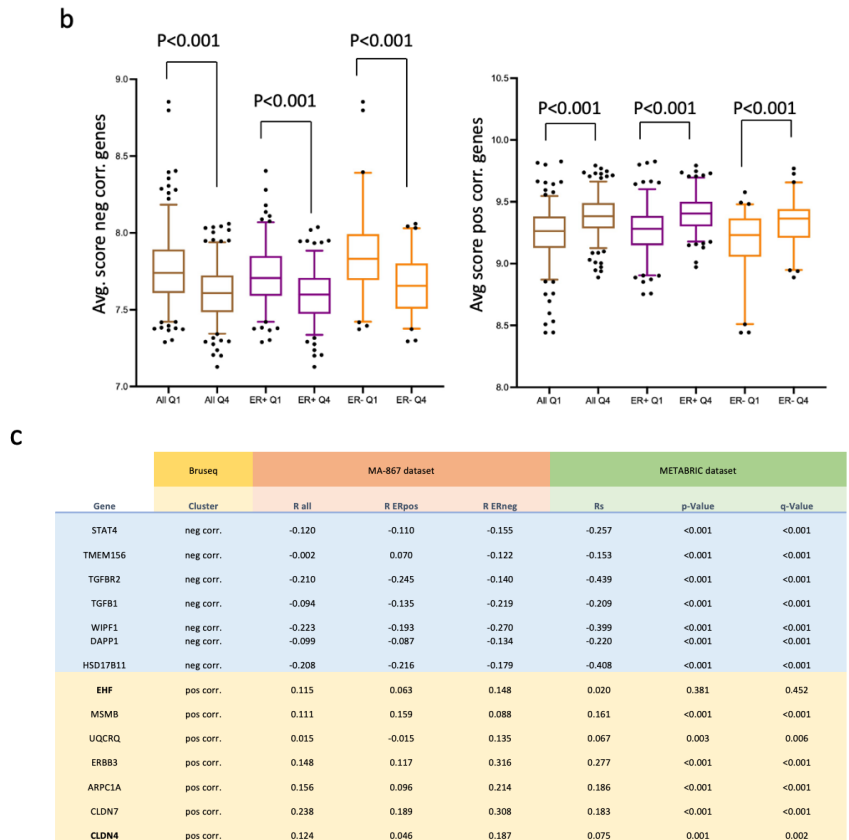


**Fig. 7. Gene clusters responding to GRHL2 depletion and their correlation with GRHL2 in breast cancer tissues. (a)** STRING derived protein interaction analysis of genes displaying sustained up- or down regulation in response to GRHL2 depletion in MCF7. GO terms are color marked as indicated. *i*, entire network with boxes showing zoom-in on indicated regions; *ii*, zoom in on indicated region showing different GO terms. # Indicates GRHL2 targets identified by promoter binding. \* Indicates TGFβ signaling axis. **(b)** Average expression (log2 scale) in the MA-867 patient dataset of the cluster of genes negatively (left panel) or positively associated with GRHL2 (right panel) in MCF7 KO model. Patients were divided in 4 quartiles according to the level of GRHL2 expression. Q1, lowest GRHL2 expression; Q4, GRHL2 highest expression; All, all patients grouped together; ER+, ER

positive patients grouped; ER-, ER negative patients grouped. Boxplots display the median with 25th–75th percentile and dots represent lower 5% and upper 95% samples. P values determined by t test (two-sided). (c) Correlation with GRHL2 in MA-867 and METABRIC datasets for indicated genes negatively or positively correlated with GRHL2 in MCF KO model analyzed by Bru-seq. For MA-867 dataset, R-values for all patients grouped together, ER positive patients, or ER negative patients are shown. For METABRIC dataset, correlation, p-value, and q-values are shown as determined in BioPortal.

We addressed to what extent GRHL2 regulated gene clusters identified in our conditional MCF7 KO model predicted associations with GRHL2 gene expression in breast cancer patients. We focused on all genes where the control sgRNA gave  $0.75 < FC < 1.5$  at each time point after GRHL2 KO while both GRHL2 sgRNAs triggered either  $FC < 0.75$  in at least 3 time points (positive correlation with GRHL2) or  $FC > 1.5$  in at least 3 time points (negative correlation with GRHL2). We made use of a cohort of 867 untreated breast cancer patients (MA-867 dataset [59]) and ranked patients in 4 quartiles according to the level of GRHL2 expression. The average expression of predicted negatively correlated and positively correlated gene clusters based on the MCF7 conditional KO model, displayed a significant correlation with GRHL2 expression in the same direction when all patients were treated as one group (**Fig. 7b**). Moreover, behavior in the MCF7 conditional KO model correctly predicted the correlation of gene clusters with GRHL2 expression when ER positive and ER negative patients were separately tested.

At the individual gene level, Pearson correlation coefficients for association with GRHL2 when all patients of the MA-867 dataset were treated as one group, were in the range  $-0.31 < R < 0.29$  indicating that associations while in the same orientation were weak. This included *EHF* and *CLDN4* that were subject to promoter binding by GRHL2 and belonged to the positively correlated gene cluster (**Fig. 4c, 6a, 7c; Table S2**). We also analyzed the METABRIC data set consisting of RNAseq data of 1904 primary breast tumors. Here, co-expression analysis using cBioPortal showed a significant correlation in the

same direction as predicted by the MCF7 conditional KO model for *CLDN4* but not *EHF* (**Fig. 7c**). For the negatively correlated gene cluster, *TGFBR2* as well as *TGFB1* showed a significant correlation in the same direction in the METABRIC data set, further establishing suppression of TGF $\beta$  signaling by GRHL2 in breast cancer cells. Notably, the large majority of genes in both clusters did not harbor promoter binding sites, further indicating that regulation at enhancer sites or indirect mechanisms prevailed.

### Discussion

We report genome-wide binding sites of the transcription factor GRHL2 that are conserved across 3 human luminal breast cancer cell lines. The match with previously published binding motifs in other cell types shows conservation of GRHL2-DNA interaction but we find that the spectrum of GRHL2 targets differs considerably from those identified in other cells. A limited number of binding sites were located at gene promoter regions. Similar to previous reports [14, 17], most binding sites were located in introns and intergenic regions. Such regions may contain enhancers interacting with GRHL2 and GRHL2 has been reported to regulate histone modifications such as H3K4me3 and H3K4me1 [17, 70]. Notably, GRHL2 can regulate ER $\alpha$  signaling output in hormone receptor positive breast cancer by co-occupying enhancer elements with FOXA1, GATA3, and ER $\alpha$  [34-36]. Co-occupation of enhancers by ER $\alpha$  and GRHL2 has been shown to be regulated by ER $\alpha$  phosphorylation at Ser118 [57]. Indeed, we detect an ER $\alpha$  binding motif in the vicinity of GRHL2 peaks, but this represents only a minor fraction of the identified GRHL2 binding sites. Moreover, intersection of our identified GRHL2 peaks with published ER $\alpha$  binding events in the same series of luminal breast cancer cells cultured under the same conditions further indicates that GRHL2 binds most of the targets found by us in absence of ER $\alpha$ , FOXA1, and GATA3. A study intersecting binding sites for GRHL2, FOXA1, and ER $\alpha$  in MCF7 cells also found that most GRHL2 binding sites did not overlap with FOXA1 or ER $\alpha$  binding but ~30% did show overlap [71]. Our exclusive focus on GRHL2 binding sites that are conserved across three luminal breast cancer cell lines may have selected for those sites binding only GRHL2. Together, these studies indicate that enhancers occupied by ER $\alpha$ , FOXA1, and GATA3 frequently also

bind GRHL2, but a majority of conserved GRHL2 binding sites in luminal breast cancer cells do not overlap with binding of the ER $\alpha$  signaling complex.

Using a conditional KO model, we identify genes whose transcription is regulated by GRHL2 in luminal breast cancer cells. Notably, the gene clusters showing up- or downregulation in response to GRHL2 loss show a significant, albeit low level of correlation with GRHL2 expression in breast cancer patients. By using Bru-seq we focus on changes in the rate of nascent RNA synthesis caused by GRHL2 depletion [72]. Differences with studies using steady state RNA-seq may be due to post transcriptional mechanisms of regulation not addressed in our analysis, including RNA stability. We observed diverse responses to GRHL2 depletion, including enhanced or repressed transcription that can be sustained, transient or dynamic type of response. The fact that patterns of transcription induction are similar to the patterns of transcription repression is in line with the fact that GRHL2 has been reported to act as a positive as well as a negative regulator of gene transcription. However, indirect mechanisms involving other transcriptional activators or repressors may also be triggered by GRHL2 depletion.

GRHL2 expression appears to support cancer growth and even disease progression in most tumor types investigated [18-22, 37]. Indeed, GRHL2 drives expression of several genes promoting cell survival and proliferation [9, 18, 19]. Our study agrees with this as GRHL2 loss rapidly affects a cluster of genes involved in cell cycle progression and causes a gradual decrease in proliferation in MCF7 cells. A group of genes whose transcription is reduced following loss of GRHL2 is involved in cell cycle progression and DNA replication including the epithelial specific ETS family transcription factor *EHF*, E2F transcription factors *E2F1* and *E2F2* and other genes such as *CDCA7L* and *MCM2* [60-63]. We show that *EHF*, *E2F2* and *CDCA7L* represent previously unidentified GRHL2 target genes that can be subject to direct regulation at promotor regions. *EHF* has been previously implicated in ovarian, gastric and prostate cancer [73-75] but our findings point to cooperative roles of GRHL2 target genes including *EHF* and E2Fs in sustaining proliferation.

Several studies have shown that GRHL2 suppresses EMT [9, 17, 23, 24, 26, 27]. This may explain its reported role as a suppressor of local tissue invasion and metastasis [9, 25]. In fact, a similar function may also be involved in the many examples where GRHL2 is positively associated with tumor progression and metastasis. GRHL2 may prevent a complete EMT and maintain cancer cells in a hybrid EMT state that is believed to be crucial for cancer cell plasticity, which supports invasion and metastasis [76, 77]. Our results concerning GRHL2 interactions with known EMT-related genes are partly in disagreement with previously published findings. First, we demonstrate that *CDH1* RNA synthesis is not altered following GRHL2 loss, despite an intronic binding site that is conserved in the three luminal cell lines. No binding site is observed in the -1000/+100 promotor region but we detect GRHL2 binding in the region from -6000 bp to -1000 bp relative to the TSS of the *CDH1* gene, consistent with an earlier study reporting a contact of GRHL2 upstream of the *CDH1* promoter [4]. Although this may facilitate long-distance interactions with the promoter region through chromatin looping [4], loss of this interaction, nor that at the intronic GRHL2 binding site, causes a reduction in *CDH1* transcription in the first 16 days after GRHL2 deletion in our study. Our findings do not rule out *CDH1* regulation through indirect, post transcriptional mechanisms including RNA stability that are not measured in Bru-seq and may underlie findings in studies using RNA-seq or PCR analyses, or at the level of translation. Second, it has been reported that *ZEB1* is regulated by GRHL2 directly and, vice versa, that *ZEB1* regulates *GRHL2* in a balance between EMT and MET [9, 20, 23, 24]. We do not detect GRHL2 binding sites in the promoter, or other regions of the *ZEB1* or *ZEB2* genes. This potential discrepancy cannot be explained by technical differences as we have confirmed the lack of GRHL2 binding in the ChIP-seq analysis by ChIP-qPCR using primers that amplified *ZEB1* and *ZEB2* regions bound by GRHL2 in human mammary epithelial cells and human ovarian cancer cells in other studies [17, 23]. Rather, this may point to differences in GRHL2 interactions in different cell types. Nevertheless, the fact that we do not detect GRHL2-binding sites in *ZEB1* or *ZEB2* is in line with our Bru-seq analysis indicating that transcription of the *ZEB1* and *ZEB2* genes is not affected by GRHL2 depletion in the first 16 days. Together, this data indicates that *CDH1*, *ZEB1*, and *ZEB2* genes do not



represent direct transcriptional targets of GRHL2 in luminal breast cancer and their regulation may occur through post-transcriptional regulation in this cellular context. Our data do confirm *CLDN4* as a direct target gene with GRHL2-binding in the promoter region and transcriptional suppression in response to GRHL2 depletion in luminal breast cancer cells.

The fact that in our study GRHL2 supports gene networks involved in cell proliferation and that a tumor/metastasis suppressing function related to its suppression of EMT is less evident, agrees with earlier studies and with the location of GRHL2 on chromosome 8q22, a region that is amplified in various cancers, including breast cancer. One explanation for the discrepancy between different studies including our own is the possibility that GRHL2 interacts with- and regulates genes in a context-dependent manner. A meta-analysis combining all RNA-seq, micro-array, and ChIP-seq experiments, identified common candidate genes for regulation by GRH or GRHL1-3. The authors noticed a striking lack of correlation between findings in normal epithelia as compared to cancerous cells with *CDH1* being identified as a target in normal epithelia but not cancer [78]. Likewise, the findings reported in our study represent candidate GRHL2-regulated genes and pathways in luminal breast cancer that partly overlap but are also distinct from GRHL2 regulation in normal epithelia and other cancer types.

### Conclusions

Taken together, this study provides a comprehensive genome-wide resource of GRHL2 binding sites conserved across luminal breast cancer cells. In a conditional KO model, we identify groups of genes whose transcription is positively or negatively controlled by GRHL2 and find 5 main patterns of dynamic regulation. The association with GRHL2 of gene clusters in the KO model predicts the correlation with GRHL2 expression in breast cancer patients. The dominant response to GRHL2 depletion in luminal breast cancer cells is suppression of proliferation and we identify clusters of genes reflecting this response including direct regulation of ETS and E2F transcription factors by GRHL2. An EMT response to GRHL2 loss is limited and our findings indicate that regulation of epithelial genes can be strikingly different in normal and

## Chapter 3

---

cancer cells involving direct GRHL2-mediated transcriptional control or indirect mechanisms.

### Abbreviations

GRHL2, Grainyhead like 2

EMT, epithelial to mesenchymal transition

HER2, human epidermal growth factor receptor 2

ChIP-seq, chromatin immunoprecipitation followed by high-throughput DNA sequencing

qPCR, quantitative polymerase chain reaction

Bru-seq, bromouridine sequencing

RIPA buffer, radioimmunoprecipitation buffer

BCA, bicinchoninic acid

PVDF, polyvinylidene difluoride

BSA, bovine serum albumin

RT, room temperature

IPA, Ingenuity Pathways Analysis

DAVID, Database for Annotation, Visualization, and Integrated Discovery

GO, Gene Ontology

PANTHER, Protein Analysis Through Evolutionary Relationships

AFC, average fold change

PPI, protein-protein interaction

### Availability of data and materials:

Chip-seq data supporting the results of this article is available at the UCSC Genome Browser [<https://genome.ucsc.edu/s/hwuRadboudumc/ZWang>].

Bru-seq data supporting the results of this article is available at Gene Expression Omnibus (GEO) database, [www.ncbi.nlm.nih.gov/geo](http://www.ncbi.nlm.nih.gov/geo) (Accession No. GSE222353).

### Competing interests:

The authors declare that they have no competing interests. Zi Wang was supported by a grant from the China Scholarship Council. Bircan Coban was supported by the Dutch Cancer Society (KWF Research Grant #10967).

### Acknowledgements:

We thank Dr. Giuseppina Carbone, Institute of Oncology Research, Bellinzona, Switzerland, for kindly providing the EHF plasmid.

### Author contributions:

ZW designed, executed and analyzed the experiments, prepared figures, and wrote the manuscript; BC analyzed experimental and patient data, prepared figures, and wrote the manuscript, HW assisted with design and analysis of the ChIP-seq experiment and critically read the manuscript; JC analyzed the ChIP-seq experiment and critically read the manuscript LD assisted with design of the ChIP-seq experiment and critically read the manuscript; MTP executed processing and sequencing of Bru-seq samples and critically read the manuscript; ML assisted with design and analysis of the Bru-seq experiment and critically read the manuscript; MS analyzed patient data and critically read the manuscript; JM analyzed patient data and critically read the manuscript; EHJD initiated the study, designed the experiments, and wrote the manuscript.

### References

1. Frisch SM, Farris JC, Pifer PM: Roles of Grainyhead-like transcription factors in cancer. *Oncogene* 2017.
2. Wang S, Samakovlis C: Grainy head and its target genes in epithelial morphogenesis and wound healing. *Curr Top Dev Biol* 2012, 98:35-63.
3. Wilanowski T, Caddy J, Ting SB, Hislop NR, Cerruti L, Auden A, Zhao LL, Asquith S, Ellis S, Sinclair R *et al*: Perturbed desmosomal cadherin expression in grainy head-like 1-null mice. *The EMBO journal* 2008, 27(6):886-897.
4. Werth M, Walentin K, Aue A, Schonheit J, Wuebken A, Pode-Shakked N, Vilianovitch L, Erdmann B, Dekel B, Bader M *et al*: The transcription factor grainyhead-like 2 regulates the molecular composition of the epithelial apical junctional complex. *Development* 2010, 137(22):3835-3845.
5. Pyrgaki C, Liu A, Niswander L: Grainyhead-like 2 regulates neural tube closure and adhesion molecule expression during neural fold fusion. *Developmental biology* 2011, 353(1):38-49.
6. Ting SB, Caddy J, Hislop N, Wilanowski T, Auden A, Zhao LL, Ellis S, Kaur P, Uchida Y, Holleran WM *et al*: A homolog of Drosophila grainy head is essential for epidermal integrity in mice. *Science* 2005, 308(5720):411-413.

7. Rifat Y, Parekh V, Wilanowski T, Hislop NR, Auden A, Ting SB, Cunningham JM, Jane SM: Regional neural tube closure defined by the Grainy head-like transcription factors. *Developmental biology* 2010, 345(2):237-245.
8. Boglev Y, Wilanowski T, Caddy J, Parekh V, Auden A, Darido C, Hislop NR, Cangkrama M, Ting SB, Jane SM: The unique and cooperative roles of the Grainy head-like transcription factors in epidermal development reflect unexpected target gene specificity. *Developmental biology* 2011, 349(2):512-522.
9. Werner S, Frey S, Riethdorf S, Schulze C, Alawi M, Kling L, Vafaizadeh V, Sauter G, Terracciano L, Schumacher U *et al*: Dual roles of the transcription factor grainyhead-like 2 (GRHL2) in breast cancer. *The Journal of biological chemistry* 2013, 288(32):22993-23008.
10. Caddy J, Wilanowski T, Darido C, Dworkin S, Ting SB, Zhao Q, Rank G, Auden A, Srivastava S, Papenfuss TA *et al*: Epidermal wound repair is regulated by the planar cell polarity signaling pathway. *Developmental cell* 2010, 19(1):138-147.
11. Gao X, Vockley CM, Pauli F, Newberry KM, Xue Y, Randell SH, Reddy TE, Hogan BL: Evidence for multiple roles for grainyhead-like 2 in the establishment and maintenance of human mucociliary airway epithelium.[corrected]. *Proceedings of the National Academy of Sciences of the United States of America* 2013, 110(23):9356-9361.
12. Senga K, Mostov KE, Mitaka T, Miyajima A, Tanimizu N: Grainyhead-like 2 regulates epithelial morphogenesis by establishing functional tight junctions through the organization of a molecular network among claudin3, claudin4, and Rab25. *Molecular biology of the cell* 2012, 23(15):2845-2855.
13. Kohn KW, Zeeberg BM, Reinhold WC, Pommier Y: Gene expression correlations in human cancer cell lines define molecular interaction networks for epithelial phenotype. *PloS one* 2014, 9(6):e99269.
14. Walentin K, Hinze C, Werth M, Haase N, Varma S, Morell R, Aue A, Potschke E, Warburton D, Qiu A *et al*: A Grhl2-dependent gene network controls trophoblast branching morphogenesis. *Development* 2015, 142(6):1125-1136.
15. Aue A, Hinze C, Walentin K, Ruffert J, Yurtdas Y, Werth M, Chen W, Rabien A, Kilic E, Schulzke JD *et al*: A Grainyhead-Like 2/Ovo-Like 2 Pathway Regulates Renal Epithelial Barrier Function and Lumen Expansion. *Journal of the American Society of Nephrology : JASN* 2015, 26(11):2704-2715.
16. Pifer PM, Farris JC, Thomas AL, Stoilov P, Denvir J, Smith DM, Frisch SM: Grainyhead-like 2 inhibits the coactivator p300, suppressing tubulogenesis and the epithelial-mesenchymal transition. *Molecular biology of the cell* 2016, 27(15):2479-2492.

17. Chung VY, Tan TZ, Tan M, Wong MK, Kuay KT, Yang Z, Ye J, Muller J, Koh CM, Guccione E *et al*: GRHL2-miR-200-ZEB1 maintains the epithelial status of ovarian cancer through transcriptional regulation and histone modification. *Scientific reports* 2016, 6:19943.
18. Dompe N, Rivers CS, Li L, Cordes S, Schwickart M, Punnoose EA, Amler L, Seshagiri S, Tang J, Modrusan Z *et al*: A whole-genome RNAi screen identifies an 8q22 gene cluster that inhibits death receptor-mediated apoptosis. *Proceedings of the National Academy of Sciences of the United States of America* 2011, 108(43):E943-951.
19. Chen W, Dong Q, Shin KH, Kim RH, Oh JE, Park NH, Kang MK: Grainyhead-like 2 enhances the human telomerase reverse transcriptase gene expression by inhibiting DNA methylation at the 5'-CpG island in normal human keratinocytes. *The Journal of biological chemistry* 2010, 285(52):40852-40863.
20. Quan Y, Jin R, Huang A, Zhao H, Feng B, Zang L, Zheng M: Downregulation of GRHL2 inhibits the proliferation of colorectal cancer cells by targeting ZEB1. *Cancer Biol Ther* 2014, 15(7):878-887.
21. Xiang X, Deng Z, Zhuang X, Ju S, Mu J, Jiang H, Zhang L, Yan J, Miller D, Zhang HG: Grhl2 determines the epithelial phenotype of breast cancers and promotes tumor progression. *PloS one* 2012, 7(12):e50781.
22. Yang X, Vasudevan P, Parekh V, Penev A, Cunningham JM: Bridging cancer biology with the clinic: relative expression of a GRHL2-mediated gene-set pair predicts breast cancer metastasis. *PloS one* 2013, 8(2):e56195.
23. Cieply B, Farris J, Denvir J, Ford HL, Frisch SM: Epithelial-mesenchymal transition and tumor suppression are controlled by a reciprocal feedback loop between ZEB1 and Grainyhead-like-2. *Cancer research* 2013, 73(20):6299-6309.
24. Cieply B, Riley Pt, Pifer PM, Widmeyer J, Addison JB, Ivanov AV, Denvir J, Frisch SM: Suppression of the epithelial-mesenchymal transition by Grainyhead-like-2. *Cancer research* 2012, 72(9):2440-2453.
25. Xiang J, Fu X, Ran W, Chen X, Hang Z, Mao H, Wang Z: Expression and role of grainyhead-like 2 in gastric cancer. *Medical oncology* 2013, 30(4):714.
26. Brabletz S, Brabletz T: The ZEB/miR-200 feedback loop--a motor of cellular plasticity in development and cancer? *EMBO reports* 2010, 11(9):670-677.
27. Gregory PA, Bracken CP, Smith E, Bert AG, Wright JA, Roslan S, Morris M, Wyatt L, Farshid G, Lim YY *et al*: An autocrine TGF-beta/ZEB/miR-200 signaling network regulates establishment and maintenance of epithelial-mesenchymal transition. *Molecular biology of the cell* 2011, 22(10):1686-1698.

28. Mlacki M, Kikulska A, Krzywinska E, Pawlak M, Wilanowski T: Recent discoveries concerning the involvement of transcription factors from the Grainyhead-like family in cancer. *Experimental biology and medicine* 2015, 240(11):1396-1401.
29. Sorlie T, Perou CM, Tibshirani R, Aas T, Geisler S, Johnsen H, Hastie T, Eisen MB, van de Rijn M, Jeffrey SS *et al*: Gene expression patterns of breast carcinomas distinguish tumor subclasses with clinical implications. *Proceedings of the National Academy of Sciences of the United States of America* 2001, 98(19):10869-10874.
30. Cancer Genome Atlas N: Comprehensive molecular portraits of human breast tumours. *Nature* 2012, 490(7418):61-70.
31. Perou CM, Sorlie T, Eisen MB, van de Rijn M, Jeffrey SS, Rees CA, Pollack JR, Ross DT, Johnsen H, Akslen LA *et al*: Molecular portraits of human breast tumours. *Nature* 2000, 406(6797):747-752.
32. Forouzanfar MH, Foreman KJ, Delossantos AM, Lozano R, Lopez AD, Murray CJ, Naghavi M: Breast and cervical cancer in 187 countries between 1980 and 2010: a systematic analysis. *Lancet* 2011, 378(9801):1461-1484.
33. Paltoglou S, Das R, Townley SL, Hickey TE, Tarulli GA, Coutinho I, Fernandes R, Hanson AR, Denis I, Carroll JS *et al*: Novel Androgen Receptor Coregulator GRHL2 Exerts Both Oncogenic and Antimetastatic Functions in Prostate Cancer. *Cancer research* 2017, 77(13):3417-3430.
34. Cocce KJ, Jasper JS, Desautels TK, Everett L, Wardell S, Westerling T, Baldi R, Wright TM, Tavares K, Yllanes A *et al*: The Lineage Determining Factor GRHL2 Collaborates with FOXA1 to Establish a Targetable Pathway in Endocrine Therapy-Resistant Breast Cancer. *Cell Rep* 2019, 29(4):889-903 e810.
35. Holding AN, Giorgi FM, Donnelly A, Cullen AE, Nagarajan S, Selth LA, Markowitz F: VULCAN integrates ChIP-seq with patient-derived co-expression networks to identify GRHL2 as a key co-regulator of ERα at enhancers in breast cancer. *Genome biology* 2019, 20(1):91.
36. Chi D, Singhal H, Li L, Xiao T, Liu W, Pun M, Jeselsohn R, He H, Lim E, Vadhi R *et al*: Estrogen receptor signaling is reprogrammed during breast tumorigenesis. *Proceedings of the National Academy of Sciences of the United States of America* 2019, 116(23):11437-11443.
37. Reese RM, Harrison MM, Alarid ET: Grainyhead-like Protein 2: The Emerging Role in Hormone-Dependent Cancers and Epigenetics. *Endocrinology* 2019, 160(5):1275-1288.
38. Tugores A, Le J, Sorokina I, Snijders AJ, Duyao M, Reddy PS, Carlee L, Ronshaugen M, Mushegian A, Watanaskul T *et al*: The epithelium-specific ETS protein EHF/ESE-3 is a context-dependent transcriptional repressor

downstream of MAPK signaling cascades. *The Journal of biological chemistry* 2001, 276(23):20397-20406.

39. Cangemi R, Mensah A, Albertini V, Jain A, Mello-Grand M, Chiorino G, Catapano CV, Carbone GM: Reduced expression and tumor suppressor function of the ETS transcription factor ESE-3 in prostate cancer. *Oncogene* 2008, 27(20):2877-2885.

40. Lin X, Tirichine L, Bowler C: Protocol: Chromatin immunoprecipitation (ChIP) methodology to investigate histone modifications in two model diatom species. *Plant Methods* 2012, 8(1):48.

41. Liu CM, Wong T, Wu E, Luo R, Yiu SM, Li Y, Wang B, Yu C, Chu X, Zhao K *et al*: SOAP3: ultra-fast GPU-based parallel alignment tool for short reads. *Bioinformatics* 2012, 28(6):878-879.

42. Ewing B, Hillier L, Wendl MC, Green P: Base-calling of automated sequencer traces using phred. I. Accuracy assessment. *Genome Res* 1998, 8(3):175-185.

43. Liao P, Satten GA, Hu YJ: PhredEM: a phred-score-informed genotype-calling approach for next-generation sequencing studies. *Genet Epidemiol* 2017, 41(5):375-387.

44. Zhang Y, Liu T, Meyer CA, Eeckhoute J, Johnson DS, Bernstein BE, Nusbaum C, Myers RM, Brown M, Li W *et al*: Model-based analysis of ChIP-Seq (MACS). *Genome biology* 2008, 9(9):R137.

45. Heinz S, Benner C, Spann N, Bertolino E, Lin YC, Laslo P, Cheng JX, Murre C, Singh H, Glass CK: Simple combinations of lineage-determining transcription factors prime cis-regulatory elements required for macrophage and B cell identities. *Mol Cell* 2010, 38(4):576-589.

46. Yu G, Wang LG, He QY: ChIPseeker: an R/Bioconductor package for ChIP peak annotation, comparison and visualization. *Bioinformatics* 2015, 31(14):2382-2383.

47. Castro-Mondragon JA, Riudavets-Puig R, Rauluseviciute I, Lemma RB, Turchi L, Blanc-Mathieu R, Lucas J, Boddie P, Khan A, Manosalva Perez N *et al*: JASPAR 2022: the 9th release of the open-access database of transcription factor binding profiles. *Nucleic Acids Res* 2022, 50(D1):D165-D173.

48. Ross-Innes CS, Stark R, Teschendorff AE, Holmes KA, Ali HR, Dunning MJ, Brown GD, Gojis O, Ellis IO, Green AR *et al*: Differential oestrogen receptor binding is associated with clinical outcome in breast cancer. *Nature* 2012, 481(7381):389-393.

49. Michaloglou C, Crafter C, Siersbaek R, Delpuech O, Curwen JO, Carnevalli LS, Staniszevska AD, Polanska UM, Cheraghchi-Bashi A, Lawson M *et al*: Combined Inhibition of mTOR and CDK4/6 Is Required for Optimal Blockade

of E2F Function and Long-term Growth Inhibition in Estrogen Receptor-positive Breast Cancer. *Mol Cancer Ther* 2018, 17(5):908-920.

50. Lai CF, Flach KD, Alexi X, Fox SP, Ottaviani S, Thiruchelvam PT, Kyle FJ, Thomas RS, Launchbury R, Hua H *et al*: Co-regulated gene expression by oestrogen receptor alpha and liver receptor homolog-1 is a feature of the oestrogen response in breast cancer cells. *Nucleic Acids Res* 2013, 41(22):10228-10240.

51. Paulsen MT, Veloso A, Prasad J, Bedi K, Ljungman EA, Magnuson B, Wilson TE, Ljungman M: Use of Bru-Seq and BruChase-Seq for genome-wide assessment of the synthesis and stability of RNA. *Methods* 2014, 67(1):45-54.

52. Paulsen MT, Veloso A, Prasad J, Bedi K, Ljungman EA, Tsan YC, Chang CW, Tarrier B, Washburn JG, Lyons R *et al*: Coordinated regulation of synthesis and stability of RNA during the acute TNF-induced proinflammatory response. *Proceedings of the National Academy of Sciences of the United States of America* 2013, 110(6):2240-2245.

53. Szklarczyk D, Gable AL, Nastou KC, Lyon D, Kirsch R, Pyysalo S, Doncheva NT, Legeay M, Fang T, Bork P *et al*: The STRING database in 2021: customizable protein-protein networks, and functional characterization of user-uploaded gene/measurement sets. *Nucleic Acids Res* 2021, 49(D1):D605-D612.

54. Curtis C, Shah SP, Chin SF, Turashvili G, Rueda OM, Dunning MJ, Speed D, Lynch AG, Samarajiwa S, Yuan Y *et al*: The genomic and transcriptomic architecture of 2,000 breast tumours reveals novel subgroups. *Nature* 2012, 486(7403):346-352.

55. Pereira B, Chin SF, Rueda OM, Vollan HK, Provenzano E, Bardwell HA, Pugh M, Jones L, Russell R, Sammut SJ *et al*: The somatic mutation profiles of 2,433 breast cancers refines their genomic and transcriptomic landscapes. *Nat Commun* 2016, 7:11479.

56. Gao X, Vockley CM, Pauli F, Newberry KM, Xue Y, Randell SH, Reddy TE, Hogan BL: Evidence for multiple roles for grainyhead-like 2 in the establishment and maintenance of human mucociliary airway epithelium. *Proceedings of the National Academy of Sciences* 2013, 110(23):9356-9361.

57. Helzer KT, Szatkowski Ozers M, Meyer MB, Benkusky NA, Solodin N, Reese RM, Warren CL, Pike JW, Alarid ET: The Phosphorylated Estrogen Receptor alpha (ER) Cistrome Identifies a Subset of Active Enhancers Enriched for Direct ER-DNA Binding and the Transcription Factor GRHL2. *Mol Cell Biol* 2019, 39(3).

58. Kas K, Finger E, Grall F, Gu X, Akbarali Y, Boltax J, Weiss A, Oettgen P, Kapeller R, Libermann TA: ESE-3, a novel member of an epithelium-specific



ets transcription factor subfamily, demonstrates different target gene specificity from ESE-1. *The Journal of biological chemistry* 2000, 275(4):2986-2998.

59. Koedoot E, Wolters L, Smid M, Stoilov P, Burger GA, Herpers B, Yan K, Price LS, Martens JWM, Le Devedec SE *et al*: Differential reprogramming of breast cancer subtypes in 3D cultures and implications for sensitivity to targeted therapy. *Scientific reports* 2021, 11(1):7259.

60. Luk IY, Reehorst CM, Mariadason JM: ELF3, ELF5, EHF and SPDEF Transcription Factors in Tissue Homeostasis and Cancer. *Molecules* 2018, 23(9).

61. Sizemore GM, Pitarresi JR, Balakrishnan S, Ostrowski MC: The ETS family of oncogenic transcription factors in solid tumours. *Nat Rev Cancer* 2017, 17(6):337-351.

62. Labib K, Tercero JA, Diffley JF: Uninterrupted MCM2-7 function required for DNA replication fork progression. *Science* 2000, 288(5471):1643-1647.

63. Ji QK, Ma JW, Liu RH, Li XS, Shen FZ, Huang LY, Hui L, Ma YJ, Jin BZ: CDCA7L promotes glioma proliferation by targeting CCND1 and predicts an unfavorable prognosis. *Mol Med Rep* 2019, 20(2):1149-1156.

64. De Craene B, Berx G: Regulatory networks defining EMT during cancer initiation and progression. *Nat Rev Cancer* 2013, 13(2):97-110.

65. Varma S, Cao Y, Tagne JB, Lakshminarayanan M, Li J, Friedman TB, Morell RJ, Warburton D, Kotton DN, Ramirez MI: The transcription factors Grainyhead-like 2 and NK2-homeobox 1 form a regulatory loop that coordinates lung epithelial cell morphogenesis and differentiation. *The Journal of biological chemistry* 2012, 287(44):37282-37295.

66. Goossens S, Vandamme N, Van Vlierberghe P, Berx G: EMT transcription factors in cancer development re-evaluated: Beyond EMT and MET. *Biochim Biophys Acta Rev Cancer* 2017, 1868(2):584-591.

67. Park SM, Gaur AB, Lengyel E, Peter ME: The miR-200 family determines the epithelial phenotype of cancer cells by targeting the E-cadherin repressors ZEB1 and ZEB2. *Genes Dev* 2008, 22(7):894-907.

68. McDougall AR, Tolcos M, Hooper SB, Cole TJ, Wallace MJ: Trop2: from development to disease. *Dev Dyn* 2015, 244(2):99-109.

69. Liburkin-Dan T, Toledano S, Neufeld G: Lysyl Oxidase Family Enzymes and Their Role in Tumor Progression. *Int J Mol Sci* 2022, 23(11).

70. Chung VY, Tan TZ, Ye J, Huang RL, Lai HC, Kappei D, Wollmann H, Guccione E, Huang RY: The role of GRHL2 and epigenetic remodeling in epithelial-mesenchymal plasticity in ovarian cancer cells. *Communications biology* 2019, 2:272.

71. Jozwik KM, Chernukhin I, Serandour AA, Nagarajan S, Carroll JS: FOXA1 Directs H3K4 Monomethylation at Enhancers via Recruitment of the Methyltransferase MLL3. *Cell Rep* 2016, 17(10):2715-2723.
72. Kirkconnell KS, Paulsen MT, Magnuson B, Bedi K, Ljungman M: Capturing the dynamic nascent transcriptome during acute cellular responses: The serum response. *Biology open* 2016, 5(6):837-847.
73. Shi J, Qu Y, Li X, Sui F, Yao D, Yang Q, Shi B, Ji M, Hou P: Increased expression of EHF via gene amplification contributes to the activation of HER family signaling and associates with poor survival in gastric cancer. *Cell Death Dis* 2016, 7(10):e2442.
74. Cheng Z, Guo J, Chen L, Luo N, Yang W, Qu X: Knockdown of EHF inhibited the proliferation, invasion and tumorigenesis of ovarian cancer cells. *Mol Carcinog* 2016, 55(6):1048-1059.
75. Albino D, Civenni G, Rossi S, Mitra A, Catapano CV, Carbone GM: The ETS factor ESE3/EHF represses IL-6 preventing STAT3 activation and expansion of the prostate cancer stem-like compartment. *Oncotarget* 2016, 7(47):76756-76768.
76. Pastushenko I, Blanpain C: EMT Transition States during Tumor Progression and Metastasis. *Trends Cell Biol* 2019, 29(3):212-226.
77. Coban B, Bergonzini C, Zweemer AJM, Danen EHJ: Metastasis: crosstalk between tissue mechanics and tumour cell plasticity. *Br J Cancer* 2021, 124(1):49-57.
78. Mathiyalagan N, Miles LB, Anderson PJ, Wilanowski T, Grills BL, McDonald SJ, Keightley MC, Charzynska A, Dabrowski M, Dworkin S: Meta-Analysis of Grainyhead-Like Dependent Transcriptional Networks: A Roadmap for Identifying Novel Conserved Genetic Pathways. *Genes* 2019, 10(11).

## Supplementary Figures and Tables

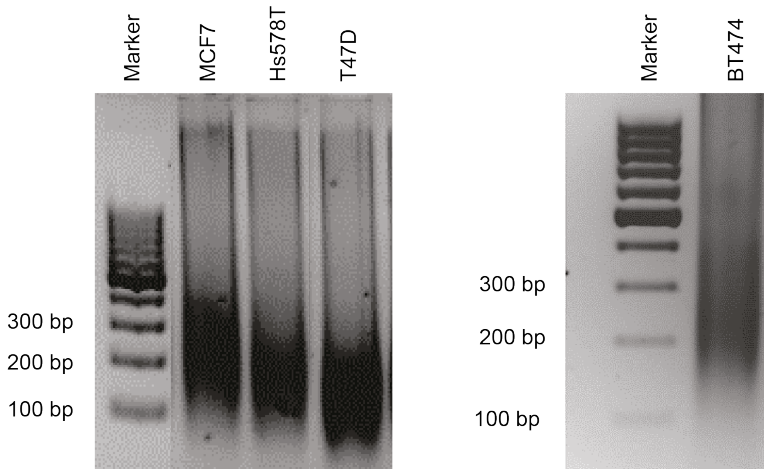


**Fig. S1. DNA fragmentation analysis by agarose gel electrophoresis.** After sonication, indicated samples were purified and loaded on 2% agarose gel.

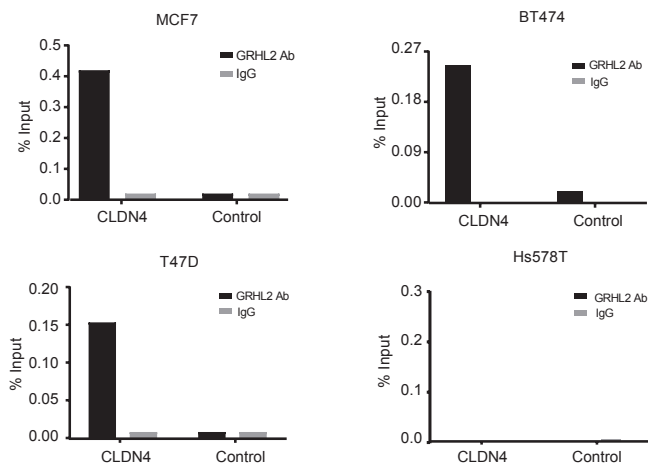


**Fig. S2. ChIP-qPCR validation of the isolated genomic DNA fragments.** Graphs represent the efficiency of *CLDN4* genomic DNA co-precipitation with anti-GRHL2

Ab (black bars) or IgG control Ab (grey bars). Detection was performed by qPCR using primers targeting the promoter region of *CLDN4* or targeting the intergenic region upstream of the *GAPDH* locus (Control). Results are shown for 3 GRHL2-positive luminal cell lines (MCF7, BT474 and T47D) and 1 GRHL2-negative basal-B cell line (Hs578T).

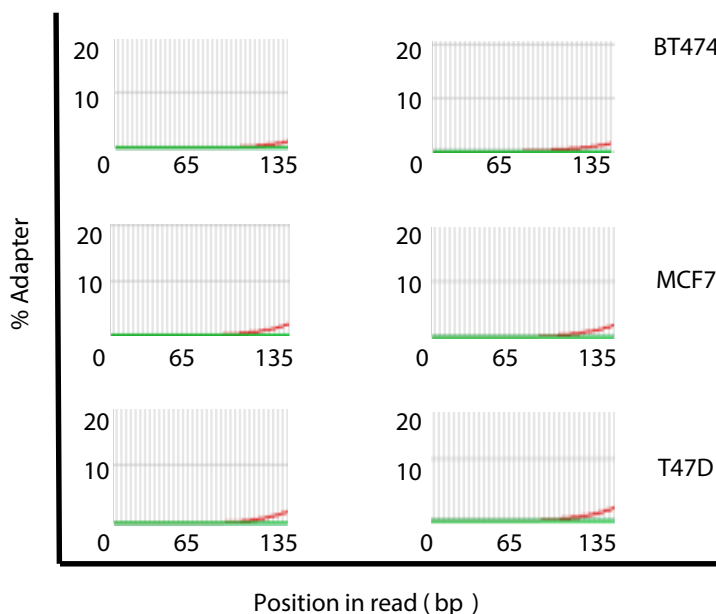


**Fig. S3. Cumulative presence of adapter sequences.** Results show that cumulative presence of adapter sequences is less than 5% in each cell sample, indicating that the data sets could be further analyzed without adapter-trimming.

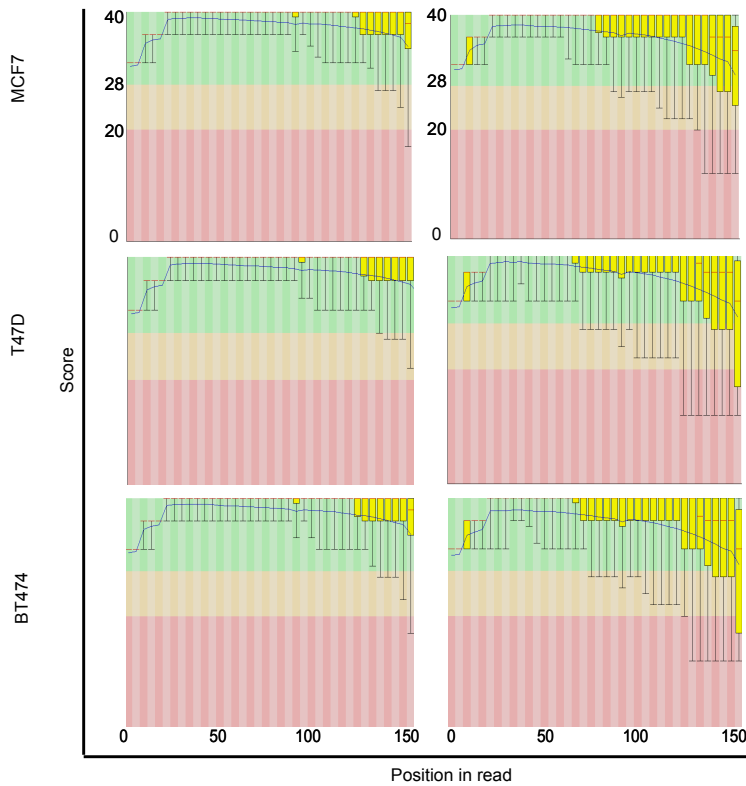


**Fig. S4. Per base sequence quality for all sequencing data sets.** Y axis is divided into high quality calls (green), reasonable quality calls (orange) and poor-quality calls (red). Analysis shows that the mean quality of base calls, indicated by the blue line, consistently remained in the green area, indicating that sequencing data sets were of high quality.

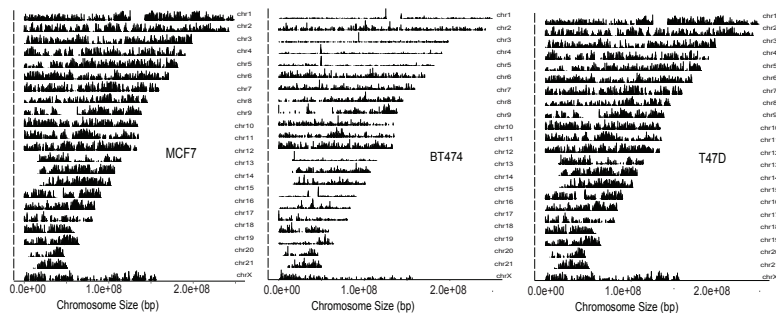


**Fig. S5. Coverage of peak regions across chromosomes.** Graphs represent the coverage of GRHL2 binding sites across all chromosomes in the indicated cell lines.

## GRHL2-controlled gene expression networks

---

ADAT3	ERBB3	LOC731157	SCOC
ADGRF4	ERP27	LRP10	SCOC-AS1
ADIPOQ	FAF1	MACC1	SEMA4A
ADK	FKBP2	MACROD1	SFTPA2
AIFM1	FLJ31356	<b>MAPK10</b>	SHPK
AIMP1	FMN1	MCEE	SLC10A5
ALDH3B2	FMO9P	MESP1	SLC25A45
AMD1	FOXA1	MGP	SLC40A1
ANKRD22	FRRS1	MIR4328	SLC41A3
ANXA9	GAR1	MIR4513	SLC4A7
ARHGAP24	GGTLC1	MIR4676	SLC9A1
ARHGAP32	GINS2	MIR6070	SLFN12
ARHGEF19	GMDS-AS1	MIR6773	SLITRK6
ARHGEF38	GMEB1	MIR6784	SMG8
ARRDC3	GMPR2	MIR8072	SNORA38
ARSD	GPNMB	MTERF2	SNORD13
ASCL2	GPR108	MUCL1	SORT1
ATAD3B	GRAMD1C	NAALADL2	SSR4P1
ATP5S	GRAMD3	NEBL-AS1	ST3GAL4
ATP6V0A4	HIST2H2AB	NEU1	STX17-AS1
B4GAT1	HIST2H2BF	NFATC4	STX19
BATF	HRH1	NIPAL2	SYTL5
BBOX1	IFRD1	NIPSNAP1	TBL1X
BCAS1	IGSF9	NME7	TGIF1
BMF	IKZF2	NXT1	TGM1
C1orf116	IQCK	OR7E91P	TIGAR
C4orf3	ITFG2	OVOL2	TJP2
CARD14	IVL	P2RY6	TMEM40
CBLB	JADE1	PAN2	TMEM79
CCDC12	JUP	PDCD2	TMPRSS11F
CD46	KCNJ13	PDE4D	<b>TMPRSS13</b>
CDC42SE1	KLK12	PDGFB	TP53INP2
CDS1	KRT80	PGAP3	TRIL
CFAP45	KRTAP3-1	<b>PGLYRP2</b>	TRPC4AP
CHD3	LACE1	PGR	TUFT1

## Chapter 3

CLCN3	LIMA1	PIK3C2G	TYSND1
<b>CLDN4</b>	LINC00346	PIM2	UBALD2
CLDN8	LINC00359	PKP2	UBE2A
CMTR2	LINC00437	PLA2G4B	URB1-AS1
CNP	LINC00456	PPEF1	VEPH1
COMT	<b>LINC00885</b>	PPOX	VGLL1
CREB3L4	LINC00938	PRIM2	VIPAS39
CRISP3	LINC01213	PROM2	WSB2
CSE1L-AS1	LINC01405	PRR15L	YAP1
CSTF1	LOC100129917	PSCA	<b>ZBTB20</b>
DAZAP1	LOC100132781	PTPN14	ZER1
DLG4	LOC100506207	PURG	ZMYND8
DLX5	LOC100506804	RAB25	ZNF20
DNAAF5	LOC100507175	RAP2B	ZNF274
DNAJC5B	LOC101927272	RASAL2	ZNF433
DSCAM-AS1	LOC101927296	RBBP8NL	ZNF44
EDEM2	LOC101927318	RBL2	ZNF440
EEA1	LOC101927391	RBM47	ZNF443
EEF1E1	LOC101927755	RIMS1	ZNF567
<b>EHF</b>	LOC101927911	RNF32	ZNF799
EIF2B5	LOC101929441	RNU5B-1	ZNF823
ELF5	LOC101929718	RNVU1-14	ZNHIT6
EPB41L1	LOC102724163	ROCK1P1	ZP1
EPHA1	LOC148709	RPL32P3	
<b>EPN3</b>	LOC344967	<b>RPL41</b>	

**Table. S1. Candidate GRHL2 target genes in luminal breast cancer cells displaying promoter interaction.** GRHL2 promotor interactions identified by ChIP-seq in 3 luminal breast cancer cell lines are listed. Genes also identified by Bru-seq in MCF7 conditional KO model showing up- or downregulation at one or more timepoints in response to GRHL2 loss are indicated in bold.



## GRHL2-controlled gene expression networks

Gene	Fold change				Cluster
	D2 AFC	D4 AFC	D8 AFC	D16 AFC	
ABCA4	0,93	2,23	5,48	3,87	
AC005821.1	2,79	6,46	12,24	6,54	Sustained induction
AC005972.4	3,53	4,29	6,38	2,59	Sustained induction
AC007952.4	0,17	0,19	0,32	0,61	Repression reset
AC008703.1	5,56	6,60	7,51	3,23	Sustained induction
AC009262.1	3,58	4,70	5,98	3,37	Sustained induction
AC010653.3	0,21	0,48	0,55	0,67	
AC013652.1	2,43	3,59	4,10	1,57	Induction reset
AC019209.3	1,43	3,61	4,91	4,29	
AC022166.1	0,00	0,00	0,00	35,23	
AC027277.2	0,26	0,23	0,38	0,68	Repression reset
AC027288.3	2,30	3,95	3,23	0,94	Induction reset
AC051619.5	5,12	4,51	3,69	2,64	Sustained induction
AC055854.1	0,50	0,32	0,27	0,45	Sustained repression
AC068633.1	7,14	0,00	0,00	12,59	Dynamic
AC083967.1	0,52	0,32	0,37	0,40	
AC084880.1	0,30	0,25	0,46	0,62	Repression reset
AC087762.1	4,99	13,04	20,78	6,49	Sustained induction
AC092167.1	8,40	7,04	5,45	2,93	Sustained induction
AC092422.1	85,82	0,02	0,04	63,37	Dynamic
AC098934.1	0,22	0,17	0,25	0,59	Repression reset
AC099520.1	2,93	4,54	5,11	2,30	Sustained induction
AC099753.1	91,52	0,00	0,00	211,15	Dynamic
AC103770.1	2,34	3,65	3,32	3,27	Sustained induction
AC109326.1	0,29	0,27	0,37	0,70	Repression reset
AC245014.3	0,26	0,23	0,32	0,56	Repression reset
ACKR3	0,70	0,61	1,36	2,68	
ACOXL	4,98	9,44	26,98	10,20	Sustained induction
ACTB	0,34	0,44	0,42	0,51	Repression reset
ACTG1	0,34	0,55	0,62	0,67	
ADCY5	1,23	2,33	4,74	6,93	
ADGRE3	3,38	0,05	0,08	11,85	Dynamic

## Chapter 3

	Fold change				
Gene	D2 AFC	D4 AFC	D8 AFC	D16 AFC	Cluster
AFF3	1,89	3,18	3,47	2,41	
AGPAT4	4,16	8,04	15,78	7,77	Sustained induction
AL049839.2	2,22	4,43	9,16	6,73	Sustained induction
AL132708.1	2,08	1,97	3,83	2,12	
AL137003.2	3,61	5,82	6,54	2,45	Sustained induction
AL137145.2	3,01	3,87	5,79	3,08	Sustained induction
AL139383.1	2,80	3,34	2,39	1,15	Induction reset
AL158066.1	0,53	0,14	0,15	0,29	
AL158847.1	1,50	2,01	3,17	3,33	
AL354740.1	2,61	4,43	4,57	2,31	Sustained induction
AL359976.1	12,40	13,35	31,68	3,11	Sustained induction
AL390726.6	8,20	8,75	9,71	4,52	Sustained induction
AL590004.4	3,58	6,52	15,14	6,33	Sustained induction
ALDH1A3	1,89	6,70	12,97	5,21	
ALDOA	0,33	0,33	0,48	0,71	Repression reset
ALOX5	3,48	5,47	10,74	8,74	Sustained induction
AMPH	1,75	2,73	6,38	4,16	
<b>ANKRD1</b>	1,39	4,68	5,06	1,90	
ANKRD29	3,32	6,49	8,05	6,63	Sustained induction
ANOS1	1,93	3,05	3,15	2,13	
ANXA3	5,19	8,86	6,80	2,41	Sustained induction
AP000880.1	0,16	0,12	0,12	0,41	Sustained repression
AP000924.1	1,55	4,57	11,84	8,49	
AP002761.4	0,23	0,26	0,40	1,11	
APRT	0,26	0,38	0,41	0,84	Repression reset
ARHGAP18	2,78	4,04	3,91	1,80	Induction reset
ARHGAP22	1,88	4,43	7,13	3,45	
ARHGAP42	2,55	4,45	4,23	1,84	Induction reset
ARHGEF28	0,68	0,57	0,44	0,42	
ARHGEF39	0,36	0,30	0,29	0,64	Repression reset
ARPC1A	0,17	0,25	0,29	0,21	Sustained repression
ARSJ	4,10	11,15	10,85	2,69	Sustained induction

## GRHL2-controlled gene expression networks

	Fold change				
Gene	D2 AFC	D4 AFC	D8 AFC	D16 AFC	Cluster
ATP10D	3,42	10,07	11,67	5,55	Sustained induction
ATP50	0,26	0,37	0,33	0,29	Sustained repression
ATP8A2	0,23	0,24	0,61	0,64	
ATXN1	2,17	3,38	3,79	2,18	Sustained induction
AURKB	0,32	0,20	0,26	0,50	Repression reset
BBC3	1,47	1,98	2,07	3,27	
BIRC5	0,38	0,25	0,25	0,49	Sustained repression
BMP1	1,99	3,51	5,20	3,49	
BOC	1,73	2,50	3,81	1,98	
C14orf80	0,28	0,34	0,36	1,28	
C1orf105	2,83	3,30	7,20	2,74	Sustained induction
C21orf58	0,42	0,27	0,32	0,73	Repression reset
C22orf34	19,17	0,00	0,04	33,04	Dynamic
<b>CADM1</b>	1,89	2,93	3,51	1,49	
<b>CADPS</b>	53,78	0,06	0,03	51,71	Dynamic
CAMK1D	1,92	3,14	3,93	1,98	
CAPN8	4,32	5,39	11,47	5,66	Sustained induction
CBX2	0,30	0,33	0,47	0,89	Repression reset
CCNF	0,38	0,28	0,31	0,72	Repression reset
CD109	2,27	2,56	4,55	2,54	Sustained induction
CDC20	0,27	0,30	0,30	0,67	Repression reset
CDCA3	0,33	0,26	0,27	0,51	Repression reset
CDCA5	0,36	0,25	0,29	0,64	Repression reset
<b>CDCA7L</b>	0,58	0,43	0,36	0,39	
CDH18	3,27	6,40	7,10	5,15	Sustained induction
CDKN2B	2,93	9,08	13,19	6,17	Sustained induction
CELF3	0,27	0,14	0,37	1,14	
CEMIP	2,07	1,74	4,07	3,24	
CENPF	0,50	0,29	0,28	0,40	Sustained repression
CFL1	0,32	0,42	0,45	0,63	Repression reset
CHTF18	0,33	0,34	0,43	1,12	
<b>CLDN4</b>	0,40	0,29	0,52	1,06	

## Chapter 3

	Fold change				
Gene	D2 AFC	D4 AFC	D8 AFC	D16 AFC	Cluster
CNTN4	22,17	0,05	5,10	26,44	Dynamic
COL4A5	3,79	7,76	10,60	5,61	Sustained induction
COL9A2	0,26	0,12	0,25	0,61	Repression reset
COLQ	2,50	2,83	3,71	1,81	Induction reset
<b>CORO2A</b>	1,50	2,23	2,49	2,76	
CPNE4	3,77	3,01	6,43	8,86	Sustained induction
CPQ	2,74	4,86	4,35	2,33	Sustained induction
CPXM2	0,40	0,27	0,29	0,62	Repression reset
CREB5	2,58	8,80	12,08	5,22	Sustained induction
CTNNA3	9,27	16,04	14,13	4,17	Sustained induction
CTNND2	2,53	3,46	3,60	1,57	Induction reset
CYB561	0,35	0,46	0,56	0,92	
CYC1	0,27	0,34	0,43	0,95	Repression reset
<b>DAPP1</b>	4,40	9,94	23,48	11,76	Sustained induction
<b>DDX11</b>	0,37	0,37	0,41	0,67	Repression reset
<b>DDX12P</b>	0,33	0,27	0,30	0,58	Repression reset
DDX41	0,33	0,48	0,52	0,77	
<b>DDX58</b>	2,25	2,17	3,26	4,00	Sustained induction
DDX60L	2,17	3,23	3,85	3,82	Sustained induction
DISC1	2,25	3,20	3,52	1,43	Induction reset
DLGAP2	20,26	0,01	0,02	24,32	Dynamic
DNAH5	3,07	4,84	6,54	3,08	Sustained induction
DNAH7	3,11	3,96	4,70	1,87	Induction reset
DNM3	1,78	2,03	3,69	1,55	
DOCK4	2,36	3,98	5,25	1,92	Induction reset
DOCK8	2,24	3,15	3,16	2,68	Sustained induction
DOK5	24,10	0,01	0,03	18,16	Dynamic
<b>DUSP10</b>	2,30	2,61	4,07	2,72	Sustained induction
E2F1	0,35	0,33	0,38	0,80	Repression reset
<b>E2F2</b>	0,31	0,28	0,33	0,77	Repression reset
EDA2R	3,81	3,40	2,15	1,75	Induction reset
EEF1A1	0,36	0,45	0,50	0,56	Repression reset

## GRHL2-controlled gene expression networks

Gene	Fold change				Cluster
	D2 AFC	D4 AFC	D8 AFC	D16 AFC	
EEF2	0,31	0,47	0,51	0,75	
EFNB2	1,18	1,44	2,17	3,08	
EHF	0,21	0,14	0,15	0,30	Sustained repression
ELL2	2,04	2,30	3,50	1,47	Induction reset
EPAS1	2,35	3,41	6,43	3,06	Sustained induction
EPB41L4A	2,23	3,14	3,26	2,28	Sustained induction
EPN3	0,22	0,30	0,46	1,10	
ERC2	2,15	4,80	8,43	8,33	Sustained induction
ESPL1	0,36	0,30	0,31	0,70	Repression reset
F2R	2,29	6,41	8,42	5,27	Sustained induction
FAM13A	2,62	2,74	5,96	3,59	Sustained induction
FAM83D	0,40	0,30	0,29	0,55	Repression reset
FANCG	0,29	0,30	0,37	0,72	Repression reset
FAU	0,26	0,29	0,33	0,38	Sustained repression
FBN2	1,94	2,24	5,55	2,60	
FBXL2	2,16	3,08	3,13	1,79	Induction reset
FEN1	0,30	0,26	0,30	0,50	Repression reset
FGF12	2,39	4,68	3,75	1,65	Induction reset
FHL2	2,47	3,00	4,81	3,10	Sustained induction
FLT1	5,25	7,58	9,04	3,34	Sustained induction
FLT3	3,73	5,93	5,81	3,09	Sustained induction
FOXP2	3,99	4,09	3,12	1,65	Induction reset
FRY	4,41	7,10	10,36	4,92	Sustained induction
FSTL4	2,31	4,03	7,89	4,83	Sustained induction
FTL	0,20	0,27	0,35	0,42	Sustained repression
FYN	1,58	3,13	4,03	2,52	
GALNT17	7,35	0,03	0,03	6,59	Dynamic
GAPDH	0,19	0,30	0,38	0,53	Repression reset
GBP2	9,04	5,34	5,68	3,34	Sustained induction
GLDN	2,12	2,36	3,32	1,39	Induction reset
GPR155	2,74	4,26	3,92	2,03	Sustained induction
GPR87	3,32	3,32	6,20	3,14	Sustained induction

## Chapter 3

	Fold change				
Gene	D2 AFC	D4 AFC	D8 AFC	D16 AFC	Cluster
GRK5	2,15	3,92	3,74	2,42	Sustained induction
GULP1	2,50	4,50	6,29	3,19	Sustained induction
H2AFZ	0,17	0,20	0,24	0,36	Sustained repression
<b>HAX1</b>	0,28	0,38	0,44	0,61	Repression reset
HDX	3,74	6,57	15,96	7,88	Sustained induction
HERC3	1,59	2,96	4,04	1,55	
HIST1H1C	0,15	0,10	0,14	0,44	Sustained repression
HIST1H1D	0,14	0,09	0,14	0,50	Sustained repression
HIST1H1E	0,12	0,11	0,14	0,37	Sustained repression
HIST1H2AB	0,16	0,08	0,12	0,47	Sustained repression
HIST1H2AE	0,20	0,10	0,15	0,40	Sustained repression
HIST1H2AI	0,12	0,08	0,11	0,38	Sustained repression
HIST1H2AJ	0,09	0,08	0,09	0,33	Sustained repression
HIST1H2AL	0,25	0,10	0,11	1,18	
HIST1H2AM	0,14	0,08	0,11	0,51	Repression reset
HIST1H2APS4	0,40	0,14	0,23	0,54	Repression reset
HIST1H2BF	0,24	0,13	0,19	0,46	Sustained repression
HIST1H2BG	0,27	0,21	0,31	0,72	Repression reset
HIST1H2BH	0,26	0,15	0,21	0,61	Repression reset
HIST1H2BI	0,13	0,10	0,11	0,31	Sustained repression
HIST1H2BK	0,14	0,10	0,13	0,30	Sustained repression
HIST1H2BM	0,16	0,10	0,11	0,29	Sustained repression
HIST1H2BO	0,14	0,09	0,14	0,41	Sustained repression
HIST1H3A	0,14	0,06	0,13	0,57	Repression reset
HIST1H3G	0,17	0,10	0,15	0,55	Repression reset
HIST1H3H	0,24	0,16	0,25	0,66	Repression reset
HIST1H3I	0,35	0,23	0,12	1,52	
HIST1H3J	0,16	0,09	0,11	0,60	Repression reset
HIST1H4A	0,12	0,12	0,11	0,49	Sustained repression
<b>HIST1H4B</b>	0,20	0,11	0,17	0,52	Repression reset
HIST1H4D	0,19	0,11	0,17	0,40	Sustained repression
<b>HIST1H4E</b>	0,19	0,17	0,25	0,54	Repression reset

## GRHL2-controlled gene expression networks

	Fold change				
Gene	D2 AFC	D4 AFC	D8 AFC	D16 AFC	Cluster
HIST1H4H	0,36	0,26	0,38	0,58	Repression reset
HIST1H4J	0,21	0,08	0,19	0,53	Repression reset
HIST2H2BE	0,39	0,27	0,34	0,66	Repression reset
HIST2H3D	0,19	0,17	0,16	2,15	Dynamic
HIST4H4	0,28	0,23	0,34	0,77	Repression reset
HJURP	0,36	0,28	0,28	0,53	Repression reset
HLA-DQB1	3,02	3,67	8,50	3,86	Sustained induction
<b>HMGB2</b>	0,25	0,23	0,29	0,46	Sustained repression
<b>HMMR</b>	0,54	0,32	0,25	0,39	
HR	0,22	0,25	0,29	0,82	Repression reset
HSD17B11	4,28	5,50	13,27	3,41	Sustained induction
HSP90AA1	0,19	0,41	0,33	0,24	Sustained repression
HSP90AB1	0,33	0,57	0,57	0,59	
HSPA8	0,26	0,35	0,37	0,41	Sustained repression
HSPE1	0,31	0,36	0,28	0,22	Sustained repression
IGSF21	3,81	0,01	0,01	7,50	Dynamic
IL18	1,84	4,63	8,54	3,08	
INCENP	0,30	0,25	0,28	0,58	Repression reset
IQCJ-SCHIP1	2,79	3,41	5,34	1,83	Induction reset
ISM1	1,75	3,28	4,45	1,57	
ITGB6	3,58	7,80	41,07	26,91	Sustained induction
JAZF1	2,15	5,12	5,89	2,88	Sustained induction
KC6	6,12	8,94	12,80	6,63	Sustained induction
KCNJ3	2,03	3,56	6,40	4,08	Sustained induction
KCNK5	0,32	0,17	0,19	0,63	Repression reset
KCNMA1	1,33	1,96	4,48	4,79	
<b>KIAA0513</b>	2,04	3,14	3,92	2,80	Sustained induction
KIAA2012	3,22	9,67	16,82	6,56	Sustained induction
KIF20A	0,26	0,23	0,20	0,37	Sustained repression
KIF2C	0,41	0,25	0,28	0,48	Sustained repression
<b>KIF5C</b>	1,26	2,82	3,91	3,14	
KIFC1	0,46	0,29	0,29	0,55	Repression reset

## Chapter 3

	Fold change				
Gene	D2 AFC	D4 AFC	D8 AFC	D16 AFC	Cluster
LAD1	0,32	0,41	0,56	1,13	
LAMA3	2,00	3,34	3,66	2,74	
<b>LAMB3</b>	2,80	4,79	12,02	8,49	Sustained induction
LAMC2	2,16	5,02	9,71	4,78	Sustained induction
LHFPL2	1,33	2,47	3,55	2,16	
<b>LIMCH1</b>	1,86	2,56	4,45	2,02	
LINC00473	7,90	6,05	6,28	2,90	Sustained induction
LINC00871	6,51	4,62	1,99	2,96	
<b>LINC00885</b>	0,30	0,17	0,19	0,42	Sustained repression
LINC01191	2,10	5,99	7,73	3,26	Sustained induction
LINC01214	9,20	17,88	43,41	27,34	Sustained induction
LINC01239	4,14	12,86	31,60	7,78	Sustained induction
LINC01619	0,83	0,51	0,51	0,42	
LIPH	2,58	3,13	3,99	1,76	Induction reset
LOXL2	2,08	4,69	7,79	4,69	Sustained induction
LRP2	3,27	4,71	4,54	2,99	Sustained induction
LUCAT1	2,68	6,05	8,36	3,28	Sustained induction
LYPD1	3,00	5,93	9,53	3,41	Sustained induction
LYPD3	0,17	0,17	0,31	0,73	Repression reset
MAF	0,00	0,00	19,71	31,48	
MAP1B	2,55	9,39	16,96	6,44	Sustained induction
<b>MAPK10</b>	2,62	3,10	2,61	1,33	Induction reset
MAPRE2	3,71	8,07	16,19	10,23	Sustained induction
MAPRE3	1,78	2,44	3,22	2,17	
MCF2L2	2,37	3,05	3,15	1,64	Induction reset
MCM2	0,34	0,33	0,33	0,68	Repression reset
MCM7	0,36	0,30	0,37	0,58	Repression reset
MCTP1	2,92	5,77	5,33	4,05	Sustained induction
MDGA2	3,42	6,23	7,58	3,42	Sustained induction
MECOM	3,20	5,13	5,05	2,54	Sustained induction
MIR222HG	1,63	3,09	5,04	3,01	
MIR3681HG	4,80	0,07	0,06	6,43	Dynamic



## GRHL2-controlled gene expression networks

	Fold change				
Gene	D2 AFC	D4 AFC	D8 AFC	D16 AFC	Cluster
MIR9-3HG	0,35	0,31	0,43	0,78	Repression reset
MITF	1,61	3,58	5,49	2,22	
MKI67	0,42	0,28	0,27	0,38	Sustained repression
MMP16	2,17	2,97	3,27	2,91	Sustained induction
MPPED2	0,75	0,59	0,41	0,35	
MRFAP1	0,33	0,47	0,50	0,59	
MRPL17	0,33	0,40	0,48	0,74	Repression reset
MRPL51	0,25	0,28	0,28	0,38	Sustained repression
MRPS34	0,25	0,28	0,29	0,65	Repression reset
MSMB	0,21	0,11	0,15	0,33	Sustained repression
<b>MTUS2</b>	2,69	2,31	5,20	2,93	Sustained induction
MYT1L	32,55	0,05	0,00	37,70	Dynamic
NBEA	2,41	3,23	3,26	1,63	Induction reset
NCF2	2,94	6,23	23,18	17,27	Sustained induction
NECTIN4	0,26	0,30	0,48	0,96	Repression reset
NEK10	1,50	2,78	6,78	2,59	
NHS	1,47	2,47	3,20	1,40	
NHSL2	3,09	4,61	6,21	3,48	Sustained induction
NLGN1	7,50	0,02	0,00	17,12	Dynamic
NME1	0,28	0,38	0,37	0,39	Sustained repression
NPAS3	2,72	4,13	3,49	1,06	Induction reset
NPM1P27	0,27	0,40	0,50	0,33	Sustained repression
<b>NPY1R</b>	0,81	0,33	0,20	0,19	
NR2C2AP	0,23	0,24	0,34	0,58	Repression reset
NRG2	3,76	8,84	10,44	3,37	Sustained induction
NRP1	2,18	3,57	3,13	1,58	Induction reset
NRXN3	10,82	0,94	1,45	11,75	
NT5DC2	0,28	0,42	0,46	0,85	Repression reset
NTN4	5,48	13,04	18,44	9,78	Sustained induction
NUDT1	0,26	0,23	0,28	0,67	Repression reset
OPCML	27,66	0,03	0,04	38,49	Dynamic
OPTN	1,69	3,76	6,50	5,12	

## Chapter 3

	Fold change				
Gene	D2 AFC	D4 AFC	D8 AFC	D16 AFC	Cluster
PACSN3	0,31	0,37	0,36	0,91	Repression reset
PALM2	2,42	4,65	4,73	1,72	Induction reset
PALM2- AKAP2	3,43	4,12	5,24	2,77	Sustained induction
PAPSS2	2,57	6,14	7,88	3,34	Sustained induction
PAQR5	1,21	1,66	1,91	3,05	
PCAT29	4,40	5,18	7,17	4,08	Sustained induction
PCSK2	63,00	0,05	0,00	99,27	Dynamic
<b>PGLYRP2</b>	0,18	0,09	0,03	0,27	Sustained repression
PGM2L1	2,30	2,73	4,43	2,62	Sustained induction
PHACTR3	40,57	0,04	0,06	47,82	Dynamic
PHGDH	0,22	0,29	0,31	0,65	Repression reset
PHLDB2	3,97	8,37	11,66	5,28	Sustained induction
PID1	1,84	3,60	10,27	7,22	
PIF1	0,45	0,28	0,28	0,55	Repression reset
PIK3IP1-AS1	5,12	6,17	7,66	3,53	Sustained induction
PIMREG	0,24	0,24	0,21	0,62	Repression reset
PKP1	0,27	0,18	0,19	0,73	Repression reset
PLCE1	2,78	9,19	9,46	2,97	Sustained induction
PLCXD2	4,35	9,62	12,79	5,07	Sustained induction
PLD1	3,98	7,92	7,69	2,78	Sustained induction
PLEKHH2	3,60	4,43	4,97	2,15	Sustained induction
PLIN4	0,11	0,03	0,09	0,34	Sustained repression
PLIN5	0,19	0,04	0,12	0,41	Sustained repression
PMP22	3,24	4,41	4,84	3,59	Sustained induction
POP7	0,30	0,30	0,40	0,71	Repression reset
PPARG	2,63	4,37	10,14	3,87	Sustained induction
PPIAP22	0,11	0,18	0,20	0,18	Sustained repression
<b>PPP1CA</b>	0,27	0,32	0,42	0,63	Repression reset
PPP1R14B	0,28	0,38	0,54	0,85	
PRELID1	0,33	0,36	0,41	0,60	Repression reset
PRICKLE2-AS1	2,03	3,23	3,48	1,32	Induction reset

## GRHL2-controlled gene expression networks

Gene	Fold change				Cluster
	D2 AFC	D4 AFC	D8 AFC	D16 AFC	
PROS1	2,99	3,62	4,27	1,93	Induction reset
<b>PRSS23</b>	2,39	4,01	5,50	5,31	Sustained induction
PSG5	2,07	7,09	9,24	7,10	Sustained induction
<b>PSMB6</b>	0,31	0,37	0,45	0,47	Sustained repression
PSMC3	0,34	0,45	0,48	0,67	Repression reset
PSMD2	0,36	0,52	0,61	0,63	
PSMG3	0,31	0,33	0,39	0,79	Repression reset
PSRC1	0,30	0,23	0,33	0,63	Repression reset
PTTG1	0,33	0,26	0,23	0,45	Sustained repression
PYCR1	0,24	0,37	0,37	0,90	Repression reset
QARS	0,30	0,44	0,43	0,66	Repression reset
RAB7B	3,72	4,73	14,45	7,71	Sustained induction
RAI2	2,11	3,70	8,48	4,74	Sustained induction
RBFOX1	2,27	0,74	0,52	3,17	
RBFOX3	34,53	0,01	0,02	39,26	Dynamic
RCAN2	9,68	1,28	20,29	16,55	
RECQL4	0,28	0,33	0,30	0,89	Repression reset
REEP4	0,24	0,27	0,34	0,99	Repression reset
RETREG1	2,37	3,64	3,37	2,27	Sustained induction
RFTN1	3,06	4,72	6,29	4,49	Sustained induction
RN7SL2	0,22	0,34	0,42	0,71	Repression reset
RN7SL3	0,29	0,45	0,54	0,86	
RN7SL4P	0,18	0,29	0,36	0,74	Repression reset
RNASEH2A	0,25	0,23	0,27	0,61	Repression reset
<b>RND3</b>	2,35	3,96	5,16	3,64	Sustained induction
RNF150	3,46	6,36	7,42	2,48	Sustained induction
RNF219-AS1	54,69	0,00	0,00	71,81	Dynamic
RNU1-120P	0,17	0,16	0,27	0,62	Repression reset
RNU1-122P	0,15	0,15	0,27	0,62	Repression reset
RNU2-63P	0,18	0,20	0,34	0,79	Repression reset
RNU4-1	0,17	0,18	0,30	0,91	Repression reset
RNU5D-1	0,14	0,29	0,43	0,53	Repression reset

## Chapter 3

	Fold change				
Gene	D2 AFC	D4 AFC	D8 AFC	D16 AFC	Cluster
RNVU1-6	0,17	0,15	0,21	0,67	Repression reset
RNVU1-7	0,20	0,22	0,24	0,59	Repression reset
RPL13A	0,32	0,41	0,49	0,64	Repression reset
RPL17	0,33	0,40	0,48	0,57	Repression reset
RPL3	0,30	0,48	0,55	0,72	
RPL35	0,32	0,38	0,41	0,58	Repression reset
RPL41	0,30	0,38	0,49	0,69	Repression reset
RPL7	0,33	0,47	0,46	0,42	Sustained repression
RPL7A	0,36	0,44	0,47	0,48	Sustained repression
RPL8	0,30	0,37	0,37	0,50	Repression reset
RPL9P9	0,15	0,27	0,18	0,25	Sustained repression
RPS10	0,32	0,37	0,34	0,28	Sustained repression
RPS11	0,35	0,37	0,40	0,46	Sustained repression
RPS2	0,28	0,34	0,35	0,61	Repression reset
RPS21	0,28	0,32	0,36	0,48	Sustained repression
RPS6KA2	2,48	2,79	3,13	2,78	Sustained induction
RPS8	0,33	0,41	0,38	0,47	Sustained repression
RTN1	2,33	5,02	4,89	2,28	Sustained induction
S100A14	0,34	0,52	0,50	0,57	
SAMD12	2,42	3,61	4,11	2,57	Sustained induction
SAMD12-AS1	3,99	6,35	7,19	4,12	Sustained induction
SAMD9	0,00	0,00	19,92	37,58	
SAPCD2	0,24	0,27	0,28	0,76	Repression reset
SCARNA12	0,14	0,20	0,26	0,26	Sustained repression
SCARNA13	0,22	0,32	0,48	0,47	Sustained repression
SCARNA21	0,08	0,10	0,10	0,22	Sustained repression
SCARNA7	0,17	0,31	0,55	0,31	
SDC1	0,28	0,35	0,48	0,97	Repression reset
SEMA6A	2,34	3,48	4,69	3,74	Sustained induction
SEPT8	0,35	0,66	0,82	1,11	
SESN3	6,90	10,94	12,91	7,02	Sustained induction
SFN	0,21	0,34	0,34	0,61	Repression reset

## GRHL2-controlled gene expression networks

	Fold change				
Gene	D2 AFC	D4 AFC	D8 AFC	D16 AFC	Cluster
SHC4	2,49	2,64	5,43	2,78	Sustained induction
SHMT2	0,22	0,39	0,42	0,82	Repression reset
SLC12A4	1,98	3,93	4,88	5,01	
<b>SLC16A3</b>	0,16	0,17	0,28	0,91	Repression reset
SLC1A1	6,72	11,29	17,89	10,80	Sustained induction
SLC22A1	1,68	4,62	6,00	3,78	
SLC22A15	2,05	2,94	3,12	1,68	Induction reset
SLC25A5	0,24	0,27	0,33	0,40	Sustained repression
SLC9A3	0,31	0,00	0,00	103,49	Dynamic
SLIT3	4,89	0,03	0,63	3,96	Dynamic
SMAGP	0,37	0,26	0,35	0,56	Repression reset
SNORD3A	0,10	0,13	0,19	0,27	Sustained repression
SNORD3B-1	0,19	0,23	0,32	0,67	Repression reset
SNORD3B-2	0,14	0,18	0,26	0,62	Repression reset
SOCS2-AS1	6,58	8,39	9,17	3,76	Sustained induction
SORCS2	1,61	2,38	3,41	2,64	
SOX9	3,49	6,38	11,38	12,66	Sustained induction
SOX9-AS1	3,93	3,43	2,82	2,14	Sustained induction
SPAG5	0,34	0,30	0,31	0,45	Sustained repression
<b>SPATA18</b>	4,04	4,13	2,47	1,69	Induction reset
SPEG	1,99	2,92	4,04	4,71	
SPOCK1	2,23	3,00	16,72	4,48	Sustained induction
SSNA1	0,22	0,27	0,39	0,74	Repression reset
SSRP1	0,33	0,44	0,45	0,58	Repression reset
ST3GAL5	1,49	2,64	4,09	3,44	
STAT4	2,50	6,67	5,66	2,00	Sustained induction
STUM	1,75	2,22	10,66	13,14	
SULF1	0,60	0,31	0,26	0,17	
SUN2	0,35	0,33	0,43	0,67	Repression reset
<b>SYNPO</b>	3,53	6,07	6,99	4,11	Sustained induction
SYNPR	8,34	0,01	0,01	10,33	Dynamic
SYT7	0,34	0,30	0,40	0,97	Repression reset

## Chapter 3

	Fold change				
Gene	D2 AFC	D4 AFC	D8 AFC	D16 AFC	Cluster
TANC2	2,06	3,16	3,40	1,56	Induction reset
TENM2	25,34	0,03	6,08	23,79	Dynamic
TFPI	1,65	2,39	3,30	2,04	
TGFB2	2,27	6,07	5,70	1,71	Induction reset
TGFB1	2,92	6,30	9,58	4,64	Sustained induction
TGFB2	3,05	6,81	8,02	2,99	Sustained induction
<b>THAP11</b>	0,20	0,23	0,29	0,81	Repression reset
THEG	0,23	0,07	0,15	0,19	Sustained repression
TIMP3	2,61	5,50	11,16	10,20	Sustained induction
TK1	0,32	0,26	0,31	0,70	Repression reset
TMC7	2,24	3,32	4,00	2,10	Sustained induction
TMEM107	0,22	0,20	0,31	0,47	Sustained repression
TMEM132C	38,52	0,00	0,00	50,13	Dynamic
TMEM132D	19,00	0,00	0,02	34,41	Dynamic
<b>TMEM140</b>	9,19	13,96	32,13	31,21	Sustained induction
TMEM156	4,33	4,22	20,11	4,15	Sustained induction
TMEM54	0,12	0,20	0,29	0,95	Repression reset
<b>TMPRSS13</b>	0,25	0,23	0,39	0,85	Repression reset
<b>TMPRSS4</b>	0,33	0,23	0,45	1,02	
TNFAIP8	2,41	2,92	3,91	1,62	Induction reset
TNIK	3,56	8,40	17,63	7,90	Sustained induction
TONSL	0,33	0,36	0,39	1,10	
TP53INP1	3,11	3,01	3,30	2,22	Sustained induction
TP63	1,61	4,51	34,52	16,43	
TPI1	0,23	0,34	0,41	0,52	Repression reset
TRAIP	0,38	0,25	0,28	0,67	Repression reset
TROAP	0,36	0,28	0,27	0,56	Repression reset
TSPAN5	2,38	3,86	6,41	2,92	Sustained induction
TUBA1B	0,19	0,22	0,25	0,45	Sustained repression
TUBB	0,30	0,33	0,36	0,56	Repression reset
TUBB4B	0,23	0,29	0,36	0,58	Repression reset
TXNIP	0,31	0,22	0,36	0,44	Sustained repression

## GRHL2-controlled gene expression networks

Gene	Fold change				Cluster
	D2 AFC	D4 AFC	D8 AFC	D16 AFC	
U1	0,24	0,18	0,33	0,79	Repression reset
U3	1,24	2,17	1,95	1,80	
UBB	0,31	0,38	0,49	0,40	Sustained repression
UBE2C	0,28	0,21	0,22	0,58	Repression reset
UBE2QL1	2,07	4,53	5,32	4,16	Sustained induction
UBL4A	0,30	0,22	0,30	0,58	Repression reset
<b>UHRF1</b>	0,33	0,27	0,32	0,68	Repression reset
UNC13C	24,62	0,10	0,06	38,12	Dynamic
UPP1	2,23	5,94	9,75	5,93	Sustained induction
UQCRQ	0,30	0,37	0,42	0,41	Sustained repression
USH2A	13,62	0,02	0,03	16,11	Dynamic
USP35	0,70	1,09	1,54	2,77	
<b>VMP1</b>	2,60	2,37	3,02	1,93	Induction reset
VSTM2B	7,96	0,00	0,00	36,91	Dynamic
WIPF1	3,54	5,91	6,80	4,04	Sustained induction
<b>WIPI1</b>	2,38	3,25	4,19	2,56	Sustained induction
WLS	2,59	3,48	3,91	2,16	Sustained induction
XRCC3	0,35	0,40	0,44	0,93	Repression reset
YPEL2	3,21	2,79	4,50	3,36	Sustained induction
Z93241.1	0,24	0,21	0,31	0,63	Repression reset
<b>ZBTB20</b>	3,17	2,79	5,25	2,21	Sustained induction
ZMAT4	1,72	5,72	14,92	5,98	
ZNF365	3,77	6,06	11,52	6,65	Sustained induction
ZNF385B	2,87	4,23	3,30	1,93	Induction reset
ZNF462	1,97	3,33	3,52	1,65	
ZNF827	2,41	3,25	3,03	1,78	Induction reset
ZWINT	0,29	0,26	0,33	0,64	Repression reset

**Table S2. GRHL2-regulated genes identified by Bru-seq in MCF7 conditional KO model.** AFC for indicated genes at the indicated timepoints (days) post induction of GRHL2 KO identified by Bru-seq in MCF7 conditional KO model and assignment

## Chapter 3

---

to clusters is shown. Genes also displaying promoter interaction identified by ChIP-seq in MCF7 cells are indicated in bold.



# Chapter 4

---

## GRHL2 regulation of growth/motility balance in luminal versus basal breast cancer

Published in: Zi Wang<sup>1</sup>, Bircan Coban<sup>1</sup>, Chen-Yi Liao<sup>1</sup>, Yao-Jun Chen<sup>1</sup>, Qiuyu Liu<sup>1</sup>, Erik HJ Danen<sup>1</sup>. GRHL2 Regulation of Growth/Motility Balance in Luminal versus Basal Breast Cancer. *Int. J. Mol. Sci.* 2023, 24, 2512.

<sup>1</sup> Division of Drug Discovery and Safety, Leiden Academic Center for Drug Research, Leiden University, The Netherlands.

\* Correspondence: Erik HJ Danen; e.danen@lacdr.leidenuniv.nl; Division of Drug Discovery and Safety, Leiden Academic Center for Drug Research, Leiden University, Einsteinweg 55, 2333CC Leiden, The Netherlands

### **Abstract:**

The transcription factor Grainyhead-like 2 (GRHL2) is a critical transcription factor for epithelial tissues that has been reported to promote cancer growth in some- and suppress aspects of cancer progression in other studies. We investigated its role in different breast cancer subtypes. In breast cancer patients, GRHL2 expression was increased in all subtypes and inversely correlated with recurrence-free and distant metastasis-free survival. In a large cell line panel, GRHL2 expression was expressed in luminal- and basal A cells but low or absent in basal B cells. Inter-section of ChIP-Seq analysis in 3 luminal and 3 basal A cell lines identified conserved GRHL2 binding sites for both subtypes. Pathway analysis of ChIP-seq data revealed cell-cell junction regulation and epithelial migration as well as epithelial proliferation as candidate GRHL2-regulated processes and further analysis of hub genes in these pathways showed similar regulatory networks in both subtypes. However, GRHL2 deletion in a luminal cell line caused cell cycle arrest while this was less prominent in a basal A cell line. Conversely, GRHL2 loss triggered enhanced migration in the basal A cells but failed to do so in the luminal cell line. ChIP-Seq and ChIP-qPCR demonstrated GRHL2 binding to CLDN4 and OVOL2 in both subtypes but not to other GRHL2 targets controlling cell-cell adhesion that were previously identified in other cell types, including CDH1 and ZEB1. Nevertheless, E-cadherin protein expression was decreased upon GRHL2 deletion especially in the luminal line and, in agreement with its selectively enhanced migration, only the basal A cell line showed concomitant induction of Vimentin and N-cadherin. To address how the balance between growth reduction and aspects of EMT upon loss of GRHL2 affected in vivo behavior, we used a mouse basal A orthotopic transplantation model in which the GRHL2 gene was silenced. This resulted in reduced primary tumor growth and a reduction in number and size of lung colonies, indicating that growth suppression was the predominant consequence of GRHL2 loss. Altogether, these findings point to largely common but also distinct roles for GRHL2 in luminal- and basal breast cancers with respect to growth and motility and indicate that, in agreement with its negative association with patient survival, growth suppression is the dominant response to GRHL2 loss.

**Keywords:** Breast cancer; luminal-like; basal-like; GRHL2.

### 1. Introduction

Breast cancer is the most prevalent malignancy in females globally. Mortality of patients with breast cancer has decreased, resulting from early diagnosis and development of therapies [1-3]. A considerable proportion of knowledge on breast cancer originates from experiments performed with breast cancer cells that cover the various subtypes of this heterogeneous disease [4]. Breast cancer is divided into luminal (luminal A and luminal B), epidermal growth factor receptor 2-enriched (HER2-enriched), basal (basal A and basal B), claudin-low, and normal-like subtypes based on gene expression profiling [5]. The most common subtype of breast cancer is luminal that originates from luminal cells in the duct [6]. It is characterized by enrichment of genes/proteins associated with the luminal epithelial phenotype (e.g., ESR1, GATA3 and FOXA1) [4,7]. Basal breast cancer is characterized by significant enrichment of basal epithelial cytokeratins, hormone receptor negativity and a high tumor grade and poor prognosis [8]. Basal breast cancer can be further divided into basal A and basal B subtypes [9]. The basal A subtype is enriched with basal markers such as cytokeratins (e.g., Cytokeratin 4), while basal-B exhibits a mesenchymal or a normal-like phenotype with overexpression of several genes related to tumor invasion and tumor stemness [4].

The Grainyhead (GRH) gene was originally discovered through a mutation that causes slack and fragile cuticles in *Drosophila* [10]. Loss of function of the GRH results in failure of neural tube closure during embryogenesis [11]. In mammals, members of the highly conserved Grainyhead like (GRHL) family directly or indirectly regulate transcription of the genes encoding epithelial cell-cell junction proteins in adherens junctions and tight junctions [12-14]. In humans, GRHL1, GRHL2 and GRHL3 are identified as GRH homologs that contain an N-terminal transcriptional activation domain, a central CP2 DNA-binding domain and a C-terminal dimerization domain [15,16]. GRHL2 has been found to serve as a pioneer factor, cooperating with FOXA1 and ER $\alpha$  to regulate gene expression [15,17,18]. >5000 GRHL2 binding sites have been reported in epithelial cells but there is limited overlap between different

tissues and regulation of several GRHL2 responsive genes has been found to be indirect [13,14,19-21].

GRHL2 has been implicated in cancer development and progression. GRHL2 has been shown to act as a tumor metastasis suppressor, by opposing epithelial-mesenchymal transition (EMT) through upregulation of epithelial markers or downregulation of mesenchymal markers [20,22,23]. In contrast, GRHL2 is located on chromosome 8q22 that is frequently amplified or overexpressed in many cancers and hence may rather have an oncogenic function [24-27]. Indeed, in prostate cancer [28], breast cancer [23], lung cancer [29] and ovarian cancer [30] downregulation of GRHL2 has been associated with inhibition of cell proliferation. Together, this suggests that GRHL2 function may vary depending on the cancer cell context.

In this study, we investigated the role of GRHL2 in different breast cancer subtypes. Our findings show that GRHL2 is absent in basal B breast cancer cells, it is expressed in luminal breast cancer cells where its depletion causes an arrested proliferation, and it is expressed in basal A where its depletion triggers a slow growth/high motility phenotype and *in vivo*, growth arrest is the dominant response to GRHL2 depletion, in line with its overexpression in breast cancer patients.

## 2. Results

### *2.1. GRHL2 is associated with poor prognosis but is downregulated in basal B subtype breast cancer*

In order to evaluate the clinical relevance of GRHL2 in breast cancer, GRHL2 alternations were examined in a series of published cohorts. GRHL2 is located on chromosome 8q22.3, a genomic region that is frequently amplified or overexpressed in many cancers [25,28]. The expression of GRHL2 mRNA and protein was significantly higher in tumor versus normal tissue for all breast cancer subtypes analyzed (Fig. 1A, B). No statistically significant association of GRHL2 mRNA expression with overall survival was detected in luminal-like breast cancer (Fig. 2C). However, GRHL2 mRNA expression was negatively associated with overall survival in basal-like breast cancer patients (Fig. 2D). In agreement with an earlier report exploring a different panel of

cell lines [22], using RNA-seq data of 52 human breast cancer cell lines [35] we found that GRHL2 mRNA was low or absent in most breast cancer cell lines representing the basal B subtype and expressed in all luminal and basal A cell lines (Fig. 2A, B). Notably, this analysis suggested that HCC1500 and SUM149PT may have been misclassified. Indeed, SUM149PT has been previously classified as basal A or basal B subtype [9,42] and reported to contain different subpopulations, according to expression level of EpCAM and CD49f surface markers [43]. Likewise, HCC1500 cells have been classified as luminal, due to a predominant population of cells that are positive for EpCAM and CD24 [3] or as basal B, owing to an enrichment for gene clusters associated with cancer stem cell- and invasive phenotypes [9]. In agreement with the RNA-seq analysis, GRHL2 protein and mRNA were not detectable in Hs578T basal B cells, whereas luminal (MCF7, T47D and BT474) and basal A cell lines (HCC1806, MDA-MB-468 and BT20) all expressed GRHL2, albeit at different levels (Fig. 2C, D). This was correlated with expression of E-cadherin, a cell adhesion receptor previously identified as a target of GRHL2 that is downregulated in cells undergoing EMT [23,44].

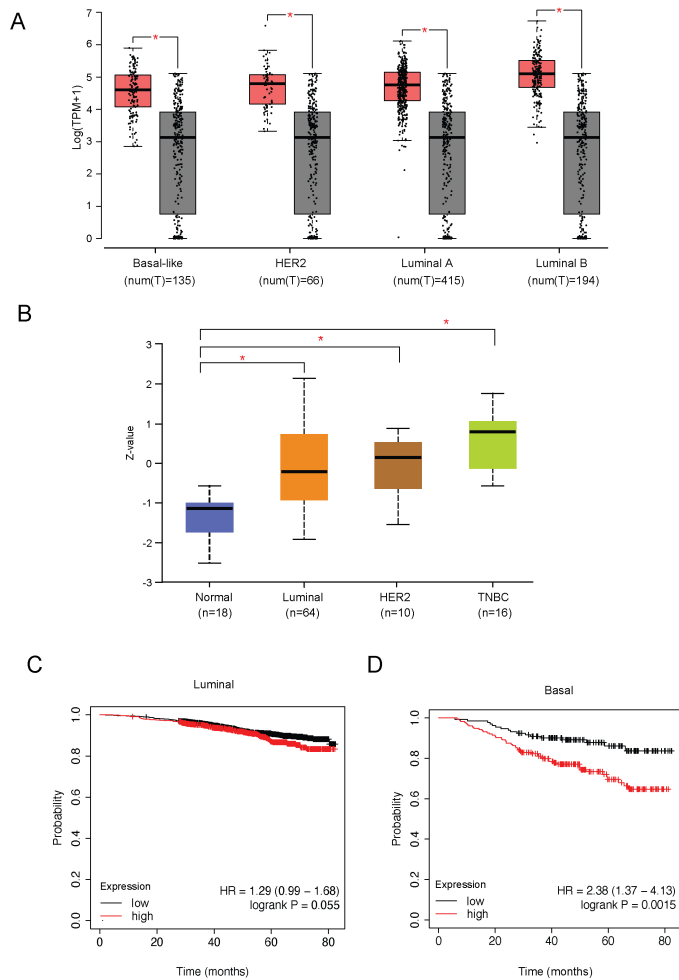


**Fig. 1. GRHL2 expression in breast cancer. (A, B)** The expression of GRHL2 mRNA **(A)** and protein **(B)** in different subtypes of breast cancer based on analyzing data from TCGA, GTEx and CPATC databases. TPM, transcripts per million. \* Indicates  $p < 0.01$ . Red and gray blocks in **(A)** represent tumor and normal samples, respectively. Dots show full distribution of all samples in the given group. **(C, D)** Association of GRHL2 expression with overall survival based on analyzing data from KM plotter database.

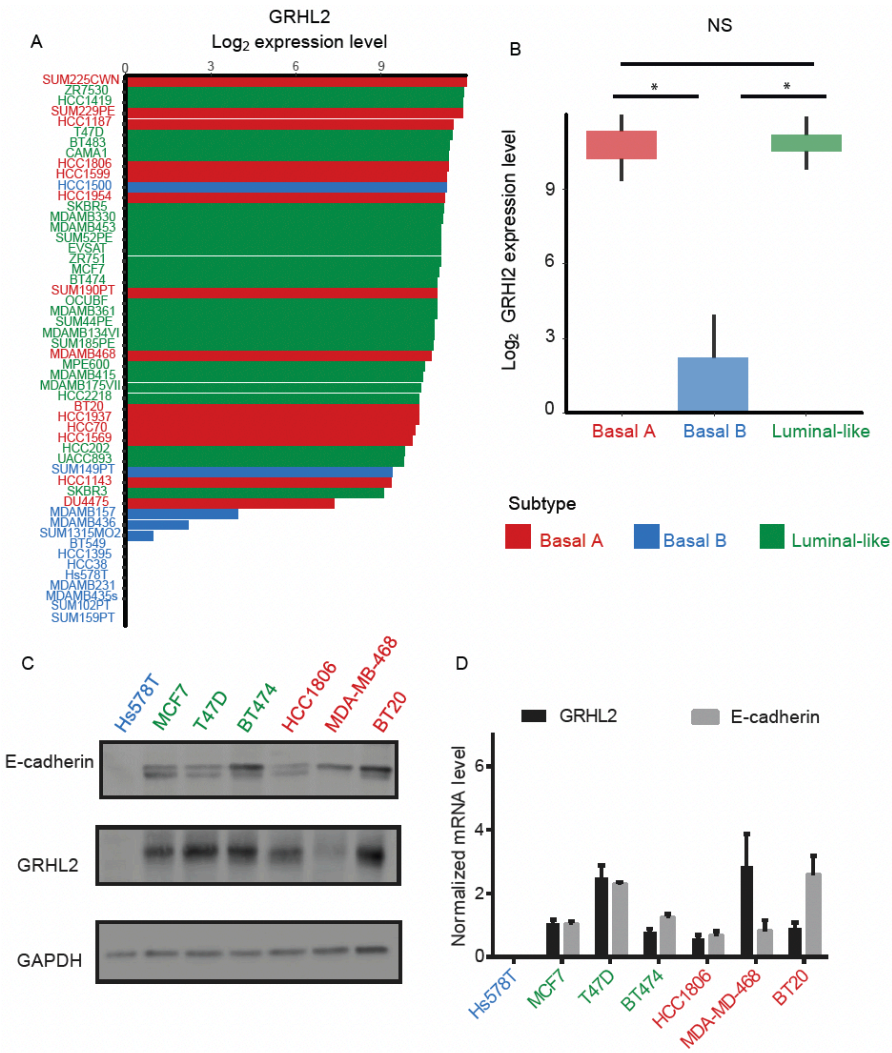


**Fig. 2. GRHL2 expression in a panel of human breast cancer cell lines representing different subtypes. (A and B)** GRHL2 expression in a panel of >50 human breast cancer cell lines covering luminal-, basal A-, and basal B subtypes extracted from RNA-seq data. \* indicates  $p < 0.05$ ; NS, not significant. **(C, D)** Western blot analysis **(C)** and qRT-PCR **(D)** showing loss of GRHL2 and its target gene CDH1 in basal B subtype breast cancer. Color codes refer to **B**.

### *2.2. Analysis of GRHL2-occupied genes in luminal and basal A breast cancer cells points to overlapping regulation of epithelial proliferation, cell-cell junctions, and cell migration*

We performed ChIP-seq in three human luminal breast cancer cell lines and three human basal A breast cancer cell lines and identified 6527 shared GRHL2 binding sites in all luminal and 13351 shared GRHL2 binding sites in all basal A cell lines (Fig 3A). Of these, 4711 GRHL2 binding sites were shared between luminal and basal A cells. MEME-ChIP identified a core GRHL2 binding motif matching previously published motifs [14, 15, 17, 56] in each cell line (Fig. 3B). Annotation of ChIP-seq data in luminal and basal A cells revealed 3155 and 5353 Ensembl annotations for GRHL2 occupied genes, respectively. These genes were interrogated using the clusterProfiler package in R for GO term enrichment. Several GO terms associated with epithelial proliferation, cell-cell junctions, and cell migration were identified (Fig 3C). We combined GO terms associated with cell-cell junction/ adhesion or GO terms associated with epithelial cell migration from Fig. 3C and used Cytoscape (cytoHubba) to identify and select hub genes. The resulting hub gene networks were not identical but did show overlap between luminal and basal A cell (Fig. 3D). I.e., CDC42 and beta-catenin (CTNNB1) were shared between luminal and basal A in the cell-cell junction/ adhesion GO terms. CDC42, PTEN, EGF, and the VEGF receptor KDR (note that the ligand VEGFA was only found in basal A) were shared between luminal and basal A in the epithelial cell migration GO terms. Together, these analyses indicated that gene networks regulated by GRHL2 in luminal and basal A cells show large overlap and may regulate, amongst others, proliferation and cell migration of both subtypes.



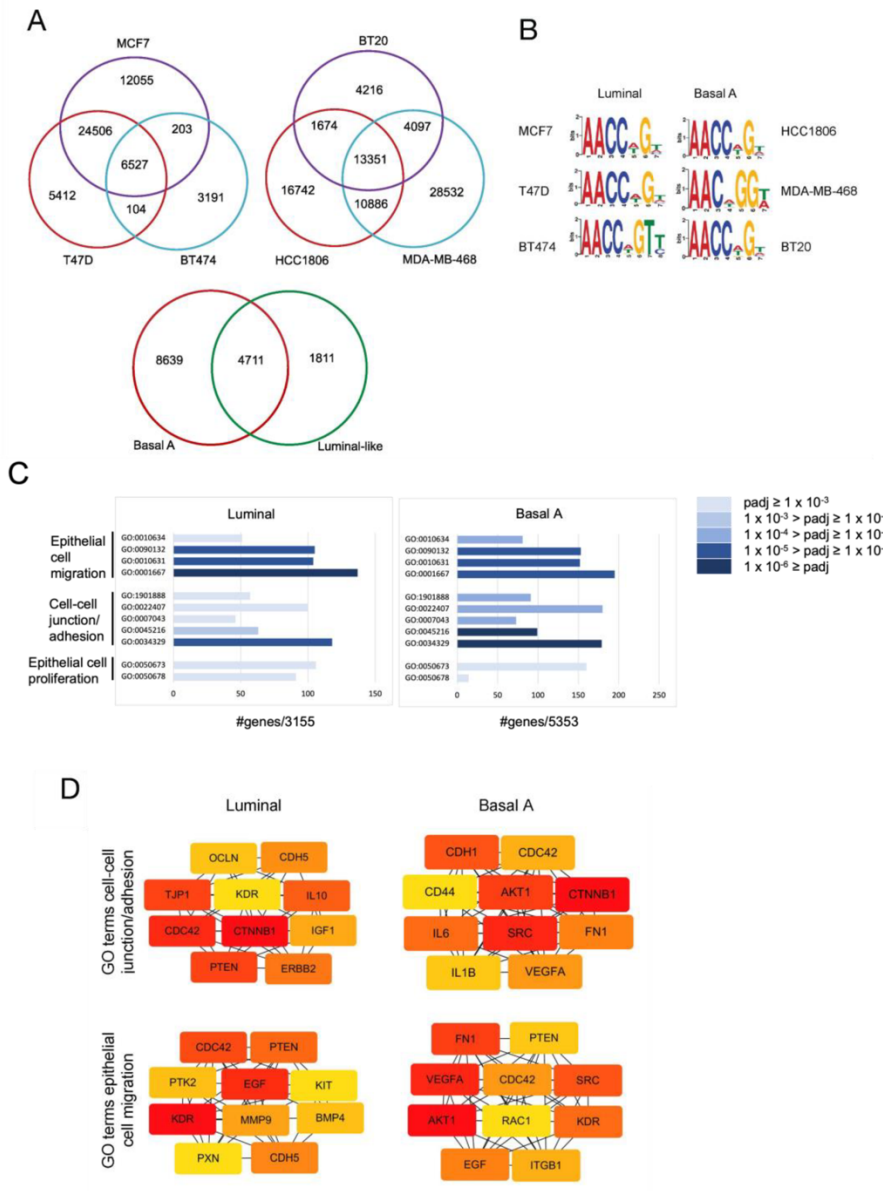


**Fig 3. ChIP-seq analysis of GRHL2 target genes in luminal and basal A cells. (A)** Venn diagrams showing overlap of GRHL2 binding sites among the indicated luminal and basal A cell lines (top panels) and overlap between shared GRHL2 binding sites in luminal and basal A cell lines (bottom panel). **(B)** GRHL2 DNA-binding

motifs identified in the indicated cell lines. **(C)** Enriched GO terms associated with the indicated functions for GRHL2-occupied genes shared between all luminal (left panel) or all basal A cell lines (right panel). Color coding according to padj values in the legend. X-axis shows the number of genes involved. **(D)** Hub genes calculated by Degree algorithm using Cytoscape (cytoHubba) software from the indicated GO terms for luminal and basal A cells. Color coding from red to yellow indicates the rank of the genes from top to low as assigned by cytoHubba.

### *2.3. Modulation of proliferation and migration in response to GRHL2 loss in luminal versus basal A breast cancer cells*

GRHL2 has been shown to promote cell survival and proliferation and to suppress EMT in epithelial cells [2,22]. Our ChIP-seq analysis suggested that both aspects could be regulated in luminal as well as basal A breast cancer cells. We studied the response to GRHL2 loss in MCF7 luminal and HCC1806 basal A cells (Fig 4A). Cell cycle analysis showed that a higher percentage of MCF7 cells were in G0/1 compared to HCC1806 cells and loss of GRHL2 resulted in a G0/1 arrest in MCF7 and a less-pronounced shift to G0/1 in HCC1806 cells (Fig. 4B). In agreement with the more robust arrest in cell cycle progression observed in MCF7, loss of GRHL2 attenuated cell proliferation of MCF7 cells at 2- and 3-days post seeding whereas a smaller, albeit significant decrease in proliferation was observed at 3 days in HCC1806 (Fig. 4C). Conversely, when random migration was analyzed, migration speed of HCC1806 cells was enhanced upon GRHL2 depletion whereas migration of MCF7 was not significantly affected (Fig. 4D). Together, these results suggested that GRHL2 loss caused suppression of growth in both subtypes, especially in the luminal cells, that was accompanied by enhanced migration predominantly in the basal A subtype.

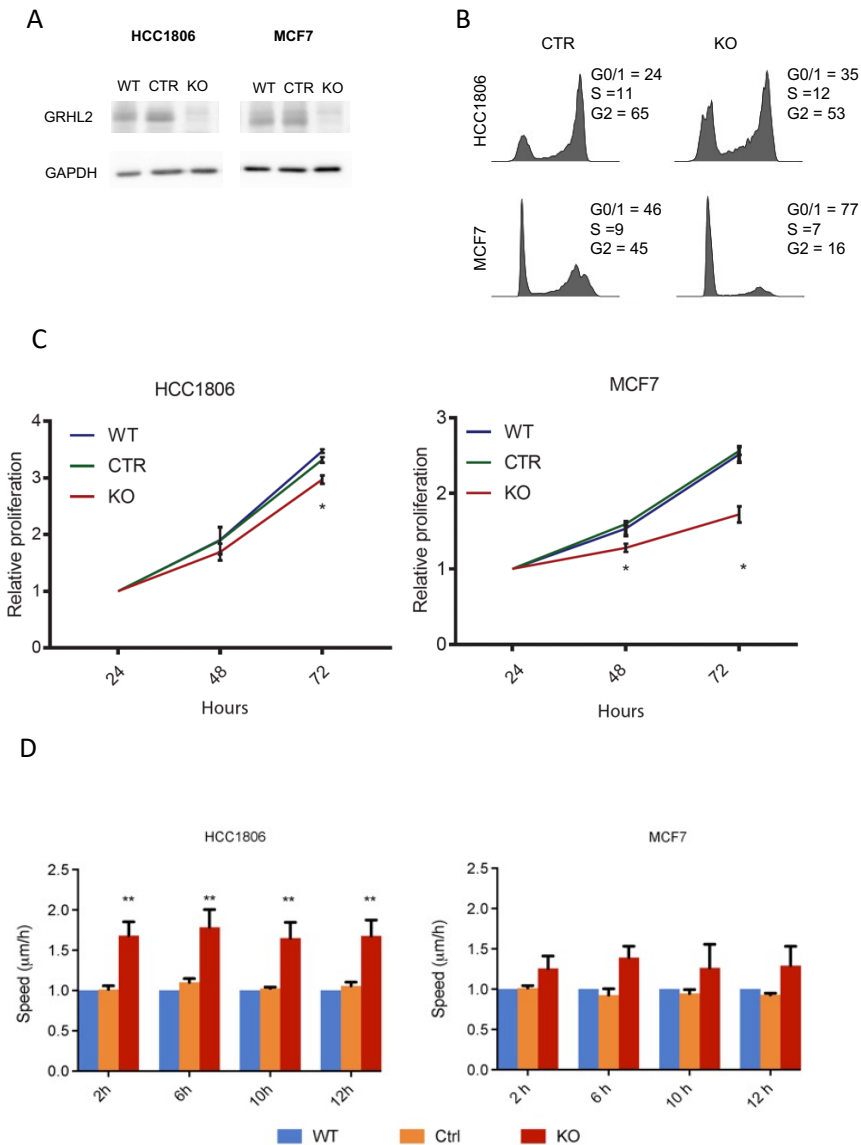
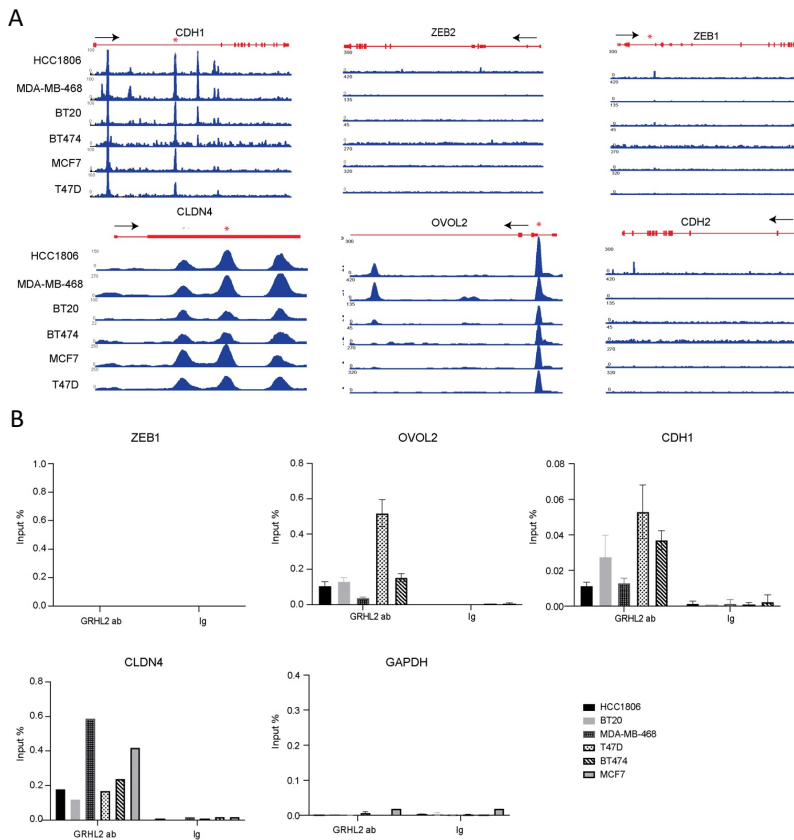


**Fig. 4. Response to GRHL2 knockout in luminal- and basal A cells. (A)** Western blot analysis showing loss of GRHL2 in KO cells. WT, wild type cells; CTR, sgCTR transduced cells; KO, sgGRHL2 transduced cells. **(B)** FACS profiles with associated quantification of cell cycle phase distribution in sgCTR (CTR) and sgGRHL2 transduced (KO) MCF7 and HCC1806 cells. Representative experiment from 2 and 3 biological replicates is shown for MCF7 and HCC1806, respectively. **(C)** Graphs showing results from SRB assay for wild type (WT) and sgCTR and sgGRHL2

transduced MCF7 and HCC1806 cells for the indicated time periods after 4 days doxycycline. Data are presented as mean  $\pm$  SEM from 3 biological replicates. Data are statistically analyzed by t-test comparing CTR and KO to WT. \* indicates  $p < 0.05$ . **(D)** Analysis of random migration assay showing the average path speed (y-axis) captured at the indicated timepoints during the assay (x-axis) for wild type (WT) and sgCTR and sgGRHL2 transduced MCF7 and HCC1806 cells 10-days post doxycycline. Data are presented as mean  $\pm$  SEM from 3 biological replicates relative to WT. Data are statistically analyzed by two-way ANOVA. \* indicates  $p < 0.05$ .

### *2.4. Signs of EMT in response to GRHL2 loss in luminal versus basal A breast cancer cells*

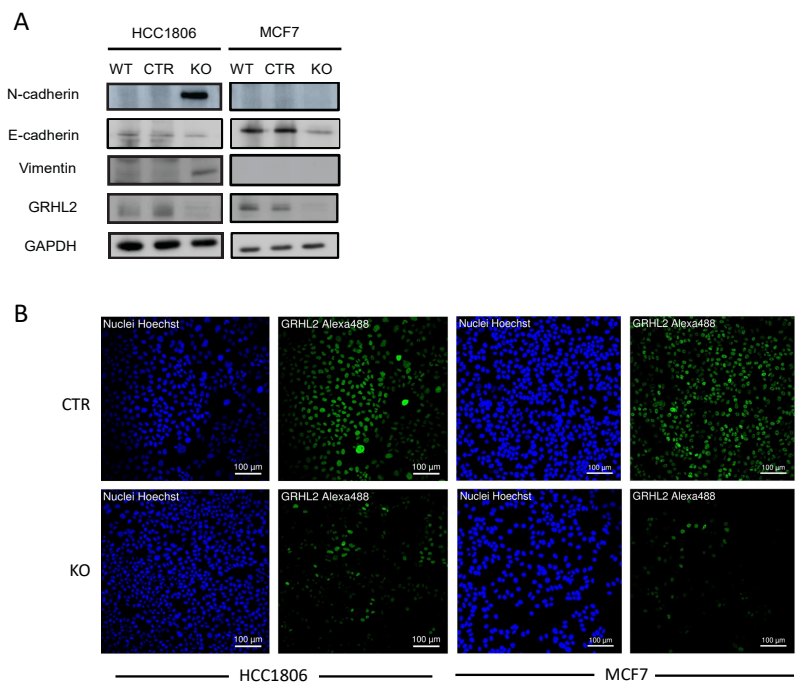
We next asked whether the selective increase in migration speed triggered by GRHL2 loss in basal A but not luminal cells may be related to differential regulation of EMT. Analysis of ChIP tracks in luminal and basal A cell lines for previously reported GRHL2 target genes revealed high similarity amongst all six cell lines (Fig. 5A). No interactions of GRHL2 with ZEB1 or ZEB2 were detected in contrast to previous findings in mammary epithelial cells [45]. This was confirmed by ChIP-qPCR using a primer set reported to amplify ZEB1 promoter DNA sequences bound by GRHL2 in human mammary epithelial cells [22] (Fig. 5B). We also did not detect GRHL2 peaks associated with CDH2 (encoding N-cadherin, a mesenchymal marker). No promoter binding but multiple in-tronic GRHL2 peaks were detected in the CDH1 gene that were conserved in all cell lines and ChIP-qPCR confirmed one of these conserved intronic GRHL2 binding sites. Lastly, GRHL2 binding at the promoter regions of CLDN4 and OVOL2 was conserved in all cell lines and validated by ChIP-qPCR.



**Fig. 5. Occupation of EMT related genes by GRHL2.** (A) ChIP tracks for the indicated genes in luminal and basal A breast cancer cell lines. The track height is scaled from 0 to the indicated number. The locus with its exon/intron structure is presented in red. (B) ChIP-qPCR validation of presence and absence of GRHL2 binding sites identified by ChIP-seq. Location of the qPCR primer set in the locus is indicated by \* in (A). Graphs represent the efficiency of indicated genomic DNA co-precipitation with anti-GRHL2 Ab or IgG control Ab. Signals for IgG control and GRHL2 antibody pulldown samples were normalized to input DNA and are presented as % input with SEM from 3 technical replicates with the exception of CLDN4 due to depletion of input material. Data were statistically analyzed by t-test and \* indicates  $p < 0.05$ .

# Chapter 4

In addition to direct binding of regulators of EMT, GRHL2 may regulate EMT indirectly. In luminal (MCF7) and basal A cells (HCC1806) GRHL2 knockout, but not control sgRNA triggered a reduction in E-cadherin protein expression (Fig. 6A). However, the induction of mesenchymal markers, Vimentin and N-cadherin was only observed in HCC1806 cells. These Western blot results were confirmed using confocal immunofluorescence microscopy. E-cadherin was expressed at cell–cell junctions and in the cytoplasm in HCC1806 and MCF7 cells and GRHL2 knockout led to reduced expression (Fig. 6B, C). A concomitant gain of Vimentin expression was only observed in HCC1806 cells. These results showed that direct binding of GRHL2 to EMT related genes is shared between luminal and basal A cells but GRHL2 depletion triggers several aspects associated with an EMT in HCC1806 whereas only reduction of E-cadherin is observed in MCF7, which may be in agreement with the enhanced migration observed in GRHL2-depleted HCC1806 but not MCF7 cells.



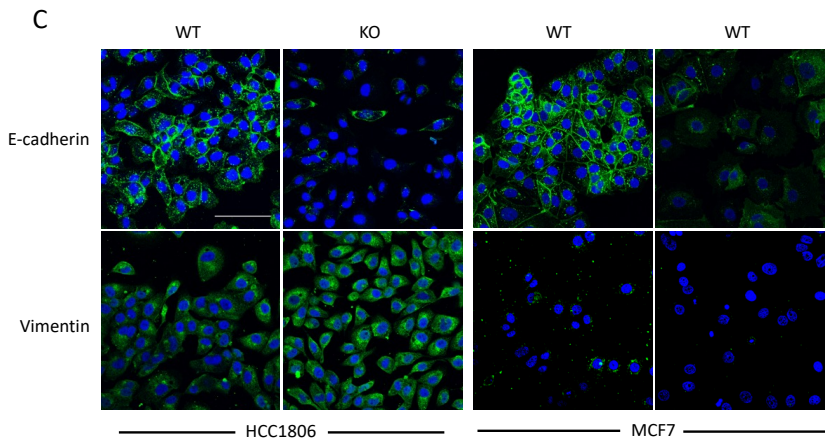


**Fig. 6. Regulation of EMT related genes by GRHL2.** (A) Western blot analysis of the indicated proteins in wild type (WT) and sgCTR (CTR) and sgGRHL2 transduced (KO) MCF7 and HCC1806 cells after 10 days doxycycline-induction. (B) Immunofluorescence analysis of HOECHST (nuclei, blue) and GRHL2 in MCF7 and HCC1806 cells expressing control sgRNA or GRHL2 sgRNA. (C) Immunofluorescence analysis of HOECHST (nuclei, blue), E-cadherin and Vimentin (Alexa-488, green), and F-actin (Rhodamine-Phalloidin, red) in WT, CTR, and KO MCF7 and HCC1806 cells after 10 days doxycycline-induction. Scale bar, 100µm.

## 2.5. GRHL2 depletion leads to reduced tumor growth and lung metastasis of 4T1 basal A cells

A shift from an epithelial towards a mesenchymal phenotype contributes to metastasis [46]. We asked whether GRHL2 depletion in basal A cells would attenuate metastasis due to reduced growth potential or promote metastasis due to the EMT shift. For this purpose, we made use of the 4T1 mouse basal A orthotopic transplantation model. Expression of shRNAs targeting GRHL2 led to ~80% reduction in GRHL2 mRNA and caused a decrease in E cadherin expression (Fig. 7A, B). Orthotopic tumor growth of shGRHL2 cells was attenuated as compared to growth of shCTR tumors (Fig. 7C). Depletion of GRHL2 also reduced lung metastasis with fewer and very small lung colonies (Fig. 7D). These results indicated that the dominant outcome of GRHL2

## Chapter 4

loss in basal A breast cancer cells in the context of tumor growth and metastasis is growth suppression.

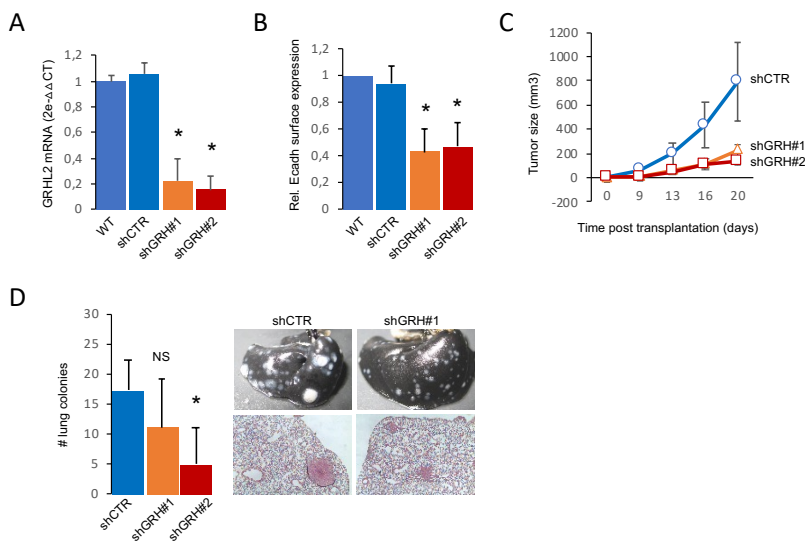


**Fig. 7. Effect of GRHL2 depletion in 4T1 basal A orthotopic transplantation model.** (A) RT qPCR analysis of efficiency of GRHL2 depletion in 4T1 cells transduced with a control or 2 GRHL2 shRNA constructs. Mean and SEM of 3 biological replicates is shown. \*  $p < 0.05$ . (B) FACS analysis of E cadherin surface expression in 4T1 variants described in A. Mean and SD of 3 experiments is determined and relative MFU (mean fluorescence units) compared to WT is shown. \*  $p < 0.05$ . (C) Graph showing mean and SD for analysis of primary tumor growth after orthotopic transplantation of control and GRHL2 shRNA transduced 4T1 cells. At least 12 mice per condition in two experiments were analyzed. (D) Graph showing mean and SD for number of detected lung colonies for the experiment as in (C). NS, not significant; \*  $p < 0.05$ . Right panel shows representative images of total lungs (top) and hematoxylin/eosin-stained lung sections derived from tumors of 4T1 cells transduced with a control or a GRHL2 shRNA construct.

### 3. Discussion

The results of this study indicate that the role of GRHL2 in luminal versus basal breast cancer cells is similar but not identical. Shared as well as distinct



gene sets are occupied by GRHL2 in these subtypes and the outcome of a reduction in GRHL2 expression may be distinct with luminal cells experiencing a robust growth arrest and basal A cells maintaining a reduced growth potential that is accompanied by enhanced migration. Nevertheless, in agreement with its overexpression and negative correlation with survival in human basal-like breast cancer patients, loss of GRHL2 in basal A cells leads to reduced growth of orthotopic tumors and lung colonies, indicating that growth suppression is the dominant response to GRHL2 loss.

GRHL2 is located on chromosome 8q22 and amplified or overexpressed in several cancer types, including breast cancer [15,47]. In vivo and clinical studies support an oncogenic role of GRHL2 [15,27-30,48,49]. Our findings corroborate such a role for GRHL2 and demonstrate an association of GRHL2 expression with poor prognosis in breast cancer. Our study using a panel of >50 human breast cancer cell lines, confirms and extends an earlier report showing that GRHL2 is downregulated in basal B breast cancer [22]. This is remarkable given its apparent relation to poor prognosis, since triple negative/basal tumors are often aggressive and have a poorer prognosis compared to the ER-positive luminal subtypes [4]. Moreover, basal B cells are enriched in EMT markers that are also associated with aggressiveness [4].

GRHL2 may play a dual role in breast cancer [15,16,23] and a tumor- or metastasis-suppressive function has been related to its ability to suppress EMT, stemness, and invasion in cell line models and clinical samples [22,23,45]. The function of GRHL2 likely is context-dependent and the consequence of GRHL2 loss depends on the cancer type and the stage of cancer progression. Here, we have explored whether luminal- and basal A breast cancer cells that are GRHL2 positive and have an epithelial phenotype with E-cadherin-mediated cell-cell contacts, respond similarly to a loss of GRHL2. We find that GRHL2 downregulation negatively impacts growth and positively impacts aspects of EMT/migration in a luminal as well as a basal A cell line, but not to the same extent. Growth inhibition upon loss of GRHL2 is robust in MCF7 but less pronounced in HCC1806 cells. Notably, expression of PCNA and TERT, which has been reported to be epigenetically controlled by GRHL2 [26,50]

was attenuated in MCF7 but not HCC1806 cells following GRHL2 depletion, indicating that replicative potential is differentially affected (data not shown).

As expected, based on earlier reports in other cell types [21,51-53], E-cadherin is downregulated in response to GRHL2 knockout in luminal as well as basal A breast cancer cells. Our findings indicate that this response may be indirect. ChIP-seq and ChIP-qPCR detect intronic GRHL2-binding sites in the CDH1 gene but no promoter binding. By contrast, we find that genes encoding the epithelial tight junction protein, CLDN4 and the epithelial zinc finger protein, OVOL2 are subject to GRHL2 promoter binding. We do not detect GRHL2 binding sites in ZEB1 or ZEB2, across all the luminal and basal A breast cancer cell lines we have analyzed, which contrasts with previous findings in other cell types [45]. Hence, regulation of E-cadherin could involve OVOL2 but not ZEBs, in breast cancer cells. Notably, GRHL2 binding to noncoding gene regions, such as the intronic binding sites in CDH1, may participate in long-distance chromatin interactions [21]. Moreover, intronic regions harbor enhancer elements and GRHL2, in some cases together with the ER-alpha transcriptional complex, can act as a pioneer factor [15-18]. As the absence or presence of promoter or intronic binding sites is shared across the luminal and basal A cells, these interactions do not explain the different response to GRHL2 loss in both subtypes. On the other hand, we observe an induction of mesenchymal markers and enhanced cell migration only in GRHL2-depleted basal A HCC1806 cells and not in GRHL2-depleted MCF7 luminal cells. It has been previously shown that loss of E-cadherin is not sufficient for enhanced cell migration, invasion, and metastasis of breast cancer cells [54-56]. The induction of mesenchymal markers, such as N-cadherin and Vimentin that we find to occur only in the HCC1806 cells may contribute to cell migration. N-cadherin junctions on the cell surface may act as migration tracks [57] and N-cadherin supports the organization of an F-actin network that drives cell migration [58]. Again, the upregulation of N-cadherin in HCC1806 cells appears to be indirect as no GRHL2 bindings sites are detected in the CDH2 gene. Vimentin, a type III intermediate filament protein, is involved in cell adhesion, migration and signal transduction and emerges in pathologies processes involving epithelial cell migration [59] but overexpression of Vimentin

by itself does not enhance cell migration in MCF7 cells [60]. Altogether, our findings and other reports indicate that in order for GRHL2 loss to trigger a shift to a more motile behavior, loss of E-cadherin is not sufficient, but a more elaborate transition is required, including loss of epithelial markers and gain of mesenchymal markers.

Despite the induction of EMT and enhanced migratory capacity in basal A breast cancer cells the ultimate outcome of GRHL2 depletion in the orthotopic tumor growth and metastasis experiment reported here, supports an oncogenic role of GRHL2. This is in agreement with earlier studies [28,30,61] and with the fact that GRHL2 is located on chromosome 8q22 that is amplified or overexpressed in several cancer types, including breast cancer [15,47]. Our findings show that GRHL2 represents a candidate therapeutic target for luminal breast cancer. Even though growth of primary tumor and metastatic colonies derived from basal breast cancer cells is suppressed in response to GRHL2 depletion, the combination of reduced growth with aspects of EMT and enhanced motility does warrant caution with strategies aimed at decreasing expression of GRHL2 in basal breast cancer.

## 4. Materials and Methods

### 4.1. Expression analysis in breast cancer cohorts and cell line panel

GRHL2 mRNA and protein expression in different subtypes were analyzed using GEPIA2 [31] and UALCAN [32,33], respectively. The KM plotter database was analyzed to evaluate the association of GRHL2 expression with survival of patients with different subclasses of breast cancer [34]. RNA-seq data for a panel of 52 breast cancer lines [35] was used to analyze GRHL2 expression across subtypes (basal A, basal B and luminal).

### 4.2. Cell lines

Human breast cancer cell lines (MCF7, T47D, BT474, HCC1806, BT20, MDA-MB-468, Hs578T) were obtained from the American Type Culture Collection. Cells were cultured in RPMI1640 medium with 10% fetal bovine serum, 25 U/mL penicillin and 25 µg/mL streptomycin in the incubator (37°C, 5% CO<sub>2</sub>). For production of lentiviral particles, VSV, GAG, REV and Cas9 or sgRNA or shRNA plasmids were transfected into HEK293 cells using Polyethylenimine

(PEI). After 2 days, lentiviral particles were harvested and filtered. Conditional Cas9 cells were generated by infecting parental cells with lentiviral particles expressing Edit-R Tre3G promoter-driven Cas9 (Dharmacon) and selected by blasticidin. Limited dilution was used to generate Cas9 monoclonal cells. Subsequently, Cas9-monoclonal MCF7 or HCC1806 cells were transduced with U6-gRNA:hPGK-puro-2A-tBFP control non-targeting or GRHL2-specific single guide (sg)RNAs (Sigma), selected by puromycin, and gene deletion was triggered by exposure to doxycycline. Control sgRNA vector was non-targeting. Human GRHL2 sgRNA was CCTCGAGACAAGAGGCTGCTGTC. For shRNA transduction of 4T1 cells, cells were transduced using lentiviral shRNA vectors (LentiExpress; Sigma-Aldrich) according to the manufacturer's procedures and selected in medium containing puromycin (2 mg/ml). Control shRNA vector targeted enhanced green fluorescent protein. Mouse GRHL2 shRNAs were CGGAGAAATTTCCGAGTACTTCTC and CGTCCTT-GTTAAGCGGATGTTCTC.

### 4.3. Western blot

Cells were lysed by radioimmunoprecipitation (RIPA) buffer (150 mM NaCl, 1% Triton X-100, 0.5% sodium deoxycholate and 0.1% Tris and 1% protease cocktail inhibitor (Sigma-Aldrich, P8340)). Then, cell lysates were sonicated and protein concentration was determined by bicinchoninic acid assay (BCA) assay. Cell lysates were mixed with protein loading buffer. Subsequently, proteins were separated by SDS-PAGE gel and transferred to methanol-activated polyvinylidene difluoride (PVDF) (Milipore, The Netherlands) membrane. Membranes were blocked with 5% bovine serum albumin (BSA, Sigma-Aldrich) for 1 hour at room temperature (RT). Membranes were stained with primary antibody overnight at 4°C and HRP-conjugated secondary antibodies for half hour at room temperature (RT). After staining with Prime ECL Detection Reagent (GE Healthcare Life science), chemoluminescence was detected by Amersham Imager 600 (GE Healthcare Life science, The Netherlands). The following antibodies were used: GRHL2 (At-las-Antibodies, hpa004820), GAPDH (SantaCruz, sc-32233), Vimentin (Abcam, ab8069), N-cadherin (BD, 610920), E-cadherin (Abcam, ab76055), Peroxidase AffiniPure Goat Anti-Rabbit IgG (Jackson ImmunoResearch, 111-035-003), Peroxidase

AffiniPure Goat Anti-Mouse IgG (Jackson ImmunoResearch, 115-035-003). Original blots are shown as supplemental data.

### 4.4. Realtime quantitative PCR (RT-qPCR)

Total RNA was isolated using RNeasy Plus Mini Kit (Qiagen). 500 ng RNA was reverse transcribed into cDNA using the RevertAid H Minus First Strand cDNA Synthesis Kit (Thermo Fisher Scientific). The cDNA was mixed with SYBR green master mix (Fisher Scientific) for qPCR. RT-qPCR data were collected and analyzed using 2- $\Delta\Delta C_t$  method. RT-qPCR primers included GRHL2 forward ggcaagtgtccttgtaaacgg / reverse atcgtcag-tctccttcctcacg; CDH1 forward: agagcttgctattgagcctgg / reverse: ccacggatcttggtgcagaaac; GAPDH forward: ccatggggaaggtgaaggtc/ reverse agttaaagcagccctggtga.

### 4.5. ChIP-seq and ChIP-qPCR

Cells were grown in RPMI-1640 complete, serum-containing medium. Cross-linking was performed by 1% formaldehyde for 10 minutes at room temperature (RT). Then 1M glycine (141  $\mu$ l of 1M glycine for 1 ml of medium) was used to quench for 5 minutes at RT. Cells were washed twice with ice-cold PBS containing 5  $\mu$ l/ml phenylmethylsulfonyl fluoride (PMSF). Cells were harvested by centrifugation (2095 g for 5 minutes at 4°C) and lysed with NP40 buffer (150 mM NaCl, 50mM Tris-HCl, 5mM EDTA, 0.5% NP40, 1% Triton X-100) containing 0.1% SDS, 0.5% sodium deoxycholate and protease inhibitor cocktail (EDTA-free Protease Inhibitor Cocktail, Sigma). Chromatin was sonicated to an average size of 300 bp and GRHL2-bound chromatin fragments were immunoprecipitated with anti-GRHL2 antibody (Sigma; HPA004820). Precipitates were washed by NP buffer, low salt (0.1% SDS, 1% Triton X-100, 2mM EDTA, 20mM Tris-HCl (pH 8.1), 150mM NaCl), high salt (0.1% SDS, 1% Triton X-100, 2mM EDTA, 20mM Tris-HCl (pH 8.1), 500mM NaCl) and LiCl buffer (0.25M LiCl, 1%NP40, 1% deoxycholate, 1mM EDTA, 10mM Tris-HCl (pH 8.1)). Chromatin was de-crosslinked by 1% SDS at 65°C and DNA was purified by Phenol:Chloroform:Isoamyl Alcohol (PCI) and then diluted in TE buffer. Library preparation and paired-end (151bp) sequencing were performed by GenomeScan (Leiden, The Netherlands). MCF7, T47D, BT474, HCC1806, MDA-MB-468, and BT20 had 87393758, 84633440, 82080866, 89366122, 114657768, 62258090 paired-end reads, respectively. ChIP-seq

data are available at the UCSC Genome Browser [<https://genome.ucsc.edu/s/hwuRadboudumc/ZWang>].

For ChIP-qPCR, the following primers were used: Control (an intergenic region upstream of the GAPDH locus): forward atgggtgccactggggatct / reverse tgccaaa-gcctaggggaaga; CLDN4: forward gtgacctcagcatgggctttga / reverse ctctctctgaccagtttctctg; ZEB1 promoter: forward gccgccgagcctccaacttt / reverse tgctagggaccggggcggttt; OVOL2 exon: forward ccttaaatcgcgagttagacc / reverse gtagcgagcttgttgacacc; CDH1 intron: forward gtagtaacggcaagcctctg / reverse caaggagccaggaagagaa. ChIP-qPCR data were analyzed using the 2- $\Delta\Delta C_t$  method.

### 4.6. ChIP-seq analysis

Less than 5% of adapter sequences were present, and the mean per base sequence quality was >30, indicating high quality reads and no requirement for adapter-trimming. Paired-end reads were mapped to the human reference genome (hg38) using BWA-MEM [36] with default parameters. Mapping of total reads to the human genome for MCF7, T47D, BT474, HCC1806, MDA-MB-468, and BT20 was 42915, 36183, 10054, 42554, 56906, 23486 respectively. Phred quality score (Q score) was used to measure base calling accuracy [37] and reads with low mapping quality ( $\leq Q30$ ) were filtered out. MACS version 2.1.0 [38] was used for peak calling by default settings. The q value was adjusted to 0.1 for BT474 cell line to avoid loss of peaks. The `annotatePeaks` and `MergePeaks` functions from HOMER [39] were used to annotate and overlap peaks, respectively. ChIPseeker was used for the analysis of ChIP-seq peaks coverage plot and the density profile of GRHL2 binding sites [40]. Motif analysis was performed using ChIP-seq peaks with high scores by the MEME-ChIP program with default settings. ChIP-seq data was visualized by the UCSC genome browser.

The `clusterProfiler` package in R was used for GO enrichment analysis using the Kyoto Encyclopedia of Genes and Genomes (KEGG) database [41]. For this purpose, gene symbols of annotated ChIP-seq data were converted to Ensembl gene annotations. For the luminal and basal A subtypes 3155 and 5353 Ensembl annotations were analyzed, respectively. Protein-protein

interaction (PPI) networks were analyzed using STRING database (<https://string-db.org/>). The cytoHubba plugin in Cytoscape software (version 3.7.2) was used to identify hub genes and their networks. The “Degree” algorithm was used to select the top genes in Cytoscape.

### *4.7. Flow cytometry*

Cell cycle analysis was performed with a Click-iT EdU Flow Cytometry Kit (Invitrogen). Cells were cultured with 50  $\mu$ M 5-ethynyl-2-deoxyuridine (EdU) for 4 h and fixed and stained according to the manufacturers protocol for analysis on a BD FACS Canto II.

### *4.8. Sulforhodamine B (SRB) assay*

Cell proliferation rate was measured by SRB assay. Cells were seeded into 96-well plates. At indicated time points, cells were fixed with 50% Trichloroacetic acid (TCA, Sigma-Aldrich) for 1 hour at 4 °C and then plates were washed with demineralized water four times and air-dried at RT. Subsequently, 0.4% SRB (60  $\mu$ l/well) was added and kept for at least 2 hours at RT. The plates were washed five times with 1% acetic acid and air-dried. 10 mM (150  $\mu$ l/well) Tris was added and kept for half hour at RT with gentle shaking. The absorbance value was measured by a plate-reader Fluostar OPTIMA.

### *4.9. Migration assay*

96 well-plates were coated with collagen (50  $\mu$ l/well, 20  $\mu$ g/ml) 1 hour 37°C and washed with PBS. Cells were seeded into the coated 96-well plates at the density of 8000 cells/well overnight and stained with Hoechst (Thermo Fisher 33242) diluted 1:7500 for 45 minutes. Images were taken every 5 minutes on a Nikon TE confocal microscope for 12 hours, at two positions per well. Tracks were analyzed using NIS Elements software and migration speed was calculated for 30 cells in each condition, tracked at 25 different timepoints.

### *4.10. Immunofluorescence*

Cells were fixed with 2% formaldehyde for 15 minutes under slow rotation, permeabilized with 1% Triton in Phosphate buffered saline (PBS) for 10 minutes, and then stained with primary antibodies and secondary

## Chapter 4

---

antibodies. The following antibodies and stains were used: Vimentin (Abcam, ab8069); E-cadherin (Abcam, ab76055); GRHL2 (Atlas-Antibodies, hpa004820); Hoechst (33258, Abcam); Goat anti-Mouse IgG (H+L) Cross-Adsorbed Secondary Antibody-Alexa Fluor 488 (Thermo Fisher, A-11001); Rhodamine-Phalloidin (Thermo Fisher, R415).

### *4.11. Animal studies*

Rag2<sup>-/-</sup>;gc<sup>-/-</sup> mice were housed in individually ventilated cages under sterile conditions. Housing and experiments were performed according to the Dutch guidelines for the care and use of laboratory animals. Sterilized food and water were provided ad libitum. Tumor cells ( $1 \times 10^5$ ) in 0.1 ml of phosphate-buffered saline were injected into the fat pad of 8- to 12-week-old female mice. Size of the primary tumors was measured using calipers. After 3 to 4 weeks, animals were anesthetized with pentobarbital. Lungs were excised and left lungs were fixed in 4% paraformaldehyde for hematoxylin and eosin staining. To quantify lung metastases, right lungs were injected with ink solution, destained in water, and fixed in Feketes [4.3% (v/v) acetic acid, 0.35% (v/v) formaldehyde in 70% ethanol].

### *4.12. Statistical analyses*

Statistical analyses were performed by GraphPad Prism 8. Details are further described in the figure legends.

**Author Contributions:** EHJD supervised the research. ZW and EHJD conceived, designed the experiments. ZW, BC, CYL and YJC performed the experiments. ZW and EHJD wrote the manuscript. All authors read, reviewed and approved the final manuscript.

**Funding:** ZW and QL were supported by a grant from the China Scholarship Council. BC was supported by a grant from the Dutch Cancer Society (KWF Research Grant #10967).



**Institutional Review Board Statement:** The animal study protocol was approved by Leiden University. Housing and experiments were performed according to the Dutch guidelines for the care and use of laboratory animals.

**Acknowledgments:** The authors thank Mrs. Chantal Pont and Jiangling Xiong (LACDR, Leiden University) for assistance with animal experiments and Haoyu Wu and Lucia Daxinger (Leiden University Hospital) for advice on ChIP-seq experiments.

**Conflicts of Interest:** The author(s) declare no competing interests.

**Data availability:** Chip-seq data supporting the results of this article is available at the UCSC Genome Browser [<https://genome.ucsc.edu/s/hwuRad-boudumc/ZWang>].

## References

1. Harbeck, N. and Gnant, M. (2017) Breast cancer. *Lancet* 389, 1134-1150. 10.1016/S0140-6736(16)31891-8
2. Ma, L. et al. (2017) Grainyhead-like 2 in development and cancer. *Tumour Biol* 39, 1010428317698375. 10.1177/1010428317698375
3. Keller, P.J. et al. (2010) Mapping the cellular and molecular heterogeneity of normal and malignant breast tissues and cultured cell lines. *Breast cancer research : BCR* 12, R87. 10.1186/bcr2755
4. Dai, X. et al. (2017) Breast Cancer Cell Line Classification and Its Relevance with Breast Tumor Subtyping. *J Cancer* 8, 3131-3141. 10.7150/jca.18457
5. Dai, X. et al. (2015) Breast cancer intrinsic subtype classification, clinical use and future trends. *American journal of cancer research* 5, 2929-2943
6. Cancer Genome Atlas, N. (2012) Comprehensive molecular portraits of human breast tumours. *Nature* 490, 61-70. 10.1038/nature11412
7. Tran, B. and Bedard, P.L. (2011) Luminal-B breast cancer and novel therapeutic targets. *Breast cancer research : BCR* 13, 221. 10.1186/bcr2904
8. Prat, A. et al. (2015) Clinical implications of the intrinsic molecular subtypes of breast cancer. *Breast* 24 Suppl 2, S26-35. 10.1016/j.breast.2015.07.008
9. Neve, R.M. et al. (2006) A collection of breast cancer cell lines for the study of functionally distinct cancer subtypes. *Cancer Cell* 10, 515-527. 10.1016/j.ccr.2006.10.008

10. Ming, Q. et al. (2018) Structural basis of gene regulation by the Grainyhead/CP2 transcription factor family. *Nucleic acids research* 46, 2082-2095. 10.1093/nar/gkx1299
11. Nüsslein-Volhard C., W.E., Kluding H. (1984) Mutations affecting the pattern of the larval cuticle in *Drosophila mel-anogaster* : I. Zygotic loci on the second chromosome. *Wilehm Roux Arch Dev Biol.* 193. 10.1007/BF00848156.
12. Werth, M. et al. (2010) The transcription factor grainyhead-like 2 regulates the molecular composition of the epitheli-al apical junctional complex. *Development* 137, 3835-3845. 10.1242/dev.055483
13. Aue, A. et al. (2015) A Grainyhead-Like 2/Ovo-Like 2 Pathway Regulates Renal Epithelial Barrier Function and Lu-men Expansion. *Journal of the American Society of Nephrology* : JASN 26, 2704-2715. 10.1681/ASN.2014080759
14. Walentin, K. et al. (2015) A Grhl2-dependent gene network controls trophoblast branching morphogenesis. *Develop-ment* 142, 1125-1136. 10.1242/dev.113829
15. Reese, R.M. et al. (2019) Grainyhead-like Protein 2: The Emerging Role in Hormone-Dependent Cancers and Epige-netics. *Endocrinology* 160, 1275-1288. 10.1210/en.2019-00213
16. Frisch, S.M. et al. (2017) Roles of Grainyhead-like transcription factors in cancer. *Oncogene*. 10.1038/onc.2017.178
17. Holding, A.N. et al. (2019) VULCAN integrates ChIP-seq with patient-derived co-expression networks to identify GRHL2 as a key co-regulator of ERa at enhancers in breast cancer. *Genome biology* 20, 91. 10.1186/s13059-019-1698-z
18. Cocce, K.J. et al. (2019) The Lineage Determining Factor GRHL2 Collaborates with FOXA1 to Establish a Targetable Pathway in Endocrine Therapy-Resistant Breast Cancer. *Cell Rep* 29, 889-903 e810. 10.1016/j.celrep.2019.09.032
19. Gao, X. et al. (2013) Evidence for multiple roles for grainyhead-like 2 in the establishment and maintenance of human mucociliary airway epithelium.[corrected]. *Proc Natl Acad Sci U S A* 110, 9356-9361. 10.1073/pnas.1307589110
20. Pifer, P.M. et al. (2016) Grainyhead-like 2 inhibits the coactivator p300, suppressing tubulogenesis and the epitheli-al-mesenchymal transition. *Molecular biology of the cell* 27, 2479-2492. 10.1091/mbc.E16-04-0249
21. Chung, V.Y. et al. (2016) GRHL2-miR-200-ZEB1 maintains the epithelial status of ovarian cancer through transcrip-tional regulation and histone modification. *Scientific reports* 6, 19943. 10.1038/srep19943
22. Cieply, B. et al. (2012) Suppression of the epithelial-mesenchymal transition by Grainyhead-like-2. *Cancer research* 72, 2440-2453. 10.1158/0008-5472.CAN-11-4038

23. Werner, S. et al. (2013) Dual roles of the transcription factor grainyhead-like 2 (GRHL2) in breast cancer. *The Journal of biological chemistry* 288, 22993-23008. 10.1074/jbc.M113.456293
24. Garnis, C. et al. (2004) Overexpression of LRP12, a gene contained within an 8q22 amplicon identified by high-resolution array CGH analysis of oral squamous cell carcinomas. *Oncogene* 23, 2582-2586. 10.1038/sj.onc.1207367
25. Dompe, N. et al. (2011) A whole-genome RNAi screen identifies an 8q22 gene cluster that inhibits death receptor-mediated apoptosis. *Proc Natl Acad Sci U S A* 108, E943-951. 10.1073/pnas.1100132108
26. Chen, W. et al. (2010) Grainyhead-like 2 enhances the human telomerase reverse transcriptase gene expression by inhibiting DNA methylation at the 5'-CpG island in normal human keratinocytes. *The Journal of biological chemistry* 285, 40852-40863. 10.1074/jbc.M110.103812
27. Quan, Y. et al. (2014) Downregulation of GRHL2 inhibits the proliferation of colorectal cancer cells by targeting ZEB1. *Cancer Biol Ther* 15, 878-887. 10.4161/cbt.28877
28. Paltoglou, S. et al. (2017) Novel Androgen Receptor Coregulator GRHL2 Exerts Both Oncogenic and Antimetastatic Functions in Prostate Cancer. *Cancer research* 77, 3417-3430. 10.1158/0008-5472.CAN-16-1616
29. Pan, X. et al. (2017) GRHL2 suppresses tumor metastasis via regulation of transcriptional activity of RhoG in non-small cell lung cancer. *Am J Transl Res* 9, 4217-4226
30. Faddaoui, A. et al. (2017) Suppression of the grainyhead transcription factor 2 gene (GRHL2) inhibits the proliferation, migration, invasion and mediates cell cycle arrest of ovarian cancer cells. *Cell Cycle* 16, 693-706. 10.1080/15384101.2017.1295181
31. Tang Z, Li C, Kang B, Gao G, Li C, Zhang Z. GEPIA: a web server for cancer and normal gene expression profiling and interactive analyses. *Nucleic Acids Res.* Jul 3 2017;45(W1):W98-W102. doi:10.1093/nar/gkx247
32. Chandrashekar DS, Bashel B, Balasubramanya SAH, et al. UALCAN: A Portal for Facilitating Tumor Subgroup Gene Expression and Survival Analyses. *Neoplasia*. Aug 2017;19(8):649-658. doi:10.1016/j.neo.2017.05.00233. Chandrashekar DS, Karthikeyan SK, Korla PK, et al. UALCAN: An update to the integrated cancer data analysis platform. *Neoplasia*. Mar 2022;25:18-27. doi:10.1016/j.neo.2022.01.001
34. Gyorffy, B. et al. (2010) An online survival analysis tool to rapidly assess the effect of 22,277 genes on breast cancer prognosis using microarray data of 1,809 patients. *Breast Cancer Res Treat* 123, 725-731. 10.1007/s10549-009-0674-9

35. Koedoot, E. et al. (2021) Differential reprogramming of breast cancer subtypes in 3D cultures and implications for sensitivity to targeted therapy. *Sci Rep* 11, 7259. 10.1038/s41598-021-86664-7
36. Liu, C.M. et al. (2012) SOAP3: ultra-fast GPU-based parallel alignment tool for short reads. *Bioinformatics* 28, 878-879. 10.1093/bioinformatics/bts061
37. Ewing, B. et al. (1998) Base-calling of automated sequencer traces using phred. I. Accuracy assessment. *Genome Res* 8, 175-185
38. Zhang, Y. et al. (2008) Model-based analysis of ChIP-Seq (MACS). *Genome biology* 9, R137. 10.1186/gb-2008-9-9-r137
39. Heinz, S. et al. (2010) Simple combinations of lineage-determining transcription factors prime cis-regulatory elements required for macrophage and B cell identities. *Mol Cell* 38, 576-589. 10.1016/j.molcel.2010.05.004
40. Yu, G. et al. (2015) ChIPseeker: an R/Bioconductor package for ChIP peak annotation, comparison and visualization. *Bioinformatics* 31, 2382-2383. 10.1093/bioinformatics/btv145
41. Yu, G. et al. (2012) clusterProfiler: an R package for comparing biological themes among gene clusters. *OMICS* 16, 284-287. 10.1089/omi.2011.0118
42. Su, Y. et al. (2016) Development and characterization of two human triple-negative breast cancer cell lines with highly tumorigenic and metastatic capabilities. *Cancer Med* 5, 558-573. 10.1002/cam4.616
43. Prat, A. et al. (2013) Characterization of cell lines derived from breast cancers and normal mammary tissues for the study of the intrinsic molecular subtypes. *Breast Cancer Res Treat* 142, 237-255. 10.1007/s10549-013-2743-3
44. Teo, K. et al. (2018) E-cadherin loss induces targetable autocrine activation of growth factor signalling in lobular breast cancer. *Sci Rep* 8, 15454. 10.1038/s41598-018-33525-5
45. Cieply, B. et al. (2013) Epithelial-mesenchymal transition and tumor suppression are controlled by a reciprocal feedback loop between ZEB1 and Grainyhead-like-2. *Cancer research* 73, 6299-6309. 10.1158/0008-5472.CAN-12-4082
46. Luond, F. et al. (2021) Distinct contributions of partial and full EMT to breast cancer malignancy. *Developmental cell* 56, 3203-3221 e3211. 10.1016/j.devcel.2021.11.006
47. Mlacki, M. et al. (2015) Recent discoveries concerning the involvement of transcription factors from the Grainyhead-like family in cancer. *Experimental biology and medicine* 240, 1396-1401. 10.1177/1535370215588924
48. Yang, X. et al. (2013) Bridging cancer biology with the clinic: relative expression of a GRHL2-mediated gene-set pair predicts breast cancer metastasis. *PloS one* 8, e56195. 10.1371/journal.pone.0056195

49. Butz, H. et al. (2014) Integrative bioinformatics analysis reveals new prognostic biomarkers of clear cell renal cell carcinoma. *Clinical chemistry* 60, 1314-1326. 10.1373/clinchem.2014.225854
50. Kang, X. et al. (2009) Regulation of the hTERT promoter activity by MSH2, the hnRNPs K and D, and GRHL2 in hu-man oral squamous cell carcinoma cells. *Oncogene* 28, 565-574. 10.1038/onc.2008.404
51. Chen, W. et al. (2018) Grainyhead-like 2 (GRHL2) knockout abolishes oral cancer development through reciprocal regulation of the MAP kinase and TGF-beta signaling pathways. *Oncogenesis* 7, 38. 10.1038/s41389-018-0047-5
52. Chen, W. et al. (2016) Grainyhead-like 2 regulates epithelial plasticity and stemness in oral cancer cells. *Carcinogenesis* 37, 500-510. 10.1093/carcin/bgw027
53. Farris, J.C. et al. (2016) Grainyhead-like 2 Reverses the Metabolic Changes Induced by the Oncogenic Epithelial-Mesenchymal Transition: Effects on Anoikis. *Mol Cancer Res* 14, 528-538. 10.1158/1541-7786.MCR-16-0050
54. Sommers, C.L. et al. (1991) Cell adhesion molecule uvomorulin expression in human breast cancer cell lines: relationship to morphology and invasive capacities. *Cell growth & differentiation : the molecular biology journal of the American Association for Cancer Research* 2, 365-372
55. Truong, H.H. et al. (2014) beta1 integrin inhibition elicits a prometastatic switch through the TGFbeta-miR-200-ZEB network in E-cadherin-positive triple-negative breast cancer. *Sci Signal* 7, ra15. 10.1126/scisignal.2004751
56. Iliina, O. et al. (2020) Cell-cell adhesion and 3D matrix confinement determine jamming transitions in breast cancer invasion. *Nat Cell Biol* 22, 1103-1115. 10.1038/s41556-020-0552-6
57. Shih, W. and Yamada, S. (2012) N-cadherin-mediated cell-cell adhesion promotes cell migration in a three-dimensional matrix. *J Cell Sci* 125, 3661-3670. 10.1242/jcs.103861
58. Ponti, A. et al. (2004) Two distinct actin networks drive the protrusion of migrating cells. *Science* 305, 1782-1786. 10.1126/science.1100533
59. Ivaska, J. et al. (2007) Novel functions of vimentin in cell adhesion, migration, and signaling. *Experimental cell research* 313, 2050-2062. 10.1016/j.yexcr.2007.03.040
60. Sommers, C.L. et al. (1992) Loss of epithelial markers and acquisition of vimentin expression in adriamycin- and vinblastine-resistant human breast cancer cell lines. *Cancer Res* 52, 5190-5197
61. Hu, F. et al. (2019) Knockdown of GRHL2 inhibited proliferation and induced apoptosis of colorectal cancer by suppressing the PI3K/Akt pathway. *Gene* 700, 96-104. 10.1016/j.gene.2019.03.051

Supplementary Figures

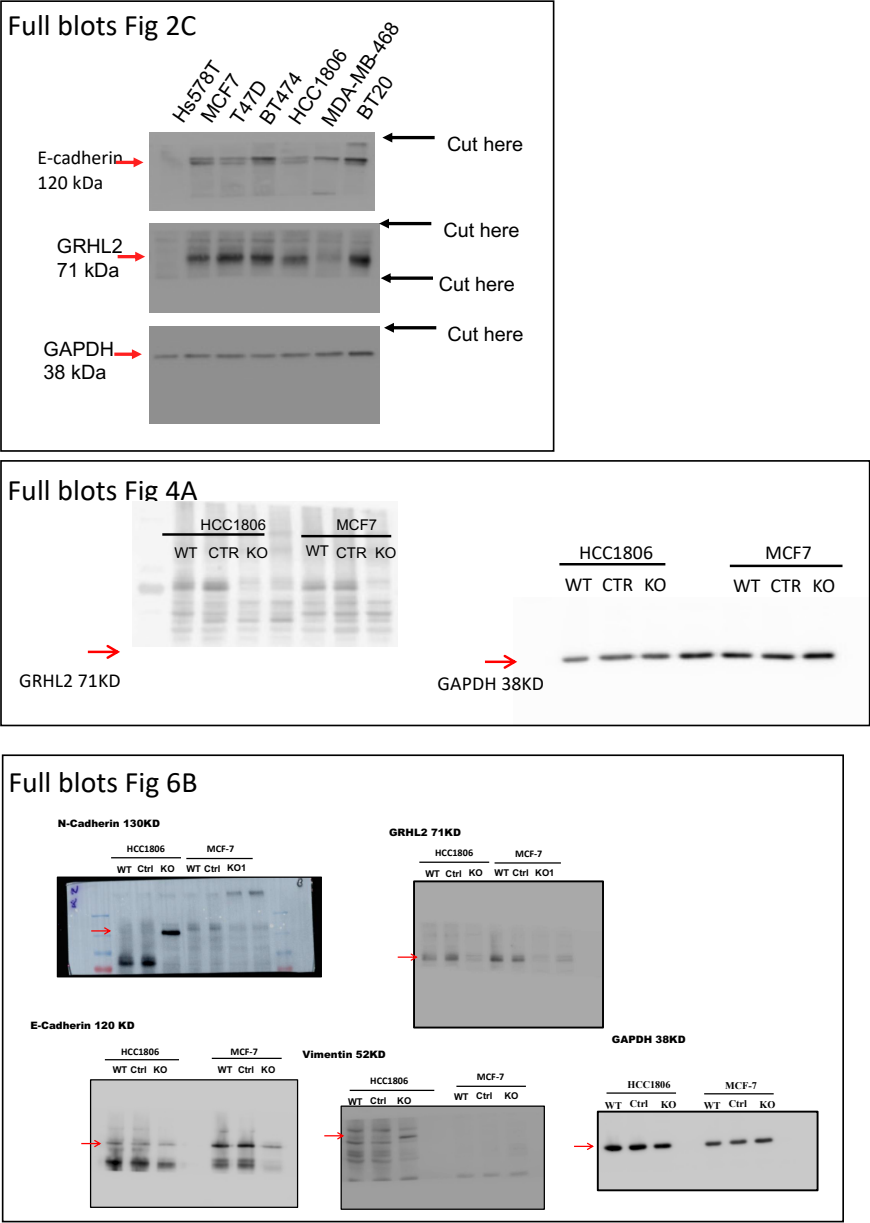


Fig. S1. Full blots for Western blots shown in Fig 2C, 4A, and 6B.

# Chapter 5

---

## Limited control of EMT/MET balance and targetable vulnerabilities by GRHL2 alone in breast cancer cells

Bircan Coban<sup>1</sup>, Zi Wang<sup>1</sup>, Julia Star Darnold<sup>1</sup>, Cecilia Bergonzini<sup>1</sup>, Annelien J.M. Zweemer<sup>1</sup>, Erik H.J. Danen<sup>1,2</sup>

<sup>1</sup>Leiden Academic Center for Drug Research, Leiden University, Leiden, The Netherlands; <sup>2</sup>correspondence: [e.danen@lacdr.leidenuniv.nl](mailto:e.danen@lacdr.leidenuniv.nl)

### Summary

Cellular plasticity is a critical factor in the development of resistance to anti-cancer drugs. Epithelial-mesenchymal transition (EMT) is one of the key processes contributing to this plasticity. In this study, we aimed to investigate the relationship between plasticity and drug resistance mediated by the epithelial transcription factor GRHL2 in Luminal and Basal B subtypes of breast cancer. We employed a GRHL2 knockout system in the Luminal subtype using MCF-7 cells and examined the changes in signaling pathways triggered by GRHL2 loss. Our findings revealed that GRHL2 deletion primarily affected the TGF $\beta$  pathway but did not provoke a complete EMT. Subsequently, we investigated whether stable or inducible overexpression of GRHL2 in Basal B subtype MDA-MB-231 cells resulted in the inverse process, mesenchymal-to-epithelial transition (MET). However, GRHL2 expression in these cells did not result in significant changes in the EMT/MET balance. Taking advantage of the possibility to explore GRHL2-regulated drug vulnerabilities without being affected by changes in the EMT/MET state, we screened a series of kinase inhibitors in MDA-MB-231 cells lacking or expressing GRHL2. Overall few differential sensitivities to these compounds were detected but four kinase inhibitors were identified that selectively inhibited proliferation of GRHL2-expressing cells in the screen. However, subsequent dose-response experiments showed that these kinases did not represent actionable GRHL2-regulated targets in MDA-MB-231 cells. These findings argue against a major change in EMT/MET balance in response to altered expression of GRHL2 and do not point to GRHL2-regulated drug vulnerabilities in breast cancer.

### Introduction

Breast cancer cells rewire signaling pathways that enhance cellular plasticity, enabling resistance to anti-cancer drugs.<sup>1–3</sup> Unraveling the mechanisms modulating the plasticity and drug responses is crucial to overcome drug resistance. This adaptive behavior of the cancer cells is often accompanied by plasticity with respect to the balance between epithelial and mesenchymal characteristics through epithelial-to-mesenchymal transitions (EMT) and mesenchymal-to-epithelial transitions (MET).<sup>4–6</sup>



EMT supports drug resistance, it enables cancer cells to become more motile, and these two responses may be interconnected.<sup>7,8</sup> Cancer cells undergoing EMT often show increased drug efflux due to the upregulation of ATP-binding cassette (ABC) transporters. These transporters pump chemotherapeutic agents out of the cells, thereby reducing their efficacy.<sup>9–11</sup> Moreover, EMT can result in changes in cell cycle regulation, rendering cancer cells less responsive to treatments that target rapidly dividing cells.<sup>12,13</sup> The mesenchymal phenotype also enhances the efficiency of DNA damage repair mechanisms, further contributing to resistance against DNA damage inducing therapies.<sup>7,14</sup>

The connection of EMT not only with cancer cell migration but also with drug resistance highlights the importance of understanding the underlying pathways to develop more effective therapeutic strategies.<sup>15,16</sup> The Grainyhead-like-2 (GRHL2) transcription factor has been shown to act as a critical epithelial suppressor of EMT.<sup>17–20</sup> During EMT, loss of GRHL2 results in a more mesenchymal phenotype with enhanced invasive properties.<sup>21,22</sup> In addition, it was shown that silencing GRHL2 expression increases the sensitivity of ovarian cancer cells to cisplatin.<sup>23</sup> GRHL2 is also implicated in the regulation of various signaling pathways associated with drug resistance, including the PI3K/AKT/mTOR pathway, the MAPK/ERK pathway, and the NF- $\kappa$ B pathway.<sup>24,25</sup>

Elucidating molecular mechanisms behind GRHL2-mediated drug responses and the signaling pathways regulated by GRHL2 could lead to the development of new targeted therapeutic strategies for breast cancer. To study this, we took two approaches: GRHL2 was deleted in Luminal breast cancer cells, or it was overexpressed in Basal B breast cancer cells. The effect on signaling pathways, EMT/MET balance, and drug sensitivity was explored.

## Materials and Methods

### Cell culture

Human breast cancer cell lines MDA-MB-231 (Basal-b subtype; triple negative breast cancer (TNBC)), MCF-7 (Luminal subtype), and the human embryonic kidney cell line HEK293T were obtained from ATCC. MCF-7 and MDA-

MB-231 were cultured in RPMI 1640 while HEK293T cells were cultured in in DMEM (Dulbecco's Modified Eagle Medium, both supplemented with 10% fetal bovine serum (FBS), 25 U/mL penicillin, and 25 µg/mL streptomycin (Fisher Scientific) and maintained in a humidified incubator with 5% CO<sub>2</sub> at 37 °C.

### **Bru-seq analysis of EMT-associated genes**

CRISPR/Cas9-mediated conditional knockout (KO) of GRHL2 in MCF-7 cells expressing one of two different GRHL2 sgRNAs or a control sgRNA in combination with an inducible Cas9 construct was induced using 1µg/ml doxycycline (dox) for 8 days as explained previously.<sup>21,26</sup> By employing the KO system, Bru-seq analysis enabled identification of GRHL2-regulated genes and pathways.<sup>27</sup> Based on their relationship with GRHL2, six EMT-associated genes (Occludin, Zonula Occludens-1/ZO-1, E-cadherin, Claudin-4/CLDN4, Vimentin, and Zinc finger E-box-binding homeobox 1/ZEB1) were chosen to explore signs of EMT following GRHL2 deletion. Changes in gene expression were calculated by comparing dox-treated KO-1 and KO-2 cells to the same cells without dox induction. The Bru-seq data is accessible in the Gene Expression Omnibus 477 (GEO) database, [www.ncbi.nlm.nih.gov/geo](http://www.ncbi.nlm.nih.gov/geo) (Accession No. GSE222353).

### **Measuring Pathway activity**

The effect of GRHL2 loss on the functional activity of signaling pathways was assessed using the Philips Pathway Activity Profiling OncoSignal platform ([https://images.philips.com/is/content/PhilipsConsumer/Campaigns/HC20140401\\_DG/Documents/HC06172020-2020-05\\_mpdf\\_fly-erpdf.pdf](https://images.philips.com/is/content/PhilipsConsumer/Campaigns/HC20140401_DG/Documents/HC06172020-2020-05_mpdf_fly-erpdf.pdf)). GRHL2 deletion was induced with 8µg/ml dox in MCF-7 cells and RNA isolation was performed using Trizol method. Purified RNA samples were used for the pathway analysis using the Oncosignal qPCR kit (Philips Molecular Pathway Diagnostics, Eindhoven, The Netherlands). The kit was designed to measure the activities of pathways driven by hormone receptors Androgen receptor (AR) and Estrogen receptor (ER), stem-cell related pathways (TGFβ and Hedgehog (HH), and growth factor pathways (PI3K) using several direct target genes within that pathway. PI3K pathway activity is

based on the inverse activity of the measured FOXO transcription factor activity score. The pathway activities are scored on 0-100 scale using a Bayesian computational model to determine whether the pathway is activated or not (0 score corresponds to the lowest and 100 corresponds to the highest probability of an active pathway).<sup>28</sup>

### **Establishment of GRHL2 overexpressing cells**

For the stable expression of GRHL2 in MDA-MB-231 cells a pLenti-GIII-CMV-GFP-2A-Puro construct (Applied Biological Materials) containing a GRHL2 insert, and an empty control construct were kindly provided by Dr. Ruby Yun-Ju Huang (National University of Singapore). Lentiviral particles were generated using HEK293T cells as previously described<sup>26</sup> and used for transduction of MDA-MB-231 cells. Transduced cells were selected using 5µg/ml Puromycin and GFP-sorted. For inducible GRHL2 expression, the Lenti-XTM Tet-On 3G System (TakaraBio, 631187) was used. For this, lentiviral particles were generated as described and MDA-MB-231 cells were transduced with a pLVX-EF1a-Tet3G construct expressing a Tet-ON 3G transactivator protein, either alone (CTR) or combined with pLVX-TRE3G-Luc expressing luciferase (Luc\*) or pLVX-TRE3G-GRHL2 expressing GRHL2 (GRHL2\*). Transduced cells were selected with Puromycin. The asterisk indicates inducible expression. For induction, MDA-MB-231 cells were treated with 125 ng/ml dox for different time periods.

### **Western Blot**

Cells were lysed using RIPA buffer. SDS-PAGE was run using 20µg lysates and transferred to PVDF membranes. The membranes were incubated overnight with the following antibodies; GRHL2 (1:1000, Atlas antibodies, hpa004820), E-cadherin (1:1000, Abcam, ab76055), CLDN4 (1:1000, Thermo Fisher, 329400), GAPDH (1:2000, Santa Cruz, sc-32233). HRP-linked anti-mouse and anti-rabbit secondary antibodies were used on the next day to detect protein expression with Prime ECL Detection Reagent. Membranes were detected with Amersham Imager 600 (GE Healthcare Life Sciences, the Netherlands).

### **Immunofluorescence**

Cells were seeded in 96well plates and fixed/permeabilized with 4% formaldehyde and 0.1% Triton X100 in Phosphate-buffered saline (PBS) for 15 mins. The cells were incubated with primary antibodies recognizing GRHL2 (1:500, Atlas-Antibodies, hpa004820), ZO-1 (1:100, Cell Signaling, 13663S), Occludin (1:300, Cell Signaling, 91131S), Claudin 4 (1:100, Thermo Fisher, 329400), E-cadherin (1:1000, Abcam, ab76055), Vimentin (1:100, Abcam, ab8069), or ZEB1 (Santa Cruz, sc-515797) overnight at 4°C. After washing, AlexaFluor-488 conjugated anti-rabbit and anti-mouse secondary antibodies were incubated with Hoechst 33258 (1:10,000, Sigma Aldrich, 861405) and Rhodamin Phalloidin (1:1000, R415, Thermo Fisher) for 1 h at room temperature. Images were taken with a Nikon ECLIPSE Ti2 confocal microscope, 20x objective. The imaging data were organized using OMERO Database.

### **Sulforhodamine B (SRB) Assay**

To examine the effect of GRHL2 overexpression in cell proliferation, MDA-MB-231 cells were seeded at a density of 3000cells/well in 96 well plates after 3 and 10 days of dox treatment. Four days later (day 7 and day 14 of GRHL2 induction), plates were fixed using 50% Trichloroacetic acid (TCA). The next day, 0.4% SRB was used to stain cells and the unbound SRB was washed away using 1% acetic acid. 10mM Tris was added to the plates and absorbance measurements were performed at 540nm using a BioTek Synergy HT plate reader (SN 269140, BioTek Instruments Inc.). The data were analyzed in Graphpad Prism, version 9.0.

### **Kinase inhibitor (KI) screening and validation**

MDA-MB-231-Luc\* and MDA-MB-231-GRHL2\* cells were treated with dox for 10 days, seeded at a density of 3000cells/well in 96 well plates and exposed for 4 days to 760 KIs from the L1200 library (Sellckchem, Munich, Germany). KIs were dissolved in 0.1% DMSO or water to a final concentration of 1uM. Cisplatin (1uM) served as a positive control. After 4 days, the cells were fixed and analyzed with SRB assay as described. & proliferation was obtained by normalizing the data to DMSO or water treated cells for each treatment plate. The screen was performed in single technical replicates and two

independent biological replicates were performed. KIs of interests (Torkinib, Mirin, A-674563 and LDC-4297) chosen based on the two biological replicates were tested together with some known DNA damaging agents (Cisplatin, Gemcitabine and Docetaxel) in a dose response curve. MDA-MB-231 cells were seeded as explained above and treated with increasing doses (0.1, 0.3, 1, 3, 10uM) of these six drugs for 4 days and processed for SRB.

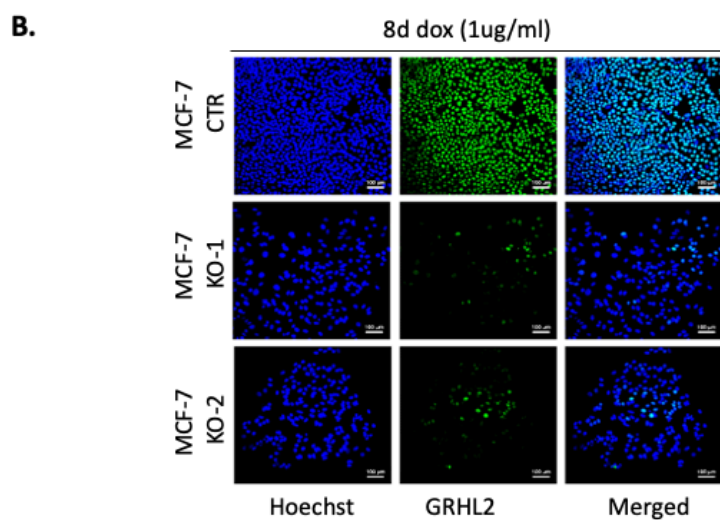
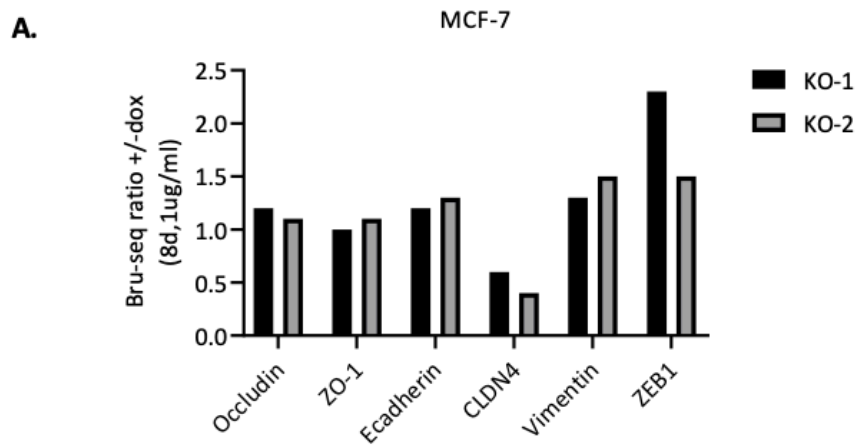
### Statistical analysis

GraphPad Prism 9 was used to perform one-way ANOVA with Tukey's multiple comparison test for statistical analysis.

## Results

### GRHL2-controlled signaling pathway activities in Luminal-like breast cancer cells

We have previously identified GRHL2-controlled gene networks in MCF-7 cells.<sup>27</sup> To investigate the effect of GRHL2 deletion on EMT progression, we employed Bru-seq data of MCF-7 cells in which GRHL2 KO was induced. We chose a timepoint of 8 days treatment with dox be in line with a subsequent experiment where changes in signaling were explored in the same system. A panel of EMT-associated genes was analyzed: epithelial markers Occludin, ZO-1, E-cadherin, CLDN4 and mesenchymal cell markers Vimentin and Zeb1. Overall, mRNA expression levels were similar for both KOs although CLDN4 was downregulated in GRHL2 KO cells (Fig. 1A). The change in CLDN4 did not reach statistical significance as compared to CTR cells at this time-point but it was significantly downregulated at other timepoints (see chapter 3). This suggested that deletion of GRHL2 alone is insufficient to trigger an EMT in Luminal-like breast cancer cells, in contrast to the EMT-related changes described previously.<sup>29,30</sup>



C.

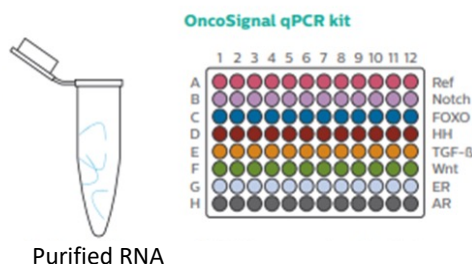
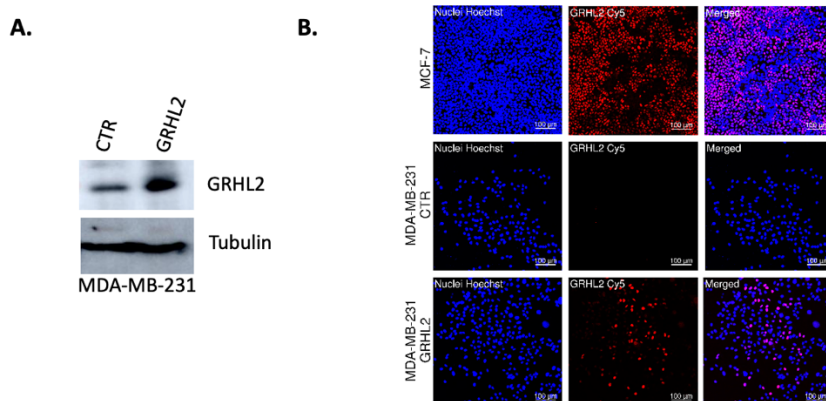


**Figure 1: Signaling pathways affected by GRHL2 deletion in luminal cells. (A)** Bru-seq analysis of EMT-associated genes in MCF-7 cells with GRHL2 KO-1 and KO-2 ; induced by 1ug/ml dox for 8 days. Graph representing fold change of transcription in response to GRHL2 deletion. **(B)** Immunofluorescence images showing GRHL2 expression after 1ug/ml dox exposure for 8 days for MCF-7 CTR, KO-1 and KO-2 cells ; Hoechst (blue), and GRHL2 Ab (green). **(C)** Cartoon explaining the OncoSignal qPCR platform to measure signaling pathway activities. Pathway activities were evaluated in RNA isolated from MCF-7 cells with or without dox induction (1ug/ml, 8 days). Scores range from 0-100 after normalization to house-keeping genes.

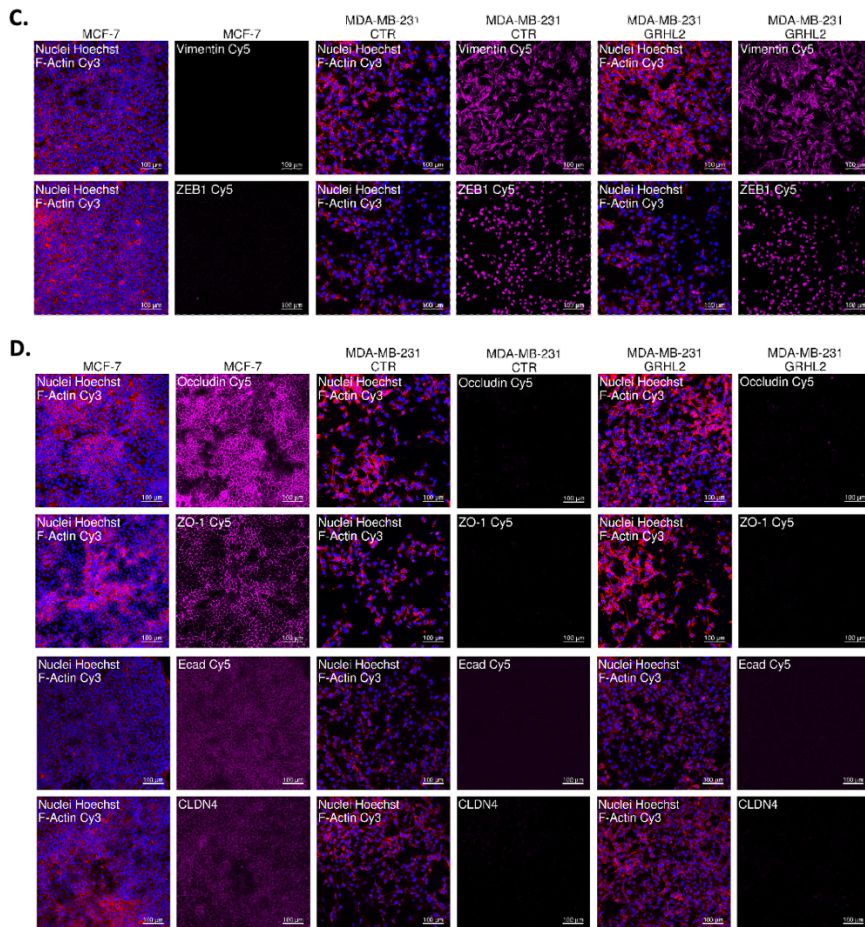
Following this, we sought to elucidate changes occurring in signaling pathways in response to GRHL2 deletion. For this, we made use of the qPCR-based Philips OncoSignal platform. A complete loss of GRHL2 was achieved in KO-1 and KO-2 cells using 8 days of dox (Fig. 1B). The activities of five different pathways that play an important role in (breast) cancer growth and progression were evaluated. No differences were observed in the activities of the ER, AR, or HH signaling pathways (Fig. 1C). Activities of the PI3K and TGFβ pathways were elevated in both KOs as compared to CTR cells. Together, these data indicate that despite upregulation of TGFβ signaling (which is a major EMT inducing pathway<sup>31,32</sup> in response to GRHL2 deletion, this is not sufficient to trigger an EMT in Luminal-like breast cancer cells.

### Stable overexpression of GRHL2 in MDA-MB-231 cells does not trigger an MET

We next performed an inverse experiment where GRHL2 was stably overexpressed in Basal-B cells. These cells express little or no GRHL2 as compared to Luminal-like breast cancer cells and have a mesenchymal phenotype. Western blot analysis confirmed that GRHL2 cDNA expressing MDA-MB-231 cells had higher GRHL2 protein expression as compared to CTR cells expressing an empty vector (Fig. 2A). This result was confirmed by immunostaining and showed that GRHL2 cDNA expression levels were comparable to the endogenous expression in MCF-7 cells, but not all MDA-MB-231-GRHL2 cells expressed the cDNA (Fig. 2B). We analyzed changes in protein expression of selected EMT/MET-associated genes induced by GRHL2 overexpression using immunostaining. Based on the expression of GRHL2 in a subset of cells, a change in the expression pattern may be expected in a subset of the cells for these markers. However, no obvious downregulation of the mesenchymal markers Vimentin and ZEB1 was observed (Fig. 2C). Moreover, no enhanced expression of the epithelial genes E-cadherin, Occludin, or ZO-1 was observed and expression of *CLDN4*, encoded by the established direct GRHL2 target gene *CLDN4*, was not affected (Fig. 2C). These results demonstrate that stable expression of GRHL2 in this TNBC cell line is insufficient to induce MET-associated changes in gene expression.



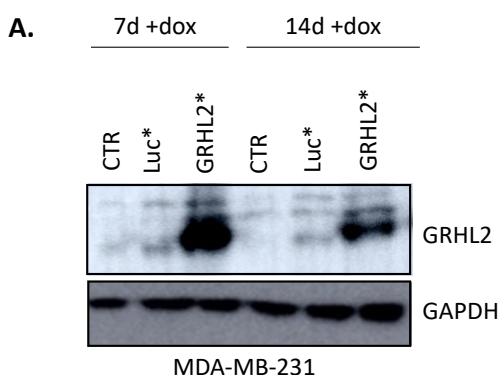




**Figure 2: Effect of stable GRHL2 overexpression in Basal-b cells on EMT-associated genes. (A, B)** GRHL2 protein expression detected by western blotting (A) and Immunofluorescence (B) in CTR and GRHL2-overexpressing MDA-MB-231 cells. Immunofluorescence analysis of GRHL2 protein expression in MCF-7 cells serves as control for endogenous expression level of GRHL2 protein. Blue, Hoechst; Red-Cy5 GRHL2 Ab. **(C, D)** Immunostaining of mesenchymal markers Vimentin and ZEB1 (C) and epithelial markers Occludin, ZO-1, E-cadherin and CLDN4 (D) in MCF-7, MDA-MB-231 CTR, and MDA-MB-231-GRHL2 cells. Blue, Hoechst; Cy5, Abs recognizing EMT /MET-associated genes; Cy3, Phalloidin.

### No MET-associated changes are observed upon inducible GRHL2 overexpression in MDA-MB-231 cells

We next sought to investigate the effect of induced, strong expression of GRHL2 in MDA-MB-231 cells. Therefore, we utilized a dox-inducible GRHL2 overexpression system to investigate possible early, but transient signs of MET triggered by GRHL2. MDA-MB-231 cells were analyzed by Western Blot after 7 and 14 days of dox treatment (Fig. 3A). A clear induction of GRHL2 was observed at both time points in GRHL2\* overexpressing cells but not in CTR or Luc\* expressing cells. We further validated this system by immunostaining of GRHL2, localized in the nucleus, upon 7 and 14 days of dox induction (Fig. 3B). Then, we examined the changes in the expression of EMT/MET associated genes after GRHL2 overexpression but, again, no induction was observed for E-cadherin or CLDN4 upon expression of GRHL2 (Fig. 3C). Altogether, these findings show that overexpression of GRHL2 by itself does not trigger MET in MDA-MB-231 cells, contradicting previously reported findings, which demonstrated GRHL2-mediated phenotypic and genetic changes in these cells.<sup>33,34</sup>



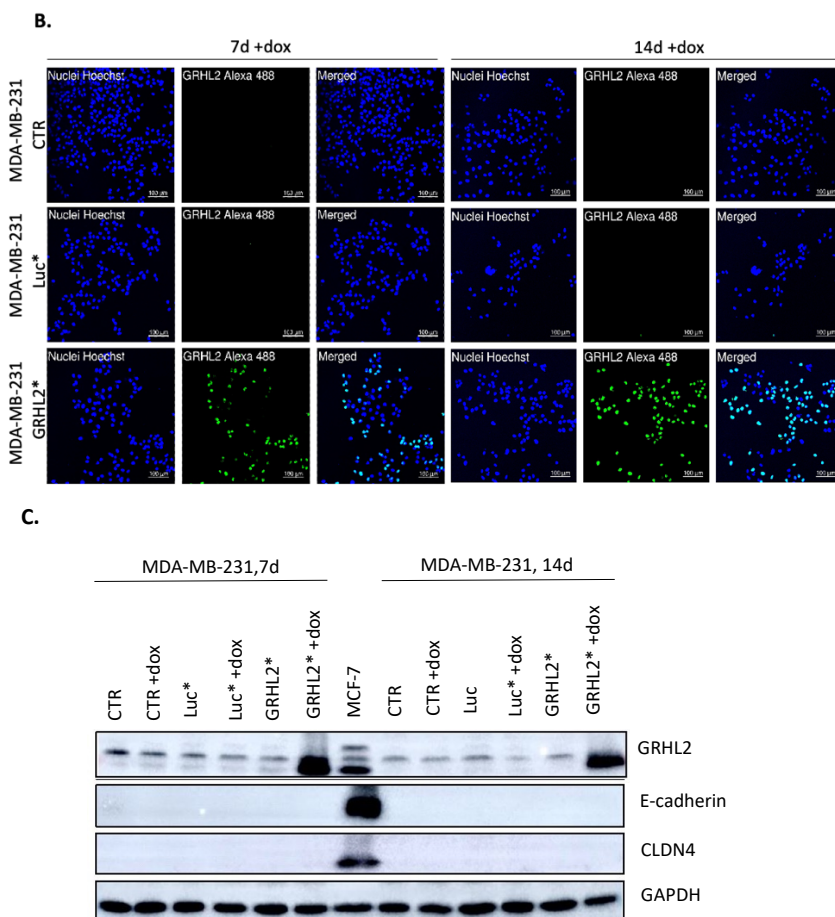


**Figure 3: Inducible GRHL2 overexpression does not confer MET-associated changes in Basal-b cells. (A, B)** Western blot (A) and immunofluorescence (B) analysis showing GRHL2 protein expression after 7 and 14 days dox induction (125ng/ml) in CTR, Luc\*, and GRHL2\* expressing MDA-MB-231 cells. Blue, Hoechst; Green, GRHL2 Ab. **(C)** Western blot showing alterations in protein expression of GRHL2 and epithelial markers CLDN4 and E-cadherin in CTR, Luc\*, and GRHL2\* expressing MDA-MB-231 cells with or without 7 and 14 days of dox (125ng/ml) exposure. MCF-7 was used to show endogenous levels of GRHL2 protein in Luminal cells.

**GRHL2 overexpression does not affect MDA-MB-231 cell growth**

Given the impact of GRHL2 deletion on cell survival and proliferation in luminal breast cancer cells,<sup>21,27</sup> we assessed the impact of GRHL2 overexpression on growth of MDA-MB-231 cells. In MDA-MB-231-GRHL2\* cells treated for 7 days with dox GRHL2 expression was detected while it was absent in MDA-MB-231-Luc\* cells (Fig. 4A). The cells were seeded after 7 days dox exposure, and cell viability was assessed after an additional 4 days growing in absence of dox using an SRB assay. This experiment did not show any significant difference in growth potential between MDA-MB-231-Luc\* or MDA-MB-231-GRHL2\* cells in absence or presence of dox (Fig. 4B).

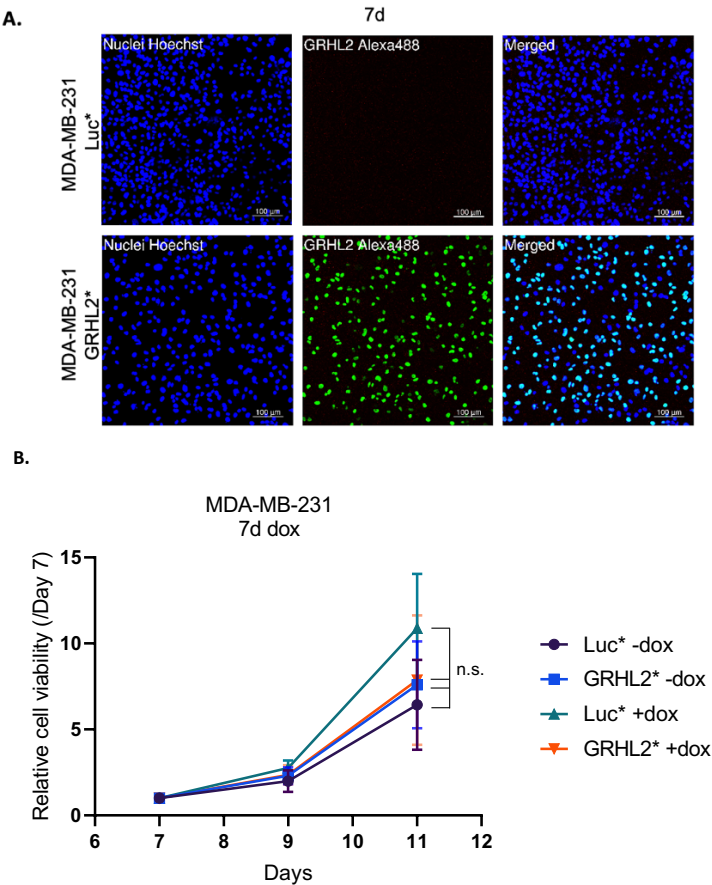


**Figure 4: Cell growth is not affected by GRHL2 overexpression in MDA-MB-231 cells. (A)** Immunostaining showing GRHL2 expression in MDA-MB-231-Luc\* and MDA-MB-231-GRHL2\* cells exposed to 125ng/ml dox for 7 days. Blue, Hoechst; Green, GRHL2 Ab. **(B)** Cell growth analyzed by SRB assay in MDA-MB-231 cells without and with 7 days dox induction of GRHL2 overexpression in MDA-MB-231-Luc\* and MDA-MB-231-GRHL2\* cells. Data was normalized to day 7. Mean  $\pm$  SD of three biological replicates is shown. ns, non-significant.

### Kinase inhibitor library screening identifies novel GRHL2-mediated vulnerabilities

The results thus far demonstrated that MDA-MB-231-GRHL2\* cells provided a model in which the impact of GRHL2 overexpression in Basal-b TNBC cells could be determined on drug vulnerabilities without confounding effects on baseline growth or EMT/MET balance. Therefore, we adopted a kinase inhibitor screening approach. First, we induced GRHL2 overexpression with 9 days of dox treatment in MDA-MB-231-GRHL2\* cells and used identically treated MDA-MB-231-Luc\* cells as control. These cells were exposed to 760 kinase inhibitors at 1uM final concentrations for four days in two biological replicates and cell viability was determined using an SRB assay (Fig.5A). 1uM Cisplatin served as a positive control since its effect on MDA-MB-231 cell viability has been studied.<sup>35,36</sup> Two biological replicates were performed. In both replicates MDA-MB-231-GRHL2\* cells were somewhat more sensitive to Cisplatin than MDA-MB-231-Luc\* cells (Fig. 5B). In addition, four kinases of interest (Torkinib, A-674563, LDC4297, Mirin) were identified that caused a reduction to <50% cell growth in MDA-MB-231-GRHL2\* cells while growth of MDA-MB-231-Luc\* cells was considerably less affected. Interestingly, the PI3K/AKT pathway, which was identified as a GRHL2-regulated signaling pathway (Fig. 1C) was a target of two of these inhibitors.

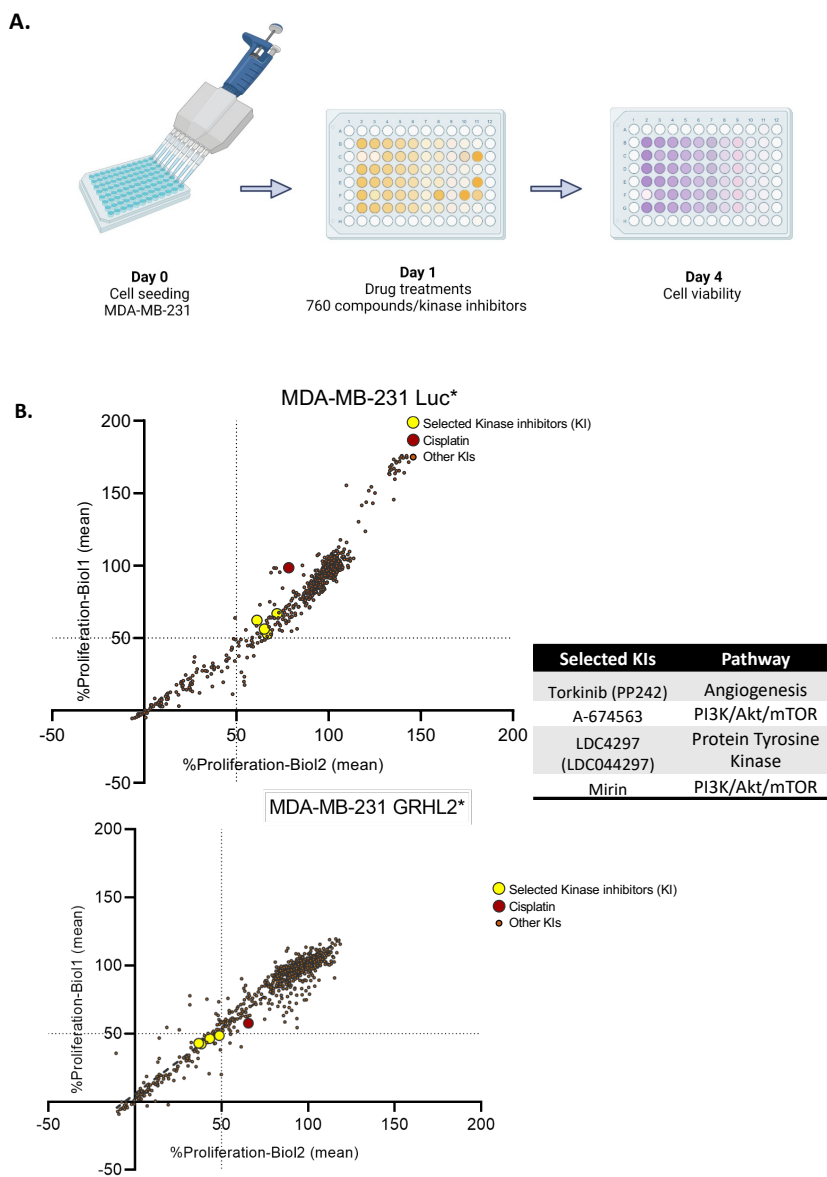


**Figure 5: Kinase inhibitor library screening in control and GRHL2 overexpressing Basal-b cells. (A)** Schematic representation of the kinase screen approach. Following the dox induction (125ng/ml) for 7 days in MDA-MB-231-Luc\* and MDA-MB-231-GRHL2\* cells, cells were treated 4 days with 1 $\mu$ M of 760 kinase inhibitors, Cisplatin, or vehicle (DMSO) followed by SRB assay. **(B)** Effect of kinase inhibitors

on growth of dox-induced MDA-MB-231-Luc\* and MDA-MB-231-GRHL2\* cells. The percentage growth is relative to DMSO condition. Two biological replicates, each performed in single technical replicates are plotted against each other. Four kinases of interest (%growth in GRHL2\* < %growth in Luc\*) are marked yellow. Cisplatin is marked red.

We subsequently analyzed the effect of concentration ranges of the 4 selected kinase inhibitors and included two additional DNA damaging chemotherapeutics, Docetaxel and Gemcitabine.<sup>37,38</sup> In this experiment, using the same strategy for the induction of GRHL2 or Luc, Cisplatin did not affect cell growth while Docetaxel and Gemcitabine strongly inhibited cell growth of MDA-MB-231-GRHL2\* as well as MDA-MB-231-Luc\* cells (Fig. 6). A674553, LDC4297, Torkinib, and Mirin inhibited cell growth in a concentration-dependent manner that was similar for MDA-MB-231-GRHL2\* and MDA-MB-231-Luc\* cells. These data demonstrate that induced expression of GRHL2 in Basal-b cells, in absence of effects on baseline growth or EMT/MET balance, does not affect sensitivity for chemotherapy or kinase inhibition.

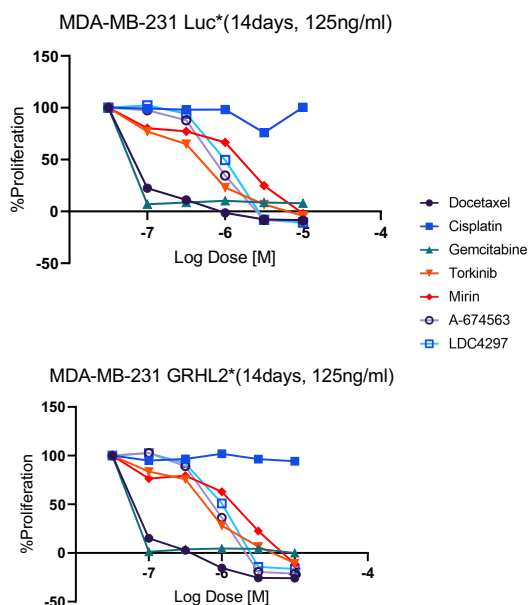


**Figure 6: Effect of selected kinase inhibitors and DNA damaging drugs on growth of control and GRHL2 overexpressing Basal-b cells. MDA-MB-231-Luc\* and MDA-**

MB-231-GRHL2\* cells were treated for 7 days using 125ng/ml dox. Induced cells were exposed to the indicated concentrations of selected kinase inhibitors Torkinib, Mirin, A-674563, or LDC4297 or DNA damaging drugs Docetaxel, Cisplatin, or Gemcitabine for 4 days. The percentage growth was determined with SRB assay and expressed relative to DMSO. Mean of three technical replicates for one experiment is shown.

### Discussion

Modulating cellular plasticity holds the potential to augment the sensitivity of cancer cells to therapies and improve patient outcomes. Prior research has highlighted the influence of EMT transcription factors (TFs) on inducing or suppressing EMT, thereby controlling anti-cancer drug resistance.<sup>8,39</sup> GRHL2, functioning as a master regulator of the epithelial phenotype, serves to inhibit more invasive and aggressive phenotypes, thereby fostering sensitivity to anti-cancer therapies.<sup>40,41</sup> Our results show that GRHL2 is not solely sufficient to disrupt the balance in EMT process. The interaction of GRHL2 with other transcription factors/genes may be required to facilitate EMT/MET. Indeed, GRHL2 operates within a network controlling gene expression of other EMT-TFs. A negative feedback loop between GRHL2 and ZEB1 has been previously reported.<sup>22,42</sup> Ultimately, EMT suppression mediated by GRHL2 requires downregulation of E-cadherin.<sup>25,43</sup>

Similar to an earlier study using MDA-MB-231 cells overexpressing GRHL2,<sup>33</sup> our study revealed no discernible impact of GRHL2 on cellular growth of this model. However, that same study showed that overexpression of GRHL2 triggers MET-like phenotypical and molecular changes (induced expression of E-cadherin) in MDA-MB-231 cells.<sup>33</sup> Our study does not support these findings. In our experiments MET-like alterations were evaluated using the mesenchymal markers Vimentin and ZEB1, and the epithelial markers Occludin, ZO-1, E-cadherin, and CLDN4. No significant changes were observed in their expression levels when GRHL2 was overexpressed. EMT progression by GRHL2 knockdown has been linked to epigenetic remodeling including histone modifications and DNA methylation in ovarian cancer.<sup>44</sup> In that study, removal of epigenetic marks on the histones using 5-azaticidine together with GRHL2 overexpression induced MET in ovarian cancer cells. It is possible that the



MDA-MB-231 cells used in our study and that of Werner et al<sup>33</sup> vary epigenetically. It is also possible that the level of GRHL2 overexpression in our experiments was less strong as compared to that achieved in the study by Werner et al. However, we confirmed that we reached GRHL2 expression levels that were similar to the endogenous level present in MCF7 Luminal breast cancer cells. Lastly, the inability of GRHL2 to stimulate MET in MDA-MB-231 cells could be explained by the lack of ER alpha (ER $\alpha$ ) signaling in MDA-MB-231 cells. Although we have demonstrated that GRHL2 rarely acts in a complex with ER $\alpha$ ,<sup>27</sup> there is evidence that GRHL2 cooperates with the ER $\alpha$ /FOXA1/GATA3 complex<sup>45</sup> and the absence of ER $\alpha$  signaling may prevent MET induction or effects on proliferation by GRHL2.

GRHL2 regulates multiple signaling pathways (MAPK, TGF $\beta$ ) that determine the anti-cancer drug response.<sup>46,47</sup> Basal-like breast cancer cells that survived after the therapy have been linked to lack of histone acetylation by H3K27ac, a well-known transcription enhancer, at regulatory sites of GRHL2.<sup>48</sup> To identify GRHL2-mediated drug vulnerabilities, we exposed CTR and GRHL2 overexpressing MDA-MB-231 cells to small molecule kinase inhibitors and chemotherapeutic agents. Interestingly, we find that besides TGF $\beta$  signaling, PI3K signaling is increased upon deletion of GRHL2 in luminal breast cancer cells, and 2/4 small molecule kinase inhibitors that appeared to selectively affect GRHL2 overexpressing MDA-MB-231 cells target PI3K signaling. Nevertheless, follow up experiments did not indicate significant vulnerabilities that are controlled by GRHL2. This implies that additional factors or mechanisms are at play in determining treatment sensitivity. The combined absence of an induction of MET and enhanced therapy sensitivity in response to GRHL2 in our study, indicates that the ability of GRHL2 to affect drug responses in breast cancer cells reported in other models may be strictly linked to its ability to shift the EMT/MET balance towards MET.

In conclusion, we find that depletion of GRHL2 in Luminal breast cancer cells or induction of GRHL2 in Basal b breast cancer cells does not necessarily lead to a shift in the EMT/MET balance. The impact of changes in GRHL2 expression must be context dependent, which also leads to apparently distinct

effects on therapy sensitivity in different models. The engagement of GRHL2 in multifaceted regulatory networks must be distinct in different breast cancer cell models thereby making a general prediction of the outcome of GRHL2 manipulation impossible.

**Acknowledgements:** We thank Dr. Ruby Yun-Ju Huang from National University of Singapore for providing the GRHL2 expression construct. We also thank to Ingelise Stringer from Molecular Pathway Diagnostics, Philips HealthWorks, The Netherlands for collaborating with us to test OncoSignal pathways technology.

**Competing interests:** The authors declare that they have no competing interests. Bircan Coban was supported by the Dutch Cancer Society (KWF Research Grant #10967).

## References

1. Wicker MN, Wagner KU. Cellular plasticity in mammary gland development and breast cancer. *Cancers Basel*. 2023;15(23). doi:10.3390/cancers15235605
2. Shi ZD, Pang K, Wu ZX, et al. Tumor cell plasticity in targeted therapy-induced resistance: mechanisms and new strategies. *Signal Transduct Target Ther*. 2023;8(1):113. doi:10.1038/s41392-023-01383-x
3. Jewer M, Lee L, Leibovitch M, et al. Translational control of breast cancer plasticity. *Nat Commun*. 2020;11(1):2498. doi:10.1038/s41467-020-16352-z
4. Forte E, Chimenti I, Rosa P, et al. EMT/MET at the crossroad of stemness, regeneration and oncogenesis: The Ying-Yang equilibrium recapitulated in cell spheroids. *Cancers Basel*. 2017;9(8):98. doi:10.3390/cancers9080098
5. Akhmetkaliyev A, Alibrahim N, Shafiee D, Tulchinsky E. EMT/MET plasticity in cancer and Go-or-Grow decisions in quiescence: the two sides of the same coin? *Mol Cancer*. 2023;22(1):90. doi:10.1186/s12943-023-01793-z
6. Jolly MK, Tripathi SC, Jia D, et al. Stability of the hybrid epithelial/mesenchymal phenotype. *Oncotarget*. 2016;7(19):27067-27084. doi:10.18632/oncotarget.8166
7. Shibue T, Weinberg RA. EMT, CSCs, and drug resistance: the mechanistic link and clinical implications. *Nat Rev Clin Oncol*. 2017;14(10):611-629. doi:10.1038/nrclinonc.2017.44
8. Marcucci F, Stassi G, De Maria R. Epithelial-mesenchymal transition: a new target in anticancer drug discovery. *Nat Rev Drug Discov*. 2016;15(5):311-325. doi:10.1038/nrd.2015.13

9. Muriithi W, Macharia LW, Heming CP, et al. ABC transporters and the hallmarks of cancer: roles in cancer aggressiveness beyond multidrug resistance. *Cancer Biol Med*. 2020;17(2):253-269. doi:10.20892/j.issn.2095-3941.2019.0284
10. Yin L, Castagnino P, Assoian RK. ABCG2 expression and side population abundance regulated by a transforming growth factor beta-directed epithelial-mesenchymal transition. *Cancer Res*. 2008;68(3):800-807. doi:10.1158/0008-5472.CAN-07-2545
11. Saxena M, Stephens MA, Pathak H, Rangarajan A. Transcription factors that mediate epithelial-mesenchymal transition lead to multidrug resistance by upregulating ABC transporters. *Cell Death Dis*. 2011;2:e179. doi:10.1038/cddis.2011.61
12. Hugo HJ, Pereira L, Suryadinata R, et al. Direct repression of MYB by ZEB1 suppresses proliferation and epithelial gene expression during epithelial-to-mesenchymal transition of breast cancer cells. *Breast Cancer Res*. 2013;15(6):R113. doi:10.1186/bcr3580
13. Yang Y, Pan X, Lei W, Wang J, Song J. Transforming growth factor-beta1 induces epithelial-to-mesenchymal transition and apoptosis via a cell cycle-dependent mechanism. *Oncogene*. 2006;25(55):7235-7244. doi:10.1038/sj.onc.1209712
14. Lee SY, Jeong EK, Ju MK, et al. Induction of metastasis, cancer stem cell phenotype, and oncogenic metabolism in cancer cells by ionizing radiation. *Mol Cancer*. 2017;16(1):10. doi:10.1186/s12943-016-0577-4
15. De Las Rivas J, Brozovic A, Izraely S, Casas-Pais A, Witz IP, Figueroa A. Cancer drug resistance induced by EMT: novel therapeutic strategies. *Arch Toxicol*. 2021;95(7):2279-2297. doi:10.1007/s00204-021-03063-7
16. Terry S, Savagner P, Ortiz-Cuaran S, et al. New insights into the role of EMT in tumor immune escape. *Mol Oncol*. 2017;11(7):824-846. doi:10.1002/1878-0261.12093
17. Xiang X, Deng Z, Zhuang X, et al. Grhl2 determines the epithelial phenotype of breast cancers and promotes tumor progression. *PLoS One*. 2012;7(12):e50781. doi:10.1371/journal.pone.0050781
18. Yang Z, Wu D, Chen Y, Min Z, Quan Y. GRHL2 inhibits colorectal cancer progression and metastasis via oppressing epithelial-mesenchymal transition. *Cancer Biol Ther*. 2019;20(9):1195-1205. doi:10.1080/15384047.2019.1599664
19. Kawabe N, Matsuoka K, Komeda K, et al. Silencing of GRHL2 induces epithelial-to-mesenchymal transition in lung cancer cell lines with different effects on proliferation and clonogenic growth. *Oncol Lett*. 2023;26(3):391. doi:10.3892/ol.2023.13977
20. Cieply B, Riley P 4th, Pifer PM, et al. Suppression of the epithelial-mesenchymal transition by Grainyhead-like-2. *Cancer Res*. 2012;72(9):2440-2453. doi:10.1158/0008-5472.CAN-11-4038
21. Wang Z, Coban B, Liao CY, Chen YJ, Liu Q, Danen EHJ. GRHL2 regulation of growth/motility balance in luminal versus basal breast cancer. *Int J Mol Sci*. 2023;24(3):2512. doi:10.3390/ijms24032512

22. Quan Y, Jin R, Huang A, et al. Downregulation of GRHL2 inhibits the proliferation of colorectal cancer cells by targeting ZEB1. *Cancer Biol Ther.* 2014;15(7):878-887. doi:10.4161/cbt.28877
23. Nie Y, Ding Y, Yang M. GRHL2 upregulation predicts a poor prognosis and promotes the resistance of serous ovarian cancer to cisplatin. *Onco Targets Ther.* 2020;13:6303-6314. doi:10.2147/OTT.S250412
24. Hu F, He Z, Sun C, Rong D. Knockdown of GRHL2 inhibited proliferation and induced apoptosis of colorectal cancer by suppressing the PI3K/Akt pathway. *Gene.* 2019;700:96-104. doi:10.1016/j.gene.2019.03.051
25. Chen W, Kang KL, Alshaikh A, et al. Grainyhead-like 2 (GRHL2) knockout abolishes oral cancer development through reciprocal regulation of the MAP kinase and TGF- $\beta$  signaling pathways. *Oncogenesis.* 2018;7(5):38. doi:10.1038/s41389-018-0047-5
26. Coban B, Wang Z, Liao CY, et al. GRHL2 suppression of NT5E/CD73 in breast cancer cells modulates CD73-mediated adenosine production and T cell recruitment. *iScience.* 2024;27(5):109738. doi:10.1016/j.isci.2024.109738
27. Wang Z, Coban B, Wu H, et al. GRHL2-controlled gene expression networks in luminal breast cancer. *Cell Commun Signal.* 2023;21(1):15. doi:10.1186/s12964-022-01029-5
28. Inda MA, van Swinderen P, van Brussel A, et al. Heterogeneity in signaling pathway activity within primary and between primary and metastatic breast cancer. *Cancers Basel.* 2021;13(6):1345. doi:10.3390/cancers13061345
29. Xiang X, Deng Z, Zhuang X, et al. Grhl2 determines the epithelial phenotype of breast cancers and promotes tumor progression. *PLoS One.* 2012;7(12):e50781. doi:10.1371/journal.pone.0050781
30. Kawabe N, Matsuoka K, Komeda K, et al. Silencing of GRHL2 induces epithelial-to-mesenchymal transition in lung cancer cell lines with different effects on proliferation and clonogenic growth. *Oncol Lett.* 2023;26(3):391. doi:10.3892/ol.2023.13977
31. Xu J, Lamouille S, Derynck R. TGF-beta-induced epithelial to mesenchymal transition. *Cell Res.* 2009;19(2):156-172. doi:10.1038/cr.2009.5
32. Hao Y, Baker D, Ten Dijke P. TGF- $\beta$ -mediated epithelial-mesenchymal transition and cancer metastasis. *Int J Mol Sci.* 2019;20(11):2767. doi:10.3390/ijms20112767
33. Werner S, Frey S, Riethdorf S, et al. Dual roles of the transcription factor grainyhead-like 2 (GRHL2) in breast cancer. *J Biol Chem.* 2013;288(32):22993-23008. doi:10.1074/jbc.M113.456293
34. Chung VY, Tan TZ, Ye J, et al. The role of GRHL2 and epigenetic remodeling in epithelial-mesenchymal plasticity in ovarian cancer cells. *Commun Biol.* 2019;2(1):272. doi:10.1038/s42003-019-0506-3
35. Wawruszak A, Luszczki JJ, Grabarska A, et al. Assessment of interactions between cisplatin and two histone deacetylase inhibitors in MCF7, T47D and MDA-MB-231 human breast cancer cell lines - an isobolographic analysis. *PLoS One.* 2015;10(11):e0143013. doi:10.1371/journal.pone.0143013

36. Prabhakaran P, Hassiotou F, Blancafort P, Filgueira L. Cisplatin induces differentiation of breast cancer cells. *Front Oncol.* 2013;3:134. doi:10.3389/fonc.2013.00134
37. Heinemann V, Boeck S, Hinke A, Labianca R, Louvet C. Meta-analysis of randomized trials: evaluation of benefit from gemcitabine-based combination chemotherapy applied in advanced pancreatic cancer. *BMC Cancer.* 2008;8(1):82. doi:10.1186/1471-2407-8-82
38. Crown J, O'Leary M, Ooi WS. Docetaxel and paclitaxel in the treatment of breast cancer: a review of clinical experience. *Oncologist.* 2004;9 Suppl 2:24-32. doi:10.1634/theoncologist.9-suppl\_2-24
39. Du B, Shim JS. Targeting epithelial-mesenchymal transition (EMT) to overcome drug resistance in cancer. *Molecules.* 2016;21(7):965. doi:10.3390/molecules21070965
40. Wang T, Li N, Jin L, Qi X, Zhang C, Hua D. The calcium pump PMCA4 prevents epithelial-mesenchymal transition by inhibiting NFATc1-ZEB1 pathway in gastric cancer. *Biochim Biophys Acta Mol Cell Res.* 2020;1867(12):118833. doi:10.1016/j.bbamcr.2020.118833
41. Cocce KJ, Jasper JS, Desautels TK, et al. The lineage determining factor GRHL2 collaborates with FOXA1 to establish a targetable pathway in endocrine therapy-resistant breast cancer. *Cell Rep.* 2019;29(4):889-903.e10. doi:10.1016/j.celrep.2019.09.032
42. Gregory PA, Bracken CP, Smith E, et al. An autocrine TGF-beta/ZEB/miR-200 signaling network regulates establishment and maintenance of epithelial-mesenchymal transition. *Mol Biol Cell.* 2011;22(10):1686-1698. doi:10.1091/mbc.E11-02-0103
43. Chen W, Yi JK, Shimane T, et al. Grainyhead-like 2 regulates epithelial plasticity and stemness in oral cancer cells. *Carcinogenesis.* 2016;37(5):500-510. doi:10.1093/carcin/bgw027
44. Chung VY, Tan TZ, Ye J, et al. The role of GRHL2 and epigenetic remodeling in epithelial-mesenchymal plasticity in ovarian cancer cells. *Commun Biol.* 2019;2:272. doi:10.1038/s42003-019-0506-3
45. Mohammadi Ghahhari N, Sznurkowska MK, Hulo N, Bernasconi L, Aceto N, Picard D. Cooperative interaction between ER $\alpha$  and the EMT-inducer ZEB1 reprograms breast cancer cells for bone metastasis. *Nat Commun.* 2022;13(1):2104. doi:10.1038/s41467-022-29723-5
46. Morrison CD, Parvani JG, Schiemann WP. The relevance of the TGF- $\beta$  Paradox to EMT-MET programs. *Cancer Lett.* 2013;341(1):30-40. doi:10.1016/j.canlet.2013.02.048
47. Nie Y, Ding Y, Yang M. GRHL2 upregulation predicts a poor prognosis and promotes the resistance of serous ovarian cancer to cisplatin. *Onco Targets Ther.* 2020;13:6303-6314. doi:10.2147/OTT.S250412
48. Pantelaiou-Prokaki G, Mieczkowska I, Schmidt GE, et al. HDAC8 suppresses the epithelial phenotype and promotes EMT in chemotherapy-treated basal-like breast cancer. *Clin Epigenetics.* 2022;14(1):7. doi:10.1186/s13148-022-01228-4



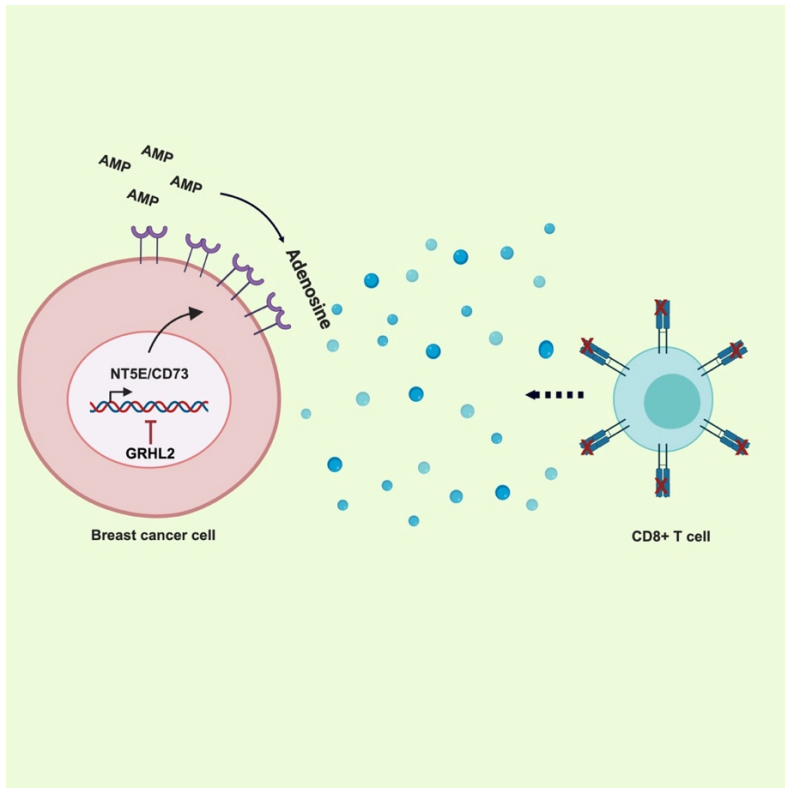
# Chapter 6

---

## GRHL2 suppression of NT5E/CD73 in breast cancer cells modulates CD73-mediated adenosine production and T cell recruitment

Published in: Bircan Coban<sup>1</sup>, Zi Wang<sup>1,2</sup>, Chen-yi Liao<sup>1</sup>, Klara Beslmüller<sup>1</sup>, Mieke A.M. Timmermans<sup>3</sup>, John W.M. Martens<sup>3</sup>, Jasmijn Hundscheid<sup>1</sup>, Bram Slutter<sup>1</sup>, Annelien J.M. Zweemer<sup>1</sup>, Elsa Neubert<sup>1</sup>, Erik H.J. Danen<sup>1,4,5</sup> GRHL2 suppression of NT5E/CD73 in breast cancer cells modulates CD73-mediated adenosine production and T cell recruitment. *iScience*. 2024 Apr 12;27(5):109738.

<sup>1</sup>Leiden Academic Center for Drug Research, Leiden University, Leiden, The Netherlands; <sup>2</sup>Department of clinical laboratory, Tianjin Medical University Cancer Institute and Hospital, National Clinical Research Center for Cancer, Tianjin, China; <sup>3</sup>Department of Medical Oncology, Erasmus MC Cancer Institute, Erasmus University Medical Center, Rotterdam, The Netherlands; <sup>4</sup> Lead contact; <sup>5</sup>correspondence: e.danen@lacdr.leidenuniv.nl



### Highlights

- GRHL2 suppresses NT5E/ CD73 expression in breast cancer cells.
- Loss of GRGL2 triggers CD73-mediated adenosine production.
- Increased adenosine production does not inhibit T cell migration.
- CD73 expression correlates with increased CD8 T cell presence in breast cancer.



### Summary

Tumor tissues often contain high extracellular adenosine, promoting an immunosuppressed environment linked to mesenchymal transition and immune evasion. Here, we show that loss of the epithelial transcription factor, GRHL2, triggers NT5E/CD73 ecto-enzyme expression, augmenting the conversion of AMP to adenosine. GRHL2 binds an intronic *NT5E* sequence and is negatively correlated with NT5E/CD73 in breast cancer cell lines and patients. Remarkably, the increased adenosine levels triggered by GRHL2 depletion in MCF-7 breast cancer cells do not suppress but mildly increase CD8 T cell recruitment, a response mimicked by a stable adenosine analog but prevented by CD73 inhibition. Indeed, NT5E expression shows a positive rather than negative association with CD8 T cell infiltration in breast cancer patients. These findings reveal a GRHL2-regulated immune modulation mechanism in breast cancers and show that extracellular adenosine, besides its established role as a suppressor of T cell-mediated cytotoxicity, is associated with enhanced T cell recruitment.

### Introduction

In solid tumors, the interaction between cancer cells and the surrounding tumor microenvironment (TME) regulates cancer growth and metastasis.<sup>1-3</sup> The TME is complex and includes altered functionality of extracellular matrix, fibroblasts, and vascular cells. In this tumor reactive stroma environment, various types of immune cells are affected. On the one hand, this involves cross talk of tumor cells with myeloid cells such as macrophages and neutrophils, and cancer-associated fibroblasts, creating an inflammatory TME that drives tumor progression.<sup>4-6</sup> On the other hand, tumors escape recognition and killing by the immune system by suppressing the activity of T cells and NK cells through a plethora of mechanisms, including the development of an immunosuppressed TME.<sup>4,7,8</sup>

One mechanism underlying the emergence of an immunosuppressed niche, involves the accumulation of adenosine in the TME.<sup>9</sup> During physiological healing of wounded or infected tissues adenosine triphosphate (ATP) released by damaged cells triggers inflammation by binding to excitatory ATP

receptors activating T cells and other immune cell types. This response is kept in check by a negative feedback loop, in which ATP and adenosine di-phosphate (ADP) are converted to adenosine monophosphate (AMP), which is further converted to adenosine, which binds inhibitory G-protein coupled receptors (GPCRs) on immune cells to dampen the inflammatory response.<sup>10</sup> In tumors, prolonged elevated levels of extracellular adenosine in the TME suppress immune cell activation and effector functions, thereby causing immune escape and therapy resistance.<sup>9,11</sup> In addition to indirect mechanisms such as leakage from necrotic cells in hypoxic areas, the accumulation of adenosine in the TME may be a consequence of genetic changes that alter nucleotide metabolism in tumor cells.

Nucleotide metabolism leading to the production of extracellular adenosine involves the conversion of ATP and ADP to AMP by ecto-enzymes, including ectonucleoside triphosphate diphosphohydrolase-1 (ENTPD1/CD39)<sup>12</sup> followed by the subsequent conversion of AMP to adenosine, mainly by the ecto-5'-nucleotidase, NT5E/CD73.<sup>13</sup> CD39 is a transmembrane protein whereas CD73 is linked to glycosylphosphatidyl inositol (GPI) in the plasma membrane and can be shed from the membrane through proteolytic cleavage or GPI hydrolysis.<sup>13</sup> Given their key role in the creation of an immunosuppressed TME, CD39 and CD73 represent candidate targets for cancer immunotherapy, and their potential has been established in preclinical models.<sup>14-22</sup> Increased levels of CD73 expression have been reported in multiple solid tumor types<sup>23-27</sup> but it is incompletely understood how tumor cells may modulate expression of this ectoenzyme. Tumor cells display plasticity and carcinomas typically contain populations of tumor cells with different epithelial versus mesenchymal characteristics.<sup>2</sup> The transition to a more mesenchymal state has been associated with immune evasion in breast- and other carcinomas.<sup>28,29</sup> Recent studies have shown that epithelial-mesenchymal transition (EMT) can modulate CD73, which may involve activation of TGF $\beta$  signaling and the SNAIL transcription factor and contributes to immune suppression.<sup>30-</sup>

32

Grainyhead-like 2 (GRHL2) is a critical transcription factor for development and function of epithelial tissues that competes with mesenchymal transcription factors such as ZEB and SNAIL to suppresses EMT.<sup>33-39</sup> We have previously identified GRHL2-regulated genes in breast cancer cells using conditional knockout (KO) cells, ChIP-seq, and Bru-seq.<sup>40,41</sup> Here, we identify the *NT5E* gene as a GRHL2 target and reveal how GRHL2 depletion induces NT5E/CD73 expression and, consequently, triggers extracellular adenosine production. We find that GRHL2 and CD73 expression are inversely correlated in a panel of human breast cancer cell lines and human breast cancer patients. We show that, in addition to its previously established role as a suppressor of T cell-mediated cytotoxicity, CD73-mediated adenosine production in fact leads to an increase in T cell recruitment and, in agreement, NT5E expression is positively rather than negatively associated with T cell infiltration in breast cancer patients.

### Results

#### Loss of GRHL2 upregulates NT5E/CD73 expression in MCF-7 cells

We explored GRHL2-regulated genes identified by nascent RNA Bru-seq in an MCF-7 conditional GRHL2 KO model. We previously developed this model using doxycycline induced Cas9 expression to trigger GRHL2 depletion.<sup>41</sup> One of the genes whose transcription was upregulated in response to loss of GRHL2 was *NT5E*. Sequence reads of NT5E nascent mRNA were mapped to the NT5E genomic sequence in Ctrl sgRNA, GRHL2 sgRNA#1 (KO-1), and GRHL2 sgRNA#2(KO-2) samples (Fig. 1A, B). An increase in the rate of synthesis of NT5E mRNA was observed upon GRHL2 deletion for both Kos and this rate decreased at the 3'end of the transcript, indicative of nascent mRNA degradation. Normalized log2-fold changes showed that nascent NT5E mRNA was induced within the first 48h of doxycycline-induced GRHL2 depletion and increased transcription was maintained for at least 16 days for one sgRNA (KO-1) whereas a second sgRNA (KO-2) showed a gradual return to baseline in this experiment (Fig. 1C).

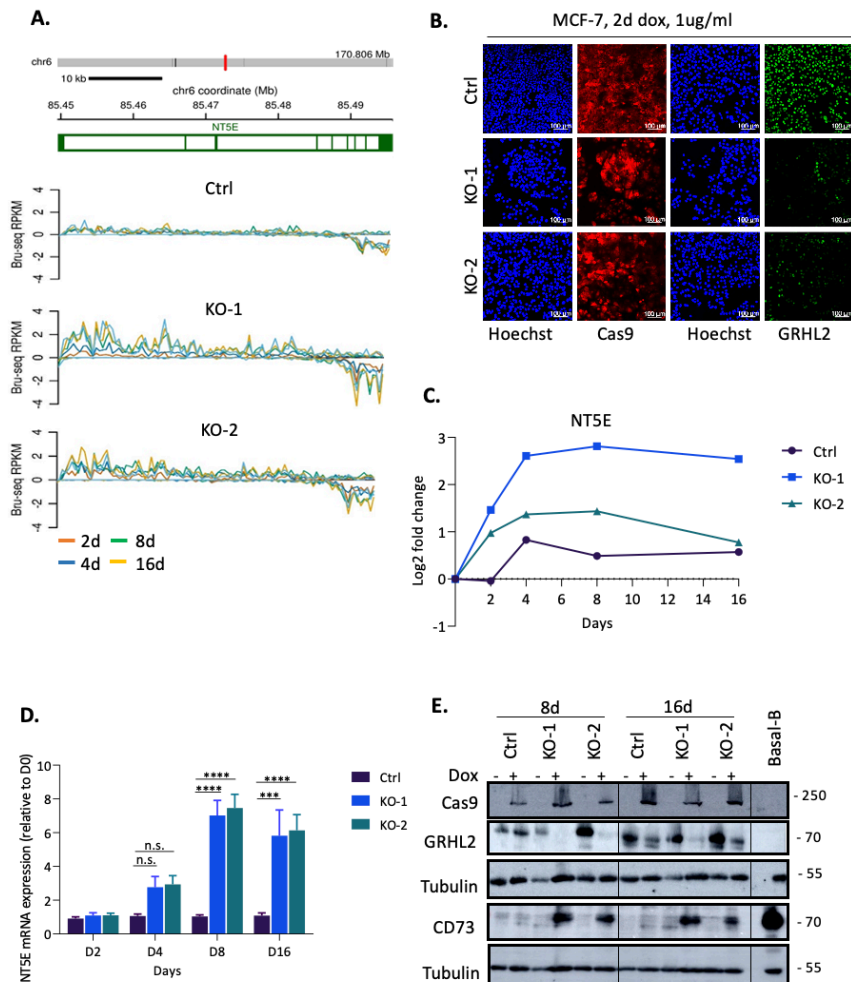


**Figure 1: Loss of GRHL2 upregulates CD73 expression in MCF-7 cells.**

**(A)** Bru-seq reads of nascent NT5E mRNA in an MCF-7 conditional GRHL2 KO model. Graphs are shown for a control sgRNA (Ctrl) and 2 GRHL2 sgRNA models (KO1 and 2) and colors represent the indicated timepoints after doxycycline induced GRHL2 deletion. The reference sequence annotation is shown above with exons in green blocks. **(B)** Immunofluorescence images of HOECHST (blue), Cas9 Ab (red), or GRHL2 Ab (green) for CTRL or GRHL2 KO MCF-7 cells after 48 hours 1 ug/ml doxycycline treatment. **(C)** Graph showing log2 fold changes of nascent

NT5E mRNA for the indicated time points after doxycycline exposure in CTR or GRHL2 KO MCF-7 cells. **(D)** qRT-PCR analysis showing changes in total NT5E mRNA expression at the indicated timepoints after doxycycline induced GRHL2 deletion. Values were normalized to the untreated samples for each time point. Data analyzed using 2- $\Delta\Delta C_t$  method. Mean and SD of three biological replicates is shown. (Two-way ANOVA test; n.s., non-significant; \*\*\* $p < 0.001$ ; \*\*\*\* $p < 0.0001$ ). **(E)** Western blot analysis of Cas9, GRHL2, and CD73 in MCF-7 control sgRNA (Ctr) and 2 GRHL2 sgRNA models (KO1 and KO2) at the indicated timepoints after doxycycline induced GRHL2 deletion. Tubulin serves as a loading control. One out of three biological replicates shown. MDA-MB-231 basal B cells serve as positive control for CD73 expression.

We confirmed the Bru-seq data by qRT-PCR on RNA samples extracted from the GRHL2 KO-induced MCF-7 cells (Fig. 1D). Total NT5E mRNA levels were increased in response to GRHL2 deletion starting from day 4 and remaining high at 8 and 16 days after loss of GRHL2. Increased NT5E mRNA levels were accompanied by an induction of the NT5E/CD73 protein (Fig 1E). CD73 protein expression emerged in GRHL2-depleted cells at 8 and 16 days after doxycycline treatment in both GRHL2 KO-1 and KO-2 models but not in the Ctrl model. A basal B cell line expressing CD73 served as a positive control. Together, these findings demonstrated that GRHL2 controls expression of the NT5E gene and, consequently, the CD73 protein.

### **NT5E/CD73 levels are inversely correlated with GRHL2 in breast cancer cell lines and breast cancer patient tumor samples**

We next addressed whether the inverse correlation between GRHL2 and NT5E identified in the MCF-7 conditional KO models was observed in a larger series of breast cancer cell lines. For this purpose, RNA-seq data from 52 human breast cancer cell lines representing distinct breast cancer subtypes was explored.<sup>42</sup> Indeed, GRHL2 mRNA was highly expressed in Her2 low and Her2+ luminal and, with more variation in TNBC basal A breast cancer cell lines while it was not or lowly expressed in TNBC basal B cell lines ( $p < 0.0001$ ), NT5E showed an opposite pattern (Fig. 2A). NT5E mRNA expression was somewhat increased in TNBC basal A cell lines as compared to the luminal breast cancer cell lines ( $p < 0.05$ ) and showed a sharp further increase in TNBC

Basal B cell lines ( $p < 0.001$ ). For basal A, NT5E expression showed a wide distribution, indicating that GRHL2/NT5E double positive lines as well as GRHL2 positive/NT5E negative lines may be present in this subtype. IHC confirmed the inverse correlation between GRHL2 and CD73 in selected luminal versus basal B cells (Fig. S1). The inverse correlation between GRHL2 and NT5E/CD73 expression was further established in a series of breast cancer cell lines representing Her2- luminal (CAMA-1 and T47D), Her2+ luminal (MDA-MB-361 and BT474), TNBC basal A (HCC1806 and HCC1143), and TNBC basal B cell lines (MDA-MB-231 and BT549). GRHL2 mRNA decreased while NT5E mRNA emerged in the basal B cell lines (Fig. 2B). In agreement, CD73 protein expression in this series was not detected in luminal cell lines, weakly expressed in basal A cell lines, and was strongly expressed in the GRHL2 negative basal B cell lines (Fig. 2C). Notably, CD73 cell surface expression as detected by flow cytometry was more heterogeneous with an increase in BT549 but not MDA-MB-231 basal B cells as compared to luminal and basal A cells (Fig. 2D). This difference between total cellular versus cell surface detected CD73 protein may be related to differences in CD73 shedding from the membrane.<sup>13</sup>

# GRHL2 suppression of NT5E/CD73 in breast cancer cells

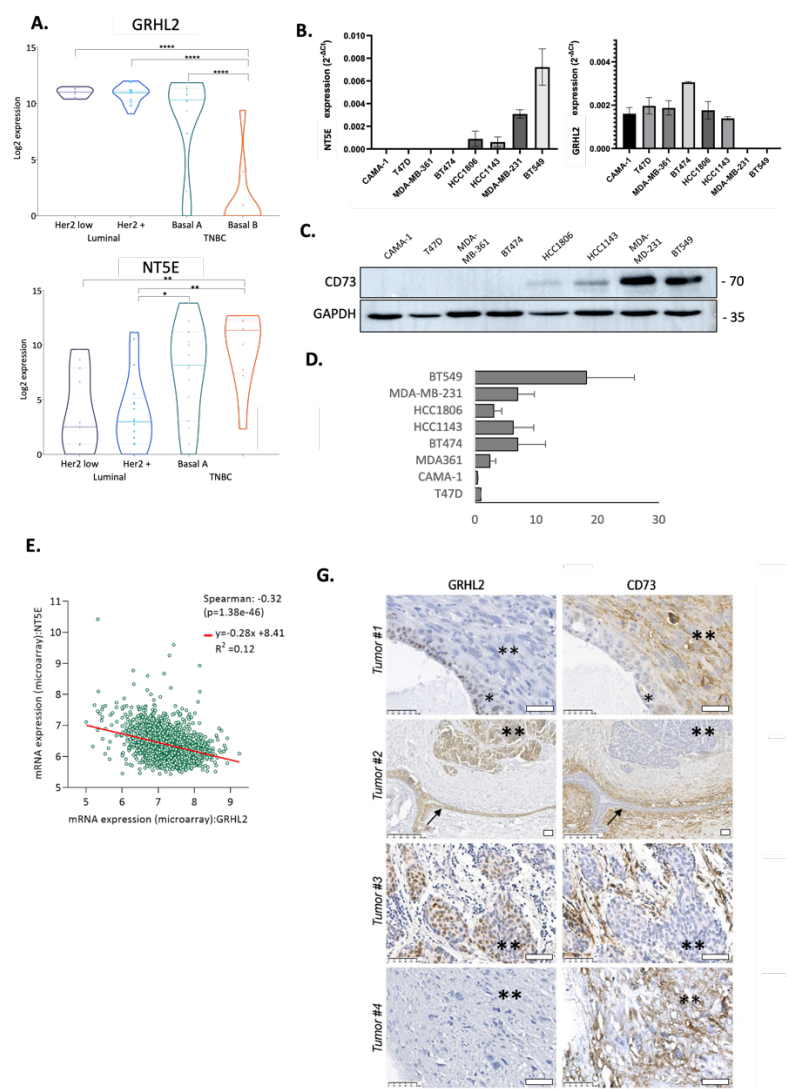


**Figure 2: NT5E/CD73 levels are inversely corelated with GRHL2 in breast cancer subtypes and breast cancer patient tumor samples. (A)** Violin plots showing gene expression levels of GRHL2 and NT5E based on RNA-seq data for 52 human breast cancer cell lines grouped according to the indicated subtypes. p-values calculated using One-way ANOVA as described in a previous study.<sup>42</sup> n.s., non-significant. **(B)** qRT-PCR analysis showing CD73 (left panel) and GRHL2 mRNA expression for the indicated cell lines. Data analyzed using 2–ΔCt method for the gene of interest corrected for GAPDH control. Mean and SD of two experiments performed in triplicate is shown. (Two-way ANOVA test) **(C)** Western blot analysis of CD73 and

GAPDH loading control in the indicated cell lines. One experiment of 2 is shown. **(D)** Flow cytometry analysis of CD73 surface expression in the indicated cell lines. Mean and SD of two experiments performed in duplicate is shown. **(E)** Correlation between gene expression levels of NT5E and GRHL2 in breast cancer tumors using METABRIC dataset. Correlation scores and p-values shown as determined in cBioPortal. **(F)** CD73 score derived from IHC, on whole slides of a series of metaplastic (TNBC) and high and low GRHL2 mRNA tumors, separated for GRHL2 IHC positive and GRHL2 IHC negative cases. Mean and SEM is shown. p-value calculated using non-parametric t-test with unequal variance. **(G)** Representative IHC images for GRHL2 and CD73 in breast cancer tissues. Tumor 1,2,4 are metaplastic tumors. **Tumor 1** containing \*area with non-invasive tumor cells staining positive for GRHL2 and negative for CD73. \*\*area with stroma containing invasive tumor cells staining negative for GRHL2 and positive for CD73. **Tumor 2** Arrow indicates milk duct with GRHL2 positive/CD73 negative epithelial cells surrounded by GRHL2 negative/CD73 positive stroma. \*\*area with invasive tumor cells staining positive for GRHL2 and negative for CD73. **Tumor 3** mRNA high tumor containing \*\*area with stroma containing invasive tumor cells staining positive for GRHL2 and negative for CD73. **Tumor 4** \*\*area containing invasive tumor cells staining negative for GRHL2 and positive for CD73. Bars, 50um; note that magnification is higher for tumor 1, 3, and 4 versus tumor 2.

To determine the clinical relevance of this inverse correlation, we used the publicly available dataset METABRIC, containing targeted sequencing mRNA data of 1,904 primary breast cancer samples, and performed a co-expression analysis using cBioPortal. The co-regulation analysis revealed a significant negative relation between GRHL2 and NT5E mRNAs in breast cancer patient tumors with a Spearman value of -0.32 ( $p < 0.001$ ) (Fig. 2E). We further investigated the relation between GRHL2 and CD73 protein expression levels by immunohistochemistry (IHC) on samples of human breast cancer tissue, choosing a set of 10 GRHL2 high, 10 GRHL2 low (based on RNAseq) and 10 metaplastic breast adenocarcinoma patient tumors as these were expected to be heterogeneous. Scoring GRHL2 nuclear staining versus CD73 membrane staining on these TMAs, further confirmed a negative correlation (Fig. 2F,G). Tumors often showed areas with GRHL2 negative and areas with positive cells. GRHL2 positive tumors or tumor areas were mostly CD73 negative; GRHL2 negative tumors or tumor areas showed a mixed pattern for CD73.



The presence of CD73 in vessels, fibroblasts, and inflammatory cells in some cases prevented accurate assessment of CD73 expression in tumor cells. Taken together, in agreement with the findings in the MCF-7 conditional KO model, these findings indicated that NT5E/CD73 is negatively correlated with GRHL2 in human breast cancer cell lines and breast cancer patients.

### **GRHL2 binds NT5E gene in multiple luminal and basal-A breast cancer cell lines**

Having established an inverse correlation between GRHL2 and NT5E/CD73 we asked whether the *NT5E* gene could be subject to direct transcriptional regulation by GRHL2 in breast cancer. Therefore, we analyzed our recent ChIP-seq data exploring genome-wide binding sites of GRHL2 in three luminal human breast cancer cell lines (MCF-7, T47D, and BT474) and three basal A human breast cancer cell lines (HCC1806, BT20, and MDA-MB-468).<sup>40,41</sup> Analysis of ChIP-seq tracks along the *NT5E* gene located on chromosome 6, revealed a GRHL2 binding site in intron 6 (intron 7 in a *NT5E* gene variant that has a short exon inserted upstream of the GRHL2 peak) that was conserved among all six cell lines (Fig. 3A). Further analysis of these peaks using MEME ChIP identified a core GRHL2 binding motif (AACC[A/C/G]GTT) (Fig. 3B). The occurrence of the GRHL2 motif in the region occupied by GRHL2 in intron 6 was also confirmed in all six breast cancer cell lines using FIMO<sup>43</sup> (Fig. 3C). Lastly, similar to the large majority of GRHL2 binding sites<sup>41</sup> no AG-GTCAnnnTGACCT ER $\alpha$  motif was detected in a -1000 to +1000 nucleotide stretch around the GRHL2 peak. This data demonstrated that GRHL2 interacts with the *NT5E* gene and the inverse relation between GRHL2 and NT5E/CD73 in breast cancer may involve GRHL2-mediated negative transcriptional regulation.

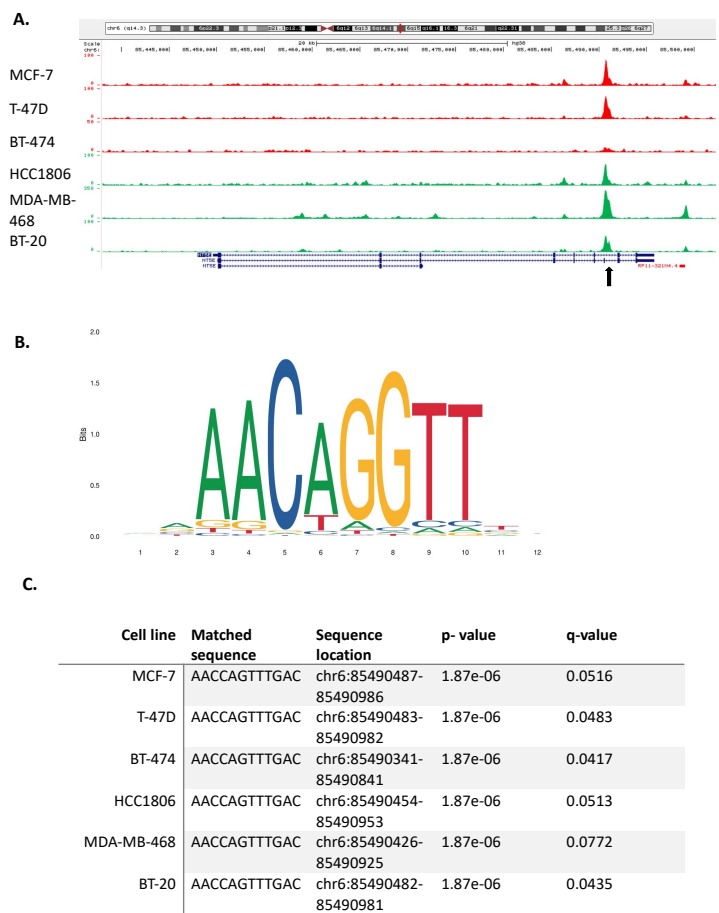


**Figure 3: Conserved GRHL2 binding site in the NT5E gene across luminal and basal-A breast cancer cell lines.**

**(A)** GRHL2 ChIP tracks showing its interactions along the NT5E DNA in the indicated luminal (labeled red) and basal-A cell lines (labeled green). Note that track heights use different scales. Annotation of the reference sequence is displayed below with exons in blue bars. **(B)** GRHL2 binding motif identified in GRHL2 ChIP-seq peaks on NT5E DNA using MEME ChIP on data retrieved from the JASPAR database. Y axis shows frequency matrix of each base occurrence. **(C)** Table showing locations and frequency of the GRHL2 motif in the NT5E gene for the indicated breast cancer cell lines as determined using FIMO. Motif occurrence measured with log-odds scores and converted into p values; q values calculated using Benjamini and Hochberg method.

### **GRHL2 regulates CD73-mediated extracellular adenosine production**

CD73 is a cell-surface ecto-nucleotidase that catalyzes the conversion of extracellular AMP into adenosine.<sup>13</sup> As we observed negative regulation of NT5E/CD73 by GRHL2 we next investigated whether loss of GRHL2 led to an increase in CD73-mediated adenosine production in MCF-7 cells. After 7 days of doxycycline exposure, we observed a strong reduction of GRHL2 protein expression in the GRHL2 KO-1, and GRHL2 KO-2 models whereas no alterations in GRHL2 protein expression were detected in the Ctrl sgRNA model condition (Fig. 4A). Parallel samples were generated for the analysis of adenosine production using Malachite Green, which detects the concentration of inorganic phosphate in the supernatant that accumulates as a result of the conversion of AMP into adenosine (Fig. 4B). Since CD73 expression is high in basal B breast cancer cells (Fig 2A), we included MDA-MB-231 and Hs578T basal B cells as positive controls. Baseline signals were similar for MCF-7 ctrl, GRHL2 KO-1 and KO-2, and the two positive controls but the addition of AMP as a substrate significantly increased adenosine production in the positive control cells and the GRHL2 depleted MCF-7 cells, while no significant increase was found for the MCF-7 ctrl cells (Fig. 4C). To demonstrate that the increase was due to the activity of CD73, we made use of an enzymatic inhibitor of CD73,  $\alpha,\beta$ -methylene ADP (APCP). Indeed, APCP prevented the conversion of AMP into adenosine in the positive control cells and the GRHL2 depleted MCF-7 cells. These data showed that, in agreement with the negative regulation of NT5E/CD73 by GRHL2, loss of GRHL2 triggers increased CD73-mediated adenosine production.

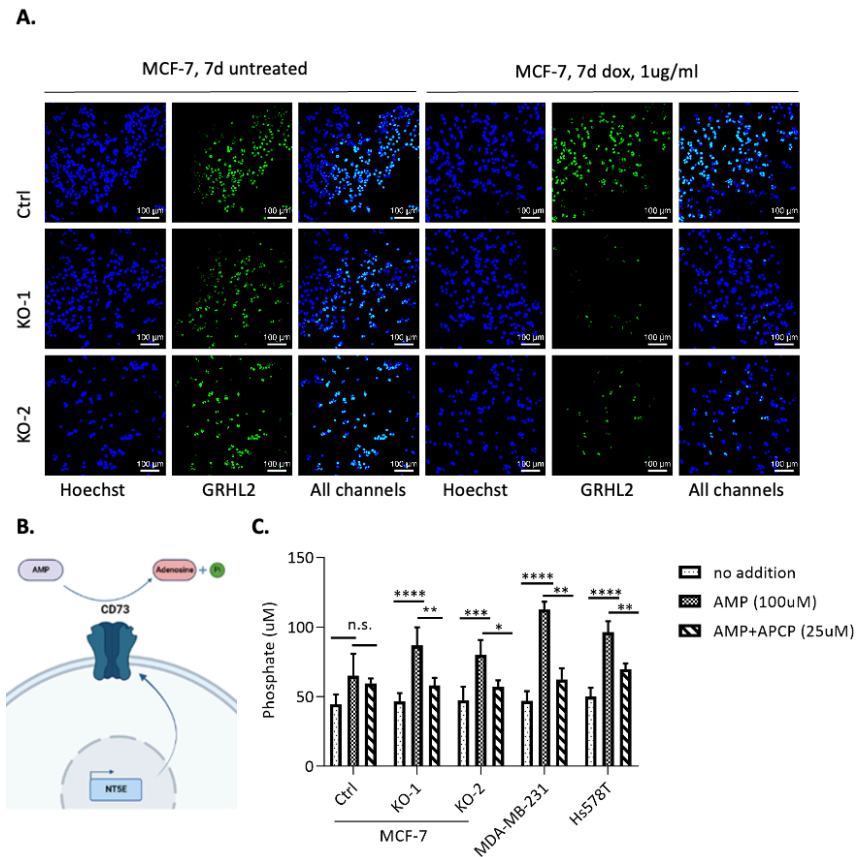


**Figure 4: GRHL2 regulates CD73-mediated extracellular adenosine production.** **(A)** Immunofluorescence staining showing GRHL2 loss at 7 days after doxycycline-mediated Cas9 induction in sgGRHL2 cells (KO-1 and KO-2) but not sgCTR cells for the experiment shown in C. Green, GRHL2 Ab; Blue, Hoechst. **(B)** Cartoon displaying the enzymatic conversion of AMP into adenosine by CD73 resulting in the production inorganic phosphate. Image created using BioRender. **(C)** Inorganic phosphate concentration measured by Malachite Green Assay in culture supernatants from the MCF-7 conditional KO model taken in parallel to images shown in A and basal B positive control cell lines MDA-MB-231 and Hs578T. Cells were incubated in absence or presence of 100μM AMP (substrate) with or without 25μM CD73 inhibitor, APCP for 125 mins. Mean ± SD of four biological replicates is shown (Two-way ANOVA test; n.s., non-significant; \*p<0.05; \*\*p<0.01; \*\*\*p<0.001; \*\*\*\*p<0.0001).

### **Enhanced CD8+ T cell recruitment due to CD73 mediated adenosine production in response to GRHL2 loss**

Adenosine is known to suppress the activation, proliferation and effector differentiation of CD8 T cells.<sup>9-11,44</sup> Yet, for melanoma and bladder cancer it has been observed that T cell specific loss of A2AR adenosine receptors leads to a reduction in tumor associated CD8+ T cells, indicating that adenosine does not interfere with T cell recruitment in solid tumors.<sup>45</sup> To address the relation between CD73 expression and CD8 T cell recruitment in breast cancer, we examined the association NT5E mRNA levels and CD8 T cell infiltration using the TIMER 2.0 patient data set.<sup>46</sup> Expression of NT5E mRNA was positively associated with CD8 T cell infiltration in all breast cancer subtypes tested (Fig. 5A,B). We next evaluated the correlation between GRHL2, CD73, and CD8 by IHC in a set of 10 GRHL2 high, 10 GRHL2 low (based on RNA-seq), and 10 metaplastic breast adenocarcinoma patient tumors. Again, there was a trend towards lower CD8 infiltration in CD73 negative tumors although CD8 IHC was heterogeneous and in this small set of tumors the difference with CD73 positive tumors was not significant (Fig 5C, D; Fig. S2). This raised the possibility that enhanced CD73-mediated adenosine production by tumor cells may in fact stimulate rather than inhibit T cell recruitment (while locally suppressing T cell function as demonstrated by others). We therefore examined how GRHL2 deletion, through increased CD73 expression and adenosine production affected recruitment of CD8 T cells to the tumor cells using the MCF-7 conditional KO model.

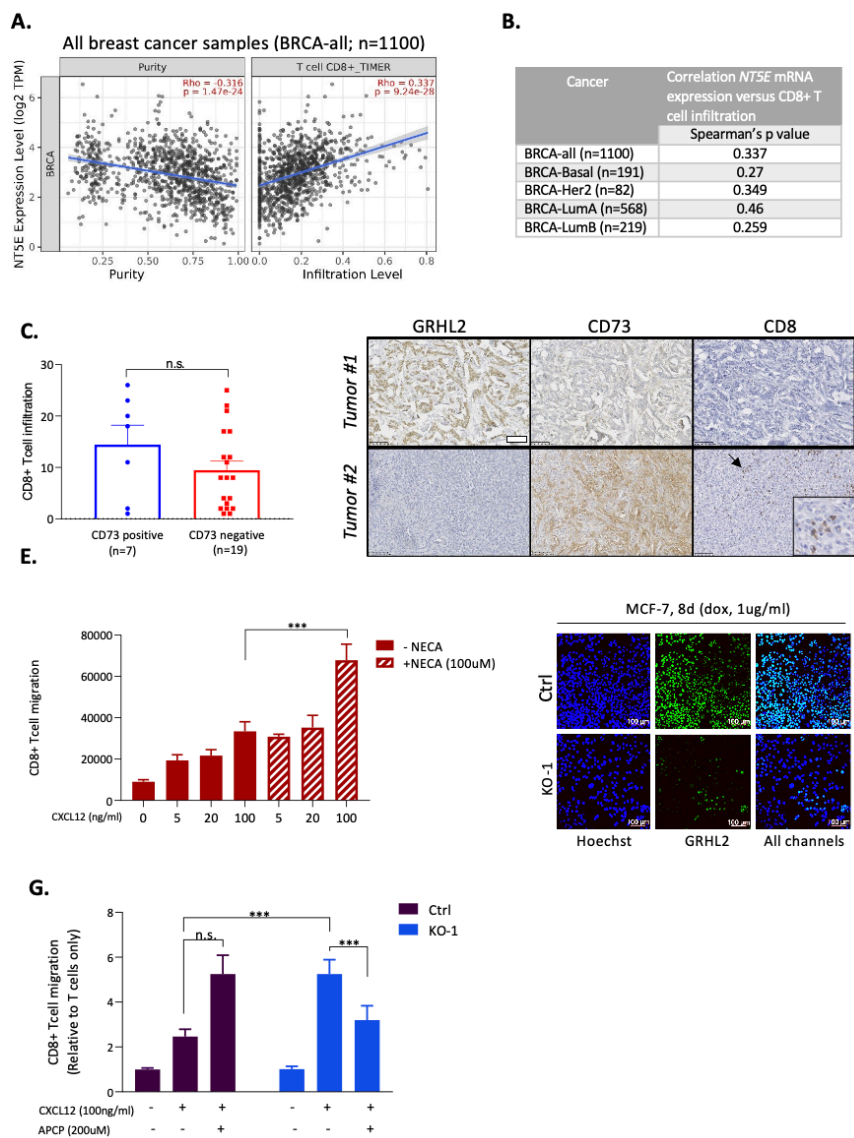


**Figure 5: Enhanced CD8+ T cell recruitment in response to GRHL2 loss.**

**(A)** TIMER 2.0 scatter plots showing the correlation of NT5E mRNA expression with tumor purity (percentage of malignant cells in a tumor tissue; left) and the predicted presence of CD8+ T cells (right) in all breast cancer (BRCA) lesions tested. **(B)** table showing TIMER 2.0 Spearman correlation scores for association between NT5E mRNA and predicted presence of CD8+ T cells across breast cancer patient tumors separated for different molecular subtypes. **(C)** CD8 score (% CD8 positive

T cells) derived from IHC, on whole slides of a series of metaplastic (TNBC) and high and low GRHL2 mRNA tumors, separated for IHC determined CD73 membrane staining positive and negative cases. Mean and SEM is shown. p-value calculated using non-parametric t-test with unequal variance. **(D)** Representative IHC images for GRHL2, CD73, and CD8 in breast cancer tissues. Arrow indicates area of infiltrated CD8 T cells in tumor 2 that is enlarged in the lower right corner. Bar, 50um. **(E)** Quantification of the number of CD8+ T cells recruited towards the lower compartment of trans-wells at increasing concentrations of CXCL12 in presence or absence of 100 uM stable adenosine analog, NECA. Average and SEM of 3 biological replicates is shown (Two-way ANOVA test; \*\*\* $p < 0.001$ ). **(F)** Immunofluorescence staining showing GRHL2 loss at 8 days after doxycycline mediated Cas9 induction in sgGRHL2 cells but not sgCTR cells for the experiment shown in G. Green, GRHL2 Ab; Blue, Hoechst. **(G)** Quantification of CD8+ T cells recruited towards

We first measured CD8+ T cell migration in the presence of a known chemo-attractant, CXCL12, in the absence or presence of a stable adenosine analog (NECA) using a trans-well assay. CXCL12 stimulated CD8+ T cell migration in a concentration dependent fashion, which was further increased by NECA (Fig. 5E; Fig. S3). At 100ng/ml CXCL12 the presence of NECA significantly increased CD8+ T cell migration ( $p < 0.0001$ ). Next, a similar setup was used to investigate the impact of seeding MCF-7 cells expressing Ctrl sgRNA or GRHL2 sgRNA cells at the bottom of the trans-well system and inducing GRHL2 depletion by incubating with doxycycline for 8 days (Fig. 5F,G; Fig. S4). No significant impact of control or GRHL2 KO cells was observed on CD8+ T cell migration in the absence of CXCL12. In the presence of CXCL12, the co-culture with GRHL2 KO cells stimulated CD8+ T cell migration more strongly as compared to the co-culture with control cells. To assess if the increase in CD8+T cell migration in the presence of GRHL2 KO cells was due to CD73 mediated adenosine production, we made use of the APCP CD73 inhibitor. Notably, while APCP did not inhibit the CD8 T cell migration in the presence of control MCF-7 cells, it attenuated the enhanced migration of CD8+ T cells towards GRHL2 KO cells (Fig. 5G; Fig. S4).

Altogether, these results indicated that CD73 mediated adenosine production is associated with increased CD8+ T cell recruitment in breast tumors.

Loss of GRHL2, through enhanced CD73 expression, stimulates CD8+ T cell migration towards breast cancer cells.

### Discussion

*GRHL2* is located on chromosome 8q22 that is frequently amplified in carcinomas.<sup>47</sup> Yet, tumors are heterogeneous and our current work and that of others<sup>39</sup> shows that *GRHL2* expression is variable in breast cancer tissues. Our findings indicate that loss of *GRHL2* can contribute to enhanced extracellular adenosine production in the TME, which has been implicated in suppression of the activation, proliferation and effector differentiation of NK cells and T cells.<sup>9,11</sup>

In the patient data as well as in the cell line panel the correlation between *GRHL2* and NT5E/CD73 is heterogeneous. We observe a significant inverse correlation but there are examples where both *GRHL2* and NT5E/CD73 are present, or both are absent. This indicates that other mechanisms regulate the expression of NT5E/CD73 besides *GRHL2*. Indeed, several additional mechanisms impinging on CD73 have been reported. EMT can modulate CD73, which may involve activation of TGF $\beta$  signaling and the SNAIL transcription factor and this may contribute to immune suppression.<sup>30-32</sup> We have previously shown that in the MCF-7 conditional KO model used in this study, deletion of *GRHL2* has limited impact on EMT markers,<sup>40,41</sup> suggesting that enhanced CD73 expression and adenosine production is not a consequence of EMT in this case. Increased transcription of NT5E through activation of hypoxia-inducible factor-1 (HIF-1) or loss of hormone receptors such as estrogen receptor (ER) have also been identified as alternative mechanisms regulating CD73 expression.<sup>48-50</sup> However, we have not observed activation of the HIF pathway or changes in ER $\alpha$  expression upon loss of *GRHL2*.<sup>41</sup> *GRHL2* has been reported to act as a pioneer factor, promoting chromatin accessibility and *GRHL2* has been found to co-occupy enhancer elements with FOXA1, GATA3, and ER $\alpha$  in hormone receptor positive breast cancers. However, we have previously found that only a minor proportion of *GRHL2* binding sites in the genome of breast cancer cell lines coincide with ER $\alpha$  binding sites<sup>41</sup> and in our current study no ER $\alpha$  motif was identified in the vicinity of the *GRHL2*



peak in the NT5E gene. Our findings point to an inhibitory interaction of GRHL2 with the NT5E gene at a conserved binding site located in an intronic region. Here, GRHL2 may interact with enhancer elements or regulate histone modifications,<sup>51,52</sup> similar to what we and others have observed for the majority of GRHL2 target genes.<sup>41,51,53</sup> Our finding that NT5E/CD73 is inversely correlated with GRHL2 in breast cancer cell lines and in patient tumors or tumor areas, suggests the negative regulation of CD73 by GRHL2 in breast cancer is common. Notably, in the scoring of CD73 in patient tissues we have focused on membrane associated CD73. The impact of alterations in CD73 expression may be further determined by the localization of CD73, a GPI-linked protein that can be membrane bound or shed from the membrane.<sup>13</sup>

GRHL2 was previously shown to support NK cell mediated tumor cytotoxicity through a mechanism involving epigenetic stimulation of ICAM-1 expression, which supported enhanced NK-target cell synapse formation.<sup>54</sup> However, GRHL2 has not been previously implicated in the interaction of tumor cells with T cells. The elevated CD73-mediated extracellular adenosine levels triggered by the loss of GRHL2, are expected to suppress T cell activity based on earlier reports. Adenosine binds to GPCRs on immune cells thereby stimulating (via A2A and A2B receptors) or suppressing (via A1 and A3 receptors) adenylyl cyclase activity, stimulating intracellular calcium release (via A1 and A3 receptors), and activating ERK and p38 MAPK signaling (via A1, A2A, A2B, A3 receptors).<sup>9</sup> Stimulation of A2AR on T cells has been reported to suppress the activation, proliferation and effector differentiation of CD8 T cells<sup>44</sup> and A2AR deletion in mouse models leads to enhanced tumor killing by CD8 cells.<sup>55</sup> Indeed, CD73 represents an actionable target to reduce extracellular adenosine levels and enhance anti-tumor immunity.<sup>16</sup> Our current work, however, shows that enhanced CD73-mediated extracellular adenosine production may stimulate rather than inhibit recruitment of CD8 T cells, and we corroborate this effect using a stable adenosine analog. Interestingly, there is precedent for a pro-migratory effect of adenosine in different contexts. Adenosine has been implicated in the migration of dendritic cells towards regulatory T cells<sup>56</sup> and T-cell-specific deletion or pharmacological inhibition of

A2AR has been shown to cause increased growth of ectopic tumors in mice as expected but in fact led to reduced CD8 T-cell accumulation in these tumors.<sup>45</sup> Our finding that CD73 expression is not negatively correlated with CD8 T cell infiltration but rather associates with a slight increase, further establishes a dual role of extracellular adenosine in T cell migration versus cytotoxic activity.

In summary, this work demonstrates that GRHL2, a key epithelial transcriptional regulator, can regulate extracellular adenosine levels produced by breast cancer cells through suppression of the gene encoding the NT5E/CD73 ecto-enzyme. Moreover, this study shows that adenosine produced by GRHL2 depleted breast cancer cells (or provided as a stable analog) can augment the recruitment of CD8 T cells, in addition to its previously established role as a suppressor of T cell-mediated cytotoxicity.

### Limitations of the study

We focused on the impact of GRHL2-NT5E/CD73-adenosine axis on T cell migration. The suppression of T cell mediated cytotoxicity by adenosine has been firmly established by others.<sup>9-11,16,44</sup> The MCF-7 conditional KO model shows decreased proliferation from 2 days after GRHL2 deletion followed by a minor decrease in viability after 1 week (in agreement with the established roles of GRHL2).<sup>35,40</sup> This precludes use of the model in assessment of T cell mediated cytotoxicity (e.g., in the context of biAbs).

CD73-mediated production of adenosine can involve tumor cells, stromal cells, regulatory T cells, and extracellular vesicles derived from these cell types.<sup>57-59</sup> Our study demonstrates that GRHL2 levels can contribute to modulation of adenosine production by tumor cells, but further (in vivo) work is required to reveal the relative contribution of adenosine produced by GRHL2 negative tumor cells in such a complex environment.

### Acknowledgements

This work was supported by grants from the Dutch Cancer Society (KWF Research Grant #10967) to Bircan Coban, the China Scholarship Council to Zi Wang, and the Dutch Research Council (NWO; Science-XL grant 2019.022) to

Erik Danen. The authors thank Mats Ljungman (Departments of Radiation Oncology and Environmental Health Sciences, University of Michigan Medical School, Ann Arbor, MI, USA) for supporting the analysis of Bru-seq data, Lucia Daxinger (Department of Human Genetics, Leiden University Medical Centre, Leiden, NL) for supporting the analysis of ChIP-seq data, Bob van de Water (LACDR, Leiden University, Leiden, NL) for supporting the analysis of RNAseq data obtained from a panel of breast cancer cell lines, Laura Heitman (LACDR, Leiden University, Leiden, NL) for providing reagents, and Sietske Luk and Mirjam Heemskerk (Department of Hematology, LUMC, Leiden, NL) for expert advice on tumor-T cell co-culture.

### Author contributions

BC designed, executed, and analyzed experiments, prepared figures, and wrote the original draft manuscript; ZW, CL, KB, and JH executed and analyzed experiments; MT and JWMM executed and analyzed IHC experiments using patient samples; BS supported isolation and flow cytometry analysis of PBMC derived CD8 T cells; AJMZ and EN analyzed experiments and co-wrote the original draft manuscript; EHJD, conceptualized the study, analyzed experiments, and reviewed and edited the manuscript. All authors read and approved the final version of the manuscript.

### References

1. Quail, D.F., and Joyce, J.A. (2013). Microenvironmental regulation of tumor progression and metastasis. *Nat Med* 19, 1423-1437. 10.1038/nm.3394.
2. Coban, B., Bergonzini, C., Zweemer, A.J.M., and Danen, E.H.J. (2021). Metastasis: crosstalk between tissue mechanics and tumour cell plasticity. *Br J Cancer* 124, 49-57. 10.1038/s41416-020-01150-7.
3. El-Kenawi, A., Hanggi, K., and Ruffell, B. (2020). The Immune Microenvironment and Cancer Metastasis. *Cold Spring Harb Perspect Med* 10. 10.1101/cshperspect.a037424.
4. Peng, W., Chen, J.Q., Liu, C., Malu, S., Creasy, C., Tetzlaff, M.T., Xu, C., McKenzie, J.A., Zhang, C., Liang, X., et al. (2016). Loss of PTEN Promotes Resistance to T Cell-Mediated Immunotherapy. *Cancer Discov* 6, 202-216. 10.1158/2159-8290.CD-15-0283.
5. Cassetta, L., and Pollard, J.W. (2023). A timeline of tumour-associated macrophage biology. *Nat Rev Cancer* 23, 238-257. 10.1038/s41568-022-00547-1.
6. Sahai, E., Astsaturov, I., Cukierman, E., DeNardo, D.G., Egeblad, M., Evans, R.M., Fearon, D., Greten, F.R., Hingorani, S.R., Hunter, T., et al. (2020). A framework for

advancing our understanding of cancer-associated fibroblasts. *Nat Rev Cancer* 20, 174-186. 10.1038/s41568-019-0238-1.

7. Ruiz de Galarreta, M., Bresnahan, E., Molina-Sánchez, P., Lindblad, K.E., Maier, B., Sia, D., Puigvehi, M., Miguela, V., Casanova-Acebes, M., Dhainaut, M., et al. (2019). B-catenin activation promotes immune escape and resistance to anti-PD-1 therapy in hepatocellular carcinoma. *Cancer Discov.* 9, 1124-1141. 10.1158/2159-8290.CD-19-0074.

8. Groth, C., Hu, X., Weber, R., Fleming, V., Altevogt, P., Utikal, J., and Umansky, V. (2019). Immunosuppression mediated by myeloid-derived suppressor cells (MDSCs) during tumour progression. *Br. J. Cancer* 120, 16-25. 10.1038/s41416-018-0333-1.

9. Antonioli, L., Blandizzi, C., Pacher, P., and Haskó, G. (2013). Immunity, inflammation and cancer: a leading role for adenosine. *Nat. Rev. Cancer* 13, 842-857. 10.1038/nrc3613.

10. Cekic, C., and Linden, J. (2016). Purinergic regulation of the immune system. *Nat. Rev. Immunol.* 16, 177-192. 10.1038/nri.2016.4.

11. Hoskin, D.W., Mader, J.S., Furlong, S.J., Conrad, D.M., and Blay, J. (2008). Inhibition of T cell and natural killer cell function by adenosine and its contribution to immune evasion by tumor cells (Review). *Int. J. Oncol.* 32, 527-535. 10.3892/ijo.32.3.527.

12. Robson, S.C., Sévigny, J., and Zimmermann, H. (2006). The E-NTPDase family of ectonucleotidases: Structure function relationships and pathophysiological significance. *Purinergic Signal.* 2, 409-430. 10.1007/s11302-006-9003-5.

13. Antonioli, L., Pacher, P., Vizi, E.S., and Haskó, G. (2013). CD39 and CD73 in immunity and inflammation. *Trends Mol. Med.* 19, 355-367. 10.1016/j.molmed.2013.03.005.

14. Perrot, I., Michaud, H.-A., Giraudon-Paoli, M., Augier, S., Docquier, A., Gros, L., Courtois, R., Déjou, C., Jecko, D., Becquart, O., et al. (2019). Blocking antibodies targeting the CD39/CD73 immunosuppressive pathway unleash immune responses in combination cancer therapies. *Cell Rep.* 27, 2411-2425.e2419. 10.1016/j.celrep.2019.04.091.

15. Yang, R., Elsaadi, S., Misund, K., Abdollahi, P., Vandsemb, E.N., Moen, S.H., Kusnierczyk, A., Slupphaug, G., Standal, T., Waage, A., et al. (2020). Conversion of ATP to adenosine by CD39 and CD73 in multiple myeloma can be successfully targeted together with adenosine receptor A2A blockade. *J. Immunother. Cancer* 8, e000610. 10.1136/jitc-2020-000610.

16. Young, A., Ngiow, S.F., Barkauskas, D.S., Sult, E., Hay, C., Blake, S.J., Huang, Q., Liu, J., Takeda, K., Teng, M.W.L., et al. (2016). Co-inhibition of CD73 and A2AR adenosine signaling improves anti-tumor immune responses. *Cancer Cell* 30, 391-403. 10.1016/j.ccell.2016.06.025.

17. Stagg, J., Divisekera, U., Duret, H., Sparwasser, T., Teng, M.W.L., Darcy, P.K., and Smyth, M.J. (2011). CD73-deficient mice have increased antitumor immunity and are resistant to experimental metastasis. *Cancer Res.* 71, 2892-2900. 10.1158/0008-5472.CAN-10-4246.

18. Stagg, J., Beavis, P.A., Divisekera, U., Liu, M.C.P., Möller, A., Darcy, P.K., and Smyth, M.J. (2012). CD73-deficient mice are resistant to carcinogenesis. *Cancer Res.* 72, 2190-2196. 10.1158/0008-5472.CAN-12-0420.
19. Wang, L., Fan, J., Thompson, L.F., Zhang, Y., Shin, T., Curiel, T.J., and Zhang, B. (2011). CD73 has distinct roles in nonhematopoietic and hematopoietic cells to promote tumor growth in mice. *J. Clin. Invest.* 121, 2371-2382. 10.1172/JCI45559.
20. Hay, C.M., Sult, E., Huang, Q., Mulgrew, K., Fuhrmann, S.R., McGlinchey, K.A., Hammond, S.A., Rothstein, R., Rios-Doria, J., Poon, E., et al. (2016). Targeting CD73 in the tumor microenvironment with MEDI9447. *Oncoimmunology* 5, e1208875. 10.1080/2162402X.2016.1208875.
21. Terp, M.G., Olesen, K.A., Arnspar, E.C., Lund, R.R., Lagerholm, B.C., Ditzel, H.J., and Leth-Larsen, R. (2013). Anti-human CD73 monoclonal antibody inhibits metastasis formation in human breast cancer by inducing clustering and internalization of CD73 expressed on the surface of cancer cells. *J. Immunol.* 191, 4165-4173. 10.4049/jimmunol.1301274.
22. Stagg, J., Divisekera, U., McLaughlin, N., Sharkey, J., Pommey, S., Denoyer, D., Dwyer, K.M., and Smyth, M.J. (2010). Anti-CD73 antibody therapy inhibits breast tumor growth and metastasis. *Proc. Natl. Acad. Sci. U. S. A.* 107, 1547-1552. 10.1073/pnas.0908801107.
23. Allard, B., Allard, D., Buisseret, L., and Stagg, J. (2020). The adenosine pathway in immuno-oncology. *Nat. Rev. Clin. Oncol.* 17, 611-629. 10.1038/s41571-020-0382-2.
24. Yang, H., Yao, F., Davis, P.F., Tan, S.T., and Hall, S.R.R. (2021). CD73, tumor plasticity and immune evasion in solid cancers. *Cancers (Basel)* 13, 177. 10.3390/cancers13020177.
25. Jeong, Y.M., Cho, H., Kim, T.-M., Kim, Y., Jeon, S., Bychkov, A., and Jung, C.K. (2020). CD73 Overexpression promotes progression and recurrence of papillary thyroid carcinoma. *Cancers (Basel)* 12, 3042. 10.3390/cancers12103042.
26. Turcotte, M., Spring, K., Pommey, S., Chouinard, G., Cousineau, I., George, J., Chen, G.M., Gendoo, D.M.A., Haibe-Kains, B., Karn, T., et al. (2015). CD73 is associated with poor prognosis in high-grade serous ovarian cancer. *Cancer Res.* 75, 4494-4503. 10.1158/0008-5472.CAN-14-3569.
27. Leclerc, B.G., Charlebois, R., Chouinard, G., Allard, B., Pommey, S., Saad, F., and Stagg, J. (2016). CD73 expression is an independent prognostic factor in prostate cancer. *Clin. Cancer Res.* 22, 158-166. 10.1158/1078-0432.CCR-15-1181.
28. Mullins, R.D.Z., Pal, A., Barrett, T.F., Heft Neal, M.E., and Puram, S.V. (2022). Epithelial-mesenchymal plasticity in tumor immune evasion. *Cancer Res.* 82, 2329-2343. 10.1158/0008-5472.CAN-21-4370.
29. Dongre, A., Rashidian, M., Reinhardt, F., Bagnato, A., Keckesova, Z., Ploegh, H.L., and Weinberg, R.A. (2017). Epithelial-to-mesenchymal transition contributes to immunosuppression in breast carcinomas. *Cancer Res.* 77, 3982-3989. 10.1158/0008-5472.CAN-16-3292.
30. Giraudo, C., Turiello, R., Orlando, L., Leonardelli, S., Landsberg, J., Belvedere, R., Rolshoven, G., Müller, C.E., Hölzel, M., and Morello, S. (2023). The CD73 is induced by TGF- $\beta$ 1 triggered by nutrient deprivation and highly expressed in dedifferentiated

- p human melanoma. Biomed. Pharmacother. 165, 115225. 10.1016/j.biopha.2023.115225.
31. Hasmim, M., Berchem, G., and Janji, B. (2022). A role for EMT in CD73 regulation in breast cancer. *Oncoimmunology* 11, 2152636. 10.1080/2162402X.2022.2152636.
  32. Hasmim, M., Xiao, M., Van Moer, K., Kumar, A., Oniga, A., Mittelbronn, M., Duhem, C., Chammout, A., Berchem, G., Thiery, J.P., et al. (2022). SNAI1-dependent upregulation of CD73 increases extracellular adenosine release to mediate immune suppression in TNBC. *Front. Immunol.* 13, 982821. 10.3389/fimmu.2022.982821.
  33. Wang, S., and Samakovlis, C. (2012). Grainy head and its target genes in epithelial morphogenesis and wound healing. *Curr. Top. Dev. Biol.* 98, 35-63. 10.1016/B978-0-12-386499-4.00002-1.
  34. Mathiyalagan, N., Miles, L.B., Anderson, P.J., Wilanowski, T., Grills, B.L., McDonald, S.J., Keightley, M.C., Charzynska, A., Dabrowski, M., and Dworkin, S. (2019). Meta-analysis of grainyhead-like dependent transcriptional networks: A roadmap for identifying novel conserved genetic pathways. *Genes (Basel)* 10, 876. 10.3390/genes10110876.
  35. Mlacki, M., Kikulska, A., Krzywinska, E., Pawlak, M., and Wilanowski, T. (2015). Recent discoveries concerning the involvement of transcription factors from the Grainyhead-like family in cancer. *Exp Biol Med (Maywood)* 240, 1396-1401. 10.1177/1535370215588924.
  36. Frisch, S.M., Farris, J.C., and Pifer, P.M. (2017). Roles of Grainyhead-like transcription factors in cancer. *Oncogene* 36, 6067-6073. 10.1038/ncr.2017.178.
  37. Cieply, B., Riley, P.t., Pifer, P.M., Widmeyer, J., Addison, J.B., Ivanov, A.V., Denvir, J., and Frisch, S.M. (2012). Suppression of the epithelial-mesenchymal transition by Grainyhead-like-2. *Cancer Res* 72, 2440-2453. 10.1158/0008-5472.CAN-11-4038.
  38. Cieply, B., Farris, J., Denvir, J., Ford, H.L., and Frisch, S.M. (2013). Epithelial-mesenchymal transition and tumor suppression are controlled by a reciprocal feedback loop between ZEB1 and Grainyhead-like-2. *Cancer Res* 73, 6299-6309. 10.1158/0008-5472.CAN-12-4082.
  39. Werner, S., Frey, S., Riethdorf, S., Schulze, C., Alawi, M., Kling, L., Vafaizadeh, V., Sauter, G., Terracciano, L., Schumacher, U., et al. (2013). Dual roles of the transcription factor grainyhead-like 2 (GRHL2) in breast cancer. *J Biol Chem* 288, 22993-23008. 10.1074/jbc.M113.456293.
  40. Wang, Z., Coban, B., Liao, C.-Y., Chen, Y.-J., Liu, Q., and Danen, E.H.J. (2023). GRHL2 regulation of growth/motility balance in luminal versus basal breast cancer. *Int. J. Mol. Sci.* 24, 2512. 10.3390/ijms24032512.
  41. Wang, Z., Coban, B., Wu, H., Chouaref, J., Daxinger, L., Paulsen, M.T., Ljungman, M., Smid, M., Martens, J.W.M., and Danen, E.H.J. (2023). GRHL2-controlled gene expression networks in luminal breast cancer. *Cell Commun. Signal.* 21, 15. 10.1186/s12964-022-01029-5.
  42. Koedoot, E., Wolters, L., Smid, M., Stoilov, P., Burger, G.A., Herpers, B., Yan, K., Price, L.S., Martens, J.W.M., Le Dévédec, S.E., and van de Water, B. (2021). Differential reprogramming of breast cancer subtypes in 3D cultures and

implications for sensitivity to targeted therapy. *Sci. Rep.* **11**, 7259. 10.1038/s41598-021-86664-7.

43. Grant, C.E., Bailey, T.L., and Noble, W.S. (2011). FIMO: scanning for occurrences of a given motif. *Bioinformatics* **27**, 1017-1018. 10.1093/bioinformatics/btr064.

44. Linnemann, C., Schildberg, F.A., Schurich, A., Diehl, L., Hegenbarth, S.I., Endl, E., Lacher, S., Müller, C.E., Frey, J., Simeoni, L., et al. (2009). Adenosine regulates CD8 T-cell priming by inhibition of membrane-proximal T-cell receptor signalling. *Immunology* **128**, e728-737. 10.1111/j.1365-2567.2009.03075.x.

45. Cekic, C., and Linden, J. (2014). Adenosine A2A receptors intrinsically regulate CD8<sup>+</sup> T cells in the tumor microenvironment. *Cancer Res.* **74**, 7239-7249. 10.1158/0008-5472.CAN-13-3581.

46. Li, T., Fu, J., Zeng, Z., Cohen, D., Li, J., Chen, Q., Li, B., and Liu, X.S. (2020). TIMER2.0 for analysis of tumor-infiltrating immune cells. *Nucleic Acids Res.* **48**, W509-W514. 10.1093/nar/gkaa407.

47. Dompe, N., Rivers, C.S., Li, L., Cordes, S., Schwickart, M., Punnoose, E.A., Amler, L., Seshagiri, S., Tang, J., Modrusan, Z., and Davis, D.P. (2011). A whole-genome RNAi screen identifies an 8q22 gene cluster that inhibits death receptor-mediated apoptosis. *Proc Natl Acad Sci U S A* **108**, E943-951. 10.1073/pnas.1100132108.

48. Samanta, D., Park, Y., Ni, X., Li, H., Zahnow, C.A., Gabrielson, E., Pan, F., and Semenza, G.L. (2018). Chemotherapy induces enrichment of CD47<sup>+</sup>/CD73<sup>+</sup>/PDL1<sup>+</sup> immune evasive triple-negative breast cancer cells. *Proc. Natl. Acad. Sci. U. S. A.* **115**, E1239-E1248. 10.1073/pnas.1718197115.

49. Synnestvedt, K., Furuta, G.T., Comerford, K.M., Louis, N., Karhausen, J., Eltzhig, H.K., Hansen, K.R., Thompson, L.F., and Colgan, S.P. (2002). Ecto-5'-nucleotidase (CD73) regulation by hypoxia-inducible factor-1 mediates permeability changes in intestinal epithelia. *J. Clin. Invest.* **110**, 993-1002. 10.1172/JCI15337.

50. Szychala, J., Lazarowski, E., Ostapowicz, A., Ayscue, L.H., Jin, A., and Mitchell, B.S. (2004). Role of estrogen receptor in the regulation of ecto-5'-nucleotidase and adenosine in breast cancer. *Clin Cancer Res* **10**, 708-717. 10.1158/1078-0432.ccr-0811-03.

51. Chung, V.Y., Tan, T.Z., Tan, M., Wong, M.K., Kuay, K.T., Yang, Z., Ye, J., Muller, J., Koh, C.M., Guccione, E., et al. (2016). GRHL2-miR-200-ZEB1 maintains the epithelial status of ovarian cancer through transcriptional regulation and histone modification. *Sci Rep* **6**, 19943. 10.1038/srep19943.

52. Chung, V.Y., Tan, T.Z., Ye, J., Huang, R.L., Lai, H.C., Kappei, D., Wollmann, H., Guccione, E., and Huang, R.Y. (2019). The role of GRHL2 and epigenetic remodeling in epithelial-mesenchymal plasticity in ovarian cancer cells. *Commun Biol* **2**, 272. 10.1038/s42003-019-0506-3.

53. Walentin, K., Hinze, C., Werth, M., Haase, N., Varma, S., Morell, R., Aue, A., Potschke, E., Warburton, D., Qiu, A., et al. (2015). A Grhl2-dependent gene network controls trophoblast branching morphogenesis. *Development* **142**, 1125-1136. 10.1242/dev.113829.

54. MacFawn, I., Wilson, H., Selth, L.A., Leighton, I., Serebriiskii, I., Bleackley, R.C., Elzamzamy, O., Farris, J., Pifer, P.M., Richer, J., and Frisch, S.M. (2019). Grainyhead-

like-2 confers NK-sensitivity through interactions with epigenetic modifiers. *Mol Immunol* 105, 137-149. 10.1016/j.molimm.2018.11.006.

55. Ohta, A., Gorelik, E., Prasad, S.J., Ronchese, F., Lukashev, D., Wong, M.K., Huang, X., Caldwell, S., Liu, K., Smith, P., et al. (2006). A2A adenosine receptor protects tumors from antitumor T cells. *Proc Natl Acad Sci U S A* 103, 13132-13137. 10.1073/pnas.0605251103.

56. Ring, S., Pushkarevskaya, A., Schild, H., Probst, H.C., Jendrossek, V., Wirsdorfer, F., Ledent, C., Robson, S.C., Enk, A.H., and Mahnke, K. (2015). Regulatory T cell-derived adenosine induces dendritic cell migration through the Epac-Rap1 pathway. *J Immunol* 194, 3735-3744. 10.4049/jimmunol.1401434.

57. Schneider, E., Winzer, R., Rissiek, A., Ricklefs, I., Meyer-Schwesinger, C., Ricklefs, F.L., Bauche, A., Behrends, J., Reimer, R., Brenna, S., et al. (2021). CD73-mediated adenosine production by CD8 T cell-derived extracellular vesicles constitutes an intrinsic mechanism of immune suppression. *Nat Commun* 12, 5911. 10.1038/s41467-021-26134-w.

58. Deaglio, S., Dwyer, K.M., Gao, W., Friedman, D., Usheva, A., Erat, A., Chen, J.F., Enjyoji, K., Linden, J., Oukka, M., et al. (2007). Adenosine generation catalyzed by CD39 and CD73 expressed on regulatory T cells mediates immune suppression. *J Exp Med* 204, 1257-1265. 10.1084/jem.20062512.

59. Clayton, A., Al-Taei, S., Webber, J., Mason, M.D., and Tabi, Z. (2011). Cancer exosomes express CD39 and CD73, which suppress T cells through adenosine production. *J Immunol* 187, 676-683. 10.4049/jimmunol.1003884.

60. Machanick, P., and Bailey, T.L. (2011). MEME-ChIP: motif analysis of large DNA datasets. *Bioinformatics* 27, 1696-1697. 10.1093/bioinformatics/btr189.

61. Curtis, C., Shah, S.P., Chin, S.F., Turashvili, G., Rueda, O.M., Dunning, M.J., Speed, D., Lynch, A.G., Samarajiwa, S., Yuan, Y., et al. (2012). The genomic and transcriptomic architecture of 2,000 breast tumours reveals novel subgroups. *Nature* 486, 346-352. 10.1038/nature10983.

62. Pereira, B., Chin, S.F., Rueda, O.M., Vollan, H.K., Provenzano, E., Bardwell, H.A., Pugh, M., Jones, L., Russell, R., Sammut, S.J., et al. (2016). The somatic mutation profiles of 2,433 breast cancers refines their genomic and transcriptomic landscapes. *Nat Commun* 7, 11479. 10.1038/ncomms11479.

### Resource availability

#### Lead contact

Erik HJ Danen ([e.danen@lacdr.leidenuniv.nl](mailto:e.danen@lacdr.leidenuniv.nl))

### Materials availability

The figures and supplementary materials contain the data. No additional materials were generated as part of this study.



### Data and code availability

Data: All data generated in the study is presented in this published article.

Code: This paper does not report original code.

The lead contact can provide the information for all relevant data and resources upon request.

### Experimental model and study participant details

#### Human subjects

The Erasmus MC medical ethics committee has declared that retrospective biomarker research on surgically resected specimen is according to Dutch law exempt of medical ethical approval (MEC 02-953). Furthermore, the study has been performed in accordance with the national guidelines of the FeDeRa, the Federation of Bio-medical research communities. (<https://www.coreon.org/wp-content/uploads/2020/04/coreon-codegoedgebruik-versie-4juli2015.pdf>). All surgically resected specimen were obtained from female breast cancer patients.

### Method details

#### Cell culture

The human breast adenocarcinoma cell lines MCF-7, CAMA-1, T47D, MDA-MB-361, BT474, HCC1806, HCC1143, MDA-MB-231, BT-549, and Hs578T were grown in RPMI 1640 (Gibco, Fisher Scientific, Landsmeer, The Netherlands) supplemented with 10% fetal bovine serum (FBS), 25 U/mL penicillin, and 25 µg/mL streptomycin (PAN Biotech) in a humidified incubator with 5% CO<sub>2</sub> at 37 °C.

#### Conditional KO procedure

Inducible Cas9 expression was generated by lentiviral transduction with Lentiviral Edit-R inducible Cas9 plasmid (Dharmacon) in MCF-7 cells. Single-cell selection was performed using 2 µg/ml blasticidin. Inducible MCF-7-Cas9 cells were then transduced with a non-targeting sgRNA and two sgRNAs targeting GRHL2 to generate inducible GRHL2 knockout cells. (Sanger Arrayed Whole Genome Lentiviral CRISPR Library (Sigma–Aldrich); sgGRHL2/1 (KO-1):

CCTCGAGACAAGAGGCTGCTGTC, sgGRHL2/2 (KO-2): AAATTCGGAG-TGCTTCAGTTGG). Bulk selection was performed using 8 µg/ml puromycin for 72hrs and induction of GRHL2 KO by doxycycline treatment was verified.

### **ChIP-seq, motif analysis, and Bru-seq**

The visualization of GRHL2 binding along the NT5E gene was obtained using the UCSC Genome Browser. ChIP-seq data supporting the results of this article is available at the UCSC Genome Browser [<https://genome.ucsc.edu/s/hwuRadboudumc/ZWang>]. Two different binding profiles of GRHL2 were retrieved from the JASPAR database (<https://jaspar.genereg.net/>). A motif discovery analysis was performed on the NT5E GRHL2 ChIP-seq peaks using the MEME-ChIP tool<sup>60</sup> from the MEME Suite 5.5.3 with default settings. The FIMO tool<sup>43</sup> was used to scan the NT5E gene for occurrences of the AACCA[C/G]GTT conserved GRHL2 motif.<sup>60</sup>

Bru-seq data supporting the results of this article is available at Gene Expression Omnibus (GEO) database, [www.ncbi.nlm.nih.gov/geo](http://www.ncbi.nlm.nih.gov/geo) (Accession No. GSE222353).

### **RNA analysis in cell lines and clinical samples**

GRHL2 and NT5E gene expression was analyzed using RNA sequencing data from a panel of 52 human breast adenocarcinoma cell lines representing luminal, basal A, and basal B subtypes (<https://zenodo.org/record/4560297/export/xm#.YVXHC5pBxQA>). Log2 normalized gene expression values were used for further analyzing. Violin plots were made by GraphPad. Co-expression analysis in clinical samples was performed using cBioPortal (<https://www.cbioportal.org/>) database. The mRNA expression data of breast cancer patients were retrieved from the METABRIC data set,<sup>61,62</sup> consisting of 1904 targeted sequenced tumor samples and visualized in cBioPortal. Co-expression z-scores (Pearson and Spearman values) were calculated on the cBioPortal website.

### **IHC on samples of human breast cancer tissue and cell lines**

Formalin-fixed paraffin-embedded (FFPE) primary metaplastic tumors (n=10) and primary tumors with high (n=10) or low (n=10) GRHL2 RNA levels were

collected from breast cancer patients who entered the Erasmus University Medical Center (Rotterdam, The Netherlands) for local treatment of their primary disease between 1985 and 2005. Sections of 4  $\mu\text{m}$  were cut, pasted on starfrost® adhesive slides, and dried overnight at 37°C. Slides were dewaxed with Xylene solution and hydrated with decreasing alcohol percentages (100%, 95%, 75% and 50%). Antigen retrieval was done using Target Retrieval Solution, Citrate pH6 (Dako Agilent, S236984-2) or Target Retrieval buffer, pH6 (S1699; for GRHL2) or pH9 (2367; for CD73 and CD8) for 20 min at 95°C followed by 20 minutes at room temperature. Subsequently, slides were immersed in 3% hydrogen peroxide/PBS for 10 minutes to block endogenous peroxidase activity. To block non-specific binding sites, a Protein Block, Serum-free solution (Dako Agilent, X090930-02) was used for 30 minutes. Then, slides were incubated for 1 hour with, 1:1250 mouse-anti-human GRHL2 antibody (Clone CL3760; Cat.nr AMAb91226; Atlas/Sigma), 1:400 mouse-anti-human 5'-Nucleotidase/ CD73 (Clone 4G6E3; Cat.nr. NBP2-37271, Novusbio), or 1:200 mouse-anti-human CD8 antibodies (Clone C8/144B; Cat.nr M7103; Dako Agilent), all diluted with Antibody Diluent (S302283-2, Dako Agilent). Negative controls were made by replacing the primary antibody with mouse immunoglobulin at identical dilution. Detection and visualization of the antibodies was done with EnVision+ Single reagent HRP, Mouse (Dako Agilent, K4001) and Liquid DAB+, 2-component system (Dako Agilent, K346811-2). Slides were counterstained with hematoxylin and dehydrated through graded alcohol and xylene and cover slides were mounted with Pertex. Results of positive control tissues of liver, skin, and intestine were compared with results in human protein atlas for the antibodies used. Results were comparable. Images were made using Nikon ECLIPSE E4000. GRHL2 was scored for absence or presence of nuclear staining in breast tumor cells. CD73 was scored for negative or weak staining (0), weak or partial membrane staining (0.5), or clear positive membrane staining (1) in breast tumor cells. CD8 was scored for the % of CD8 positive cells in the tumor area.

### Immunofluorescence

Cells were fixed and permeabilized by incubation with 4% formaldehyde and 0.1% Triton X100 in Phosphate-buffered saline (PBS) for 15 mins, followed by

a blocking step with 0.5% w/v bovine serum albumin (BSA, Sigma Aldrich) in (PBS) for 30 mins. Then, cells were incubated with the GRHL2 primary antibody (1:500, Atlas-Antibodies, hpa004820) in 0.5% w/v BSA in PBS overnight at 4°C. The cells were washed three times in PBS supplemented with 0.5% BSA (BSA-PBS) and subsequently stained with AlexaFluor-488 conjugated anti-rabbit secondary antibody (1:1000, Mol Probes, A11008) and Hoechst 33258 (1:10,000, Sigma Aldrich, 861405) for 1 h at room temperature, followed by three times washing steps with 0.5% BSA-PBS. Cell preparations were imaged using a Nikon ECLIPSE Ti2 confocal microscope.

### **Western blotting and flow cytometry**

Cells were lysed for total protein isolation and protein samples (20 µg/lane) were run on sodium dodecyl sulfate–polyacrylamide gel electrophoresis (SDS-PAGE). The gels were transferred onto a polyvinylidene difluoride (PVDF) membrane (Millipore) followed by blocking with 5% BSA in Tris-buffered saline (TBS), with 0.05% Tween-20 (TBS-T). Membranes were incubated with GRHL2 (Atlas-Antibodies, hpa004820), cas9 (Cell Signaling, 14697S), CD73 (Abcam, ab202122), and  $\alpha$ -tubulin (Sigma Aldrich, T-9026) antibodies at 4 °C, overnight. Horseradish peroxidase-conjugated secondary antibodies (Jackson ImmunoResearch, anti-rabbit 111-035-003, anti-mouse 115-035-003) and Alexa-647-linked anti-mouse (Jackson ImmunoResearch, 115-605-146) were used at room temperature, 1h. Primary and secondary antibodies were prepared in 1% BSA in TBS-T. Signals were detected with an Amersham Imager 600 (GE Healthcare Life Sciences, Eindhoven, The Netherlands) using Cy5 fluorescence and ECL (Prime) Western Blotting Detection Reagent (GE Healthcare Life Sciences). Band intensities were quantified with Image J.

For flowcytometry, cells were detached with 0.02% EDTA. Surface expression levels were determined using CD73 (Clone 4G6E3; Cat.nr. NBP2-37271, Novusbio), CD8 (Clone SK1; Cat.nr 344702; Biolegend), or isotype control primary antibodies, followed by fluorescence-conjugated secondary antibodies. For analysis of T cells the CD8 staining was combined with a live/dead stain (fixable viability dye, Invitrogen). Samples were measured on a CytoFLEX S (Beckman Coulter) and analyzed using FlowJo (version 10).

### qRT-PCR

Total RNA was extracted using Trizol (TRI reagent, AM9738, Invitrogen). cDNA was synthesized using the RevertAid H minus first-strand cDNA synthesis kit (Thermo Fisher Scientific) according to the manufacturer's protocol. Gene expression was normalized to the Actin gene and further analyzed with the  $2^{-\Delta\Delta C_t}$  method.

### Malachite Green Assay

GRHL2 KO was induced in MCF-7 Ctrl, KO-1, KO-2 cells with 1  $\mu\text{g}/\text{ml}$  doxycycline for 7 days. On day 7, MCF-7 cells together with Hs578T and MDA-MB-231 were seeded as 25,000 cells per well in triplicate in a 96-well plate. Cell media was discarded 24h later and the cells were washed with phosphate-free buffer (2 mM  $\text{MgCl}_2$ , 1 mM KCl, 10 mM glucose, 125 mM NaCl, 10 mM Hepes pH 7.2, diluted in ddH<sub>2</sub>O). Then, cells were treated with a CD73 inhibitor Adenosine 5'-( $\alpha,\beta$ -methylene) diphosphate (APCP) (25  $\mu\text{M}$  final concentration; Sigma Aldrich) for 15 mins at 37 °C. Adenosine monophosphate (AMP; 100  $\mu\text{M}$  final; Sigma Aldrich) was added and incubated for 110 mins at 37 °C. Only phosphate-free buffer was added to the wells indicated as the control condition. Inorganic phosphate production in the cell supernatants was measured using the malachite green phosphate detection kit (R&D Systems) following the manufacturer's instructions.

### Trans-well T cell migration assay and flow cytometry

MCF-7 Ctrl, KO-1, and KO-2 cells were seeded in 24-well plates (20,000 cells per well) after 5 days of doxycycline treatment (1  $\mu\text{g}/\text{ml}$ ). Human peripheral blood mononuclear cells (PBMCs) were isolated from peripheral blood from healthy volunteers by Histopaque®-1077 (10771, Sigma-Aldrich) density gradient centrifugation and enriched for CD8<sup>+</sup> T cells with the CD8<sup>+</sup> T Cell Isolation Kit (130-096-495, Miltenyi Biotec) according to manufacturer's instructions. Enriched CD8<sup>+</sup> T cells were stained with Cell Tracker™ Green CMFDA Dye (1  $\mu\text{M}$ ) (C2925, Invitrogen) for 45 min and added (200,000 cells per transwell) on top of the filter membrane of the transwell insert (6.5 mm Transwell with 3.0  $\mu\text{m}$  pore, Corning). The cancer cells and CD8<sup>+</sup> T cells were cultured with RPMI 1640, supplemented with 10% human plasma isolated

freshly from the healthy blood donors, 25 U/ml penicillin, 25 µg/mL Streptomycin at 37 °C in a humidified 5% CO<sub>2</sub> incubator. After 48 hours, filters were discarded and 20 fluorescence (488nm) and phase-contrast images per well were taken with 20x magnitude imaging using ZOE™ Fluorescent Cell Imager. The supernatant from the lower chamber was also collected to quantify migrated T cells by using a hemocytometer after Trypan blue staining (1450021, Biorad).

### **Quantification and Statistical analyses**

Data were represented as the mean ± standard deviation (SD) or means ± standard error of the mean (SEM) of at least two independent experiments. Two-way analysis of variance (ANOVA) with Bonferroni's multiple comparison test was performed unless otherwise stated. Non-parametric t-test with unequal variance was employed to determine statistical significance of the difference between groups in IHC experiments. Statistical data were obtained using GraphPad Prism 8 (GraphPad Software, La Jolla, CA, USA). ns, not significant; \*P < 0.05, \*\*P < 0.01, \*\*\*P < 0.001 and \*\*\*\*P < 0.0001.

## Supplementary Figures

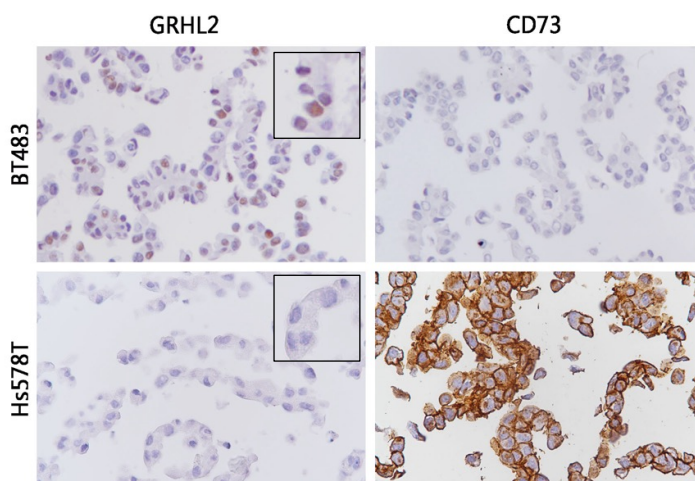


**Figure S1: GRHL2 and CD73 protein expression in breast cancer cell lines (related to Figure 2).**

GRHL2 and CD73 IHC results for a luminal cell line, showing nuclear GRHL2 expression (BT483) versus a basal B cell line lacking GRHL2 (Hs578T).

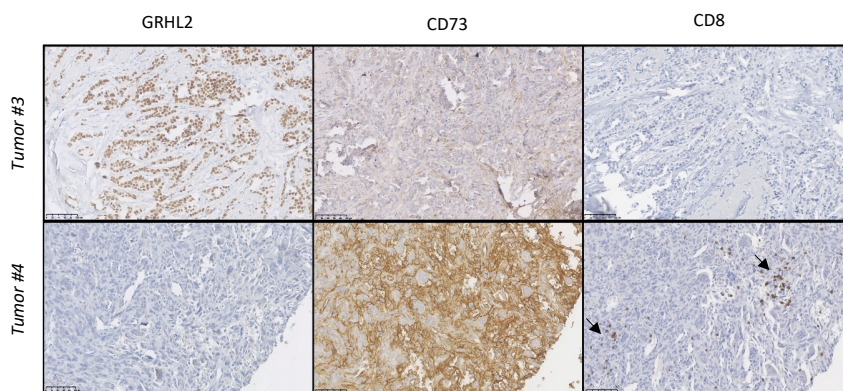


**Figure S2: IHC for GRHL2, CD73, and CD8 in breast cancer lesions (related to Figure 5C, D).**

Representative IHC images for GRHL2, CD73, and CD8 in breast cancer tissues. Arrows indicate infiltrated CD8 T cells in tumor 4.

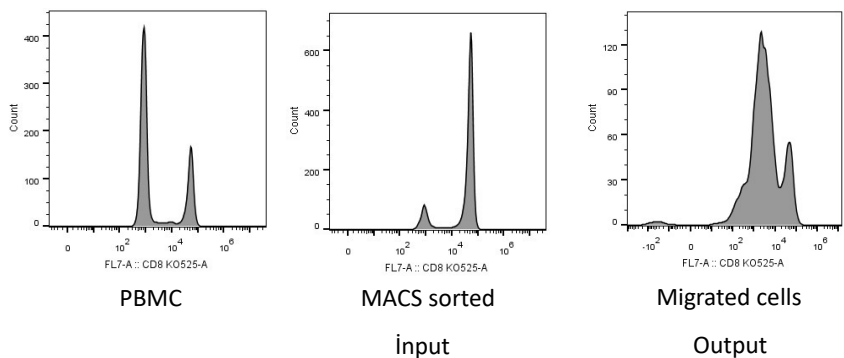


**Figure S3: Flow cytometry analysis of CD8 T cells in trans-well assay (related to Figure 5E).**

CD8 surface expression determined by flow cytometry for PBMCs (left), purified CD8 T cells that were added to the upper compartment of trans-wells (middle), and for the T cells migrated to the bottom compartment in presence of CXCL12 (right).

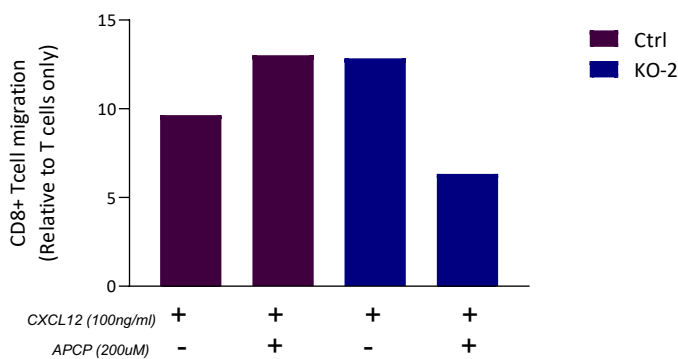


**Figure S4: CD8 T cell recruitment in presence of control or GRHL2 KO MCF-7 cells (related to Figure 5G).**

Quantification of CD8+ T cells recruited towards the lower compartment of trans-wells seeded with control or GRHL2 KO-2 MCF-7 cells (8 days 1ug/ml doxycycline treatment) in absence or presence of 100 ng/ml CXCL12 and 200uM



## **GRHL2 suppression of NT5E/CD73 in breast cancer cells**

---

APCP CD73 inhibitor. Data normalized to the T cells only condition. One experiment is shown.



# Chapter 7

---

Summary, Discussion and Future  
Perspectives

Breast cancer is the most prevalent cancer among women globally<sup>1</sup> and the therapeutic interventions remain limited due to the metastatic nature of the disease. Targeting metastasis is challenging due to the adaptive behavior of tumor cells.<sup>2</sup> Therefore, identifying the key regulators like epithelial-mesenchymal transition (EMT) is crucial.<sup>3</sup> Although EMT is not considered as the only prerequisite for the metastasis,<sup>4,5</sup> multiple studies have demonstrated its significant role in promoting metastasis and tumor progression.<sup>6,7</sup> EMT is controlled by a regulatory network of transcription factors; EMT transcription factors (EMT-TFs).<sup>8,9</sup> In this thesis, I focused on a master epithelial regulator of EMT, Grainyhead-like 2 transcription factor (GRHL2) and identified its diverse roles across breast cancer subtypes, providing novel mechanistic insights. Our initial literature study explored the interactions between molecular and physical cues that reshape tumor microenvironment and provide cellular plasticity, required for metastasis in **chapter 2**. We then examined distinct signaling networks and molecular processes regulated by GRHL2 in the luminal and basal A subtypes of breast cancer in **chapter 3-4**. Following these findings, we analyzed the function of GRHL2 in controlling kinase signaling, how central its role is in the EMT/mesenchymal-epithelial transition (MET) balance, and whether it regulates therapy response using a luminal and a basal-b model (**chapter 5**). Lastly, a novel immune modulatory role was discovered for GRHL2 in breast cancer (**chapter 6**). Here, we explain the key findings of the thesis and their significance for cancer research. We also provide recent advancements for the future research.

### **Diverse mechanisms controlling cellular plasticity in cancer metastasis**

Intratumor heterogeneity, characterized by tumor cells harboring distinct phenotypical and molecular features within the same tumor bulk, facilitates significant adaptability, often acquired through cellular plasticity.<sup>10</sup> This plasticity is further sustained by alterations in the genomic and phenotypic landscapes through EMT. EMT is influenced by various stimuli such as hypoxia and pH levels in the tumor microenvironment, as well as downstream signaling pathways including transforming growth factor- $\beta$  (TGF $\beta$ ), Wnt, and EGF.<sup>9</sup> In Chapter 1, we present a comprehensive investigation into the essential roles

played by the GRHL family, including GRHL1-3, both in embryogenesis and cancer.

It has been previously reported that mechanical stimuli also have an impact on maintaining the plasticity.<sup>11</sup> The tumor cells manipulate the interplay between several signaling pathways and mechanical cues, supporting their growth and survival to adapt to alterations within the tumor microenvironment. We discuss two distinct mechanisms; EMT and jamming/unjamming that remodel the tumor microenvironment to establish an optimal niche for the metastatic outgrowth (**chapter 2**). Additionally, we have outlined a roadmap for therapeutic interventions targeting these mechanisms.

### **Subtype-specific actions of GRHL2 across breast cancer subtypes**

In **Chapter 3**, we analyzed GRHL2 binding sites and motifs in three luminal estrogen receptor (ER) (+) breast cancer cell lines using ChIP-seq.<sup>12,13</sup> Multiple studies have demonstrated a regulatory role for GRHL2 in ER-mediated transcriptional activity.<sup>14–16</sup> Hence, we examined the presence of GRHL2 binding regions in the binding sites for ER alpha and its regulators; FOXA1 and GATA3. However, only a surprisingly small subset of intersecting binding sites was found, consistent with the findings reported by Jozwik et al.<sup>17</sup>

While genome-wide distribution of GRHL2 motifs identified putative candidate target genes of GRHL2, we further investigated their transcriptional regulation by GRHL2 in luminal breast cancer. A conditional knock-out model in a luminal breast cancer cell model; MCF-7 was employed to measure dynamic changes in nascent mRNA using Bru-seq. Differential transcriptional changes were observed in response to GRHL2 deletion. We evaluated direct and indirect regulation of such genes by integrating ChIP-seq and Bru-seq results. A significant reduction was observed in the transcriptional activity of a set of genes associated with cell-cycle and DNA replication; EHF, E2F2 and CDCA7L.<sup>18–20</sup> Our study elucidated a direct transcriptional regulation of some of these genes facilitated by GRHL2 binding to their respective promoter regions. The loss of GRHL2 in MCF-7 cells also resulted in downregulation of cell growth, and our attempts to rescue this phenotype through EHF

upregulation were unsuccessful, suggesting the involvement of additional cell-cycle regulatory genes or factors.

The interactions between GRHL2 and a set of EMT-TFs were also evaluated after GRHL2 deletion. Epithelial EMT-TFs; OVOL2 and CDLN4 were identified as direct targets of GRHL2 while only CLDN4 mRNA was altered in response to GRHL2 loss. A critical target of the EMT-TF; CDH1 which encodes the E-cadherin cell-cell adhesion receptor, is a known direct target of GRHL2. However, unlike other studies,<sup>21</sup> it remained unaffected by the loss of GRHL2 expression in our study. In addition, no GRHL2 binding in the promoter region of ZEB1 was found in contrast to the earlier reports showing direct negative regulatory feedback loop between GRHL2 and ZEB1.<sup>13,22,23</sup> These findings highlight the cell-type specific actions of GRHL2 and suggest the involvement of other mechanisms like post-transcriptional regulations.

Nest, a similar integrative approach was taken in three luminal and three basal-a breast cancer lines to unveil the different biological functions of GRHL2 in distinct breast cancer subtypes (**chapter 4**). Analysis of ChIP-seq data showed common changes in cell migration, epithelial proliferation and cell-cell junctions in both subtypes. Dual roles have been attributed to GRHL2 as a tumor suppressor and promoter in many cancers.<sup>24–27</sup> In agreement with our conclusion in chapter 3, cell-cycle arrest was the dominant response to GRHL2 loss in luminal cell line, MCF-7. This effect was less pronounced in a basal A cell line, HCC1806. Indeed, this points to distinct roles for GRHL2 in different breast cancer subtypes. The differential response in growth might be explained by the enhanced activities of hormone receptors in luminal breast cancer. Elevated ER signaling in tumors is correlated with poor prognosis<sup>28,29</sup> and is linked to increased cell proliferation. ER $\alpha$  signaling supports the cell proliferation in MCF-7 cells by increasing the transcriptional activities of PCNA/E2F1 and inhibiting the induction of cell-cycle arrest via p53/p21 axis.<sup>30</sup>

In contrast to the findings in MCF-7, the deletion of GRHL2 resulted in increased cell migration in HCC1806 cells, accompanied by upregulation of N-

cadherin and Vimentin; mesenchymal genes.<sup>31,32</sup> Previous studies have linked the enhanced activation of mesenchymal markers to increased cell migration.<sup>33,34</sup> Although the downregulation of E-cadherin occurred as a common finding in both cell types, it didn't further induce a full EMT in luminal breast cancer, suggesting the necessity of other changes co-existing also in the mesenchymal spectrum of EMT.<sup>35,36</sup> Our findings indicate that such changes are already present in basal A breast cancer cells and here depletion of GRHL2 does activate an EMT. Altogether, these results point to a subtype-specific role for GRHL2 in breast cancer.

*In vivo* experiments supported the oncogenic role of GRHL2, given its location in the frequently amplified region (8q22) in many cancers.<sup>36–38</sup> The aspects of EMT induced by GRHL2 deletion in HCC1806 suggested that GRHL2 may have tumor- or metastasis suppressive roles in this model, as opposed to luminal cells where our findings pointed to a largely tumor promoting role. We investigated this in a basal A orthotopic transplantation model. However, these experiments indicated that despite the more obvious EMT upon GRHL2 depletion, also in basal-A cells tumor growth as well as metastasis are supported rather than suppressed by GRHL2.

### **Multifaceted roles of GRHL2 in cancer cell signaling and targeted therapies**

Our findings in chapter 3 and 4 delineated the landscape of gene networks regulated by GRHL2 in luminal and basal A breast cancer subtypes. By using the data obtained in chapter 3, we evaluated the changes in a set of EMT-related genes after the induction of GRHL2 loss in MCF-7 cells (**chapter 5**). Our data revealed no changes in the expression patterns of epithelial markers and mesenchymal cell markers other than CLDN4. This indicated the absence of EMT-induction by GRHL2 deletion in luminal cancer, corroborating the results presented in chapter 4.

To understand the mechanisms underlying differential regulation of cellular processes controlled by GRHL2, we next profiled the kinase activities associated with the breast cancer signaling in luminal breast cancer. Several signaling pathways; estrogen receptor (ER), PI3K, Hedgehog (HH), TGF $\beta$  and

androgen receptor (AR) were analyzed with a qPCR-based platform, designed for its use in the clinic to determine personalized therapies for breast cancer patients.<sup>39</sup> GRHL2 exerts its diverse functions by rewiring signaling pathways in many cancer types.<sup>15,40</sup> The elevated GRHL2 expression was shown to induce MAPK activity, resulting in suppression of TGF $\beta$  mediated epithelial plasticity and carcinogenesis in oral cancer.<sup>41</sup> However, we have not observed any changes in MAPK activity in GRHL2 deleted cells. This pattern was also observed across other pathways except for PI3K and TGF $\beta$ , being upregulated upon GRHL2 loss. The importance of TGF $\beta$  signaling and its function in inducing EMT to sustain tumorigenesis have been implicated by several studies.<sup>42,43</sup> The tumor suppressing function of GRHL2 is often linked to the down-regulation of TGF $\beta$  signaling,<sup>44,45</sup> supporting our analysis in luminal breast cancer. The potential rationale for the pathways remaining unaffected by GRHL2 deletion could be attributed to the utilization of a conditional CRISPR-Cas9 knockout system. The analyzed samples for the pathway analysis were originated from a knockout study conducted for 8 days in MCF-7 cells. It is possible that a longer duration for GRHL2 knock-out is necessary for the modifications of the post transcriptional machinery and signaling pathways.

EMT is defined by the balance between epithelial and mesenchymal states, and its progression is characterized by the gain of mesenchymal characteristics which is associated with therapy resistance.<sup>5,46</sup> As elucidated in chapter 3 and 4, GRHL2 plays a pivotal role in determining the balance between EMT and MET in breast cancer but, its deletion in luminal cells is not sufficient to drive an EMT. The basal B subtype of breast cancer is characterized by its enhanced mesenchymal features, limiting the response to the therapies.<sup>47</sup> Consequently, our investigation centered on understanding whether expression of GRHL2 would be sufficient to suppress the mesenchymal phenotype and affect the therapy response in basal B breast cancer.

Overexpression of GRHL2 in the basal B subtype breast cancer cell line, MDA-MB-231 did not induce alterations in the expression patterns of any epithelial markers (Occludin, CLDN4, E-cadherin, ZO-1) or mesenchymal markers (Vimentin and Zeb1). Differing from our findings, overexpression of GRHL2 has



been shown to induce MET-like changes, both phenotypically and genotypically, including increased E-cadherin expression.<sup>22</sup> However, both studies showed that cell growth remained unaffected, unlike the changes observed in Chapter 4 in the luminal and basal A subtypes of breast cancer. This indicates that GRHL2 manipulation on its own, does not suffice to drive an EMT in a basal B model suggesting that other, critical regulators of the epithelial/mesenchymal balance must be altered.

We next assessed the drug responses facilitated by GRHL2 in absence of confounding influences of changes in the EMT/MET balance. MDA-MB-231 cells, with and without GRHL2 overexpression, were treated with a small kinase inhibitor library, and drug responses were evaluated based on changes in cell growth. Similar to a previous study showing the co-operation of GRHL2 with PI3K/Akt pathway in colorectal cancer,<sup>48</sup> we also found two candidate kinases targeting PI3K pathway, exhibiting GRHL2 mediated sensitivity. However, this vulnerability wasn't further validated. Altogether, the findings in chapter 5 indicate that GRHL2 loss in basal B cells is not sufficient to drive an EMT and in absence of such an effect, the impact on therapy response is limited or absent.

### **Studying tumor-immune cell interactions in the context of GRHL2-mediated immune evasion**

The interaction between GRHL2 and immune regulatory mechanisms has been only minimally addressed by studies thus far. By integrating the data from breast cancer cell lines and breast adenocarcinoma patient tumors, we detected a significant negative correlation of GRHL2 with expression of the ecto-enzyme, NT5E/CD73 (**chapter 6**). Based on our findings in chapter 3 and 4, we identified the CD73 encoding gene, NT5E as one of the direct targets of GRHL2 in luminal breast cancer.

Several studies have emphasized the role of elevated adenosine levels, facilitated by CD73 in tumor cells, in immune evasion.<sup>49,50</sup> Our investigation revealed that the loss of GRHL2 in luminal breast cancer increases CD73-mediated extracellular adenosine production. However, tumor cells are not the

sole contributors to the adenosine production. Studies have demonstrated that immune cells with pro and anti-tumor capabilities including NK cells,<sup>51</sup> macrophages,<sup>52</sup> and cytotoxic (CD8+) T cells,<sup>53</sup> also significantly contribute to elevated adenosine levels within the tumor microenvironment.

To delineate the impact of GRHL2-controlled adenosine production on luminal breast cancer, we employed a trans-well migration model to study tumor-immune cell interactions in response to GRHL2 loss. Surprisingly, we found that the absence of GRHL2 increased the CD8+ T cell migration, which could be reverted by a CD73 inhibitor. The finding that CD73-mediated adenosine production in tumors may actually increase, rather than decrease immune infiltration was supported in clinical samples showing a positive relation between CD73 and Cd8+ T cell presence although the correlation was weak. This unveiled a novel role for GRHL2 in shaping the immune response within luminal breast cancer. Other studies have focused on the impact of extracellular adenosine on the cytotoxic activity of CD8+ T cells.<sup>54,55</sup> As previously displayed in chapter 4, GRHL2 deletion induces cell-cycle arrest in luminal breast cancer. Therefore, we were unable to investigate the cytotoxic effects mediated by adenosine using our conditional knockout model.

Studying the immune evasion related mechanisms in 2D might underestimate the complexity of the tumor microenvironment. During tumor progression, remodulation of the tumor microenvironment, including the formation of a collagen-rich, stiff extracellular matrix (ECM) occurs.<sup>56</sup> It has been reported that the highly dense ECM had an impact on the cytotoxic activity of immune cells<sup>56,57</sup> and the profile of T cells,<sup>58</sup> representing a mechanism of tumor immune evasion. Hence, it will be interesting to further explore the impact of GRHL2 loss on interactions with the immune system in 3D co-culture systems and using *in vivo* models.

### **Conclusion and future perspectives**

In conclusion, this thesis examines multifaceted roles of GRHL2 across breast cancer subtypes. We explore the underlying mechanisms that support cellular plasticity and their implication for the cancer therapy. We outline the

signaling networks orchestrated by GRHL2 in luminal breast cancer and discern differential roles of GRHL2 in cell growth and cell migration between luminal vs. basal A subtypes of breast cancer. Our research highlights that altering GRHL2 expression is, by itself, not sufficient to drive EMT in luminal, or MET in basal B subtype breast cancers. This may also explain that in our studies, no significant correlation is identified between GRHL2 expression and therapy responses tested. Moreover, a novel immunomodulatory function via the NT5E/CD73-extracellular adenosine axis is identified in luminal breast cancer.

It will be important to unravel the interaction between co-factors and GRHL2 in different breast cancer subtypes using co-immunoprecipitation and other approaches, to understand the mechanisms underlying context-dependent GRHL2 controlled cell functions. The use of patient derived xenografts or organoid models will provide more insights for the tumor heterogeneity in different breast cancer subtypes. This will allow the identification of more clinically relevant GRHL2-regulated mechanisms underlying its role in tumor growth, metastasis, and therapy response. 2D tumor models lack the complexity of the tumor microenvironment and lack the abundance of metabolites and cytokines, secreted by numerous cell types in the tumor microenvironment. With respect to the novel GRHL2-regulated interaction with CD8+ T cells we discover, further exploration of this mechanism in complex 3D or *in vivo* models are warranted to place in context of the diverse tumor microenvironment components that also contribute to extracellular adenosine production. Overall, this thesis illuminates novel insights into the context and subtype-specific roles of GRHL2 in breast cancer subtypes and offers opportunities for targeted vulnerabilities in breast cancer therapy.

## References

1. Arnold M, Morgan E, Rumgay H, et al. Current and future burden of breast cancer: Global statistics for 2020 and 2040. *Breast*. 2022;66:15-23. doi:10.1016/j.breast.2022.08.010
2. Welch DR, Hurst DR. Defining the hallmarks of metastasis. *Cancer Res*. 2019;79(12):3011-3027. doi:10.1158/0008-5472.CAN-19-0458
3. Nieto MA, Huang RYJ, Jackson RA, Thiery JP. EMT: 2016. *Cell*. 2016;166(1):21-45. doi:10.1016/j.cell.2016.06.028

4. Zheng X, Carstens JL, Kim J, et al. Epithelial-to-mesenchymal transition is dispensable for metastasis but induces chemoresistance in pancreatic cancer. *Nature*. 2015;527(7579):525-530. doi:10.1038/nature16064
5. Fischer KR, Durrans A, Lee S, et al. Epithelial-to-mesenchymal transition is not required for lung metastasis but contributes to chemoresistance. *Nature*. 2015;527(7579):472-476. doi:10.1038/nature15748
6. Caramel J, Papadogeorgakis E, Hill L, et al. A switch in the expression of embryonic EMT-inducers drives the development of malignant melanoma. *Cancer Cell*. 2013;24(4):466-480. doi:10.1016/j.ccr.2013.08.018
7. Ye X, Brabletz T, Kang Y, et al. Upholding a role for EMT in breast cancer metastasis. *Nature*. 2017;547(7661):E1-E3. doi:10.1038/nature22816
8. Puisieux A, Brabletz T, Caramel J. Oncogenic roles of EMT-inducing transcription factors. *Nat Cell Biol*. 2014;16(6):488-494. doi:10.1038/ncb2976
9. Li W, Kang Y. Probing the fifty shades of EMT in metastasis. *Trends Cancer*. 2016;2(2):65-67. doi:10.1016/j.trecan.2016.01.001
10. Hanahan D, Weinberg RA. Hallmarks of cancer: the next generation. *Cell*. 2011;144(5):646-674. doi:10.1016/j.cell.2011.02.013
11. Oswald L, Grosser S, Smith DM, Käs JA. Jamming transitions in cancer. *J Phys Appl Phys*. 2017;50(48):483001. doi:10.1088/1361-6463/aa8e83
12. Aue A, Hinze C, Walentin K, et al. A grainyhead-like 2/ovo-like 2 pathway regulates renal epithelial barrier function and lumen expansion. *J Am Soc Nephrol*. 2015;26(11):2704-2715. doi:10.1681/ASN.2014080759
13. Chung VY, Tan TZ, Tan M, et al. GRHL2-miR-200-ZEB1 maintains the epithelial status of ovarian cancer through transcriptional regulation and histone modification. *Sci Rep*. 2016;6(1):19943. doi:10.1038/srep19943
14. Reese RM, Helzer KT, Allen KO, Zheng C, Solodin N, Alarid ET. GRHL2 enhances phosphorylated estrogen receptor (ER) chromatin binding and regulates ER-mediated transcriptional activation and repression. *Mol Cell Biol*. 2022;42(10):e0019122. doi:10.1128/mcb.00191-22
15. Cocce KJ, Jasper JS, Desautels TK, et al. The lineage determining factor GRHL2 collaborates with FOXA1 to establish a targetable pathway in endocrine therapy-resistant breast cancer. *Cell Rep*. 2019;29(4):889-903.e10. doi:10.1016/j.celrep.2019.09.032
16. Holding AN, Giorgi FM, Donnelly A, et al. Correction to: VULCAN integrates ChIP-seq with patient-derived co-expression networks to identify GRHL2 as a key co-regulator of ERα at enhancers in breast cancer. *Genome Biol*. 2019;20(1):122. doi:10.1186/s13059-019-1733-0
17. Jozwik KM, Chernukhin I, Serandour AA, Nagarajan S, Carroll JS. FOXA1 directs H3K4 monomethylation at enhancers via recruitment of the methyltransferase MLL3. *Cell Rep*. 2016;17(10):2715-2723. doi:10.1016/j.celrep.2016.11.028
18. Hsu T, Trojanowska M, Watson DK. Ets proteins in biological control and cancer. *J Cell Biochem*. 2004;91(5):896-903. doi:10.1002/jcb.20012

19. Chen HZ, Tsai SY, Leone G. Emerging roles of E2Fs in cancer: an exit from cell cycle control. *Nat Rev Cancer*. 2009;9(11):785-797. doi:10.1038/nrc2696
20. Li H, Weng Y, Wang S, et al. CDCA7 facilitates tumor progression by directly regulating CCNA2 expression in esophageal squamous cell carcinoma. *Front Oncol*. 2021;11:734655. doi:10.3389/fonc.2021.734655
21. Werner S, Frey S, Riethdorf S, et al. Dual roles of the transcription factor grainyhead-like 2 (GRHL2) in breast cancer. *J Biol Chem*. 2013;288(32):22993-23008. doi:10.1074/jbc.M113.456293
22. Werner S, Frey S, Riethdorf S, et al. Dual roles of the transcription factor grainyhead-like 2 (GRHL2) in breast cancer. *J Biol Chem*. 2013;288(32):22993-23008. doi:10.1074/jbc.M113.456293
23. Cieply B, Farris J, Denvir J, Ford HL, Frisch SM. Epithelial-mesenchymal transition and tumor suppression are controlled by a reciprocal feedback loop between ZEB1 and Grainyhead-like-2. *Cancer Res*. 2013;73(20):6299-6309. doi:10.1158/0008-5472.CAN-12-4082
24. Nishino H, Takano S, Yoshitomi H, et al. Grainyhead-like 2 (GRHL2) regulates epithelial plasticity in pancreatic cancer progression. *Cancer Med*. 2017;6(11):2686-2696. doi:10.1002/cam4.1212
25. Pan X, Zhang R, Xie C, et al. GRHL2 suppresses tumor metastasis via regulation of transcriptional activity of RhoG in non-small cell lung cancer. *Am J Transl Res*. 2017;9(9):4217-4226.
26. Faddaoui A, Sheta R, Bachvarova M, et al. Suppression of the grainyhead transcription factor 2 gene (GRHL2) inhibits the proliferation, migration, invasion and mediates cell cycle arrest of ovarian cancer cells. *Cell Cycle*. 2017;16(7):693-706. doi:10.1080/15384101.2017.1295181
27. Chen W, Yi JK, Shimane T, et al. Grainyhead-like 2 regulates epithelial plasticity and stemness in oral cancer cells. *Carcinogenesis*. 2016;37(5):500-510. doi:10.1093/carcin/bgw027
28. Lønning PE. Poor-prognosis estrogen receptor- positive disease: present and future clinical solutions. *Ther Adv Med Oncol*. 2012;4(3):127-137. doi:10.1177/1758834012439338
29. Prat A, Pineda E, Adamo B, et al. Clinical implications of the intrinsic molecular subtypes of breast cancer. *Breast*. 2015;24 Suppl 2:S26-35. doi:10.1016/j.breast.2015.07.008
30. Liao XH, Lu DL, Wang N, et al. Estrogen receptor  $\alpha$  mediates proliferation of breast cancer MCF-7 cells via a p21/PCNA/E2F1-dependent pathway. *FEBS J*. 2014;281(3):927-942. doi:10.1111/febs.12658
31. Wang M, Ren D, Guo W, et al. N-cadherin promotes epithelial-mesenchymal transition and cancer stem cell-like traits via ErbB signaling in prostate cancer cells. *Int J Oncol*. 2016;48(2):595-606. doi:10.3892/ijo.2015.3270
32. Usman S, Waseem NH, Nguyen TKN, et al. Vimentin is at the heart of epithelial mesenchymal transition (EMT) mediated metastasis. *Cancers Basel*. 2021;13(19):4985. doi:10.3390/cancers13194985

33. Nguyen T, Duchesne L, Sankara Narayana GHN, et al. Enhanced cell-cell contact stability and decreased N-cadherin-mediated migration upon fibroblast growth factor receptor-N-cadherin cross talk. *Oncogene*. 2019;38(35):6283-6300. doi:10.1038/s41388-019-0875-6
34. De Pascalis C, Pérez-González C, Seetharaman S, et al. Intermediate filaments control collective migration by restricting traction forces and sustaining cell-cell contacts. *J Cell Biol*. 2018;217(9):3031-3044. doi:10.1083/jcb.201801162
35. Pastushenko I, Brisebarre A, Sifrim A, et al. Identification of the tumour transition states occurring during EMT. *Nature*. 2018;556(7702):463-468. doi:10.1038/s41586-018-0040-3
36. Jolly MK, Tripathi SC, Jia D, et al. Stability of the hybrid epithelial/mesenchymal phenotype. *Oncotarget*. 2016;7(19):27067-27084. doi:10.18632/oncotarget.8166
37. Dompe N, Rivers CS, Li L, et al. A whole-genome RNAi screen identifies an 8q22 gene cluster that inhibits death receptor-mediated apoptosis. *Proc Natl Acad Sci U A*. 2011;108(43):E943-51. doi:10.1073/pnas.1100132108
38. Kang X, Chen W, Kim RH, Kang MK, Park NH. Regulation of the hTERT promoter activity by MSH2, the hnRNPs K and D, and GRHL2 in human oral squamous cell carcinoma cells. *Oncogene*. 2009;28(4):565-574. doi:10.1038/onc.2008.404
39. Inda MA, van Swinderen P, van Brussel A, et al. Heterogeneity in signaling pathway activity within primary and between primary and metastatic breast cancer. *Cancers Basel*. 2021;13(6):1345. doi:10.3390/cancers13061345
40. Nie Y, Ding Y, Yang M. GRHL2 upregulation predicts a poor prognosis and promotes the resistance of serous ovarian cancer to cisplatin. *Onco Targets Ther*. 2020;13:6303-6314. doi:10.2147/OTT.S250412
41. Chen W, Kang KL, Alshaikh A, et al. Grainyhead-like 2 (GRHL2) knockout abolishes oral cancer development through reciprocal regulation of the MAP kinase and TGF- $\beta$  signaling pathways. *Oncogenesis*. 2018;7(5):38. doi:10.1038/s41389-018-0047-5
42. Xu J, Lamouille S, Derynck R. TGF-beta-induced epithelial to mesenchymal transition. *Cell Res*. 2009;19(2):156-172. doi:10.1038/cr.2009.5
43. Morrison CD, Parvani JG, Schiemann WP. The relevance of the TGF- $\beta$  Paradox to EMT-MET programs. *Cancer Lett*. 2013;341(1):30-40. doi:10.1016/j.canlet.2013.02.048
44. He J, Feng C, Zhu H, Wu S, Jin P, Xu T. Grainyhead-like 2 as a double-edged sword in development and cancer. *Am J Transl Res*. 2020;12(2):310-331.
45. Xiang J, Fu X, Ran W, Wang Z. Grhl2 reduces invasion and migration through inhibition of TGF $\beta$ -induced EMT in gastric cancer. *Oncogenesis*. 2017;6(1):e284. doi:10.1038/oncsis.2016.83
46. Byers LA, Diao L, Wang J, et al. An epithelial-mesenchymal transition gene signature predicts resistance to EGFR and PI3K inhibitors and identifies Axl as a therapeutic target for overcoming EGFR inhibitor resistance. *Clin Cancer Res*. 2013;19(1):279-290. doi:10.1158/1078-0432.CCR-12-1558

47. Dine JL, O'Sullivan CC, Voeller D, et al. The TRAIL receptor agonist drozitumab targets basal B triple-negative breast cancer cells that express vimentin and Axl. *Breast Cancer Res Treat.* 2016;155(2):235-251. doi:10.1007/s10549-015-3673-z
48. Hu F, He Z, Sun C, Rong D. Knockdown of GRHL2 inhibited proliferation and induced apoptosis of colorectal cancer by suppressing the PI3K/Akt pathway. *Gene.* 2019;700:96-104. doi:10.1016/j.gene.2019.03.051
49. Kellner M, von Neubeck B, Czogalla B, et al. A novel anti-CD73 antibody that selectively inhibits membrane CD73 shows antitumor activity and induces tumor immune escape. *Biomedicines.* 2022;10(4):825. doi:10.3390/biomedicines10040825
50. Stagg J, Divisekera U, Duret H, et al. CD73-deficient mice have increased anti-tumor immunity and are resistant to experimental metastasis. *Cancer Res.* 2011;71(8):2892-2900. doi:10.1158/0008-5472.CAN-10-4246
51. Neo SY, Yang Y, Record J, et al. CD73 immune checkpoint defines regulatory NK cells within the tumor microenvironment. *J Clin Invest.* 2020;130(3):1185-1198. doi:10.1172/JCI128895
52. Murphy PS, Wang J, Bhagwat SP, et al. CD73 regulates anti-inflammatory signaling between apoptotic cells and endotoxin-conditioned tissue macrophages. *Cell Death Differ.* 2017;24(3):559-570. doi:10.1038/cdd.2016.159
53. Schneider E, Winzer R, Rissiek A, et al. CD73-mediated adenosine production by CD8 T cell-derived extracellular vesicles constitutes an intrinsic mechanism of immune suppression. *Nat Commun.* 2021;12(1):5911. doi:10.1038/s41467-021-26134-w
54. Ray A, Du T, Wan X, et al. A novel small molecule inhibitor of CD73 triggers immune-mediated multiple myeloma cell death. *Blood Cancer J.* 2024;14(1):58. doi:10.1038/s41408-024-01019-5
55. Briceño P, Rivas-Yañez E, Roseblatt MV, et al. CD73 ectonucleotidase restrains CD8+ T cell metabolic fitness and anti-tumoral activity. *Front Cell Dev Biol.* 2021;9:638037. doi:10.3389/fcell.2021.638037
56. Kuczek DE, Larsen AMH, Thorseth ML, et al. Collagen density regulates the activity of tumor-infiltrating T cells. *J Immunother Cancer.* 2019;7(1):68. doi:10.1186/s40425-019-0556-6
57. Robertson C, Sebastian A, Hinckley A, et al. Extracellular matrix modulates T cell clearance of malignant cells in vitro. *Biomaterials.* 2022;282(121378):121378. doi:10.1016/j.biomaterials.2022.121378
58. Chirivi M, Maiullari F, Milan M, et al. Tumor extracellular matrix stiffness promptly modulates the phenotype and gene expression of infiltrating T lymphocytes. *Int J Mol Sci.* 2021;22(11):5862. doi:10.3390/ijms22115862





# Appendix

---

Nederlandse samenvatting

List of commonly used abbreviations

Curriculum vitae

List of publications

### Nederlandse samenvatting

Borstkanker is wereldwijd de meest voorkomende vorm van kanker bij vrouwen en uitzaaiing beperkt de effectiviteit van doelgerichte therapieën. Daarom zijn er nieuwe strategieën nodig om uitzaaiing tegen te gaan. De snelle aanpassing van tumorcellen vereist de identificatie van belangrijke regulatoren zoals epitheliale-mesenchymale transitie (EMT). Hoewel EMT niet de enige factor is in uitzaaiing, bevordert het dit wel en wordt het gereguleerd door een netwerk van transcriptiefactoren (EMT-TF's). Dit proefschrift richtte zich specifiek op de verschillende rollen van Grainyhead-like 2 (GRHL2) in verschillende borstkankersubtypes, met als doel nieuwe mechanistische en doelgerichte inzichten te verschaffen.

**Hoofdstuk 1** geeft een overzicht van de biologie van borstkanker, met de nadruk op een belangrijke familie van transcriptiefactoren -Grainyhead-like- die de progressie en uitzaaiing van borstkanker beïnvloeden en hun rol in normale fysiologie en maligniteiten. **In hoofdstuk 2** gingen we verder met het begrijpen van de moleculaire en fysische factoren in de nabije omgeving van de tumorcellen (de “tumor microenvironment” (TME)) die leiden tot uitzaaiing. We hebben de mechanische aspecten van de TME en het aanpassen van de TME door tumorcellen uitgewerkt op basis van de bestaande literatuur. Later bespraken we de migratiestrategieën van tumorcellen en hoe deze worden gestuurd door twee fenomenen: “unjamming” en gedeeltelijke EMT. Potentiële therapeutische benaderingen voor het aanpakken van de TME en de gedeeltelijke EMT werden voorgesteld om uitzaaiing te overwinnen. Deze analyse biedt inzicht in de wisselwerking tussen fysieke en moleculaire signalen die de verspreiding van tumorcellen vanuit de primaire tumor ondersteunen en hoe nieuwe doelgerichte strategieën kunnen worden ontwikkeld.

GRHL2 blijkt een dubbele rol te spelen als bevorderaar van tumor groei en onderdrukker van metastasering in verschillende kankertypes, waaronder borstkanker. De specifieke functies van GRHL2 in verschillende borstkankersubtypes zijn echter slecht gedefinieerd in de literatuur. In **hoofdstuk 3** analyseerden we de genregulatiernetwerken van GRHL2 in het lumbinale borstkankersubtype. Genomische gebieden die door GRHL2 worden bezet, zijn

geïdentificeerd met behulp van een ChIP-seq studie en dit heeft mogelijke doelen van GRHL2 in luminale borstkanker afgebakend. Er is eerder gemeld dat GRHL2 betrokken is bij de regulatie van de oestrogeen receptor (ER) en zijn pioniersfactoren GATA3 en FOXA1. Daarom onderzochten wij in hoeverre GRHL2 bindingsplaatsen deelt met deze factoren en ontdekten dat de overlap beperkt was. Om het GRHL2-gereguleerde transcriptoom te bepalen, ontwikkelden we een induceerbaar GRHL2 knock-out (KO) model in de MCF-7 luminale borstkankercellijn en voerden we Bru-seq analyse uit. Een geïntegreerde aanpak die ChIP- en Bru-seq-studies combineerde, identificeerde nieuwe directe GRHL2-doelwitgenen, waaronder zijn rol in proliferatie door de transcriptionele activering van ETS- en E2F-transcriptiefactoren. Aangezien GRHL2 een hoofdregulator van EMT is, beoordeelden wij de transcriptionele controle over EMT-gerelateerde genen. GRHL2 bleek CLDN4 rechtstreeks te reguleren. Echter, zowel ChIP- als Bru-seq-analyses sloten de directe controle van andere targets, zoals CDH1 en ZEB1, door GRHL2 in luminale borstkankercellen uit. De relatie tussen GRHL2 en zijn transcriptionele targets werd verder klinisch gevalideerd in zowel ER-positieve als ER-negatieve borstkankerpatiënten. Het onderzoek toonde nieuwe gennetwerken en doelen aan die door GRHL2 worden gecontroleerd, evenals de unieke rol van GRHL2 bij het reguleren van EMT.

**Hoofdstuk 4** onderzocht de invloed van GRHL2-verlies in diverse biologische processen in luminale en basale borstkankers. Er werden verschillende niveaus van GRHL2 expressie waargenomen in de verschillende borstkankersubtypes. GRHL2 expressie bleek geassocieerd te zijn met een slechtere uitkomst voor de patiënt en was significant gedownreguleerd in het basale B subtype vergeleken met andere borstkankersubtypes. Wij toonden aan dat GRHL2-verlies in luminale en basale A-subtypes resulteerde in celcyclusstilstand. Bovendien verbeterde het de migratiemogelijkheden van basale A-cellen, maar had het geen invloed op de migratie van luminale cellen. In luminale cellen was er een afname van de epitheliale marker E-cadherine, terwijl er daarnaast in basale cellen ook nog een toename was van de mesenchymale markers Vimentine en N-cadherine. Om de invloed van GRHL2 op groei en EMT te evalueren, onderzochten we een basaal A tumormodel waarin

GRHL2 niveaus experimenteel verlaagd waren in vivo. De verlaagde GRHL2 niveaus resulteerden in verminderde tumorgroei en verminderde uitzaaiing naar de longen, wat bevestigt dat groeionderdrukking, maar niet een verhoogde EMT-gestimuleerde uitzaaiing, een gevolg is van GRHL2-verlies.

**In hoofdstuk 5**, concentreerden we ons op de rol van GRHL2 in EMT en de signaalwegen die het reguleert in het basale B-subtype. In overeenstemming met hoofdstuk 4 zagen we weinig GRHL2 expressie in basale B cellen. Daarom hebben we de expressie van GRHL2 in deze cellen verhoogd, zowel stabiel als conditioneel. Deze overexpressie induceerde echter geen mesenchymale naar epitheliale overgang (MET), wat erop wijst dat GRHL2 overexpressie op zichzelf onvoldoende is om de EMT/MET-balans in het basale B-subtype te beïnvloeden. Het overheersende effect van GRHL2 op celgroei gold niet voor dit subtype. Om de GRHL2-gereguleerde signalering van basale B-cellen te onderzoeken, gebruikten we een high-throughput screening met kinase remmers. Het effect van vier kinase remmers leek beïnvloed te zijn door GRHL2, maar verdere validatie is nodig om GRHL2-gemedieerde reacties te bevestigen.

**Hoofdstuk 6** bracht een nieuwe rol voor GRHL2 in immuunmodulatie aan het licht. Er werd ontdekt dat NT5E, dat codeert voor het ecto-enzym CD73, dat verantwoordelijk is voor de productie van adenosine in de TME, een direct doelwit is van GRHL2 in luminale cellen. Verlies van GRHL2 leidde tot verhoogde expressie van NT5E op zowel mRNA- als eiwitniveau, wat resulteerde in hogere extracellulaire adenosine niveaus. Eerder onderzoek heeft aangetoond dat hoge adenosine niveaus in de TME het gedrag van T-cellen beïnvloedt en hun cytotoxiciteit remt. Wij toonden aan dat deze verhoging de migratie van CD8+ T-cellen bevordert. Deze studie heeft ons inzicht in de rol van GRHL2 en de invloed ervan in de immuunoncologie vergroot door een nieuwe signalerings route te identificeren. In **hoofdstuk 7** bespraken we de conclusies van elk hoofdstuk in dit proefschrift en schetsten we toekomstige onderzoeksperspectieven.

---

**List of commonly used abbreviations**

A2AR	Adenosine A2A receptor
ABC	ATP-binding cassette
ADP	Adenosine di-phosphate
AFC	Average fold change
AMP	Adenosine mono-phosphate
ANOVA	Analysis of variance
APCP	An enzymatic inhibitor of CD73, $\alpha,\beta$ -methylene ADP
AR	Androgen receptor
ATP	Adenosine triphosphate
BCA	Biicinchoninic acid
CAFs	Cancer-associated fibroblasts
CD39	Cluster of Differentiation 39; ectonucleoside triphosphate diphosphohydrolase-1
CD73	Cluster of Differentiation 73; ecto-5'-nucleotidase
CD8	Cluster of Differentiation 8;
CDCA7L	Cell division cycle-associated 7-like protein
CDH1	Cadherin-1
CDH2	Cadherin-2
cDNA	CopyDNA of complement DNA
ChIP	Chromatin immunoprecipitation
CLDN4	Claudin-4
CO2	Carbon dioxide
CRC	Cancer,30 colo-rectal cancer
CTR	Cell cycle phase distribution in sgCTR
CXCL12	C-X-C motif chemokine ligand 12
DMSO	Dimethylsulfoxide
DNA	Deoxyribonucleic acid
ECL	Electrochemiluminescence
ECM	Extracellular matrix
EDTA	Ethylenediaminetetraacetic acid
EGF	Epidermal growth factor
EHF	ETS homologous factor

## Appendix

---

EMT	Epithelial-mesenchymal transition
EMT-TFs	Epithelial-mesenchymal transition transcription factors
ER	Estrogen receptor
ERa	Estrogen receptor alpha
EV	Empty vector
FACS	Fluorescence-activated cell sorting
FAK	Focal adhesion kinase
FC	Fold-change
FIMO	Find Individual Motif Occurrences
FOXA1	Forkhead box protein A1
GAPDH	Glyceraldehyde 3-phosphate dehydrogenase
GATA3	GATA binding protein 3
GEO	Gene Expression Omnibus
GO	Gene Ontology
GRHL	Grainyhead like
HA	Hyaluronic acid
HER2	Human epidermal growth factor re-ceptor 2
HH	Hedgehog
hTERT	Human telomerase reverse transcriptase
IHC	Immunohistochemistry
IP	Immunoprecipitation
IPA	Ingenuity pathway analysis
KO	Knock out
LOXL2	Lysyl oxidase homolog 2
MACS	Model-based analysis of ChIP-Seq
MAPK	Mitogen-activated protein kinase
MCM2	Mini-chromosome maintenance protein-2
MET	Mesenchymal-to-epithelial transition
METABRIC	Molecular Taxonomy of Breast Cancer International Consortium
mRNA	Messenger-ribonucleic acid
NaCl	Sodium chloride
NECA	5'-N-ethylcarboxamide adenosine
NK	Natural killer cells

NT5E	Ecto-5'-nucleotidase
OVOL2	Ovo like zinc finger 2
PBS	Phosphate buffered saline
PCR	Polymerase chain reaction
PI3K	Phosphoinositide 3-kinase
PR	Progesterone receptor
PVDF	Polyvinylidene difluoride
qPCR	Quantitative polymerase chain reaction
RNA	Ribonucleic acid
ROCK	Rho-associated kinase
RPMI	Roswell Park Memorial Institute medium
RT	Room temperature
RT-qPCR	Realtime quantitative PCR
SD	Sented as the mean $\pm$ standard deviation
SDS-PAGE	Sodium do-decyl sulfate–polyacrylamide gel electrophoresis
SE	Standard error
SEM	Standard error of the mean
SRB	Sulforhodamine B
TCA	Trichloroacetic acid
TERT	Telomerase reverse transcriptase
TFs	Transcription factors
TGF	Transforming growth factor
TME	Tumor microenvironment
TNBC	Triple negative breast cancer
TSS	Transcription start site
UCSC	University of California Santa Cruz
WT	Wild type
YAP	Yes1 associated transcriptional regulator
ZEB1	Zinc finger E-box binding homeobox 1
ZO-1	Zonula occludens-1

### Curriculum vitae

Bircan Çoban was born on April 20, 1990, in Izmir, Türkiye. In 2008, she began her Bachelor's degree in Biology at Hacettepe University in Ankara, Türkiye. During her undergraduate studies, she participated in the Erasmus Mundus Summer Training program, working on the role of RNA binding protein, HuD, in the onset and progression of childhood tumor neuroblastoma under the supervision of Dr. Daniele Peroni at the Centre for Integrative Biology at the University of Trento, Italy in 2011.

After completing her B.Sc. in 2012, she joined the lab of Dr. Tolga Emre at Bogazici University in Istanbul, Türkiye, as a trainee student from 2013 to 2014. There, she focused on the characterization of IRF4 in melanoma cell lines. In 2014, she received a tuition waiver to pursue her Master's in Molecular Biology and Genetics, supervised by Dr. Ozlen Konu at Bilkent University in Ankara, Türkiye. Her research on the regulation of Mineralocorticoid receptor (MR) and its downstream targets by Estrogen and Aldosterone in breast cancer sparked her curiosity about protein biology, leading her to a short-term scientific mission at the University of Lausanne, Switzerland in 2015. At Lausanne, she worked with interdisciplinary researchers in the group of Prof. Olivier Staub, obtaining preliminary results for her Master's thesis.

After successfully obtaining her M.Sc. degree in 2016, she moved to Munich to further her career as a graduate student at the Technical University of Munich, Germany. She spent seven months there, gaining experience with *in vivo* mouse models and organoid cultures of pancreatic adenocarcinoma.

In 2018, she began her Ph.D. studies under the supervision of Prof. Erik Danen at Leiden Academic Centre for Drug Research, Leiden University, the Netherlands. Her project, supported by Dutch Cancer Society, focused on identifying the context-specific roles of the Grainyhead-like transcription factor-2 across breast cancer subtypes. After completing her experiments in the lab, she worked as a Research Scientist at ProteoNic BV in 2023-2024. Currently, she is on sabbatical and dedicating her time to travels and personal development.



**List of publications**

- **Coban B**, Wang Z, Liao CY, Beslmüller K, Timmermans MAM, Martens JWM, Hundscheid JHM, Slutter B, Zweemer AJM, Neubert E, Danen EHJ. GRHL2 suppression of NT5E/CD73 in breast cancer cells modulates CD73-mediated adenosine production and T cell recruitment. *iScience*. 2024 Apr 12;27(5):109738.
- Bergonzini C, Gregori A, Hagens TMS, van der Noord VE, van de Water B, Zweemer AJM, **Coban B**, Capula M, Mantini G, Botto A, Finamore F, Garajova I, McDonnell LA, Schmidt T, Giovannetti E, Danen EHJ. ABCB1 overexpression through locus amplification represents an actionable target to combat paclitaxel resistance in pancreatic cancer cells. *J Exp Clin Cancer Res*. 2024 Jan 2;43(1):4.
- Wang, Z.; **Coban, B.**; Liao, C.-Y.; Chen, Y.-J.; Liu, Q.; Danen, E.H.J. GRHL2 Regulation of Growth/Motility Balance in Luminal versus Basal Breast Cancer. *Int. J. Mol. Sci.* 2023, 24, 2512.
- Wang Z, **Coban B**, Wu H, Chouaref J, Daxinger L, Paulsen MT, Ljungman M, Smid M, Martens JWM, Danen EHJ. GRHL2-controlled gene expression networks in luminal breast cancer. *Cell Commun Signal*. 2023 Jan 23;21(1):15.
- Liu Q, Stel WV, Noord VEV, Leegwater H, **Coban B**, Elbertse K, Pruijs JTM, Béquignon OJM, Westen GV, Dévédec SEL, Danen EHJ. Hypoxia Triggers TAZ Phosphorylation in Basal A Triple Negative Breast Cancer Cells. *Int J Mol Sci*. 2022 Sep 4;23(17):10119
- **Coban B**, Bergonzini C, Zweemer AJM, Danen EHJ. Metastasis: cross-talk between tissue mechanics and tumour cell plasticity. *Br J Cancer*. 2021 Jan;124(1):49-57



